

SYNTHETIC UTILIZATION OF THE REDOX PROPERTIES OF SOME
GROUP 6 ORGANOMETALLIC NITROSYL COMPLEXES

By

GEORGE BANNERMAN RICHTER-ADDO

B.Sc. (Hons), University of Cape Coast, 1982
Dip.Ed., University of Cape Coast, 1982

A THESIS SUBMITTED IN PARTIAL FULFILLMENT
OF THE REQUIREMENTS FOR THE DEGREE OF
DOCTOR OF PHILOSOPHY

in

THE FACULTY OF GRADUATE STUDIES

(Department of Chemistry)

We accept this thesis as conforming
to the required standard

THE UNIVERSITY OF BRITISH COLUMBIA
September 1988

© George Bannerman Richter-Addo, 1988

In presenting this thesis in partial fulfilment of the requirements for an advanced degree at the University of British Columbia, I agree that the Library shall make it freely available for reference and study. I further agree that permission for extensive copying of this thesis for scholarly purposes may be granted by the head of my department or by his or her representatives. It is understood that copying or publication of this thesis for financial gain shall not be allowed without my written permission.

Department of CHEMISTRY

The University of British Columbia
Vancouver, Canada

Date 12TH OCTOBER, 1988.

Abstract

The redox behavior of a series of organometallic complexes containing $\text{Cp}'\text{M}(\text{NO})$ groups ($\text{Cp}' = \eta^5\text{-C}_5\text{H}_5(\text{Cp})$ or $\eta^5\text{-C}_5\text{Me}_5(\text{Cp}^*)$; $\text{M} = \text{Mo}$ or W) has been investigated both by cyclic voltammetry and by chemical means. The neutral 16-electron $\text{Cp}'\text{Mo}(\text{NO})\text{X}_2$ compounds ($\text{X} = \text{Cl}, \text{Br}$ or I) undergo a single, essentially reversible, one-electron reduction in $\text{CH}_2\text{Cl}_2/0.1\text{M} [\text{n-Bu}_4\text{N}]\text{PF}_6$ at relatively low potentials (< -0.1 V vs SCE). The electrochemically observed reductions can be effected on a preparative scale by employing Cp_2Co as the chemical reductant. The isolable 17-electron $[\text{Cp}'\text{Mo}(\text{NO})\text{X}_2]^{\bullet-}$ radical anions are cleanly reconverted to their 16-electron neutral precursors by treatment with $[\text{Cp}_2\text{Fe}]\text{BF}_4$. In contrast, the $\text{Cp}'\text{W}(\text{NO})\text{I}_2$ compounds undergo rapid decomposition to their $[\text{Cp}'\text{W}(\text{NO})\text{I}]_2$ monohalo dimers upon electrochemical reduction.

Electrophiles NE^+ ($\text{E} = \text{O}$ or $\text{p-O}_2\text{NC}_6\text{H}_4\text{N}$) undergo unprecedented insertions into the Cr-C σ -bonds of $\text{CpCr}(\text{NO})_2\text{R}$ complexes ($\text{R} = \text{Me}, \text{CH}_2\text{SiMe}_3$ or Ph) to afford $[\text{CpCr}(\text{NO})_2\{\text{N}(\text{E})\text{R}\}]^+$ cationic complexes. Present evidence is consistent with these insertions occurring via charge-controlled, intermolecular attacks by NE^+ at the Cr-R groups in classical $\text{S}_{\text{E}}2$ processes. The newly-formed $\text{N}(\text{E})\text{R}$ ligands function as Lewis bases through nitrogen atoms toward the formally 16-electron $[\text{CpCr}(\text{NO})_2]^+$ cations and may be displaced from the chromium's coordination sphere by the more strongly coordinating Cl^- anion. The resulting $\text{CpCr}(\text{NO})_2\text{Cl}$ can be reconverted to $\text{CpCr}(\text{NO})_2\text{R}$, thereby completing a cycle by regenerating the initial organometallic reactant. The entire sequence of stoichiometric reactions forming the cycle thus constitutes a selective method

(iii)

for the formation of new carbon-nitrogen bonds, the net organic conversions mediated by the CpCr(NO)_2 group being $\text{NE}^+ + \text{R}^- \rightarrow \text{N(E)R}$.

The electrophilic $[\text{Cp}'\text{M(NO)}_2]^+$ cations ($\text{Cp}' = \text{Cp}$ or Cp^* ; $\text{M} = \text{Cr}, \text{Mo}$ or W) condense with methyl propiolate and 2,3-dimethyl-2-butene to afford cationic organometallic lactone complexes. These complexes undergo facile O -dealkylation to yield the neutral $\text{Cp}'\text{M(NO)}_2(\eta^1\text{-lactone})$ derivatives. Furthermore, the neutral $\text{Cp}'\text{W(NO)}_2(\eta^1\text{-lactone})$ compounds decompose in air to their $\text{Cp}'\text{W(O)}_2(\eta^1\text{-lactone})$ dioxo products.

TABLE OF CONTENTS

Abstract	ii
List of Tables	vii
List of Figures	ix
Acknowledgement	xii
List of Abbreviations.....	xiii
Chapter 1 General Introduction	1
Chapter 2 Electrochemical Studies of the Complexes $[\text{Cp}'\text{M}(\text{NO})\text{X}_2]_n$ $\text{M} = \text{Mo or W}; \text{Cp}' = \eta^5\text{-C}_5\text{H}_5(\text{Cp}) \text{ or } \eta^5\text{-C}_5\text{Me}_5(\text{Cp}^*); \text{X} = \text{Cl},$ $\text{Br or I}; n = 1 \text{ or } 2]: \text{ Synthesis and Characterization}$ of the $[\text{Cp}'\text{Mo}(\text{NO})\text{X}_2]^{\bullet-}$ Radical Anions and $[\text{Cp}^*\text{W}(\text{NO})\text{I}]_2$	5
- Introduction	6
- Experimental Section	8
Electrochemical Measurements	9
ESR Measurements	11
- Results and Discussion	17
Molybdenum Complexes	17
Cyclic Voltammetry Studies	17
Preparation of the Radical Anion Complexes	24
Direct Evidence for the Involvement of Single Electron Transfer (SET) During the Reactions of Grignard Reagents with the $\text{Cp}'\text{Mo}(\text{NO})\text{X}_2$ Complexes. Implications for the Improved Syntheses of the $\text{Cp}'\text{Mo}(\text{NO})\text{R}_2$ Compounds	31
Tungsten Complexes	35

	The Cp'W(NO)X ₂ Complexes	35
	The Tungsten Cp'W(NO)(CH ₂ SiMe ₃) ₂ Dialkyl Complexes ..	39
	- Summary	43
	- References and Notes	45
Chapter 3	Insertions of Electrophiles into Metal-Carbon Bonds:	
	Formation of New Carbon-Nitrogen Linkages Mediated by the	
	CpCr(NO) ₂ Group	52
	- Introduction	53
	- Experimental Section	54
	- Results and Discussion	66
	Insertions of the Nitrosonium Ion into Chromium-Carbon	
	Bonds	66
	Possible Mechanisms for the Nitrosonium Insertion	
	Reactions	73
	A Stoichiometric Cycle for the Formation of New Carbon-	
	Nitrogen Bonds	83
	Deprotonation of the Formaldoxime Ligand in	
	[CpCr(NO) ₂ {N(OH)CH ₂ }]PF ₆	89
	- Summary	96
	- References and Notes	98
Chapter 4	Some Characteristic Chemistry of the Electrophilic	
	[Cp'M(NO) ₂]BF ₄ Complexes (Cp' = Cp or Cp [*] ; M = Cr, Mo or W)	102
	- Introduction	103
	- Experimental Section	105
	- Results and Discussion	112

Generation of $[\text{Cp}'\text{M}(\text{NO})_2]\text{BF}_4$ ($\text{Cp}' = \text{Cp}$ or Cp^* ; $\text{M} = \text{Cr}$, Mo or W)	112
Reactions of $[\text{Cp}'\text{M}(\text{NO})_2]\text{BF}_4$ with 2,3-Dimethyl-2-butene and Methyl Propiolate	115
Preparation of the Neutral $\text{Cp}'\text{M}(\text{NO})_2$ - $\overline{\text{C}=\text{C}(\text{H})\text{C}(\text{Me})_2\text{C}(\text{Me})_2\text{OC}(=\text{O})}$ Lactone Complexes (7-12)	124
Decomposition of the $\text{Cp}'\text{W}(\text{NO})_2$ - $\overline{\text{C}=\text{C}(\text{H})\text{C}(\text{Me})_2\text{C}(\text{Me})_2\text{OC}(=\text{O})}$ Complexes in Air	132
- Summary	133
- References and Notes	136
Epilogue	140
Appendix	141

LIST OF TABLES

Table 2.1	Data for the Reduction of Dihalo Complexes of Molybdenum	18
Table 2.2	A Comparison of the Nitrosyl-Stretching Frequencies of the New 17-electron Radical Anion Complexes with their Neutral Precursors.	26
Table 2.3	Electron Spin Resonance Data for the $[\text{Cp}_2\text{Co}][\text{Cp}'\text{Mo}(\text{NO})\text{X}_2]$ Radical Anion Complexes	28
Table 2.4	Electrochemical Data for the Electroreduction of $\text{Cp}^*\text{W}(\text{NO})\text{I}_2$ in CH_2Cl_2 for a Variety of Scan Rates	41
Table 3.1	Cyclic Voltammetry Data for the Oxidations of Some $\text{CpCr}(\text{NO})_2\text{R}$ Complexes	76
Table 3.2	Selected Bond Lengths (Å) and Angles (deg) for $[\text{CpCr}(\text{NO})_2\{\text{N}(\text{NC}_6\text{H}_4\text{NO}_2)\text{Me}\}]^+\text{BF}_4^-$	85
Table 3.3	Selected Bond Lengths (Å) and Angles (deg) for the $[\{\text{CpCr}(\text{NO})_2\}_2\{\mu,\eta^2\text{-N}(\text{CH}_2)\text{O}\}]^+$ cation as it exists in its BPh_4^- salt	91
Table 4.1	IR Data for Various $\text{Cp}'\text{M}(\text{NO})_2\text{X}$ Complexes in CH_2Cl_2	113
Table 4.2	Numbering Scheme for the Cationic and Neutral Lactone Complexes	116
Table 4.3	Physical Data for the Cationic Lactone Complexes 1-6	119
Table 4.4	^1H NMR Chemical Shifts of the Cationic Lactone Complexes 1-6	120
Table 4.5	^{13}C NMR Chemical Shifts of Some Lactone Complexes	121
Table 4.6	Physical and Mass Spectral Data for the Neutral Lactone Complexes	126

Table 4.7	^1H NMR Chemical Shifts of the Neutral Lactone Complexes	127
Table 4.8	Selected Bond Lengths (Å) for the $\text{CpMo}(\text{NO})_2(\eta'\text{-lactone})$ compound 9	130
Table 4.9	Selected Bond Angles (deg) for the $\text{CpMo}(\text{NO})_2(\eta'\text{-lactone})$ compound 9	131

LIST OF FIGURES

Figure 2.1	The low-temperature cyclic voltammetry cell: (A) Pt-bead working electrode; (B) Pt-wire auxiliary electrode; (C) aqueous saturated calomel reference electrode; (D) fine-fritted reference cell holder; (E) Luggin probe; (F) glass jacket for coolant	10
Figure 2.2	Ambient temperature cyclic voltammogram of $\text{CpMo}(\text{NO})\text{I}_2$ in CH_2Cl_2 containing 0.1 M $[\text{n-Bu}_4\text{N}]\text{PF}_6$ measured at a platinum-bead electrode at a scan rate of 0.24 V s^{-1}	20
Figure 2.3	Cyclic voltammogram of $\text{CpMo}(\text{NO})\text{I}_2$ in CH_2Cl_2 at a scan rate of 0.44 V s^{-1}	22
Figure 2.4	Cyclic voltammogram of $[\text{CpMo}(\text{NO})\text{I}]_2$ in CH_2Cl_2 at a scan rate of 0.14 V s^{-1}	23
Figure 2.5	The ESR spectrum of $[\text{Cp}_2\text{Co}][\text{CpMo}(\text{NO})\text{Cl}_2]$ in DMF	29
Figure 2.6	The ESR spectrum of $[\text{Cp}_2\text{Co}][\text{Cp}^*\text{Mo}(\text{NO})\text{Br}_2]$ in DMF	30
Figure 2.7	The ESR spectrum of a DMF solution of an equimolar mixture of $\text{Me}_3\text{SiCH}_2\text{MgCl}$ and $\text{Cp}^*\text{Mo}(\text{NO})\text{Br}_2$ at 20°C	33
Figure 2.8	Cyclic voltammograms of $\text{CpW}(\text{NO})\text{I}_2$ in CH_2Cl_2 at a scan rate of 0.32 V s^{-1} . (a) scanning positive potentials first, and (b) scanning negative potentials first	36
Figure 2.9	Cyclic voltammograms of $\text{Cp}^*\text{W}(\text{NO})\text{I}_2$ in CH_2Cl_2 at different scan rates (a) 2.64 V s^{-1} (b) at 0.53 V s^{-1} and (c) at 0.13 V s^{-1}	38
Figure 2.10	Plot of $i_{\text{p,a}}/i_{\text{p,c}}$ vs scan rate for the first reversible redox couple of $\text{Cp}^*\text{W}(\text{NO})\text{I}_2$ in CH_2Cl_2	40

- Figure 2.11** Temperature dependence of $\frac{i_{p,a}}{i_{p,c}}$ values as a function of scan rate for the first reversible redox couple of $\text{Cp}^*\text{W}(\text{NO})\text{I}_2$ in THF 42
- Figure 3.1** The solid-state molecular structure of the $[\text{CpCr}(\text{NO})_2\{\text{N}(\text{OH})\text{CH}_2\}]^+$ cation 68
- Figure 3.2** Ambient temperature cyclic voltammogram of 5×10^{-4} M $\text{CpCr}(\text{NO})_2\text{Me}$ in CH_2Cl_2 containing 0.1 M $[\text{n-Bu}_4\text{N}]\text{PF}_6$ measured at a platinum-bead electrode at a scan rate of 0.30 V s^{-1} 75
- Figure 3.3** The 300 MHz ^1H NMR spectrum of $[\text{CpCr}(\text{NO})_2\{\text{N}(\text{NC}_6\text{H}_4\text{NO}_2)\text{Me}\}]\text{BF}_4$ in CD_3NO_2 (*) 82
- Figure 3.4** Views of the molecular structure of the $[\text{CpCr}(\text{NO})_2\{\text{N}(\text{NC}_6\text{H}_4\text{NO}_2)\text{Me}\}]^+$ cation (a) approximately parallel to the Cp ligand and (b) approximately perpendicular to the Cp ligand. Only non-hydrogen atoms are shown 84
- Figure 3.5** Solid-state molecular structure of the $[\{\text{CpCr}(\text{NO})_2\}_2\{\mu, \eta^2\text{-N}(\text{CH}_2)\text{O}\}]^+$ cation as it exists in its BPh_4^- salt. Hydrogen atoms have been omitted for clarity 90
- Figure 3.6** The 300 MHz ^1H NMR spectrum of $[\{\text{CpCr}(\text{NO})_2\}_2\{\mu, \eta^2\text{-N}(\text{CH}_2)\text{O}\}]\text{PF}_6$ in CD_2Cl_2 93
- Figure 3.7** The 75 MHz ^{13}C NMR spectrum of $[\{\text{CpCr}(\text{NO})_2\}_2\{\mu, \eta^2\text{-N}(\text{CH}_2)\text{O}\}]\text{PF}_6$ in CD_3NO_2 . The inset contains an expansion of the signals due to the Cp carbons at δ 105.94 and 105.06 ppm 94

Figure 4.1	The 300 MHz ^1H NMR spectrum of complex 3 in acetone- d_6	118
Figure 4.2	The 300 MHz ^1H NMR spectrum of complex 9 in acetone- d_6	128
Figure 4.3	Solid-state molecular structure of the $\text{CpMo}(\text{NO})_2(\eta^1\text{-lactone})$ complex 9	129

ACKNOWLEDGMENTS

My sincere gratitude goes to my research supervisor, Professor Peter Legzdins, for being a constant source of support to me (both academically and personally) over the years. Without question, whatever I have achieved academically over the last 4 years has been largely due to his high standards and energetic enthusiasm for hard work.

I also want to thank the occupants of 319/325 (Neil, Jeff, Bé, Teen, Nancy and Everett) for providing the friendly research environment, and Neil and Nancy for proofreading this thesis. My gratitude goes to Drs. F.G. Herring, L. Weiler and F. Aubke for reading portions of this thesis and making suggestions for improvement.

I would also like to thank Ms. Lani Collins and Ms. Bev Gray for typing this thesis. I also acknowledge the financial support of the University of British Columbia in the form of a Graduate Fellowship (1985-87).

Finally, I thank a very special friend, Ms. Lethika Raveendran, for her loving friendship and support.

LIST OF ABBREVIATIONS

Cp	-	η^5 -cyclopentadienyl
Cp [*]	-	η^5 -pentamethylcyclopentadienyl
Me	-	CH ₃ , methyl
Ph	-	C ₆ H ₅ , phenyl
Et ₂ O	-	(CH ₃ CH ₂) ₂ O, diethyl ether
THF	-	C ₄ H ₈ O, tetrahydrofuran
C ₆ D ₆	-	benzene-d ₆
CDCl ₃	-	chloroform-d ₁
CD ₂ Cl ₂	-	dichloromethane-d ₂
CD ₃ NO ₂	-	nitromethane-d ₃
(CD ₃) ₂ CO	-	acetone-d ₆
IR	-	infrared
NMR	-	nuclear magnetic resonance
MS	-	mass spectrometry
<u>m/z</u>	-	mass-to-charge ratio in the mass spectrum
P ⁺	-	molecular ion (in the mass spectrum)
CV	-	cyclic voltammetry
SCE	-	saturated calomel electrode
V	-	volts
¹³ C { ¹ H}	-	proton decoupled carbon-13

(xiv)

ESSE QUAM VIDERI:

TO BE IS BETTER THAN TO SEEM TO BE.

-Motto of the Accra Academy, Ghana

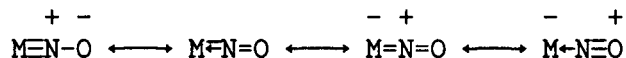
CHAPTER 1

General Introduction

Organometallic nitrosyl complexes are compounds that contain both nitric oxide and organic groups coordinated in some fashion to one or more metal centers. In monometallic nitrosyl complexes, the nitrosyl ligands may participate in two principal bonding modes:

- a) terminal, linear M-NO
- b) terminal, bent M-NO

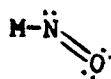
The terminal, linear bonding mode of the NO ligand is very common in organometallic nitrosyl chemistry, and four simple resonance forms for this bonding mode can be envisaged,



When linearly bonded, the nitrosyl ligand is considered to be a formal three-electron donor. Furthermore, the MNO bonding involves a synergic combination of σ -donation from the nitrosyl ligand to the metal and $\text{M}\pi \rightarrow \text{NO}\pi^*$ back-bonding. As expected, the extent of metal π -donation is largely dependent on the degree of electron-richness of the metal center. In principle, therefore, an increase in the electron-richness of the metal center should result in increased back-bonding to the nitrosyl ligand and thus decrease the NO bond order and its infrared (IR) stretching frequency (ν_{NO}). Indeed, this shift in ν_{NO} is one of the most sensitive probes to changes in the electron-richness of the metal center in an organometallic nitrosyl complex.

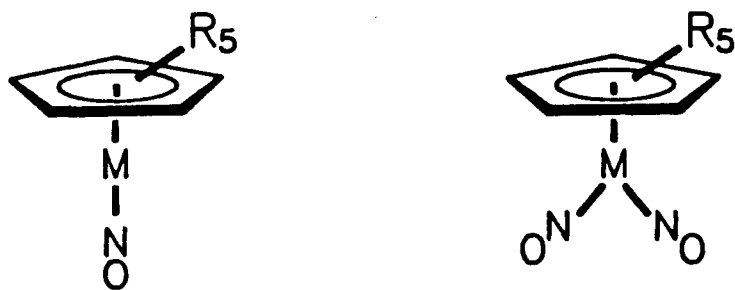
The terminal, bent bonding mode of the nitrosyl ligand is by far less common than its linear form. Formally, the bent NO ligand is an analogue of an organic nitroso group or the NO group in ClNO. The MNO linkage consists of a

doubly bonded NO group, a single σ -bond between the nitrogen and the metal, and a lone pair of electrons on the nitrogen atom, i.e.



The nitrogen atom in this case is sp^2 hybridized and the resulting M-N-O is bent. When bonded in this way, the nitrosyl ligand is a formal one-electron donor.

The work presented in this thesis deals primarily with the determination and synthetic utilization of the redox properties of some Group 6 organometallic nitrosyl complexes containing the $\text{Cp}'\text{M}(\text{NO})$ or $\text{Cp}'\text{M}(\text{NO})_2$ fragments ($\text{Cp}' = \eta^5\text{-C}_5\text{H}_5$ (Cp) or $\eta^5\text{-C}_5\text{Me}_5$ (Cp^*); $\text{M} = \text{Cr}, \text{Mo}$ or W).



($\text{M} = \text{Cr}, \text{Mo}$ or W ; $\text{R} = \text{H}$ or Me)

A major impetus for this research is embodied in the belief that a knowledge of the redox properties of a class of compounds will provide a clearer understanding of their known chemistry as well as facilitate the development of new chemistry. Chapter 2 of this thesis deals with the results of cyclic voltammetry studies of various mononitrosyl complexes of molybdenum and tungsten. In particular, the $[\text{Cp}'\text{M}(\text{NO})\text{I}_2]_n$ ($\text{M} = \text{Mo}$ or W ; $n = 1$ or 2) compounds were studied in detail since these compounds were then the sole precursors used to obtain a variety of alkyl, hydride and diene derivatives containing the $\text{Cp}'\text{M}(\text{NO})$ group. Chapter 3 centers on the oxidation electrochemistry of various dinitrosyl complexes of chromium. Results of the reactions of these $\text{CpCr}(\text{NO})_2\text{R}$ complexes ($\text{R} = \text{alkyl}$ or aryl) with nitrogen-containing electrophiles are presented in the light of a stoichiometric cycle for carbon-nitrogen bond formation. Finally, Chapter 4 describes the synthetic utility of the electrophilic $[\text{Cp}'\text{M}(\text{NO})_2]^+$ cations ($\text{M} = \text{Cr}, \text{Mo}$ or W) in organic synthesis. Of particular interest is the condensation reaction involving these cations, methyl propiolate and 2,3-dimethyl-2-butene to form organometallic lactone complexes of the form $\text{Cp}'\text{M}(\text{NO})_2(\eta^1\text{-lactone})$.

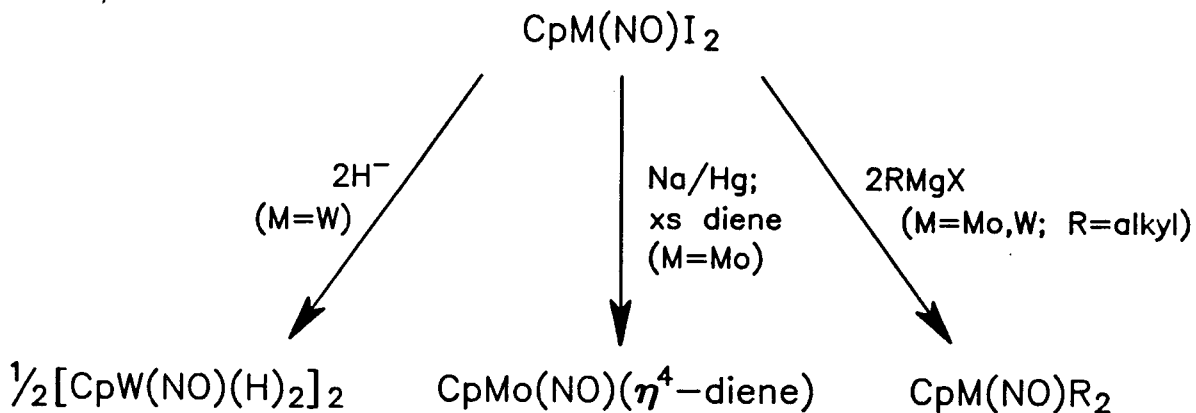
Since the bonding in organometallic nitrosyl complexes is largely dominated by covalent interaction with the metal atom, assignment of oxidation states to the metal atom and the NO is undesirable. Throughout this thesis, therefore, rationales involving formal oxidation states are avoided, and all ligands are considered to be neutral (for example, the Cp ligand is formally a neutral five-electron donor whereas the halide ligand is considered a neutral one-electron donor).

CHAPTER 2

Electrochemical Studies of the Complexes $[\text{Cp}'\text{M}(\text{NO})\text{X}_2]_n$ $[\text{M} = \text{Mo or W};$
 $\text{Cp}' = \eta^5\text{-C}_5\text{H}_5(\text{Cp}) \text{ or } \eta^5\text{-C}_5\text{Me}_5(\text{Cp}^*); \text{X} = \text{Cl, Br or I}; n = 1 \text{ or } 2]:$ Synthesis
and Characterization of the $[\text{Cp}'\text{Mo}(\text{NO})\text{X}_2]^{\bullet-}$ Radical Anions and $[\text{Cp}^*\text{W}(\text{NO})\text{I}]_2$.

Introduction

During previous work in our laboratories, several alkyl,¹ hydride² and diene³ derivatives of complexes containing the CpM(NO) group [M = Mo or W] have been synthesized by utilizing the diiodo precursors [CpM(NO)I₂]_n (n = 1 or 2) as shown in Scheme 2.1 (for n = 1).



Scheme 2.1

Curiously, it had not been possible to extend these reactions to prepare the analogous hydride complexes of molybdenum, the diene complexes of tungsten, and the aryl analogues of the formally 16-electron dialkyl complexes. Most disturbingly, the Cp^{*}Mo(NO)R₂ (R = alkyl) complexes could not be obtained in more than marginal yields starting from the diiodo precursor.⁴ In an effort to try to understand the factors that govern the outcome of these halide substitution reactions, I undertook an electrochemical study of the

$[\text{Cp}'\text{M}(\text{NO})\text{I}_2]_n$ precursor complexes ($\text{M} = \text{Mo}$ or W ; $\text{Cp}' = \text{Cp}$ or Cp^*) and later extended it to encompass the analogous dichloro and dibromo complexes of molybdenum.

This Chapter contains (1) the results of the electrochemical studies (2) the description of the isolation of a series of molybdenum dihalo radical anions, and (3) spectroscopic evidence for the occurrence of single electron transfer (SET) during the reactions of Grignard reagents with the $[\text{Cp}'\text{Mo}(\text{NO})\text{X}_2]_n$ complexes. To avoid the controversy of the value of n in the $[\text{Cp}'\text{Mo}(\text{NO})\text{X}_2]_n$ complexes in the solid state,⁵ I shall simply refer to these complexes as monomers ($n = 1$) since evidence presented in this Chapter is most consistent with their formulation as monomers in solution.

Experimental Section

All reactions and subsequent manipulations involving organometallic reagents were performed under anhydrous conditions and under an atmosphere of prepurified dinitrogen. Conventional techniques⁶ were employed unless otherwise noted. All solvents were purified according to published procedures.⁷ Tetrahydrofuran (THF) and diethylether were distilled from Na/benzophenone; toluene from Na; and CH_2Cl_2 from P_2O_5 . The solvents were freshly distilled and purged with N_2 for ~10 min prior to use. All chemicals were of reagent grade or comparable purity, and were either purchased from commercial suppliers or prepared by published procedures. Standard analytical and spectroscopic techniques were used to ascertain their purity. The $[\text{CpMo}(\text{NO})\text{X}_2]_n$ complexes ($\text{X} = \text{Cl}, \text{Br}, \text{I}; n = 1 \text{ or } 2$),⁸ $[\text{CpMo}(\text{NO})\text{I}]_2$ ⁹ and the $[\text{Cp}'\text{W}(\text{NO})\text{I}_2]_n$ complexes ($\text{Cp}' = \text{Cp}^{10a} \text{ or } \text{Cp}^{*10b}$) were prepared by known procedures. The $[\text{Cp}^*\text{Mo}(\text{NO})\text{X}_2]_n$ compounds (for $\text{X} = \text{Br}, \text{I}$)¹¹ were prepared from $\text{Cp}^*\text{Mo}(\text{NO})(\text{CO})_2$ and elemental X_2 in a manner similar to the preparation of their perhydro analogues, and their purity was checked by elemental analyses.

Infrared spectra were obtained with a Nicolet Model 5DX FT-IR instrument (internally calibrated with a He/Ne laser). ^1H NMR and ^{13}C NMR spectra were obtained with a Varian Associates XL-300 NMR spectrometer or a Bruker WP-80 NMR spectrometer. Low-resolution mass spectra were recorded at 70 eV on an Atlas CH4B or a Kratos MS50 spectrometer using the direct-insertion method by the staff of the Mass Spectrometry Laboratory headed by Dr. G.K. Eigendorf. Elemental analyses were performed by Mr. P. Borda of this Department.

Electrochemical Measurements

Electrochemical measurements were accomplished with a PAR Model 173 potentiostat equipped with a Model 176 current-to-voltage converter and a Model 178 electrometry probe. The triangular waveform potential required during cyclic voltammetry studies was obtained with a Wavetek Model 143 function generator in conjunction with a unity-gain inverter (± 15 V, 50 mA) constructed in the Electronics Shop under the direction of Mr. Joe Sallos. Cyclic voltammograms were recorded on a Hewlett-Packard Model 7090A X-Y recorder. A Fisher Model 5000 strip-chart recorder was used for the current-time plot during bulk electrolyses measurements.

Each electrochemical study employed cyclic voltammetry (CV) measurements, and the three-electrode cell employed for CV has been previously described.¹² A similar cell was employed for low-temperature CV and is shown in Figure 2.1. The cell was constructed by Mr. Steve Takacs of the Departmental glassblowing shop.

All potentials are reported versus the aqueous saturated calomel electrode (SCE), and E^0 values were determined as the average of cathodic and anodic peak potentials, i.e. $(E_{p,c} + E_{p,a})/2$. Compensation for iR drop in potential measurements was not employed in this study. The $[n\text{-Bu}_4\text{N}]\text{PF}_6$ support electrolyte was prepared by metathesis of $[n\text{-Bu}_4\text{N}]\text{I}$ with NH_4PF_6 in hot acetone and was recrystallized thrice from ethanol.¹² Solvents (THF, CH_2Cl_2 , CH_3CN) were obtained from BDH Chemicals (spectral grade) and were stirred over alumina (Woelm neutral, activity 1) whilst simultaneously being purged with N_2 for 15 min just prior to use. The solutions employed during CV were typically $(5\text{--}7) \times 10^{-4}$ M in the organometallic complex and 0.1 M in $[n\text{-Bu}_4\text{N}]\text{PF}_6$ and were

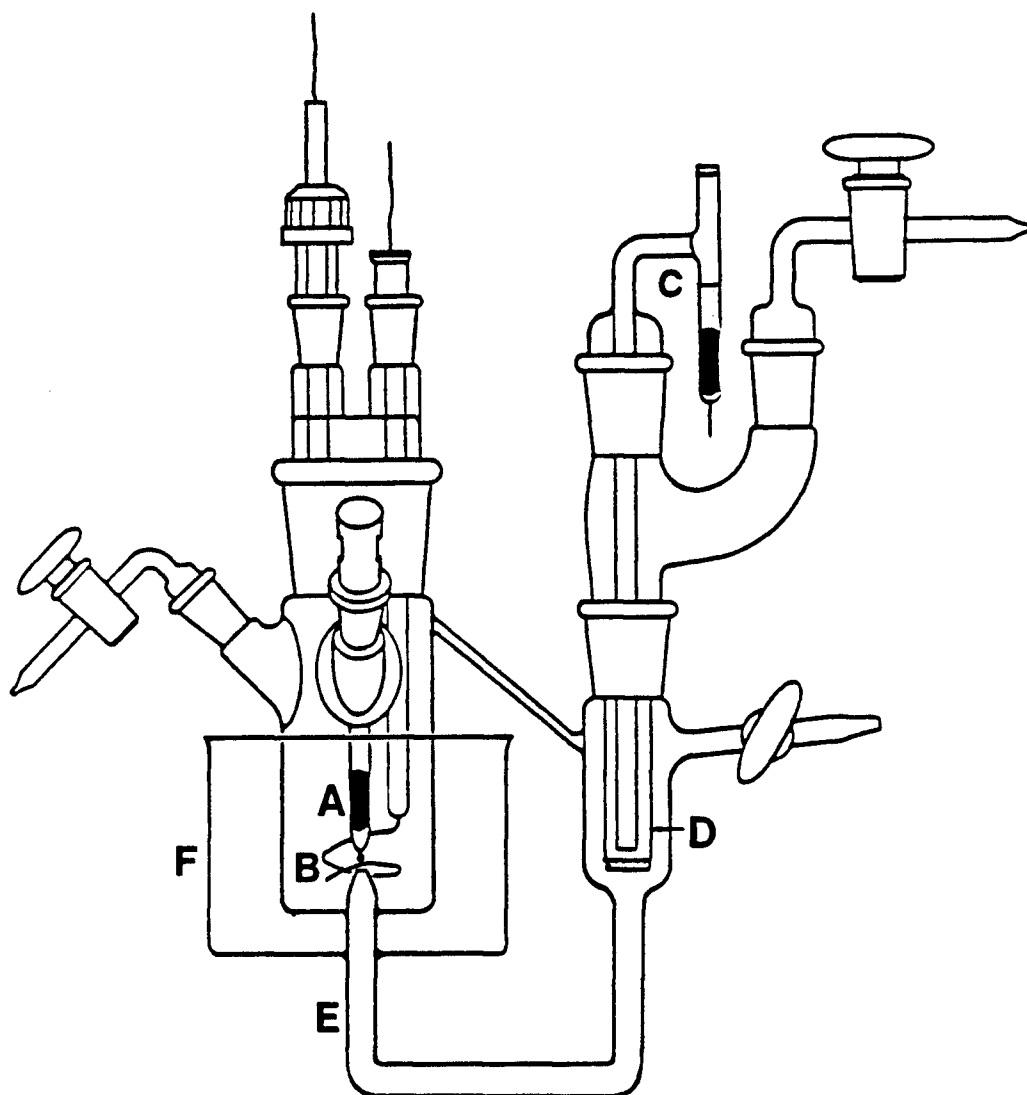


Figure 2.1. The low-temperature cyclic voltammetry cell: (A) Pt-bead working electrode; (B) Pt-wire auxiliary electrode; (C) aqueous saturated calomel reference electrode; (D) fine-fritted reference cell holder; (E) Luggin probe; (F) glass jacket for coolant.

maintained under an atmosphere of N_2 . Under these conditions, the Cp_2Fe/Cp_2Fe^+ couple is measured at $E^{O'} = +0.46$ V versus SCE in CH_2Cl_2 . The ratio of the cathodic peak current to anodic peak current $(i_{p,c}/i_{p,a})^{13}$ is 1. Furthermore, the cathodic peak current $(i_{p,c})$ increases linearly with $v^{1/2}$.¹⁴ The separation of the cathodic and anodic peak potentials (ΔE) increases somewhat with a rise in scan rate, from 67 mV at 0.14 V s^{-1} to 78 mV at 0.28 V s^{-1} . Consequently, redox couples exhibiting similar behavior to that of the Cp_2Fe/Cp_2Fe^+ couple (which is known to be highly reversible)¹⁵ are considered to be reversible. In general, reversible processes observed in cyclic voltammetry experiments were studied in detail first before irreversible waves.

ESR Measurements

Dimethylformamide (DMF) was dried over BaO overnight, filtered through Celite and then deaerated with N_2 prior to use. Samples for ESR measurements were prepared in a Vacuum Atmospheres Model HE-43 Dry Box as follows: a weighed amount of the solid radical anion complex was dissolved in enough DMF to make up a 5×10^{-5} M solution. A portion of this solution was then transferred by disposable syringe into a sealed melting-point capillary tube to a height of about 0.5 cm. The capillary tube was then sealed at the open end with silicone grease (Dow Corning, High Vacuum). The X-band ESR spectra were then recorded using the spectrometer and interfaced computer system described by Phillips and Herring.¹⁶ The spectra were recorded by Dr. F.G. Herring.

Preparation of $Cp^*Mo(NO)Cl_2$. This compound was obtained as a byproduct from the preparation of $Cp^*Mo(NO)_2Cl$ by the stoichiometric reaction of

$\text{Cp}^*\text{Mo}(\text{NO})(\text{CO})_2$ with NOCl in CH_2Cl_2 at room temperature.¹⁷ The red precipitate formed in the reaction mixture was collected by filtration and recrystallized from large quantities of CH_2Cl_2 to obtain $\text{Cp}^*\text{Mo}(\text{NO})\text{Cl}_2$ as a red-brown powder in ~20% yield.

Anal. Calcd for $\text{C}_{10}\text{H}_{15}\text{NOCl}_2\text{Mo}$: C, 36.14; H, 4.52; N, 4.22. Found: C, 36.03; H, 4.65; N, 4.31. IR (Nujol mull) ν_{NO} 1645 (s) cm^{-1} .

Reactions of $\text{Cp}'\text{Mo}(\text{NO})\text{X}_2$ ($\text{Cp}' = \text{Cp}$ or Cp^* ; $\text{X} = \text{Cl}$, Br or I) with Cobaltocene. All of these reactions were carried out in THF in a similar manner. However, the procedures described below vary slightly, and enable the desired complexes to be obtained in optimum yields.

Preparation of $[\text{Cp}_2\text{Co}][\text{CpMo}(\text{NO})\text{Cl}_2]$. To a rapidly stirred, green solution of $\text{CpMo}(\text{NO})\text{Cl}_2$ (0.22 g, 0.84 mmol) in THF (30 mL) was added solid Cp_2Co ¹⁸ (0.16 g, 0.83 mmol). A green solid precipitated over a 2 min period. This solid was collected by filtration, washed with THF (2 x 5 mL) and dried in vacuo (5×10^{-3} mm) for 1 h to obtain 0.31 g (83% yield) of $[\text{Cp}_2\text{Co}][\text{CpMo}(\text{NO})\text{Cl}_2]$.

Anal. Calcd for $\text{C}_{15}\text{H}_{15}\text{NOCl}_2\text{MoCo}$: C, 39.91; H, 3.33; N, 3.10. Found: C, 40.08; H, 3.41; N, 2.91. IR (Nujol mull) ν_{NO} 1552 (s) cm^{-1} ; also 3076 (m), 1640 (m), 1527 (sh), 1413 (m), 1063 (w), 1010 (m), 1004 (sh), 864 (m), 805 (m) cm^{-1} .

Preparation of $[\text{Cp}_2\text{Co}][\text{Cp}^*\text{Mo}(\text{NO})\text{Cl}_2]$. To a stirred, green solution of $\text{Cp}^*\text{Mo}(\text{NO})\text{Cl}_2$ (0.33 g, 1.0 mmol) in THF (70 mL) was added solid Cp_2Co (0.188 g, 1.0 mmol). A green solid precipitated over a 5 min period. Diethylether (80 mL) was added to the reaction mixture to complete the precipitation, and the

green microcrystalline solid was collected by filtration, washed with Et₂O (20 mL) and then dried in vacuo for 1 h to obtain 0.42 g (80% yield) of [Cp₂Co][Cp^{*}Mo(NO)Cl₂].

Anal. Calcd for C₂₀H₂₅NOCl₂MoCo: C, 46.07; H, 4.80; N, 2.69. Found: C, 46.13; H, 4.92; N, 2.67. IR (Nujol mull) ν_{NO} 1523 (s) cm⁻¹; also 3091 (m), 1610 (w), 1415 (m), 1063 (w), 1009 (w), 864 (m) cm⁻¹.

Preparation of [Cp₂Co][CpMo(NO)Br₂]. To a stirred, red-brown solution of CpMo(NO)Br₂ (0.351 g, 1.0 mmol) in THF (30 mL) was added solid Cp₂Co (0.186 g, 0.98 mmol). A dark green, powdery precipitate formed after ~2 min, and the reaction mixture was stirred for an additional 3 min to ensure complete reaction. Et₂O (50 mL) was added to complete the precipitation, and the solid was collected by filtration and dried in vacuo for 1 h to obtain 0.47 g (87% yield) of [Cp₂Co][CpMo(NO)Br₂].

Anal. Calcd for C₁₅H₁₅NOBr₂MoCo: C, 33.33; H, 2.78; N, 2.59. Found: C, 33.44; H, 2.95; N, 2.45. IR (Nujol mull) ν_{NO} 1557 (s) cm⁻¹; also 3090 (m), 1652 (w), 1414 (m), 1063 (w), 1009 (m), 1004 (sh), 862 (m), 804 (m) cm⁻¹.

Preparation of [Cp₂Co][Cp^{*}Mo(NO)Br₂]. To a stirred, green solution of Cp^{*}Mo(NO)Br₂ (0.357 g, 0.848 mmol) in THF (50 mL) was added solid Cp₂Co (0.153 g, 0.810 mmol). The reaction mixture was stirred for 3 min whereupon a green microcrystalline solid precipitated, leaving a light brown supernatant solution. This green solid was collected by filtration, washed with THF (20 mL) and dried in vacuo for 1.5 h to obtain 0.43 g (82% yield) of [Cp₂Co][Cp^{*}Mo(NO)Br₂].

Anal. Calcd for C₂₀H₂₅NOBr₂MoCo: C, 39.34; H, 4.10; N, 2.30. Found: C,

39.70; H, 4.09; N, 2.20. IR (Nujol mull) ν_{NO} 1534 (s) cm^{-1} ; also 3086 (m), 1638 (w), 1414 (m), 1065 (w), 1009 (w), 864 (m) cm^{-1} .

Preparation of $[\text{Cp}_2\text{Co}][\text{CpMo}(\text{NO})\text{I}_2]$. To a stirred, red solution of $\text{CpMo}(\text{NO})\text{I}_2$ (0.45 g, 1.0 mmol) in THF (30 mL) was added solid Cp_2Co (0.19 g, 1.0 mmol). The solution turned brown instantly, and a dark brown solid precipitated. Diethylether (30 mL) was added to complete precipitation of the solid, which was collected by filtration, washed with Et_2O (2 x 10 mL) and dried in vacuo for 2 h to obtain 0.54 g (84% yield) of brown $[\text{Cp}_2\text{Co}][\text{CpMo}(\text{NO})\text{I}_2]$.

Anal. Calcd for $\text{C}_{15}\text{H}_{15}\text{NOI}_2\text{MoCo}$: C, 28.39; H, 2.37; N, 2.21. Found: C, 28.30; H, 2.36; N, 2.38. IR (Nujol mull) ν_{NO} 1557 (s) cm^{-1} ; also 3065 (w), 1653 (w), 1412 (m), 1059 (m), 1007 (m), 999 (sh), 862 (m), 804 (m) cm^{-1} .

Attempts to obtain crystals of this complex from THF/ Et_2O at -20°C only resulted in the formation of black micro-crystals of $[\text{CpMo}(\text{NO})\text{I}_2]$ readily identifiable by its characteristic IR and mass spectra,⁹ and by elemental analyses.

Preparation of $[\text{Cp}_2\text{Co}][\text{Cp}^*\text{Mo}(\text{NO})\text{I}_2]$. To a stirred, red solution of $\text{Cp}^*\text{Mo}(\text{NO})\text{I}_2$ (0.515 g, 1.0 mmol) in THF (30 mL) was added solid Cp_2Co (0.19 g, 1.0 mmol). The color changed from red to green in ~2 min, and a green microcrystalline solid precipitated. The green solid was collected by filtration, washed with THF (2 x 10 mL) and then Et_2O (3 x 10 mL), and dried in vacuo for 2 h to obtain 0.49 g (70% yield) of $[\text{Cp}_2\text{Co}][\text{Cp}^*\text{Mo}(\text{NO})\text{I}_2]$.

Anal. Calcd for $\text{C}_{20}\text{H}_{20}\text{NOI}_2\text{MoCo}$: C, 34.09; H, 2.84; N, 1.99. Found: C, 33.76; H, 3.05; N, 1.89. IR (Nujol mull) ν_{NO} 1541 (s) cm^{-1} ; also 3083 (w),

1636 (w), 1412 (m), 1113 (w), 1007 (w), 862 (m) cm^{-1} .

Oxidation of the Radical Anion Complexes of Molybdenum. Oxidation of the $[\text{Cp}_2\text{Co}][\text{Cp}'\text{Mo}(\text{NO})\text{X}_2]$ radical anion complexes (obtained above) by equimolar amounts of $[\text{Cp}_2\text{Fe}]\text{BF}_4$ in acetonitrile resulted in all cases in the clean conversion of the radical anions to their neutral dihalo precursor complexes. The reactions were monitored (and nitrosyl-containing products identified) by IR spectroscopy.

Attempted Synthesis of $[\text{CpFe}(\eta^6\text{-C}_6\text{Me}_6)][\text{CpW}(\text{NO})(\text{CH}_2\text{SiMe}_3)_2]$. To a vigorously stirred Et_2O solution (20 mL) of $\text{CpW}(\text{NO})(\text{CH}_2\text{SiMe}_3)_2$ (0.15 g, 0.33 mmol) was added a filtered Et_2O solution (20 mL) of $\text{CpFe}(\eta^6\text{-C}_6\text{Me}_6)$ ¹⁹ (0.093 g, 0.33 mmol). The initial violet color of the reaction mixture (due to the dialkyl complex) became red-brown after ~1 min, and the reaction mixture was stirred for 0.5 h to ensure complete reaction. Removal of the solvent in vacuo resulted only in the deposition of an intractable red tar.

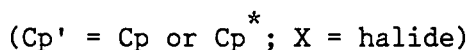
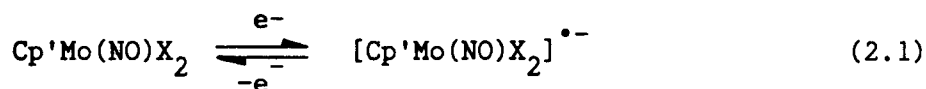
Preparation of $[\text{Cp}^*\text{W}(\text{NO})\text{I}]_2$. To an orange toluene solution (50 mL) of $\text{Cp}^*\text{W}(\text{NO})(\text{CO})_2$ (1.04 g, 2.57 mmol) was added solid $\text{Cp}^*\text{W}(\text{NO})\text{I}_2$ (1.55 g, 2.57 mmol). The resulting green solution was then refluxed at ~110°C for 2 h during which time the color turned a darker green. The final reaction mixture was allowed to cool to room temperature, filter-cannulated into a separate flask, and then kept at -20°C for 3 days. A dark green crystalline solid precipitated during this time, and it was collected by filtration, washed with cold toluene (2 x 5 mL) [**Caution:** this solid is soluble in toluene to an appreciable extent] and dried in vacuo overnight to obtain 0.89 g (36% yield) of $[\text{Cp}^*\text{W}(\text{NO})\text{I}]_2$ as air-sensitive green crystals.

Anal. Calcd for $C_{20}H_{30}N_2O_2I_2W_2$: C, 25.21; H, 3.15; N, 2.94. Found: C, 25.29; H, 3.21; N, 2.86. IR (Nujol mull) ν_{NO} 1597 (s) cm^{-1} . 1H NMR (C_6D_6) δ 1.98 (s). $^{13}C\{^1H\}$ NMR (C_6D_6) δ 118.68, 114.84, 12.48, 11.57. Low resolution mass spectrum (probe temperature 120°C) m/z 952 (P^+).

Results and Discussion

Molybdenum Complexes

Cyclic Voltammetry Studies. The electrochemical behavior of all the $\text{Cp}'\text{Mo}(\text{NO})\text{X}_2$ compounds ($\text{Cp}' = \text{Cp}$ or Cp^*) are similar. [Data for the reductions of these compounds are summarized in Table 2.1.]²⁰ All of these complexes undergo very facile one-electron reductions in CH_2Cl_2 , representable by the general equation shown below,



In general, the pentamethylcyclopentadienyl (Cp^*) compounds are more difficult to reduce (by ~ 0.2 V) than their perhydro analogues, consistent with the expected increase in electron density at the metal center.¹⁹ The electrochemical behavior of a representative example is now discussed in detail.

A cyclic voltammogram of $\text{CpMo}(\text{NO})\text{I}_2$ in CH_2Cl_2 is shown in Figure 2.2. This compound exhibits a reversible one-electron reduction at $\underline{E}^{\circ'} = -0.04$ V vs SCE. At a scan rate (ν) of 0.12 V s^{-1} , the separation in peak potentials ($\Delta \underline{E}$) is 65 mV, and the anodic to cathodic peak current ratio ($i_{p,a}/i_{p,c}$)¹³ is 0.93. The $i_{p,a}/i_{p,c}$ value increases with a rise in scan rate from 0.93 at 0.12 V s^{-1} to 0.99 at 0.24 V s^{-1} . Furthermore, a linear plot of $i_{p,c}$ vs $\nu^{1/2}$ is obtained over the scan-rate range available.¹⁴ In addition, the peak potentials do

Table 2.1. Data for the Reduction of Dihalo Complexes of Molybdenum.^a

Compound	Scan Rate (v, V s ⁻¹)	$E^{o'}$ ^b (V)	ΔE^c (mV)	$i_{p,a}/i_{p,c}$	Comments
CpMo(NO)Cl ₂	0.06	-0.10	65	0.85	
	0.13	-0.10	71	0.92	
Cp [*] Mo(NO)Cl ₂	0.06	-0.35	73	1.00	
	0.25	-0.35	89	1.00	
CpMo(NO)Br ₂	0.09	-0.05	67	0.86	second weak wave at $E_{p,c} = -1.73$ V (0.51 V s ⁻¹)
	0.21	-0.05	89	0.91	
CpMo(NO)Br ₂ ^e	0.14	-0.12	72	0.94	second weak wave at $E_{p,c} = -1.72$ V (0.51 V s ⁻¹)
Cp [*] Mo(NO)Br ₂	0.06	-0.29	69	0.90	
	0.24	-0.29	80	1.00	
CpMo(NO)I ₂	0.12	-0.04	65	0.93	second weak wave at $E_{p,c} = -1.60$ V (0.44 V s ⁻¹)
	0.24	-0.04	68	0.99	
CpMo(NO)I ₂ ^e	0.24	-0.13	80	0.98	second weak wave at $E_{p,c} = -1.61$ V
CpMo(NO)I ₂ ^f	0.07	-0.21	64	0.90	smaller waves at -1.01 and -1.78 V (0.13 V s ⁻¹)

continued...

Table 2.1 (continued)

$\text{Cp}^*\text{Mo}(\text{NO})\text{I}_2$	0.05	-0.25	57	0.98	second wave at $E_{p,c} = -1.79 \text{ V}$ (0.55 V s^{-1})
$\text{CpMo}(\text{NO})\text{I}_2(\text{PMePh}_2)$	0.12	-0.98	60	0.90	

^a In CH_2Cl_2 containing 0.1 M $[\text{n-Bu}_4\text{N}]\text{PF}_6$, at a Pt-bead electrode, unless otherwise stated. Potentials are measured vs SCE. ^b Defined as the average of cathodic and anodic peak potentials. ^c Defined as the difference between anodic and cathodic peak potentials, i.e. $|E_{p,a} - E_{p,c}|$ in mV. ^d Ratio of anodic peak current to cathodic peak current.¹³ ^e in THF. ^f in CH_3CN .

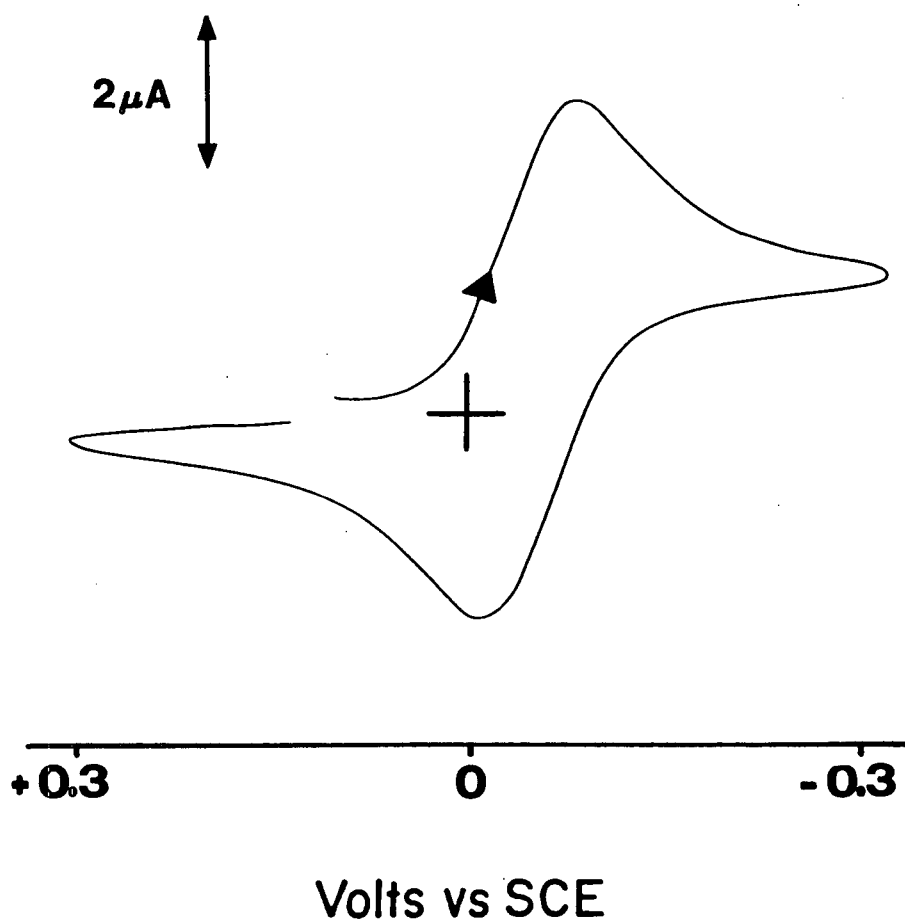
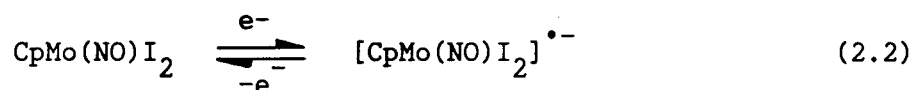
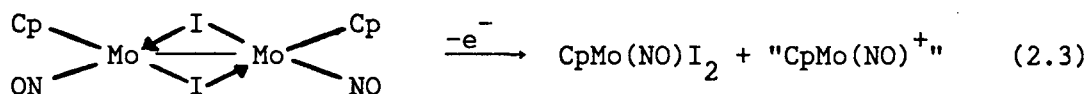


Figure 2.2. Ambient temperature cyclic voltammogram of $\text{CpMo}(\text{NO})\text{I}_2$ in CH_2Cl_2 containing 0.1 M $[\text{n-Bu}_4\text{N}]\text{PF}_6$ measured at a platinum-bead electrode at a scan rate of 0.24 V s^{-1} .

separate somewhat with increasing scan rate, being 65 mV at 0.12 V s^{-1} and 68 mV at 0.24 V s^{-1} . Bulk electrolysis of a THF solution of this compound consumes 1 faraday per mole of monomeric $\text{CpMo}(\text{NO})\text{I}_2$. All the above data are consistent with the one-electron stoichiometry of the reduction of the 16-electron $\text{CpMo}(\text{NO})\text{I}_2$ to its 17-electron radical anion, i.e.



As shown in Figure 2.3, if the scan is extended to the solvent limit ($\sim -2 \text{ V}$), a second wave is evident at $E_{p,c} = -1.60 \text{ V}$ (0.44 V s^{-1}) which gives rise to corresponding anodic peaks (at $+0.46 \text{ V}$ and $+0.69 \text{ V}$) due to the release of I^- in solution.²¹ This second reduction wave is assigned to the formation of $[\text{CpMo}(\text{NO})\text{I}]_2$, which arises from the decomposition of the $[\text{CpMo}(\text{NO})\text{I}_2]^{\bullet-}$ radical anion.²² This assignment is confirmed by the recording of a cyclic voltammogram of an authentic sample of $[\text{CpMo}(\text{NO})\text{I}]_2$. The latter compound exhibits a single (irreversible) reduction peak at -1.6 V . Interestingly, oxidation of the $[\text{CpMo}(\text{NO})\text{I}]_2$ compound results in the heterolytic cleavage of the $\text{Mo}(\mu\text{-I})_2\text{Mo}$ unit to regenerate $\text{CpMo}(\text{NO})\text{I}_2$ as shown in Equation 2.3.



The cyclic voltammogram indicating this particular transformation is shown in Figure 2.4. Thus, when the anodic scan is reversed after the oxidation peak at $+1.05 \text{ V}$, a reversible redox couple is observed at -0.04 V ($i_{p,a}/i_{p,c} = 0.90$,

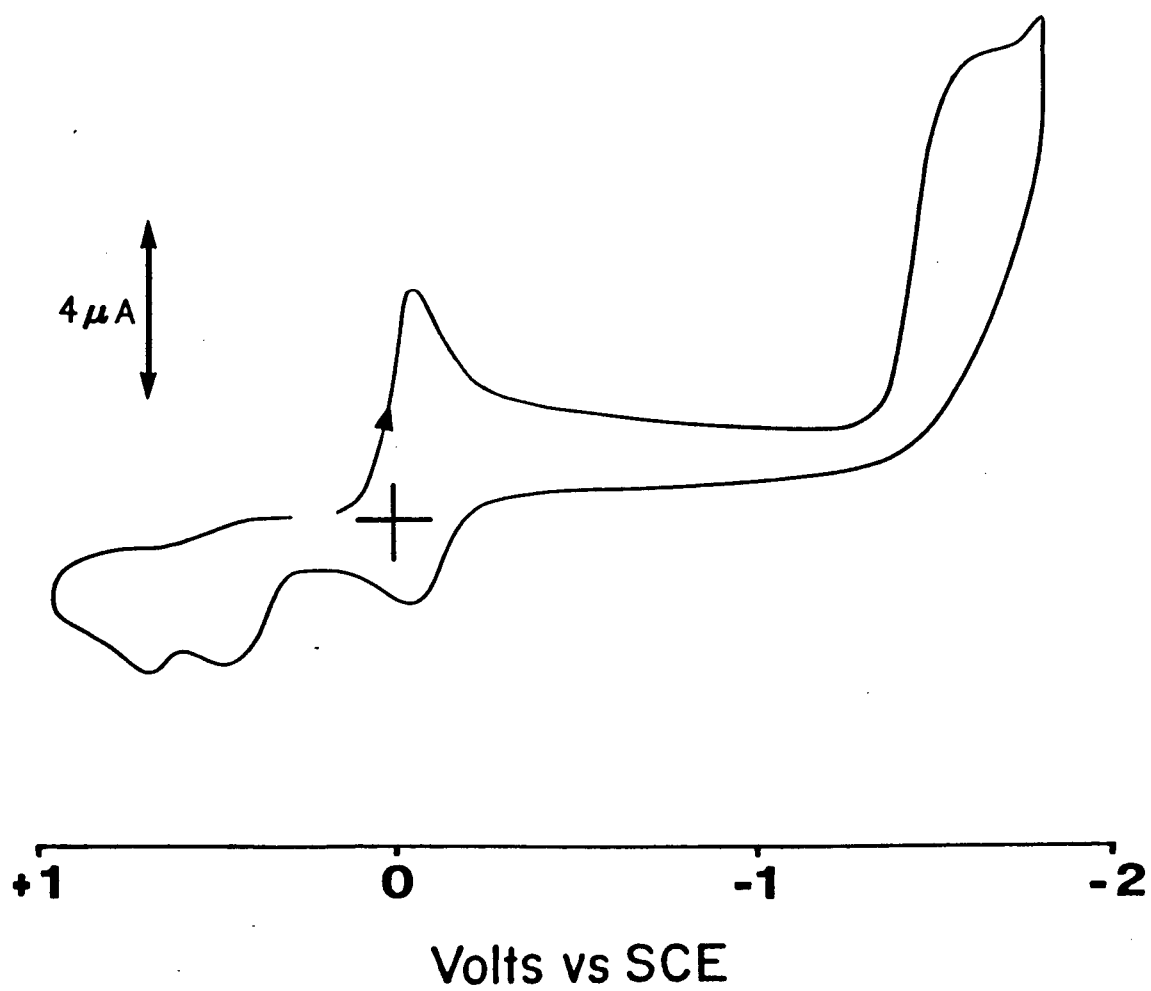


Figure 2.3. Cyclic voltammogram of $\text{CpMo}(\text{NO})\text{I}_2$ in CH_2Cl_2 at a scan rate of 0.44 V s^{-1} .

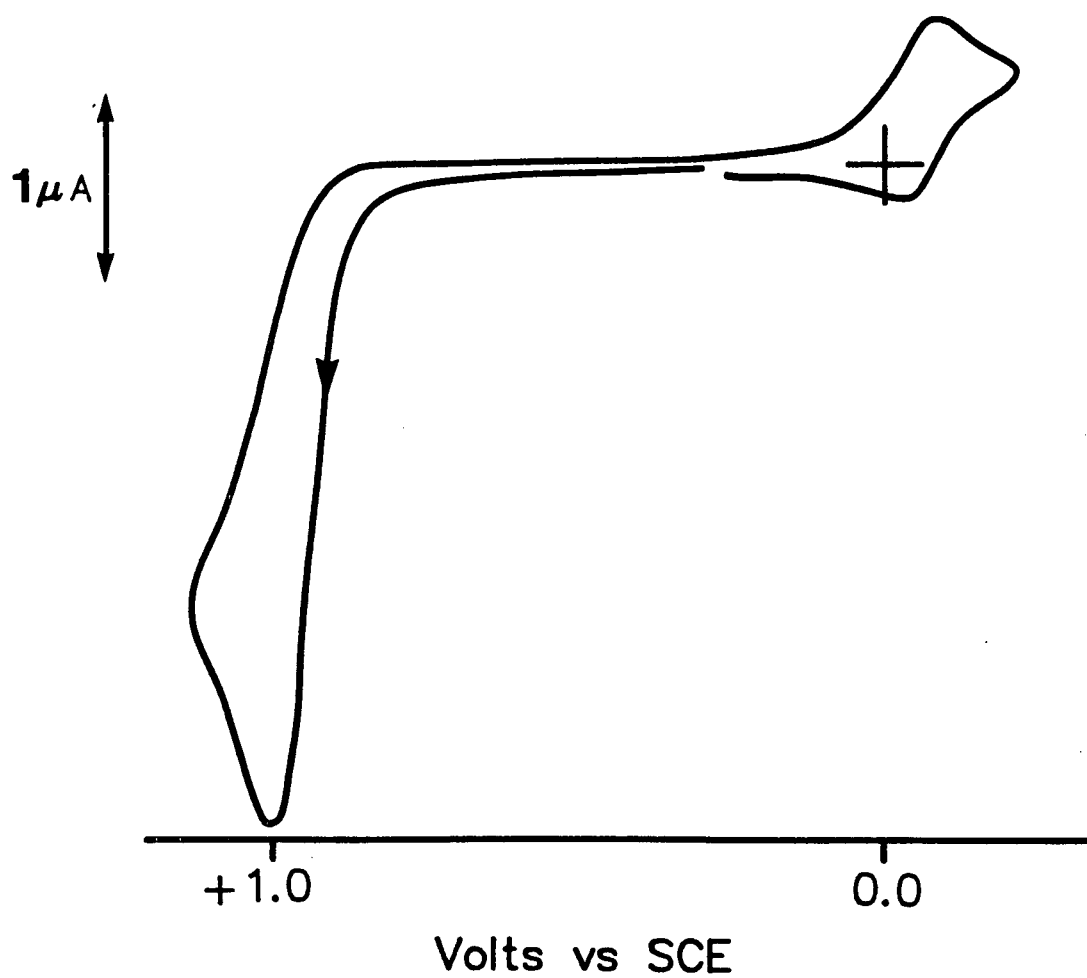
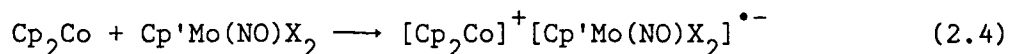


Figure 2.4. Cyclic voltammogram of $[\text{CpMo}(\text{NO})\text{I}]_2$ in CH_2Cl_2 at a scan rate of 0.14 V s^{-1} .

$\Delta E = 70$ mV) which is due to the formation of $\text{CpMo}(\text{NO})\text{I}_2$ (vide supra). The formally 13-electron " $\text{CpMo}(\text{NO})^+$ " byproduct of the reaction probably decomposes in the absence of any trapping ligands.²³

The lower $i_{p,a}/i_{p,c}$ ratios of the redox couples of the $\text{CpMo}(\text{NO})\text{X}_2$ complexes upon reduction at low scan rates, and the observation (for some of these complexes, Table 2.1) of second reduction waves at more negative potentials, is consistent with the slow decomposition of the $[\text{CpMo}(\text{NO})\text{X}_2]^{\bullet-}$ radical anions to their respective $[\text{CpMo}(\text{NO})\text{X}]_2$ monohalo dimers.²⁴

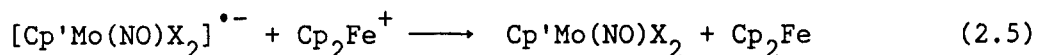
Preparation of the Radical Anion Complexes. Cobaltocene may be used to effect the reductions outlined in Equation 2.1 on a preparative scale.²⁵ When solid Cp_2Co is added to THF solutions of the $\text{Cp}'\text{Mo}(\text{NO})\text{X}_2$ compounds, the 17-electron $[\text{Cp}'\text{Mo}(\text{NO})\text{X}_2]^{\bullet-}$ radical anion complexes precipitate as green to brown solids. The general equation for this reaction is outlined in Equation 2.4.



Isolated in this manner, these radical anion salts are obtained in high yields as analytically pure solids which are very soluble in DMF, slightly soluble in THF, and insoluble in Et_2O . These radical anion salts are air- and moisture-sensitive, especially in solutions. However, as solids, they are stable at -10°C under an atmosphere of N_2 for at least three weeks (for $\text{X} = \text{Cl}$ or Br). The iodo complexes decompose in less than two days even at -20°C .

Not surprisingly, the chemical oxidation of the $[\text{Cp}'\text{Mo}(\text{NO})\text{X}_2]^{\bullet-}$ complexes

by $[\text{Cp}_2\text{Fe}]\text{BF}_4$ ²⁶ in acetonitrile cleanly regenerates the neutral dihalo precursor complexes,²⁷ i.e.



The IR data for the $[\text{Cp}'\text{Mo}(\text{NO})\text{X}_2]^{\bullet-}$ radical anion complexes are listed in Table 2.2, and are compared with those of their dihalo precursors. As may be noted, a decrease in the nitrosyl stretching frequency (ν_{NO}) of $\sim 120 \text{ cm}^{-1}$ is observed upon reduction of the neutral dihalo compounds.²⁸ The ν_{NO} values for the radical anions are, however, indicative of the NO ligands being linear and terminal (i.e. not adopting bent geometries upon reduction of the compounds). A striking observation is that the ν_{NO} 's of the anionic 17-electron $[\text{Cp}'\text{Mo}(\text{NO})\text{X}_2]^{\bullet-}$ complexes are in the same range as those of the neutral 18-electron $\text{CpMo}(\text{NO})\text{L}_2$ compounds (L = phosphine or phosphite).³⁰ For instance, $[\text{Cp}_2\text{Co}]^+[\text{CpMo}(\text{NO})\text{I}_2]^{\bullet-}$ has a ν_{NO} of 1570 cm^{-1} in THF, compared to the ν_{NO} of 1568 cm^{-1} for the $\text{CpMo}(\text{NO})(\text{Ph}_2\text{PCH}_2\text{CH}_2\text{PPh}_2)$ compound in the same solvent.³⁰ The nitrosyl ligand in the latter compound is also distinctly linear. Consequently, it appears that not enough electron density is backdonated to the NO ligands in these $[\text{Cp}'\text{Mo}(\text{NO})\text{X}_2]^{\bullet-}$ complexes to cause them to bend. Interestingly, it has also been computed that the lowest unoccupied molecular orbital (LUMO) of the related 16-electron $\text{CpMo}(\text{NO})\text{Me}_2$ model compound is localized on the metal center and contains no NO 2π character.¹ Therefore, the reduction of the 16-electron $\text{CpMo}(\text{NO})\text{Me}_2$ compound to its 17-electron $[\text{CpMo}(\text{NO})\text{Me}_2]^{\bullet-}$ radical anion is not expected to result in a significant

Table 2.2. A Comparison of the Nitrosyl-Stretching Frequencies of the New 17-electron Radical Anion Complexes with Their Neutral Precursors.^a

Complex	$\nu_{\text{NO}}, \text{ cm}^{-1}$					
	X = Cl		X = Br		X = I	
	Cp' = Cp	Cp' = Cp [*]	Cp' = Cp	Cp' = Cp [*]	Cp' = Cp	Cp' = Cp [*]
Cp'Mo(NO)X ₂	1665	1647	1670 ^b	1649	1670 ^b	1663
[Cp ₂ Co][Cp'Mo(NO)X ₂]	1552	1523	1557	1534	1557	1541

^a as Nujol mulls, unless otherwise stated.

^b as KBr pellets.⁸

bending of the nitrosyl ligand in the radical anion complex. In contrast, the added electron density in $[\text{CpMo}(\text{NO})(\text{CO})_2]^{\bullet-}$ [obtained by electroreduction of the 18-electron $\text{CpMo}(\text{NO})(\text{CO})_2$ precursor] is localized largely in the Mo-NO group, a feature which is believed to result in the concomitant bending of the nitrosyl ligand.³¹ That the added electron density in the $[\text{Cp}'\text{Mo}(\text{NO})\text{X}_2]^{\bullet-}$ complexes is not localized on their Mo-NO groups is clearly evident in their ESR spectra which exhibit no ^{14}N hyperfine coupling. The ESR data for all the molybdenum radical anion complexes synthesized in this study are listed in Table 2.3.

The ESR spectra obtained for the dichloro and diiodo radical anion complexes are similar, each consisting of a single, strong central resonance flanked by molybdenum satellite signals. The ESR spectrum of $[\text{Cp}_2\text{Co}][\text{CpMo}(\text{NO})\text{Cl}_2]$ is shown as a representative example in Figure 2.5. A strong central resonance ($g = 1.9819$) with five broad satellite signals due to ^{95}Mo and ^{97}Mo hyperfine coupling ($I = 5/2$, nat. abund. 15.9% and 9.6% respectively) is observed.³² No ^{14}N or ^1H hyperfine coupling is evident in this spectrum, and this is so for the spectra of all the complexes. However, in sharp contrast to the ESR spectra for the dichloro (and diiodo) radical anion complexes, those for the dibromo analogues exhibit halide hyperfine interactions. For example, the ESR spectrum of $[\text{Cp}_2\text{Co}][\text{Cp}^*\text{Mo}(\text{NO})\text{Br}_2]$, shown in Figure 2.6, consists of a 7-line central pattern due to coupling of the unpaired electron to two Br nuclei ($I = 3/2$; ^{79}Br , 50.54% nat. abund.; ^{81}Br , 49.46% nat. abund.) ($a_{\text{Br}} = 10.4 \text{ G}$).³³ The spectrum of the perhydro analogue, $[\text{Cp}_2\text{Co}][\text{CpMo}(\text{NO})\text{Br}_2]$, also displays a pattern similar to that shown in Figure

Table 2.3. Electron Spin Resonance Data for the $[\text{Cp}_2\text{Co}][\text{Cp}^*\text{Mo}(\text{NO})\text{X}_2]$ Radical Anion Complexes.^a

Complex	$[\text{CpMo}(\text{NO})\text{Cl}_2]^{\bullet-}$	$[\text{Cp}^*\text{Mo}(\text{NO})\text{Cl}_2]^{\bullet-}$	$[\text{CpMo}(\text{NO})\text{Br}_2]^{\bullet-}$
g-value	1.9819	1.9840	2.0103
Temp(°C)	14.5	22.6	22.7

Complex	$[\text{Cp}^*\text{Mo}(\text{NO})\text{Br}_2]^{\bullet-}$	$[\text{CpMo}(\text{NO})\text{I}_2]^{\bullet-}$	$[\text{Cp}^*\text{Mo}(\text{NO})\text{I}_2]^{\bullet-}$
g-value	2.0092	2.0596	2.0582
Temp(°C)	22.8	18.5	19.9

^a As DMF solutions, except for the iodo complexes which were examined as THF solutions.

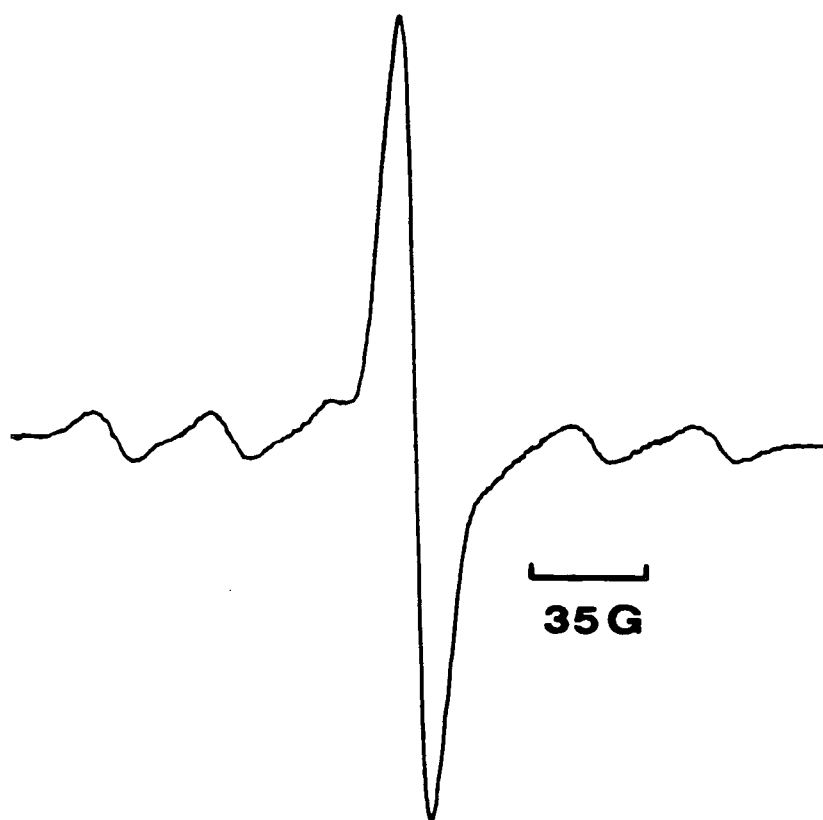


Figure 2.5. The ESR spectrum of $[\text{Cp}_2\text{Co}][\text{CpMo}(\text{NO})\text{Cl}_2]$ in DMF.

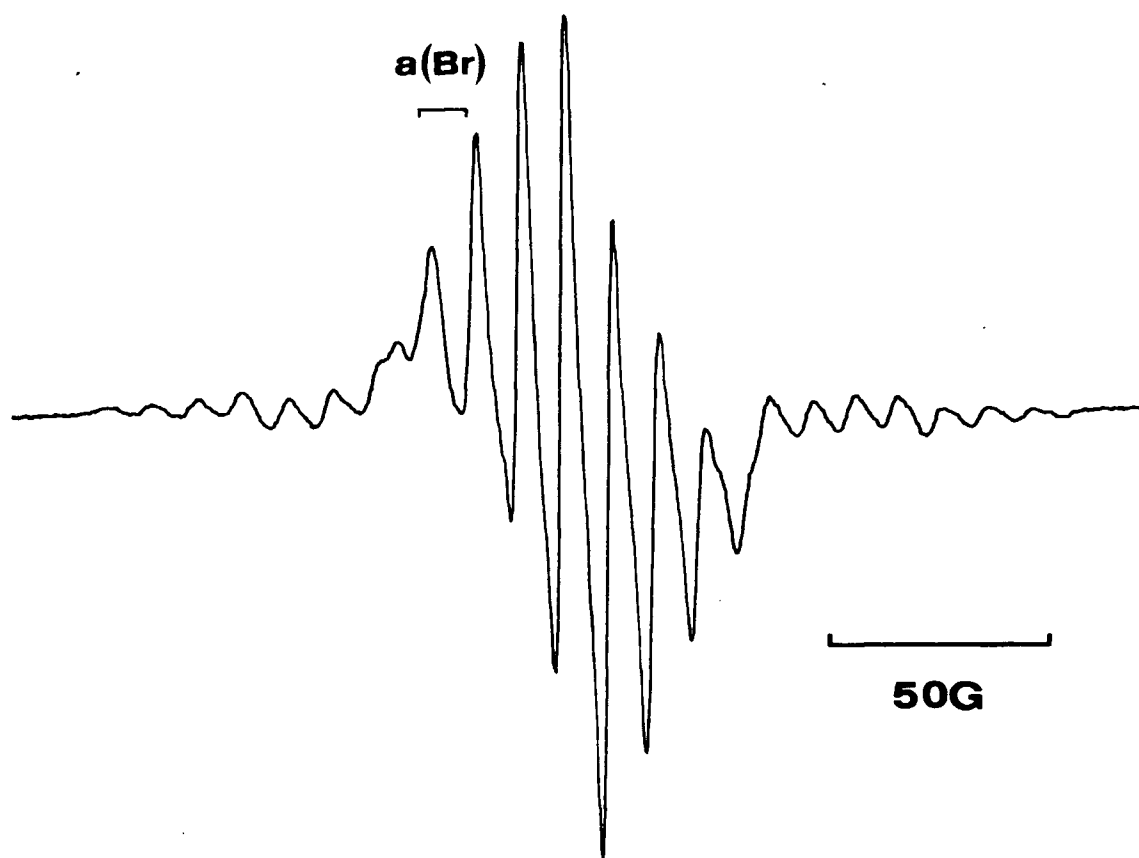
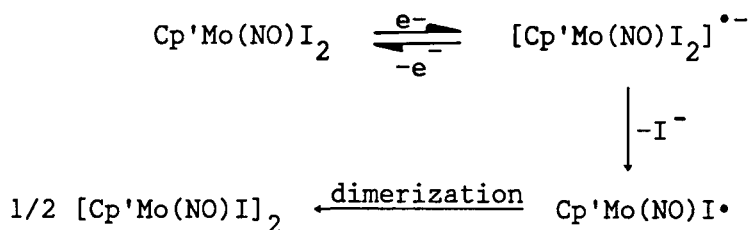


Figure 2.6. The ESR spectrum of $[\text{Cp}_2\text{Co}][\text{Cp}^*\text{Mo}(\text{NO})\text{Br}_2]$ in DMF.

2.6. Like the dichloro radical anion complexes, these dibromo analogues are stable in DMF solution for at least 3 h at room temperature. In contrast, the diiodo radical anions are relatively unstable in DMF. For example, the initial spectrum of $[\text{Cp}^*\text{Mo}(\text{NO})\text{I}_2]^{\bullet-}$ as the cobalticinium salt in DMF displays a strong central resonance ($g = 2.0142$) and an identical Mo isotope pattern as in Figure 2.5. This central signal gradually gives way to a new broad signal (at $g = 2.064$) attributed to the neutral $\text{Cp}^*\text{Mo}(\text{NO})\text{I}^\bullet$ radical, formed by I^- loss from the radical anion.³⁴ This latter feature is in agreement with the cyclic voltammetric results discussed earlier. Therefore, the processes outlined in Scheme 2.2 plausibly account for the formation of $[\text{Cp}'\text{Mo}(\text{NO})\text{I}]_2$ from their diiodo precursors upon reduction.



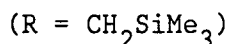
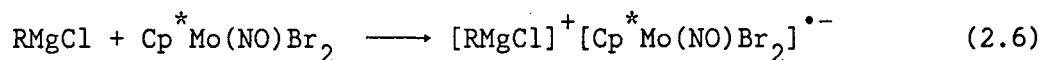
Scheme 2.2

Consistent with Scheme 2.2 is the observation that attempts to grow crystals of $[\text{Cp}_2\text{Co}][\text{CpMo}(\text{NO})\text{I}_2]$ only result in the formation of $[\text{CpMo}(\text{NO})\text{I}]_2$. It is probable, therefore, that the analogous dichloro and dibromo radical anion complexes eventually undergo similar decomposition to their monohalo dimers, albeit at much slower rates.³⁵

Direct Evidence for the Involvement of Single Electron Transfer (SET)

During the Reactions of Grignard Reagents with the Cp'Mo(NO)X₂ Complexes.

Implications for the Improved Syntheses of the Cp'Mo(NO)R₂ Compounds. The ESR spectrum of an equimolar mixture of Me₃SiCH₂MgCl and Cp^{*}Mo(NO)Br₂ in DMF is shown in Figure 2.7. This spectrum is qualitatively identical to that of [Cp₂Co][Cp^{*}Mo(NO)Br₂] (Figure 2.6) and provides evidence for the occurrence of SET from the Grignard reagent to the dibromo complex,^{36,39} i.e.



Although Grignard reagents are known to function as SET agents to organic compounds such as ketones⁴⁰ and to organic groups bound to transition metals,⁴¹ very little is presently known about the nature of their reactions with organometallic halo compounds. Thus, the formation of the [Cp^{*}Mo(NO)Br₂]^{•-} radical anion in reaction 2.6 is of fundamental significance. Presumably, the very low potentials required for the reductions of the Cp'Mo(NO)X₂ compounds facilitate SET from the Grignard reagents to these complexes. It is reasonable, therefore, to assume that if the dihalo radical anions are indeed intermediates in the reactions of the Cp'Mo(NO)X₂ compounds with Grignard reagents to generate ultimately the Cp'Mo(NO)R₂ complexes, then a sufficient lifetime for these radical anions is necessary to allow halide-alkyl metathesis (i.e. R for X) to occur to yield the final alkyl complexes. If this is not so, then rapid decomposition of these [Cp'Mo(NO)X₂]^{•-} radical anions may then lead

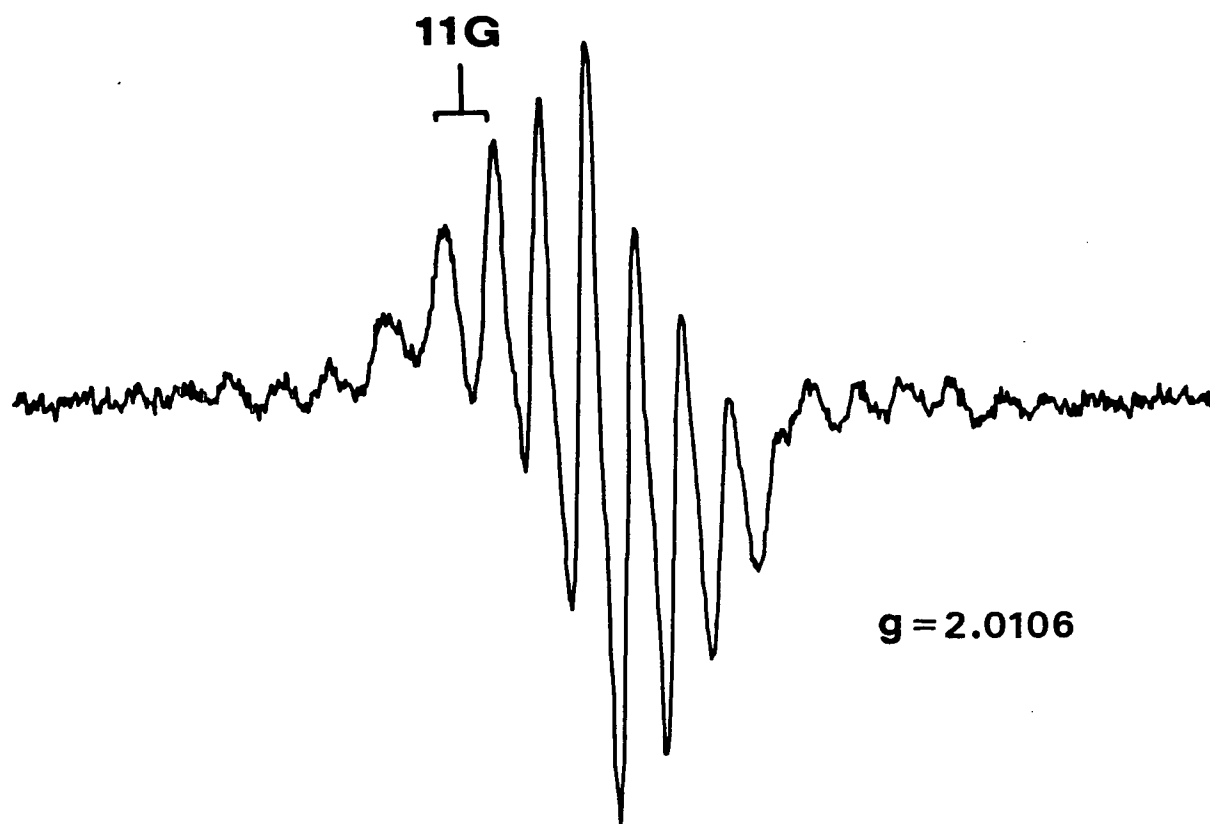
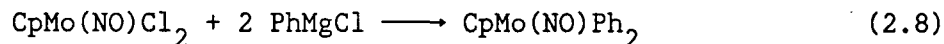
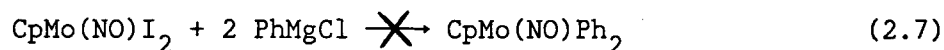
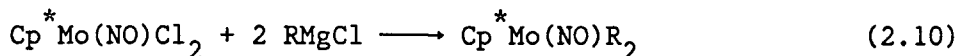
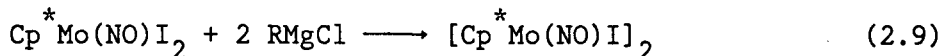


Figure 2.7. The ESR spectrum of a DMF solution of an equimolar mixture of $\text{Me}_3\text{SiCH}_2\text{MgCl}$ and $\text{Cp}^*\text{Mo}(\text{NO})\text{Br}_2$ mixture at 20°C .

only to the formation of the monohalo dimers (vide supra). Since the order of stability of the radical anions [both in solutions (by ESR) and in the solid state (by IR)] is in the order $\text{Cl} > \text{Br} \gg \text{I}$, it seems logical, then, that the highest yields (and perhaps the 'cleanest' formation reactions) of the $\text{Cp}'\text{Mo}(\text{NO})\text{R}_2$ complexes from this synthetic route should be obtained when the dichloro precursors are used. Indeed, many previously unobtainable $\text{Cp}'\text{Mo}(\text{NO})\text{R}_2$ compounds ($\text{R} = \text{alkyl or aryl}$) are now synthesizable cleanly by this route. For example,



Also, it is now understandable why attempts to synthesize the $\text{Cp}^*\text{Mo}(\text{NO})\text{R}_2$ complexes from $\text{Cp}^*\text{Mo}(\text{NO})\text{I}_2$ and RMgCl ($\text{R} = \text{alkyl}$) only lead to the formation of $[\text{Cp}^*\text{Mo}(\text{NO})\text{I}]_2$ in high yields,⁴ i.e.



To summarize, it therefore appears that a sufficiently stable $[\text{Cp}'\text{Mo}(\text{NO})\text{X}_2]^{\bullet-}$ complex is desirable for the overall halide-alkyl (or aryl)

metathesis reaction. Nevertheless, a more detailed systematic study needs to be done to unravel the individual steps that lead finally to dialkylation (or arylation). It should be noted, however, that although we have not been able to achieve monoalkylation from the dihalo precursors with the RMgX (or RLi) reagents, the monoalkylated complex $[\text{CpMo}(\text{NO})\text{Br}(\text{Me})]_2$ ⁴² is obtainable by employing the less nucleophilic trimethylaluminum as the alkylating agent on the dibromo precursor.⁴³ This procedure may well circumvent the initial formation of the molybdenum containing radical anion as outlined in equations 2.1 and 2.6.⁴⁴

Tungsten Complexes

The $\text{Cp}'\text{W}(\text{NO})\text{I}_2$ Complexes. In the previous section, the electrochemistry of the $\text{Cp}'\text{Mo}(\text{NO})\text{I}_2$ complexes was discussed. As noted earlier, both complexes ($\text{Cp}' = \text{Cp}$ or Cp^*) exhibit similar reduction behavior in CH_2Cl_2 solution, undergoing facile reversible reductions. Unlike the molybdenum analogues, however, the $\text{Cp}'\text{W}(\text{NO})\text{I}_2$ complexes exhibit somewhat different electrochemical behavior when Cp is replaced by Cp^* . The cyclic voltammograms of these complexes will now be discussed in some detail.

Cyclic voltammograms of $\text{CpW}(\text{NO})\text{I}_2$ in CH_2Cl_2 are shown in Figure 2.8. This compound undergoes an irreversible reduction at $E_{\text{p,c}} = -0.35 \text{ V}$ and a somewhat reversible reduction at $E^{\text{O}'} = -0.64 \text{ V}$ ($\Delta E = 88 \text{ mV}$). The first reduction, however, remains irreversible even at higher scan rates up to 15 V s^{-1} . The observed anodic peaks at positive potentials (in Figure 2.8b) are due to the release of I^- in solution (vide supra)²¹ and are notably absent when the anodic scan is performed first (Figure 2.8a). These peaks due to the I^-/I_3^- system

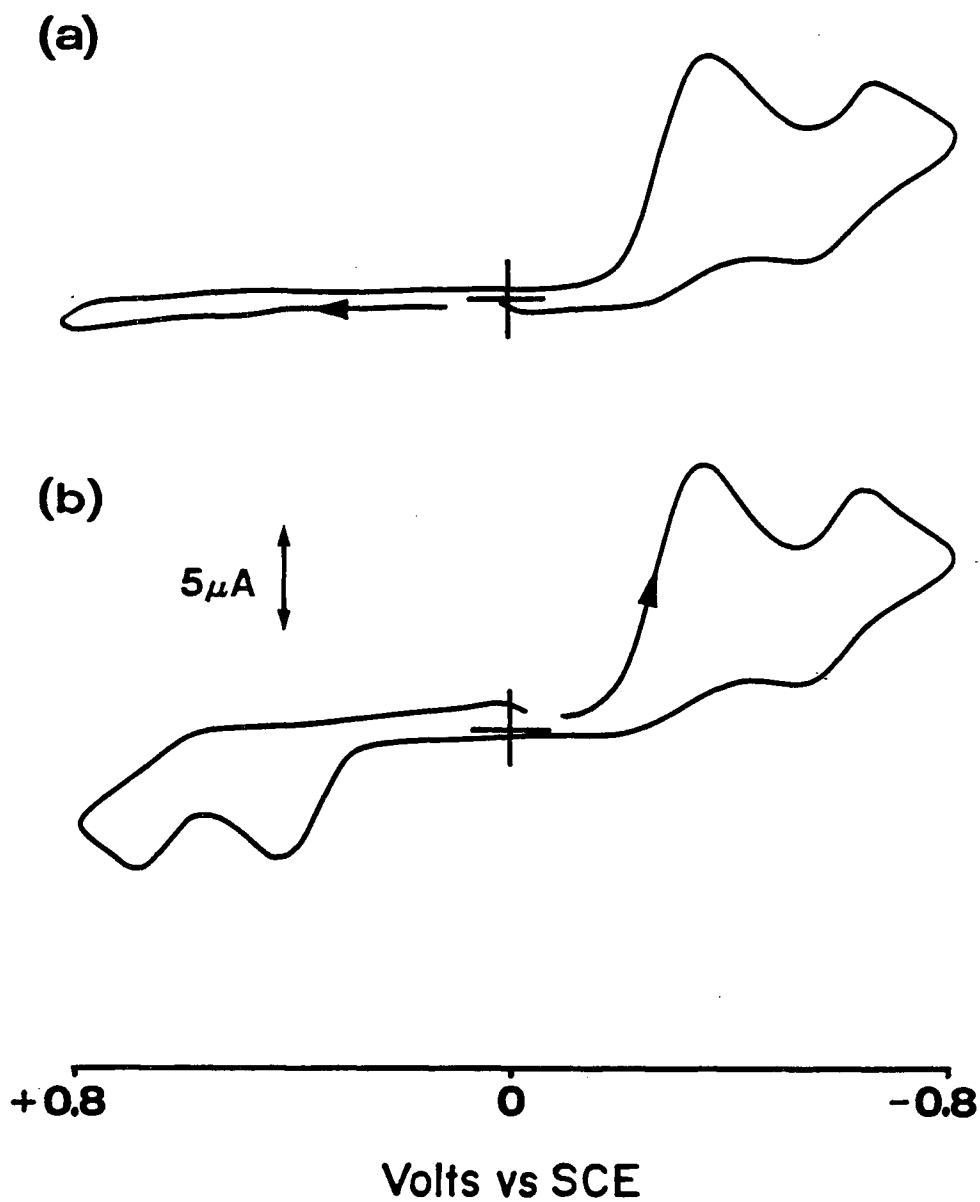
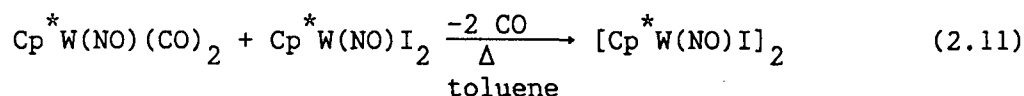


Figure 2.8. Cyclic voltammograms of CpW(NO)I_2 in CH_2Cl_2 at a scan rate of 0.32 V s^{-1} . (a) scanning positive potentials first, and (b) scanning negative potentials first.

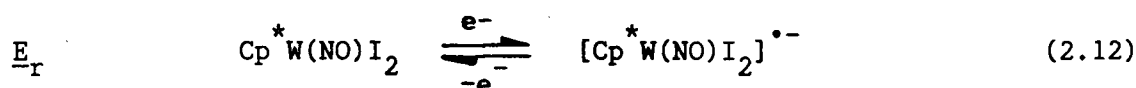
are similarly observed if only the first reduction wave is passed.

Cyclic voltammograms of the permethylated analogue, $\text{Cp}^*\text{W}(\text{NO})\text{I}_2$, in CH_2Cl_2 are shown in Figure 2.9. In contrast to the $\text{CpW}(\text{NO})\text{I}_2$ compound, the first reduction of this complex is largely reversible and occurs at $\underline{E}^{0'} = -0.52$ V. The magnitude of the return anodic current ($i_{p,a}$) for this couple is enhanced at higher scan rates (Figure 2.9a). Furthermore, the intensity of the wave for the second redox couple at $\underline{E}^{0'} = -1.06$ V is more pronounced at lower scan rates (Figure 2.9c) and is enhanced by the addition of an authentic sample of $[\text{Cp}^*\text{W}(\text{NO})\text{I}]_2$. This latter compound can be synthesized independently as outlined in Equation 2.11.⁴⁵



It is thus concluded that $[\text{Cp}^*\text{W}(\text{NO})\text{I}]_2$ is being generated electrochemically by the reduction of the diiodo precursor. This parallels the behavior of the molybdenum complexes presented earlier, although in the tungsten cases the moniodo dimers are reversibly reduced, presumably to their $[\text{Cp}^*\text{W}(\text{NO})\text{I}]_2^{\bullet-}$ bimetallic radical anions.

Electrochemically, therefore, the overall process to generate $[\text{Cp}^*\text{W}(\text{NO})\text{I}]_2$ may be classified as a reversible electron transfer (\underline{E}_r) followed by an irreversible chemical reaction (\underline{C}_1).⁴⁶



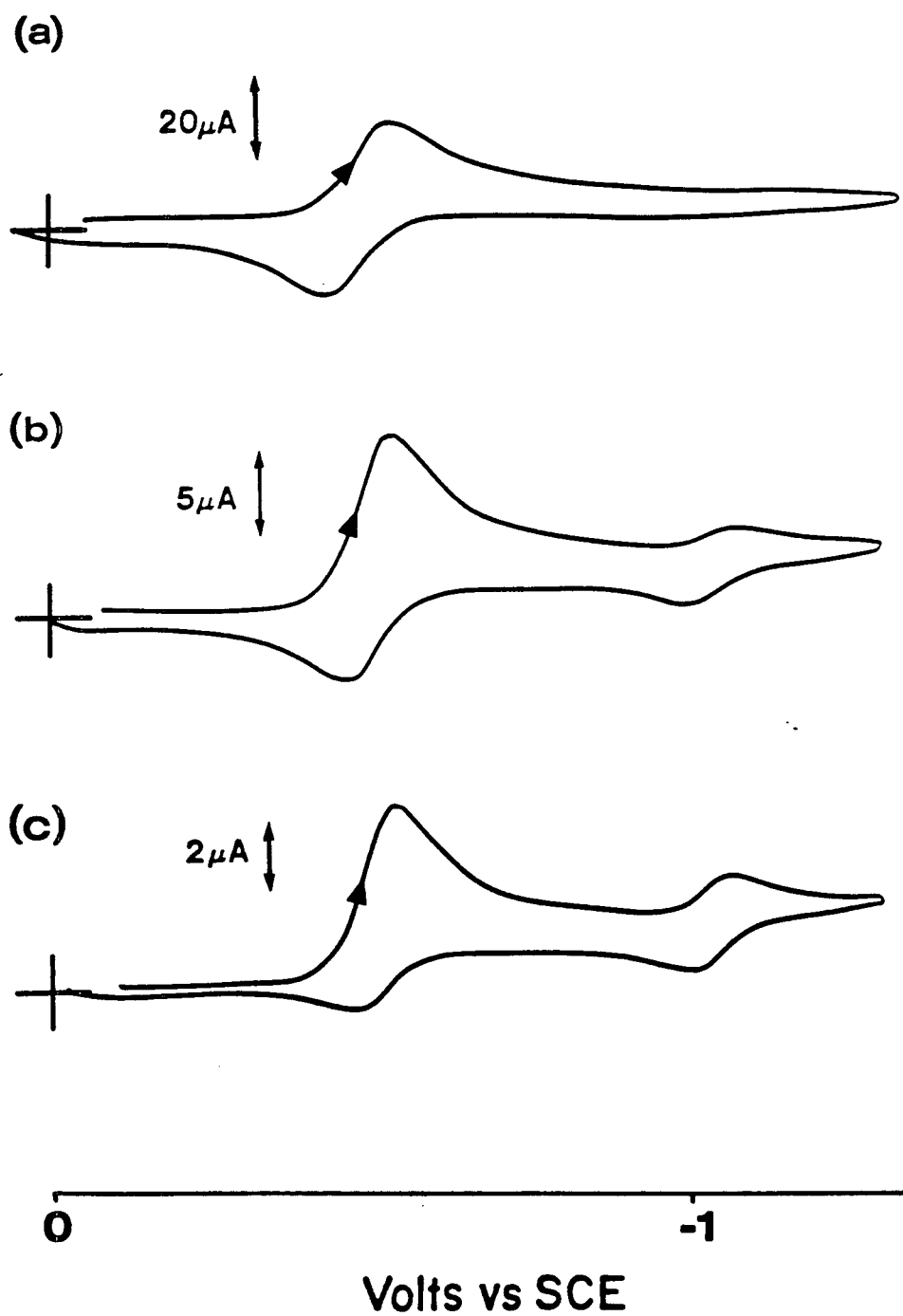
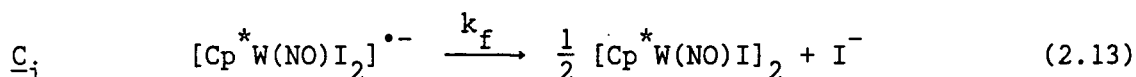


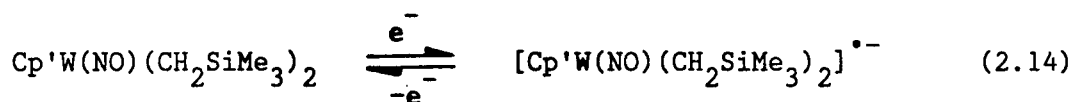
Figure 2.9. Cyclic voltammograms of $\text{Cp}^*\text{W}(\text{NO})\text{I}_2$ in CH_2Cl_2 at different scan rates (a) 2.64 V s^{-1} (b) at 0.53 V s^{-1} and (c) at 0.13 V s^{-1} .



The $i_{p,a}/i_{p,c}$ dependence on scan rate (v) for the \underline{E}_r step (Equation 2.12) is shown in Figure 2.10, and the observed trend of higher $i_{p,a}/i_{p,c}$ values (increased chemical reversibility) at higher scan rates is consistent with the proposed $\underline{E}_r \underline{C}_i$ mechanism.^{46,47} This variation of $i_{p,a}/i_{p,c}$ for the electroreduction (\underline{E}_r) as a function of scan rate (v) may then be used to estimate the rate constant (k_f in s^{-1}) for the coupled chemical reaction (\underline{C}_i) by employing the method of Nicholson and Shain.⁴⁷ The results are collected in Table 2.4.

As might have been expected, the stability of the electrogenerated $[\text{Cp}^* \text{W}(\text{NO}) \text{I}_2]^{\bullet -}$ radical anion is markedly enhanced by lower temperatures (Figure 2.11).⁴⁸ For instance, the redox couple (for the first reduction) in THF at $\underline{E}^{0'} = -0.49 \text{ V}$ (at 0.07 V s^{-1}) has an $i_{p,a}/i_{p,c}$ value of 0.74 at -30°C , whereas at 0°C it is only 0.46. It is thus conceivable that the $[\text{Cp}^* \text{W}(\text{NO}) \text{I}_2]^{\bullet -}$ complex may well be chemically accessible at lower temperatures. This hypothesis has not, however, been tested experimentally.

The Tungsten $\text{Cp}^* \text{W}(\text{NO}) (\text{CH}_2\text{SiMe}_3)_2$ Dialkyl Complexes. Cyclic voltammetry of the tungsten dialkyl compounds reveals that they are reduced reversibly, i.e.



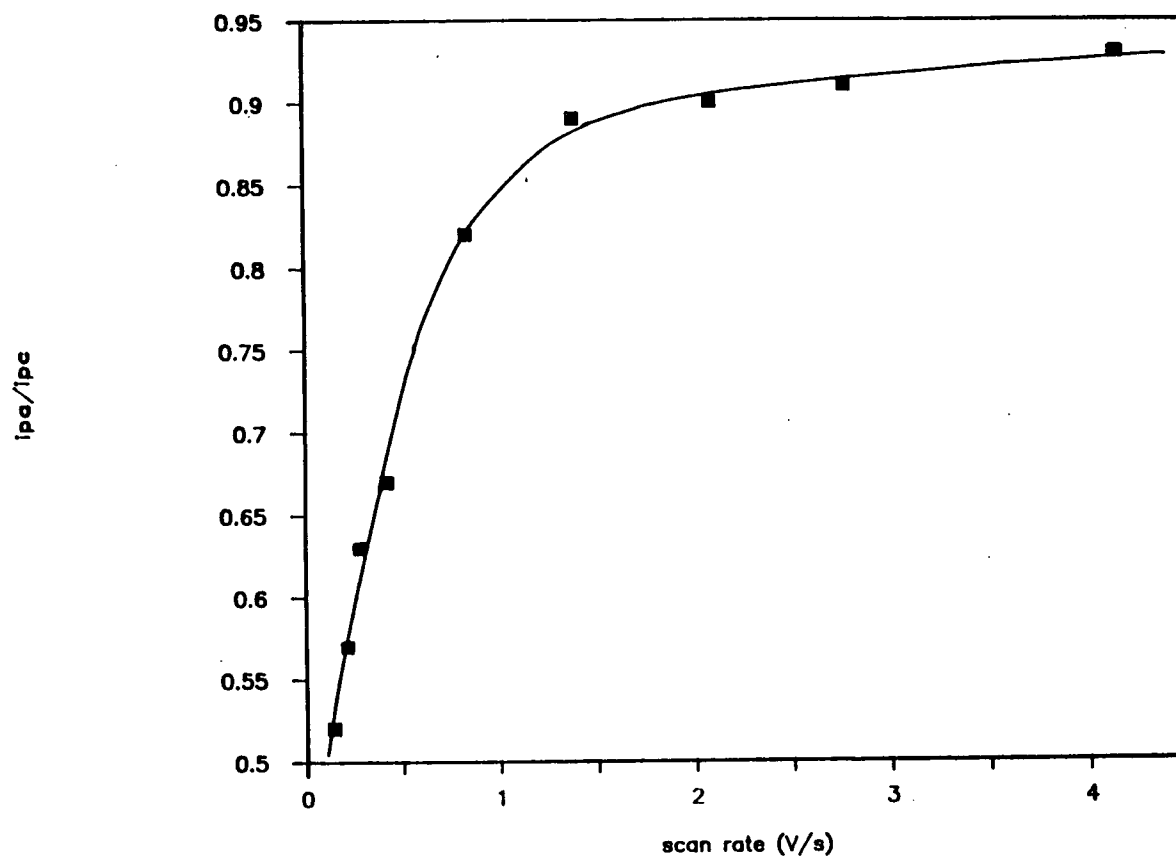


Figure 2.10. Plot of $i_{p,a}/i_{p,c}$ vs scan rate for the first reversible redox couple of $\text{Cp}^*\text{W}(\text{NO})\text{I}_2$ in CH_2Cl_2 .

Table 2.4. Electrochemical Data for the Electroreduction of $\text{Cp}^*\text{W}(\text{NO})\text{I}_2$ in CH_2Cl_2 for a Variety of Scan Rates.^a

Scan Rate (v , V s^{-1})	$E^{o'}$ (V)	Current ($i_{p,c}$) (μA)	ΔE (mV)	$i_{p,a}/i_{p,c}$	k_f^b
0.14	-0.52	5.52	58	0.52	0.94
0.21	-0.52	6.57	59	0.57	1.13
0.28	-0.52	7.58	64	0.63	1.16
0.42	-0.52	9.42	66	0.67	1.46
0.83	-0.52	12.8	68	0.82	1.25
1.38	-0.52	16.7	78	0.89	1.32

^a Various symbols used are defined in the Experimental Section.

^b Rate of irreversible chemical reaction (C_i) following the reversible electron transfer (E_r). Estimated from $i_{p,a}/i_{p,c}$ using the method of Nicholson and Shain,⁴⁷ assuming a simple first-order reaction.

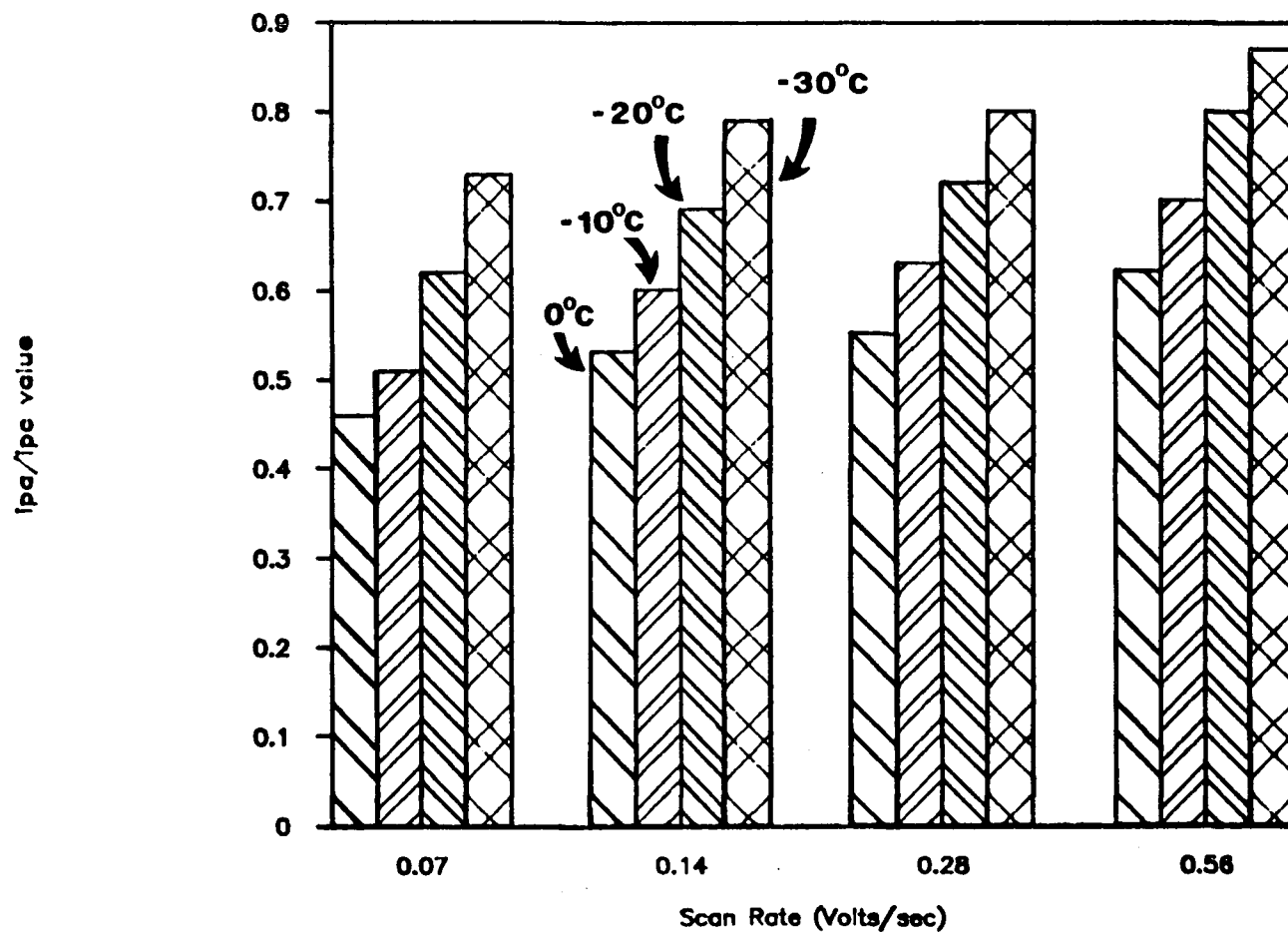


Figure 2.11. Temperature dependence of $i_{p,a}/i_{p,c}$ values as a function of scan rate for the first reversible redox couple of $\text{Cp}^*\text{W}(\text{NO})\text{I}_2$ in THF.

For $\text{Cp}' = \text{Cp}$, the reversible redox couple occurs (in CH_2Cl_2) at $\underline{E}^{\text{O}'} = -1.51 \text{ V}$ (0.15 V s^{-1} , $\Delta E = 90 \text{ mV}$, $i_{\text{p,a}}/i_{\text{p,c}} = 0.97$) and for $\text{Cp}' = \text{Cp}^*$ this wave occurs at $\underline{E}^{\text{O}'} = -1.64 \text{ V}$ (0.19 V s^{-1} , $i_{\text{p,a}}/i_{\text{p,c}} = 0.90$). The cathodic shift in the $\underline{E}^{\text{O}'}$ value in moving from Cp to Cp^* is consistent with the increased electron density on the metal center due to the greater electron donating capability of the permethylated ring. These dialkyl complexes are significantly more difficult to reduce than their dialkyl precursors, and this is not expected since alkyl ligands are sufficiently better donor ligands than are halides.⁴⁹ Unfortunately, attempts to isolate these $[\text{Cp}'\text{W}(\text{NO})\text{R}_2]^{\bullet-}$ radical anions have so far been unsuccessful.^{50,51} For example, no reaction occurs between $\text{CpW}(\text{NO})(\text{CH}_2\text{SiMe}_3)_2$ and Cp_2Co in Et_2O at room temperature over a 3 h period. This is not too surprising since Cp_2Co ($\underline{E}^{\text{O}'} = -0.82 \text{ V}$, vide supra) may not be a suitable reducing agent for the reduction of the dialkyl compounds ($\underline{E}^{\text{O}'} = -1.61 \text{ V}$). Regrettably, employing the more potent reducing agent, $\text{CpFe}(\eta^6\text{-C}_6\text{Me}_6)$ ($\underline{E}_{1/2} = -1.78 \text{ V}$)^{19a} for the reduction of the dialkyl compound only results in the production of an intractable tar.

Summary

All the $\text{CpMo}(\text{NO})\text{X}_2$ complexes undergo one-electron reversible reductions at $0 > \underline{E}^{\text{O}'} \geq -0.1 \text{ V}$ vs SCE in dichloromethane solution. Their Cp^* analogues are more difficult to reduce (by $\sim 0.2 \text{ V}$), reflecting the greater electron-donating capability of the Cp^* ligand. Furthermore, the W complexes are more difficult to reduce (by $\sim 0.3 \text{ V}$) than their Mo congeners. The radical anion complexes of the form $[\text{Cp}'\text{Mo}(\text{NO})\text{X}_2]^{\bullet-}$ can be isolated as their cobalticinium salts. ESR

measurements on solutions of these radical anions show the unpaired electron to be coupled only to the molybdenum center, or also to the halide (for $X = \text{Br}$).

In the case of tungsten, the $[\text{Cp}^* \text{W}(\text{NO})\text{I}_2]^{\bullet -}$ complex, generated electrochemically, is unstable and rapidly decomposes to $[\text{Cp}^* \text{W}(\text{NO})\text{I}]_2$, which has also been synthesized independently.

This study has shown that the successful accomplishment of the $\text{Cp}'\text{Mo}(\text{NO})\text{X}_2 \longrightarrow \text{Cp}'\text{Mo}(\text{NO})\text{R}_2$ metathesis reaction can be predicted by understanding the electrochemical behavior of the precursor $\text{Cp}'\text{Mo}(\text{NO})\text{X}_2$ compounds. As a result of this work, several new $\text{Cp}'\text{Mo}(\text{NO})(\text{alkyl})_2$ compounds have been made. Also, the previously unknown $\text{Cp}'\text{M}(\text{NO})(\text{aryl})_2$ compounds have now been successfully synthesized in our laboratories by employing the dichloro precursor complexes (and not the diiodo compounds) for the metathesis reaction. The work presented in this Chapter (and the predictions derived from it) is invaluable to our research group since a large portion of our research deals with studies involving the $\text{Cp}'\text{M}(\text{NO})\text{R}_2$ compounds or complexes derived from them.

References and Notes

1. Legzdins, P.; Rettig, S. J.; Sánchez, L.; Bursten, B. E.; Gatter, M. G. *J. Am. Chem. Soc.* **1985**, *107*, 1411.
2. (a) Legzdins, P.; Martin, J. T.; Oxley, J. C. *Organometallics* **1985**, *4*, 1263. (b) Legzdins, P.; Martin, J. T.; Einstein, F. W. B.; Jones, R. H. *Organometallics* **1987**, *6*, 1826.
3. (a) Hunter, A. D.; Legzdins, P.; Nurse, C. R.; Einstein, F. W. B.; Willis, A. C. *J. Am. Chem. Soc.* **1985**, *107*, 1791. (b) Hunter, A. D.; Legzdins, P.; Einstein, F. W. B.; Willis, A. C.; Bursten, B. E.; Gatter, M. G. *J. Am. Chem. Soc.* **1986**, *108*, 3843.
4. Phillips, E. C. unpublished observations.
5. (a) Hunter, A. D. Ph.D. Dissertation, The University of British Columbia, 1985. (b) Martin, J. T. Ph.D. Dissertation, The University of British Columbia, 1987.
6. Shriver, D. F.; Dreznor, M. A. *The Manipulation of Air-Sensitive Compounds*; 2nd. Ed. Wiley-Interscience: New York, N.Y. 1986.
7. Perrin, D. D.; Armarego, W. L. F.; Perrin, D. R. *Purification of Laboratory Chemicals*; 2nd Ed.; Pergamon: Oxford, 1980.
8. Seddon, D.; Kita, W. G.; Bray, J.; McCleverty, J. A. *Inorg. Synth.* **1976**, *16*, 24.
9. James, T. A.; McCleverty, J. A. *J. Chem. Soc. A.*, **1971**, 1068.
10. (a) Legzdins, P.; Martin, D. T.; Nurse, C.R. *Inorg. Chem.* **1980**, *19*, 1560. (b) Dryden, N. H.; Legzdins, P.; Einstein, F. W. B.; Jones, R. H. *Can. J. Chem.* in press.

11. (a) Malito, J. T.; Shakir, R.; Atwood, J. L. *J. Chem. Soc., Dalton Trans.* **1980**, 1253. (b) Nurse, C. R. Ph.D. Dissertation, The University of British Columbia, 1983.
12. Legzdins, P.; Wassink, B. *Organometallics*, **1984**, *3*, 1811.
13. Nicholson, R. S. *Anal. Chem.* **1966**, *38*, 1406.
14. Diffusion control was tested for in all redox processes during cyclic voltammetry experiments by observing the behavior of peak currents (i_p) as a function of scan rate (v) over at least one order of magnitude of scan rate. For all reversible couples in this study, i_p varied linearly with $v^{1/2}$ and not with v . Representative examples are displayed in the Appendix.
15. Holloway, J. D. L.; Geiger, W. E. *J. Am. Chem. Soc.* **1979**, *101*, 2038.
16. Phillips, P. S.; Herring, F. G. *J. Magn. Reson.* **1984**, *57*, 43.
17. The $[\text{CpMo}(\text{NO})\text{Cl}_2]_2$ analogue can also be formed in low yields by this route: Legzdins, P.; Malito, J. T. *Inorg. Chem.* **1975**, *14*, 1875.
18. King, R. B. *Organometallic Syntheses*; Academic: New York, **1965**, Vol. 1, pp 70-71.
19. (a) Hamon, J.-R.; Astruc, D.; Michaud, P. *J. Am. Chem. Soc.* **1981**, *103*, 758. (b) Robbins, J. L.; Edelstein, N.; Spencer, B.; Smart, J. C. *J. Am. Chem. Soc.*, **1982**, *104*, 1882.
20. The data for the electrochemical oxidations of all the complexes studied are summarized in the Appendix. All of these complexes undergo irreversible oxidations. With the exception of the oxidation of

- [CpMo(NO)I]₂, these oxidations were not investigated further.
21. These anodic peaks are enhanced by the addition of Bu₄NI and are assigned to the oxidation of I⁻ and I₃⁻: Samuel, E.; Guery, D.; Vedel, J. *J. Organomet. Chem.* **1984**, 263, C43.
 22. It is unlikely that this peak is due to the reduction of the radical anion to give the dianion, since its current value is so low. However, [Cp₂ZrI₂]^{•-} is reported to be reduced to the dianion: El Murr, N; Chaloyard, A.; Tirouflet, J. *J. Chem. Soc., Chem. Commun.* **1980**, 446.
 23. In this connection, it has recently been discovered that [CpCr(NO)I]₂ is oxidized by 2 equiv. of AgPF₆ to [CpCr(NO)(CH₃CN)₂]^{•+}[PF₆]⁻ in acetonitrile: Chin, T. T. unpublished observation.
 24. Other examples of this kind of halide loss can be found, see: Connelly, N. G.; Geiger, W. E. *Adv. Organomet. Chem.* **1984**, 23, 1.
 25. Under identical experimental conditions, the Cp₂Co/C₂Co⁺ couple occurs at -0.82 V vs SCE, in CH₂Cl₂. This E° value is sufficiently negative of those of the dihalo complexes and yet sufficiently positive of the second reduction peaks; a situation that is ideal for effecting the desired single-electron transfer.
 26. The Cp₂Fe⁺ cation is a well-known one-electron oxidant in organometallic chemistry: Schumann, H. *J. Organomet. Chem.* **1986**, 304, 341.
 27. Although Cp₂Fe⁺ does not react with CpMo(NO)I₂ in CH₃CN, NO⁺ does to give a flocculent yellow powder of elemental composition [CpMo(NO)(CH₃CN)₃](I)(PF₆): IR (Nujol mull) ν_{NO} 1707 (s) cm⁻¹; also

- 2328 (m) and 2299 (m) cm^{-1} (ν_{CN} region), ν_{PF_6} 841 (s) cm^{-1} . ^1H NMR (CD_3NO_2) δ 6.68 (s, 5H, C_5H_5), 2.65 (s, 9H, CH_3CN). ^{13}C $\{^1\text{H}\}$ NMR (CD_3NO_2) δ 141.10 (s, CH_3CN), 113.18 (s, C_5H_5), 5.04 (s, CH_3CN).
28. In contrast, a decrease of $\sim 200\text{--}180\text{ cm}^{-1}$ is observed after reduction of various $\text{CpM}(\text{NO})_2\text{X}$ complexes ($\text{M} = \text{Mo}$ or W).²⁹
29. Legzdins, P.; Wassink, B. *Organometallics* **1988**, 7, 482.
30. Hunter, A. D.; Legzdins, P. *Organometallics* **1986**, 5, 1001.
31. Geiger, W. E.; Rieger, P. H.; Tulyathan, B.; Rausch, M. *J. Am. Chem. Soc.* **1984**, 106, 7000.
32. The individual contributions of the ^{95}Mo and ^{97}Mo isotopes are unresolved, and this is not unusual: (a) Atherton, N. M.; Denti, G.; Ghedini, M.; Oliva, C. *J. Magn. Reson.* **1981**, 43, 167. (b) Hanson, G. R.; Wilson, G. L.; Bailey, T. D.; Pibrow, J. R.; Wedd, A. G. *J. Am. Chem. Soc.* **1987**, 109, 2609.
33. The extent of hyperfine coupling is of similar magnitude to that found for the $[\text{Cp}_2\text{MoBr}_2]^+$ cation, where $a_{\text{Br}} = 15.8\text{ G}$: Cooper, R. L.; Green, M. L. H. *J. Chem. Soc. A.* **1967**, 1155.
34. A similar argument has been used regarding the electrogeneration of $\text{HB}(\text{Me}_2\text{pz})\text{Mo}(\text{NO})\text{I}^\bullet$ ($\text{Me}_2\text{pz} = 3,5\text{-dimethylpyrazolyl}$): Briggs, T. N.; Jones, C. J.; McCleverty, J. A.; Neaves, B. D.; El Murr, N.; Colquhoun, H. M. *J. Chem. Soc., Dalton Trans.* **1985**, 1249.
35. In this connection, the very weak bands at $\sim 1620\text{ cm}^{-1}$ evident in the IR spectra of the $[\text{Cp}_2\text{Co}][\text{Cp}'\text{Mo}(\text{NO})\text{X}_2]$ complexes may be due to some

$\text{Cp}'\text{Mo}(\text{NO})\text{X}^\bullet$, resulting from decomposition of the radical anion in the solid state.

36. Integration of this signal to ascertain the concentration has not been performed. As a matter of caution, however, it must be noted that in related organic systems, integrations (concentrations) have been found to be dependent on the nature of R,³⁷ or even on the purity of the Mg used in making the Grignard reagent.³⁸
37. Ashby, E. C.; Goel, A. B. *J. Am. Chem. Soc.* **1981**, *103*, 4983.
38. Ashby, E. C.; Wiesemann, T. L. *J. Am. Chem. Soc.* **1978**, *100*, 189.
39. In general, it is believed that organometallic cation radicals such as $\text{R}_4\text{M}^{\bullet+}$ (M = Sn or Pb) are short-lived due to their tendency to cleave the M-R bond. It is entirely possible that the $[\text{RMgX}]^{\bullet+}$ radical cation is stabilized by some means such as solvation or aggregation: Maruyama, K.; Katagiri, T. *J. Am. Chem. Soc.* **1986**, *108*, 6263.
40. For leading references on Grignard reagents as SET agents to organic compounds, see (a) Kochi, J.K. *Organometallic Mechanisms and Catalysis*; Academic: New York, N.Y., 1978, Chapter 17. (b) Jones, P.R. *Adv. Organomet. Chem.* **1977**, *15*, 274. (c) Ashby, E. C.; Bowers, J.; Depriest, R. *Tetrahedron Lett.* **1980**, *21*, 3541. (d) Ashby, E. C.; Goel, A. B. *J. Am. Chem. Soc.* **1981**, *103*, 4983. (e) Ashby, E. C. *Pure Appl. Chem.* **1980**, *52*, 545.
41. In a few cases, Grignard reagents have been known to function as SET agents to organic groups bound to transition metals. (a) Top, S.; Jaouen, G. *J. Organomet. Chem.* **1987**, *336*, 143. (b) Astruc,

- D. In *The Chemistry of the Metal-Carbon Bond*; Hartley, F. R., Ed.; Wiley-Interscience: Chichester, 1987; Vol. 4, p. 630.
42. Alegre, B.; de Jesús, E.; de Miguel, A. V.; Royo, P.; Lanfredi, A. M. M.; Tiripicchio, A. *J. Chem. Soc., Dalton Trans.* **1988**, 819.
43. Trialkylaluminum reagents (R_3Al) are capable of abstracting halide to form $[R_3AlX]^-$. For general discussions, see (a) Yamamoto, A. *J. Organomet. Chem.* **1986**, 300, 347. (b) Mole, T.; Jeffrey, E. A. *Organoaluminum compounds*; Elsevier: New York, N.Y.; 1972, p. 374.
44. (p-tol)Li is reported to react with $HB(Me_2pz)Mo(NO)I_2$ to form a complex formulated as $HB(Me_2pz)_3Mo(NO)I_2 \cdot Li(OEt_2)$.³⁴
45. A similar method has been used to synthesize $[CpMo(NO)I]_2$,⁹ but the W analogues were unknown prior to this work.
46. For simplified reviews concerning the characterization of electrode processes, see (a) Mabbott, G. A. *J. Chem. Ed.* **1983**, 60, 697. (b) Heinze, J. *Angew. Chem. Int. Ed. Engl.* **1984**, 23, 831. More rigorous treatments are also available.⁴⁷
47. Nicholson, R. S.; Shain, I. *Anal. Chem.* **1964**, 36, 706.
48. For excellent references on low-temperature electrochemistry, see (a) Van Duyne, R. P.; Reilley, C. N. *Anal. Chem.* **1972**, 44, 142. (b) *ibid*, p. 153. (c) *ibid*, p. 158.
49. Kochi, J. K. *Pure Appl. Chem.* **1980**, 52, p. 578.
50. A few related Cp_2TiR_2 dialkyl complexes also undergo one-electron reversible reductions. (a) Kira, M.; Bock, H.; Umino, H.; Sakurai, H. *J. Organomet. Chem.* **1979**, 173, 39. (b) Koch, L.; Fakhr, A.;

Mugnier, Y.; Roullier, L.; Moise, C.; Laviron, E. *J. Organomet. Chem.* **1986**, 314, C17.

51. Compounds of the type $\text{Na}^+[\text{Cp}_2\text{ZrR}_2]^{\bullet-}$ have been reported in the literature,^{52a} although this is at variance with cyclic voltammetry results which show the *irreversible* nature of the reduction of the dialkyl precursors.^{52b}
52. (a) Lappert, M. F.; Riley, P. I.; Yarrow, P. I. W. *J. Chem. Soc., Chem. Commun.* **1979**, 305. (b) Lappert, M. F.; Pickett, C. J.; Riley, P. I.; Yarrow, P. I. W. *J. Chem. Soc., Dalton Trans.* **1981**, 805.

CHAPTER 3

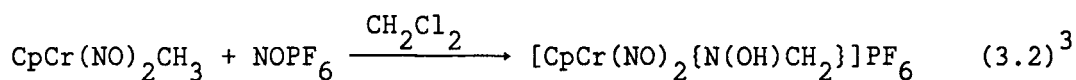
Insertions of Electrophiles into Metal-Carbon Bonds: Formation of New
Carbon-Nitrogen Linkages Mediated by the $\text{CpCr}(\text{NO})_2$ Group.

Introduction

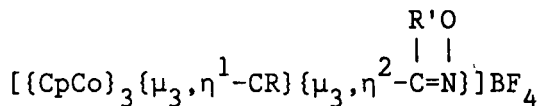
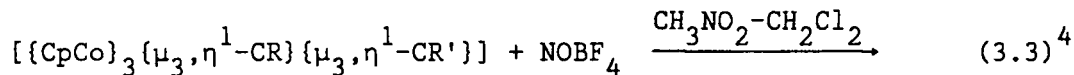
Complexes containing σ -bonded organic ligands play a central role in transition-metal organometallic chemistry.¹ Of the various chemical properties exhibited by these complexes, probably none is more important than their ability to undergo insertion reactions of the type



where XY can be a variety of entities.² The particular examples of reactions 3.1 having XY = CO have been the most studied and are the best understood mechanistically.² In contrast, virtually nothing is presently known about the cases when XY = NO⁺ which is isoelectronic with CO. Indeed, it was only recently that the first examples of the insertion of NO⁺ into transition-metal-carbon bonds were initially communicated by this research group³ and then by other investigators,⁴ i.e.



and



where Cp = $\eta^5-C_5H_5$ and R or R' = alkyl or aryl. Yet, reactions such as 3.2 and

3.3 are of fundamental significance since they lead to the formation of new carbon-nitrogen bonds, an intriguing goal in its own right from the viewpoint of organic synthesis.⁵ Thus, I was interested in studying further the chemistry presented in eqn 3.2 with a view to determining the origin of the formaldoxime ligand in the product. Furthermore, the product complex had only been obtained in somewhat low yield (46% based on Cr) and no intermediates had been detected during the course of the reaction.

In this Chapter, I present the results of the extension of the chemistry outlined in reaction 3.2 to encompass the insertions of not only the nitrosonium ion but also the aryldiazonium cation into the Cr-C σ -bonds of several $\text{CpCr(NO)}_2\text{R}$ (R = alkyl or aryl) complexes. Furthermore, I also describe some derivative chemistry of the products resulting from insertion that has led to the development of a stoichiometric cycle for the formation of new C-N linkages, each step of the cyclic process being mediated by the CpCr(NO)_2 group.

Experimental Section

All reactions and subsequent manipulations were performed under anaerobic and anhydrous conditions. General procedures routinely employed in this study have been described in the previous Chapter. The commercially available reagents AgPF_6 (Strem), NOPF_6 (Alfa), $[\text{PPN}]\text{Cl}$ (bis(triphenylphosphine)iminium chloride, Alfa), CD_3MgI (Aldrich), and Proton Sponge (1,8-bis(dimethylamino)-naphthalene, Aldrich) were used as received without further purification.

Reaction of $\text{CpCr(NO)}_2\text{Me}$ with NOPF_6 . A green solution of $\text{CpCr(NO)}_2\text{Me}$ ⁷ (0.576 g, 3.00 mmol) in CH_2Cl_2 (45 mL) was treated with finely ground NOPF_6

(0.525 g, 3.00 mmol), and the mixture was stirred vigorously at room temperature. After 1 h, a green-brown precipitate began to form, and an IR spectrum of the supernatant solution revealed new bands at 1842 (s), 1834 (w), 1742 (s), 1734 (w) and 1710 (w) cm^{-1} in addition to the ν_{NO} 's characteristic of $\text{CpCr(NO)}_2\text{Me}$ in this solvent at 1776 and 1669 cm^{-1} . After 1.5 h, stirring was stopped, and the green-brown precipitate was permitted to settle. The green supernatant solution was removed by filter cannulation. The remaining precipitate was washed with CH_2Cl_2 (5 mL) and dried in vacuo (5×10^{-3} mm) at 20°C for 1 h to obtain 0.806 g (73% yield) of a brown solid. This solid contained a mixture of the isomers $[\text{CpCr(NO)}_2\{\text{N(O)Me}\}]\text{PF}_6$, and $[\text{CpCr(NO)}_2\{\text{N(OH)CH}_2\}]\text{PF}_6$, in an approximate ratio of 2:3 as judged by its ^1H NMR spectrum.

Anal. Calcd for $\text{C}_6\text{H}_8\text{N}_3\text{O}_3\text{PF}_6\text{Cr}$: C, 19.63; H, 2.20; N, 11.45. Found: C, 19.71; H, 2.30; N, 11.33. IR (Nujol mull) ν_{OH} 3482 (s) cm^{-1} ; ν_{NO} 1852 (s), 1759 (vs), 1559 (w) cm^{-1} . ^1H NMR (CD_2Cl_2 , -20°C) δ 8.92 (br s, 1H, $\text{H}_\text{X}\text{ONCH}_\text{A}\text{H}_\text{B}$), 7.66 (d, 1H, $^2\text{J}_{\text{H}_\text{A}-\text{H}_\text{B}} = 5.2$ Hz, $\text{H}_\text{X}\text{ONCH}_\text{A}\text{H}_\text{B}$), 7.14 (d, 1H, $\text{H}_\text{X}\text{ONCH}_\text{A}\text{H}_\text{B}$), 5.98 (s, 7H, C_5H_5), 1.81 (br s, 2H, NOCH_3).

Recrystallization of the brown solid from CH_2Cl_2 afforded dark green microcrystals of $[\text{CpCr(NO)}_2\{\text{N(OH)CH}_2\}]\text{PF}_6$ as the sole product. Its spectroscopic properties are the same as those exhibited by the mixture (vide supra) except for the absence of the 1559 cm^{-1} band in its IR spectrum and the methyl proton signal at δ 1.81 in its ^1H NMR spectrum. Single crystals of this salt suitable for X-ray crystallographic analysis were grown by maintaining a saturated CH_2Cl_2 solution of the complex under N_2 at -20°C for 2 days.

Preparation of $\text{CpCr(NO)}_2\text{CD}_3$. To a stirred, green slurry of

$\text{CpCr}(\text{NO})_2\text{Cl}^8$ (3.83 g, 18.0 mmol) in Et_2O (160 mL) at room temperature was added dropwise over 10 min a clear solution of CD_3MgI (1.0 M in Et_2O , 18.0 mL, 18.0 mmol) in Et_2O (40 mL total volume). The supernatant solution became darker green in color as the nitrosyl reagent was consumed and a green-brown precipitate formed. After the addition of the Grignard reagent had been completed, the reaction mixture was further stirred for 15 min and was then filtered through a short (3 x 5 cm) column of alumina (Woelm neutral, activity 1) supported on a medium porosity frit to obtain a green filtrate. Solvent removal from the filtrate under reduced pressure and sublimation of the remaining residue at 80–90°C and 5×10^{-3} mm onto a water-cooled probe afforded 1.97 g (57% yield) of $\text{CpCr}(\text{NO})_2\text{CD}_3$ as a dark green, microcrystalline solid. IR (Et_2O) ν_{NO} 1779 (s), 1676 (vs) cm^{-1} . ^2H NMR (CH_3NO_2) δ 0.12 (s, CD_3). Low-resolution mass spectrum (probe temperature 150°C) m/z 194 (P^+).

Preparation of $[\text{CpCr}(\text{NO})_2\{\text{N}(\text{OD})\text{CD}_2\}]\text{PF}_6$. This complex was prepared by treating $\text{CpCr}(\text{NO})_2\text{CD}_3$ with NOPF_6 in CH_2Cl_2 at room temperature for 4 h. It was isolated in a manner identical to that employed for its perhydro analogue (vide supra) in 61% yield. IR (Nujol mull) ν_{NO} 1852 (s), 1759 (vs) cm^{-1} ; ν_{OD} 2581 (m) cm^{-1} . ^2H NMR (CH_3NO_2) δ 8.89 (br s, 1D, OD), 7.61 (br s, 1D, $\text{ONCD}_{\text{A}}\text{D}_{\text{B}}$), 7.25 (br s, 1D, $\text{ONCD}_{\text{A-B}}$). In the presence of even trace amounts of H_2O , the complex undergoes facile deuterium-hydrogen exchange at the OD position.

Preparation of $\text{CpCr}(\text{NO})_2\text{CH}_2\text{SiMe}_3$. A stirred, green slurry of $\text{CpCr}(\text{NO})_2\text{Cl}$ (4.25 g, 20.0 mmol) in Et_2O (200 mL) was treated dropwise over 5 min with a solution of $\text{Me}_3\text{SiCH}_2\text{MgCl}^9$ (1.25 M in Et_2O , 25 mL, 31 mmol) at room

temperature. The reaction mixture became red-brown in color and a brown precipitate deposited. After an additional 10 min of stirring, an IR spectrum of the final red-brown supernatant solution was devoid of the nitrosyl absorptions at 1811 and 1705 cm^{-1} characteristic of $\text{CpCr}(\text{NO})_2\text{Cl}$, but did exhibit new bands at 1775 and 1674 cm^{-1} . Solvent was removed from the final reaction mixture in vacuo, and the residue remaining was extracted with hexanes (3 x 100 mL) until the extracts were colorless. The volume of the combined extracts was reduced to 30 mL under reduced pressure, and the resulting green solution was transferred to the top of an alumina column (Woelm neutral, activity 1, 3 x 15 cm) made up in Et_2O . Elution of the column with Et_2O developed a single green band which was eluted from the column and collected. Solvent removal from the eluate in vacuo afforded a green oil which upon cooling to -196°C at 5×10^{-3} mm solidified into needle-like crystals of analytically pure $\text{CpCr}(\text{NO})_2\text{CH}_2\text{SiMe}_3$ (3.03 g, 57% yield).

Anal. Calcd for $\text{C}_9\text{H}_{16}\text{N}_2\text{O}_2\text{SiCr}$: C, 40.91; H, 6.06; N, 10.61. Found: C, 40.87; H, 6.06; N, 10.53. IR (CH_2Cl_2) ν_{NO} 1772 (s), 1669 (vs) cm^{-1} . ^1H NMR (CD_2Cl_2) δ 5.49 (s, 5H, C_5H_5), 0.29 (s, 2H, CH_2), 0.08 (s, 9H, CH_3). Low-resolution mass spectrum (probe temperature 150°C) m/z 249 ($[\text{P}-\text{CH}_3]^+$).

Reaction of $\text{CpCr}(\text{NO})_2\text{CH}_2\text{SiMe}_3$ with NOPF_6 . To a mixture of $\text{CpCr}(\text{NO})_2\text{CH}_2\text{SiMe}_3$ (0.528 g, 2.00 mmol) and finely ground NOPF_6 (0.350 g, 2.00 mmol) was added CH_2Cl_2 (25 mL), and the mixture was stirred rapidly at room temperature for 25 min. The reaction mixture became darker green in color as the NOPF_6 was consumed. An IR spectrum of the final green solution displayed new ν_{NO} 's at 1840, 1740 and 1613 cm^{-1} in addition to weak bands at 1772 and

1669 cm^{-1} due to the nitrosyl ligands of the $\text{CpCr}(\text{NO})_2\text{CH}_2\text{SiMe}_3$ reactant. The addition of hexanes (120 mL) to the final solution induced the separation of a green oil. The supernatant solution was removed by cannulation, and the oil was reprecipitated from CH_2Cl_2 (10 mL)/hexanes (100 mL) and dried at 5×10^{-3} mm and 20°C for 2 h to obtain 0.71 g (81% yield) of $[\text{CpCr}(\text{NO})_2\{\text{N}(\text{O})\text{CH}_2\text{SiMe}_3\}]\text{PF}_6$ as a slightly impure, viscous green oil.

Anal. Calcd for $\text{C}_9\text{H}_{16}\text{N}_3\text{O}_3\text{SiPF}_6\text{Cr}$: C, 24.60; H, 3.64; N, 9.57. Found: C, 23.16; H, 3.06; N, 10.00. IR (neat) ν_{NO} 1838 (s), 1736 (vs), 1628 (w) cm^{-1} . ^1H NMR (CD_2Cl_2) δ 7.80 (s, 2H, CH_2), 5.89 (s, 5H, C_5H_5), 0.30 (s, 9H, $\text{Si}(\text{CH}_3)_3$).

Reaction of $[\text{CpCr}(\text{NO})_2\{\text{N}(\text{O})\text{CH}_2\text{SiMe}_3\}]\text{PF}_6$ with H_2O . A stirred, green solution of $[\text{CpCr}(\text{NO})_2\{\text{N}(\text{O})\text{CH}_2\text{SiMe}_3\}]\text{PF}_6$ (0.680 g, 1.55 mmol) in CH_2Cl_2 (15 mL) was treated with 3 drops of distilled H_2O whereupon a green solid began to precipitate after ~ 2 min. After 45 min, the almost colorless supernatant solution was removed by filter cannulation. The remaining green solid was washed with CH_2Cl_2 (5 mL) and was dried at 20°C and 5×10^{-3} mm to obtain 0.31 g (55% yield) of $[\text{CpCr}(\text{NO})_2\{\text{N}(\text{OH})\text{CH}_2\}]\text{PF}_6$ which was identified by its characteristic spectroscopic properties (vide supra).

Similar treatment of $[\text{CpCr}(\text{NO})_2\{\text{N}(\text{O})\text{CH}_2\text{SiMe}_3\}]\text{PF}_6$ with D_2O afforded a comparable yield of $[\text{CpCr}(\text{NO})_2\{\text{N}(\text{OD})\text{CH}_2\}]\text{PF}_6$: IR (Nujol mull) ν_{OD} 2577 (m) cm^{-1} ; ν_{NO} 1852 (s), 1759 (vs), 1559 (w) cm^{-1} . ^2H NMR (CH_3NO_2) δ 8.77 (s).

Reaction of $\text{CpCr}(\text{NO})_2\text{CH}_2\text{SiMe}_3$ with I_2 . A violet solution of I_2 (0.127 g, 0.50 mmol) in Et_2O (20 mL) was added dropwise by cannula to a stirred green solution of $\text{CpCr}(\text{NO})_2\text{CH}_2\text{SiMe}_3$ (0.264 g, 1.00 mmol) in Et_2O (20 mL) at

room temperature. The reaction mixture darkened in color, and some dark solid precipitated. After 10 min, the reaction mixture was quickly filtered through a short (3 x 5 cm) column of alumina (Woelm neutral, activity 1) supported on a medium porosity frit. The brown-black filtrate was taken to dryness in vacuo, and the remaining black residue was recrystallized from Et₂O at -5°C to obtain 0.06 g (20% yield based on Cr) of CpCr(NO)₂I as a black, crystalline solid.

Anal. Calcd for C₅H₅N₂O₂CrI: C, 19.74; H, 1.64; N, 9.21. Found: C, 19.90; H, 1.66; N, 9.19. IR (Nujol mull) ν_{NO} 1812 (s), 1695 (vs) cm⁻¹. Low resolution mass spectrum (probe temperature 120°C) m/z 304 (P⁺).

Treatment of CpCr(NO)₂CH₂SiMe₃ with MeOH. A stirred CH₂Cl₂ (20 mL) solution of green CpCr(NO)₂CH₂SiMe₃ (0.264 g, 1.00 mmol) was treated with an excess (~1 mL) of deaerated methanol. After being stirred at ambient temperature for 5 days, the reaction mixture had not changed in color, and its IR spectrum exhibited only ν_{NO} 's due to the organometallic reactant at 1774 and 1669 cm⁻¹.

Reaction of CpCr(NO)₂Ph with NOPF₆. A green solution of CpCr(NO)₂Ph⁷ (0.220 g, 0.866 mmol) in CH₂Cl₂ (10 mL) was treated with solid, finely ground NOPF₆ (0.152 g, 0.866 mmol), and the mixture was stirred rapidly at ambient temperature. The supernatant solution became red as the nitrosonium salt dissolved. An IR spectrum of this solution displayed new nitrosyl absorptions at 1848 and 1744 cm⁻¹ in addition to those due to the phenyl reactant. Dark red microcrystals began to precipitate from this solution after ~10 min. Hexanes (60 mL) were added to complete the precipitation of this solid which was then collected by filtration and dried at 20°C and 5 x 10⁻³ mm for 1 h to obtain 0.28 g (76% yield) of [CpCr(NO)₂{N(O)Ph}]PF₆ as a red, microcrystalline solid.

Anal. Calcd for $C_{11}H_{10}N_3O_3PF_6Cr$: C, 30.77; H, 2.33; N, 9.79. Found: C, 31.02; H, 2.29; N, 9.59. IR (Nujol mull) ν_{NO} 1850 (s), 1766 (vs), 1489 (m) cm^{-1} . 1H NMR (CD_2Cl_2) δ 8.21–7.60 (m, 5H, C_6H_5), 6.01 (s, 5H, C_5H_5).

Reaction of $CpCr(NO)_2Me$ with $NSPF_6$. Over a 20-min period, an orange solution of $NSPF_6$ in CH_3NO_2 (2 mmol in 30 mL, generated in situ from 1/3 $(NSCl)_3$ and $AgPF_6$)¹⁰ was filter-cannulated onto a stirred, olive-green solution of $CpCr(NO)_2Me$ (0.384 g, 2.00 mmol) in CH_2Cl_2 (30 mL) held at 0°C by means of an ice bath. As the reaction progressed, the reaction mixture darkened in color. The ice bath was then removed, and the mixture was allowed to warm slowly to room temperature as stirring was continued for an additional 2.5 h. Hexanes (100 mL) were then added to the final reaction mixture whereupon two immiscible liquid phases separated. The upper hexanes layer containing unreacted $CpCr(NO)_2Me$ was removed by cannulation and discarded. Solvent was removed from the lower nitromethane layer in vacuo to obtain a viscous green oil. Trituration of this oil with CH_2Cl_2 (10 mL) resulted in the formation of 0.31 g of a green powder. IR (Nujol mull) ν_{NO} 1829 (s), 1723 (vs) cm^{-1} ; also 3331 (s) and 1659 (w) cm^{-1} . Unfortunately, this green powder was unstable, decomposing even when maintained at -20°C overnight. Consequently, a consistent elemental analysis of this material could not be obtained.

Reaction of $CpCr(NO)_2Me$ with $[p-O_2NC_6H_4N_2]BF_4$. The paranitrophenyl-diazonium salt, $[p-O_2NC_6H_4N_2]BF_4$ (0.474 g, 2.00 mmol)¹¹ was dissolved in CH_3NO_2 (50 mL), and the resulting light orange solution was transferred dropwise by cannula onto a stirred CH_2Cl_2 (50 mL) solution of $CpCr(NO)_2Me$

(0.384 g, 2.00 mmol) at ambient temperature. The reaction mixture was stirred for a total of 2 h, during which time the originally green solution became red, and IR monitoring revealed replacement of the original ν_{NO} 's at 1777 and 1669 cm^{-1} by new bands at 1846 and 1746 cm^{-1} . Solvent was removed from the final mixture in vacuo, and the remaining oily residue was reprecipitated from CH_2Cl_2 -hexanes. Trituration of the oil thus obtained with CH_2Cl_2 afforded a green-brown microcrystalline solid and a red supernatant solution. The crystals were collected by filtration, washed quickly with CH_2Cl_2 (2 x 5 mL), and dried at 20°C and 5×10^{-3} mm for 1 h to obtain 0.212 g (25% yield) of analytically pure $[\text{CpCr}(\text{NO})_2\{\text{N}(\text{NC}_6\text{H}_4\text{NO}_2)\text{Me}\}]\text{BF}_4$. Single crystals of this salt were grown by maintaining a concentrated solution of this complex in CH_2Cl_2 at -20°C for 3 days.

Anal. Calcd for $\text{C}_{12}\text{H}_{12}\text{O}_4\text{N}_5\text{BF}_4\text{Cr}$: C, 33.58; H, 2.80; N, 16.32. Found: C, 33.44; H, 2.87; N, 16.20. IR (Nujol mull) ν_{NO} 1833 (s), 1726 (vs) cm^{-1} ; also 1605 (m), 1590 (m), 1560 (w) cm^{-1} . ^1H NMR (CD_3NO_2) δ 8.43 (d, 2H, meta $\underline{\text{H}}$, $^3J_{\text{H}_\text{A}\text{H}_\text{X}} = 9.3$ Hz), 7.29 (d, 2H, ortho $\underline{\text{H}}$), 6.12 (s, 5H, C_5H_5), 4.26 (s, 3H, CH_3). Definitive assignment of the ν_{NN} of the diazene ligand in the IR spectrum requires a proper ^{15}N labeling study.

Reaction of $[\text{CpCr}(\text{NO})_2\{\text{N}(\text{O})\text{Ph}\}]\text{PF}_6$ with $[\text{PPN}]\text{Cl}$. To a stirred, red solution of $[\text{CpCr}(\text{NO})_2\{\text{N}(\text{O})\text{Ph}\}]\text{PF}_6$ (0.268 g, 0.625 mmol) in CH_2Cl_2 (25 mL) at ambient temperature was added a slight excess of $[\text{PPN}]\text{Cl}$ (0.40 g, 0.70 mmol) whereupon the solution immediately became green. After 1 min, an IR spectrum of this solution was devoid of absorptions due to the nitrosobenzene-containing complex, but did exhibit strong bands attributable to $\text{CpCr}(\text{NO})_2\text{Cl}$ (ν_{NO} 1817

(s), 1711 (vs) cm^{-1}) and uncomplexed PhNO (1506, 1439 cm^{-1}). Removal of solvent from the final reaction mixture in vacuo and sublimation of the residue at 20°C and 5×10^{-3} mm onto a Dry-Ice-cooled probe produced 0.02 g (34% yield) of PhNO which was identified by comparison of its spectroscopic properties with those exhibited by an authentic sample. The relatively low isolated yield of PhNO from this clean (by IR) conversion was undoubtedly a reflection of the nitroso compound's considerable volatility.

Sequential Treatment of $\text{CpCr(NO)}_2\text{Ph}$ with $[\text{p-O}_2\text{NC}_6\text{H}_4\text{N}_2]\text{BF}_4$ and $[\text{PPN}]\text{Cl}$.

A stirred, green solution of $\text{CpCr(NO)}_2\text{Ph}$ (0.31 g, 1.2 mmol) in CH_3NO_2 (5 mL) at room temperature was treated with solid $[\text{p-O}_2\text{NC}_6\text{H}_4\text{N}_2]\text{BF}_4$ (0.24 g, 1.0 mmol) whereupon the reaction mixture became red-brown within 10 min. After 5 h, the reaction mixture was filtered through a medium-porosity glass frit, and solvent was removed from the filtrate in vacuo. The remaining brown residue was dissolved in CH_2Cl_2 (40 mL), $[\text{PPN}]\text{Cl}$ (0.63 g, 1.1 mmol) was added, and the resulting solution was stirred for 15 min whereupon it became green-orange in color. The final reaction mixture was taken to dryness under reduced pressure, and the residue thus obtained was extracted with hexanes (2 x 70 mL) to leave behind a green-brown powder. Solvent was removed from the combined orange extracts in vacuo, the resulting residue was dissolved in Et_2O (10 mL), and this solution was transferred to the top of an alumina column (Woelm neutral, activity 1, 2 x 10 cm) made up in Et_2O . Elution of the column in air with Et_2O developed a single orange band which was eluted from the column and collected. Solvent removal from the eluate in vacuo afforded an orange solid which was recrystallized from hexanes to obtain 0.08 g (35% yield) of $\text{p-O}_2\text{NC}_6\text{H}_4\text{N}_2\text{Ph}$ as an orange microcrystalline solid.

Anal. Calcd for $\text{C}_{12}\text{H}_9\text{N}_3\text{O}_2$: C, 63.43; H, 3.99; N, 18.49. Found: C,

63.50; H, 4.01, N, 18.44. Low-resolution mass spectrum (probe temperature 150°C) m/z 227 (P^+).

The green-brown powder remaining after the hexanes extraction was recrystallized from CH_2Cl_2 -hexanes to obtain 0.16 g (75% yield) of golden $CpCr(NO)_2Cl$ which was readily identifiable by its characteristic IR and mass spectra.⁸

Reaction of $[CpCr(NO)_2\{N(OH)CH_2\}PF_6]$ with $CpCr(NO)_2Me$. To a stirred, green CH_2Cl_2 solution (25 mL) of $CpCr(NO)_2Me$ (1.92 g, 1.00 mmol) was added solid $[CpCr(NO)_2\{N(OH)CH_2\}]PF_6$ (0.367 g, 1.00 mmol). The mixture was stirred vigorously for 10 days at ambient temperature [**Caution:** a gas is evolved during this reaction, and appropriate steps must be taken to avoid excessive pressure build-up in the reaction vessel]. After this period the reaction mixture was filtered. Addition of hexanes (100 mL) to the filtrate resulted in the precipitation of a green flocculent powder. This powder was collected by filtration and dried in vacuo for 3 h to obtain 0.46 g (85% yield based on Cr) of green $[(CpCr(NO)_2)_2\{\mu, \eta^2-N(CH_2)_2O\}]PF_6$.

Anal. Calcd for $C_{11}H_{12}N_5O_5PF_6Cr_2$: C, 24.31; H, 2.21; N, 12.89. Found: C, 24.22; H, 2.24; N, 12.71. IR (Nujol) ν_{NO} 1832(s), 1809(s), 1716(s), 1700(s) cm^{-1} ; ν_{NC} 1567(w) cm^{-1} . IR (CH_2Cl_2) ν_{NO} 1833(s), 1811(s), 1731(s), 1709(s) cm^{-1} . 1H NMR (CD_2Cl_2) δ 7.25 (d, 1H, $-ONCH_{AB}$, $^2J_{H_A-H_B} = 6.3$ Hz), 7.13 (d, 1H, $-ONCH_{AB}$), 5.81 (s, 5H, C_5H_5), 5.74 (s, 5H, C_5H_5). $^{13}C\{^1H\}$ NMR (CD_2Cl_2) δ 151.41 (s, CH_2), 104.59 (s, C_5H_5), 103.76 (s, C_5H_5). ^{13}C NMR (CD_3NO_2) δ 153.33 (dd, CH_{AB} , $^1J_{^{13}C-H} = 185$ Hz, 173.4 Hz), 105.94 (dq, C_5H_5 , $^1J_{^{13}C-H} = 182.2$

Hz, $^nJ_{13C-1H} = 6.5$ Hz), 105.06 (dq, C_5H_5 , $^1J_{13C-1H} = 182.6$ Hz, $^nJ_{13C-1H} = 6.5$ Hz).

This compound was also obtainable in comparable yield by the direct reaction of $CpCr(NO)_2Me$ with $NOPF_6$ in a 2:1 ratio. The evolution of CH_4 was established by GC-MS¹² analysis of the atmosphere in the reaction flask.

Reaction of $[CpCr(NO)_2\{N(OH)CH_2\}]PF_6$ with Proton Sponge. To a stirred, green slurry of $[CpCr(NO)_2\{N(OH)CH_2\}]PF_6$ (0.07 g, 0.20 mmol) in CH_2Cl_2 (10 mL) was added solid Proton Sponge (0.04 g, 0.19 mmol). The reaction mixture immediately turned red-brown. An IR spectrum of the red-brown solution displayed new strong bands at 1800 and 1690 cm^{-1} attributable to ν_{NO} . However, these bands were gradually replaced over a 1.5 h period by new bands at 1833, 1809, 1731 and 1701 cm^{-1} . A yellow solid also precipitated during this time. Removal of the solid by filtration, and addition of hexanes (30 mL) to the green-brown filtrate resulted in the precipitation of a green solid. This solid was collected by filtration, washed with hexanes (5 mL) and dried in vacuo for 1 h to obtain 0.03 g (55% yield based on Cr) of $[(CpCr(NO)_2)_2\{\mu, \eta^2-N(CH_2)_2O\}]PF_6$ which was readily identifiable by its characteristic spectroscopic properties (vide supra).

Preparation of $[(CpCr(NO)_2)_2\{\mu, \eta^2-N(CH_2)_2O\}]BPh_4$. To a stirred, green methanol solution (100 mL) of $[(CpCr(NO)_2)_2\{\mu, \eta^2-N(CH_2)_2O\}]PF_6$ (0.46 g, 0.85 mmol) in air was added solid $NaBPh_4$ (0.29 g, 0.85 mmol). A shiny, green micro-crystalline solid precipitated after ~5 min. This solid was collected by filtration, washed with methanol (10 mL) and then dried in vacuo for 6 h to obtain 0.40 g (66% yield based on Cr) of golden-brown

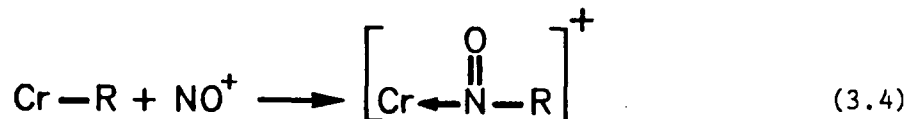
$[\{\text{CpCr}(\text{NO})_2\}_2\{\mu, \eta^2\text{-N}(\text{CH}_2)_2\text{O}\}]\text{BPh}_4$. Suitable crystals of this salt for X-ray crystallographic analysis were grown by slow evaporation of a saturated solution of the complex in a 1:1 mixture of CH_2Cl_2 /hexanes at room temperature.

Anal. Calcd for $\text{C}_{35}\text{H}_{32}\text{Cr}_2\text{N}_5\text{O}_5\text{B}$: C, 58.58; H, 4.46; N, 9.76. Found: C, 58.31; H, 4.68; N, 9.67. IR (Nujol mull) ν_{NO} 1817(s), 1786(s), 1722(s) and 1696(s) cm^{-1} . ^1H NMR (d_6 -acetone) δ 7.48-6.73 (m, 22H, CH_2 and 4 x C_6H_5), 6.07 (s, 5H, C_5H_5), 6.02 (s, 5H, C_5H_5).

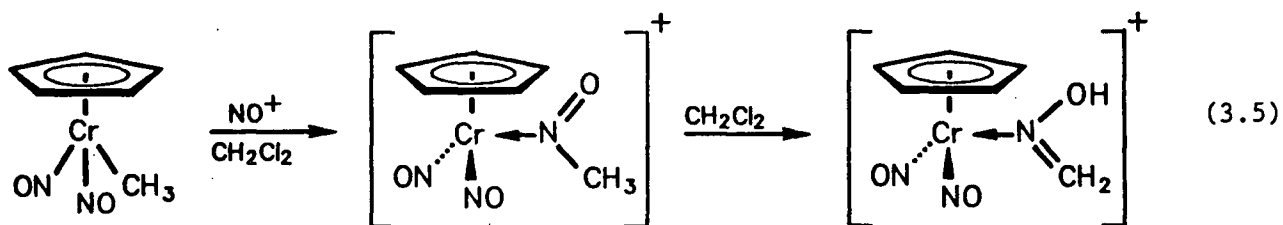
Results and Discussion

Insertions of the Nitrosonium Ion into Chromium-Carbon Sigma Bonds.

Treatment of various $\text{CpCr}(\text{NO})_2\text{R}$ complexes (R = alkyl or aryl) with NO^+ results in the clean insertion of the nitrosonium ion into the $\text{Cr}-\text{C}$ σ bonds, i.e.



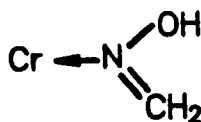
the cationic products resulting from transformations 3.4 generally being isolable in good yields as their PF_6^- salts. In the special case when $\text{R} = \text{Me}$, the insertion first generates a brown complex whose spectroscopic properties are consistent with it containing the $[\text{CpCr}(\text{NO})_2\{\text{N}(\text{O})\text{Me}\}]^+$ cation. Specifically, its IR spectrum (Nujol mull) exhibits a band at 1559 cm^{-1} and its ^1H NMR spectrum (CD_2Cl_2 , -20°C) displays a singlet at δ 1.81, both features being attributable to the nitrosomethane ligand.¹³ In solutions, however, this brown complex isomerizes irreversibly to the novel formaldoxime complex, i.e.



The isomerization step depicted in eqn 3.5 is rapid in poorly coordinating

solvents such as CH_2Cl_2 and CH_3NO_2 ,¹⁴ and the final green formaldoxime complex, $[\text{CpCr}(\text{NO})_2\{\text{N}(\text{OH})\text{CH}_2\}]\text{PF}_6$, is best isolated by crystallization from CH_2Cl_2 . In the solid state, the latter salt may be handled in air for short periods of time, but it is best stored under dry N_2 .

A single-crystal X-ray crystallographic analysis¹⁵ of $[\text{CpCr}(\text{NO})_2\{\text{N}(\text{OH})\text{CH}_2\}]\text{PF}_6$ ³ establishes that the organometallic cation possesses a normal "three-legged piano stool" molecular structure. A thermal ellipsoid plot of this structure is shown in Figure 3.1, and pertinent intramolecular dimensions are tabulated in the caption. Within the cation, the $\text{CpCr}(\text{NO})_2$ fragment is normal, closely resembling that found in $\text{CpCr}(\text{NO})_2\text{Cl}$.¹⁶ The $\text{CrN}(\text{OH})\text{CH}_2$ portion of the cation is essentially planar, and the intramolecular dimensions of the formaldoxime ligand resemble those of free formaldoxime.¹⁷ Consequently, in valence-bond terms, the bonding within this grouping is representable as



with the formaldoxime ligand functioning as a formal two-electron donor to the metal center. The spectroscopic properties of $[\text{CpCr}(\text{NO})_2\{\text{N}(\text{OH})\text{CH}_2\}]\text{PF}_6$ can be readily understood in terms of its solid-state molecular structure, thereby indicating that the basic structural units persist in solutions. For instance, the ^1H NMR spectrum of the salt in CD_2Cl_2 exhibits a broad singlet at δ 8.92 and an AB pattern at δ 7.66 and 7.14 attributable to the hydroxyl and methylene protons, respectively, of the formaldoxime ligand.

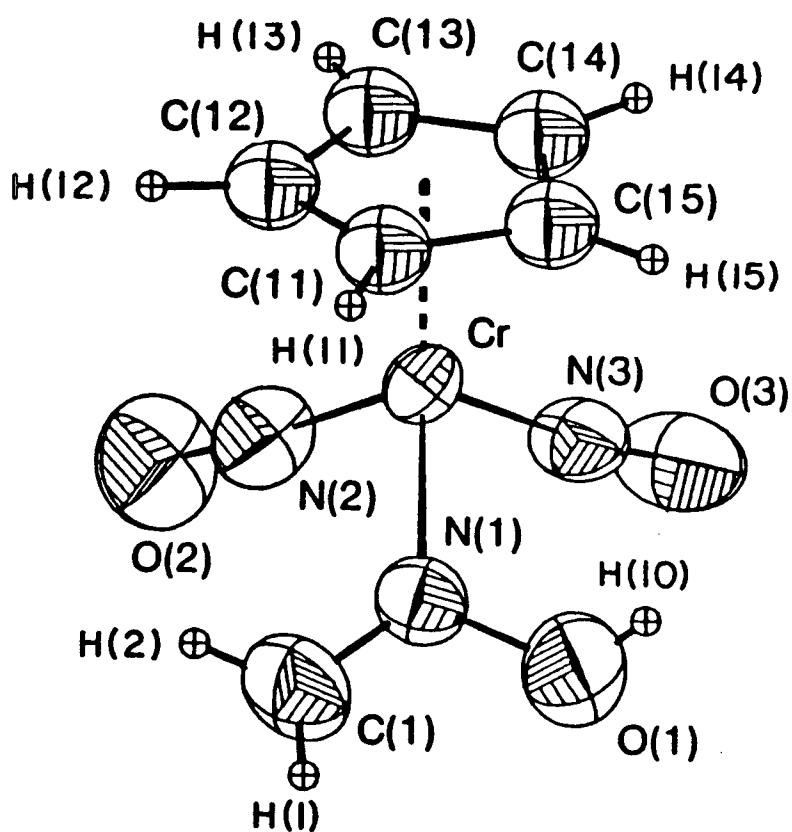
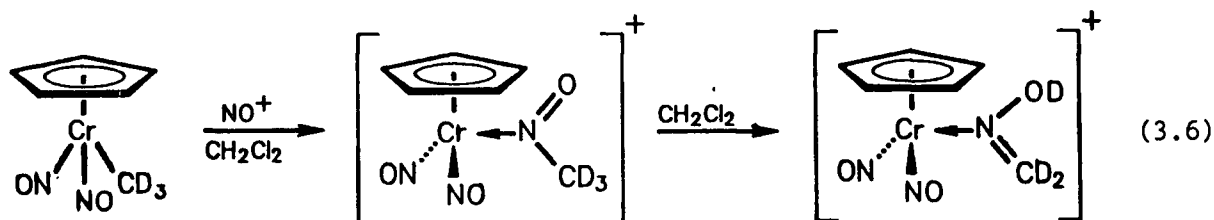
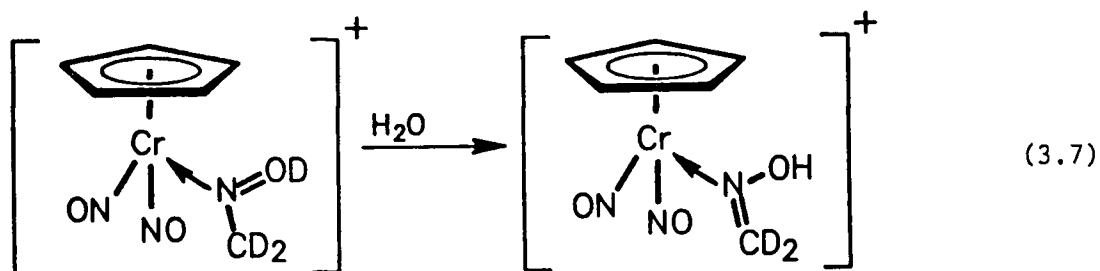


Figure 3.1. The solid-state molecular structure of the $[\text{CpCr}(\text{NO})_2\{\text{N}(\text{OH})\text{CH}_2\}]^+$ cation. Selected bond distances (Å) and angles (deg) are C(1)-N(1) = 1.253(9), N(1)-O(1) = 1.392(7), Cr-N(1) = 2.034(5), Cr-N(2) = 1.702(6), Cr-N(3) = 1.709(5), N(2)-O(2) = 1.163(6), N(3)-O(3) = 1.152(6), Cr-C₅H₅ (centroid) = 1.843, Cr-N(1)-C(1) = 128.9(5), C(1)-N(1)-O(1) = 111.5(6), O(1)-N(1)-Cr = 119.6(4), N(2)-Cr-N(3) = 93.5(3), O(2)-N(2)-Cr = 174.5(6), O(3)-N(3)-Cr = 172.2(5).

The reaction between the perdeutero methyl complex, $\text{CpCr}(\text{NO})_2\text{CD}_3$, and NO^+ apparently proceeds in an analogous manner, i.e.

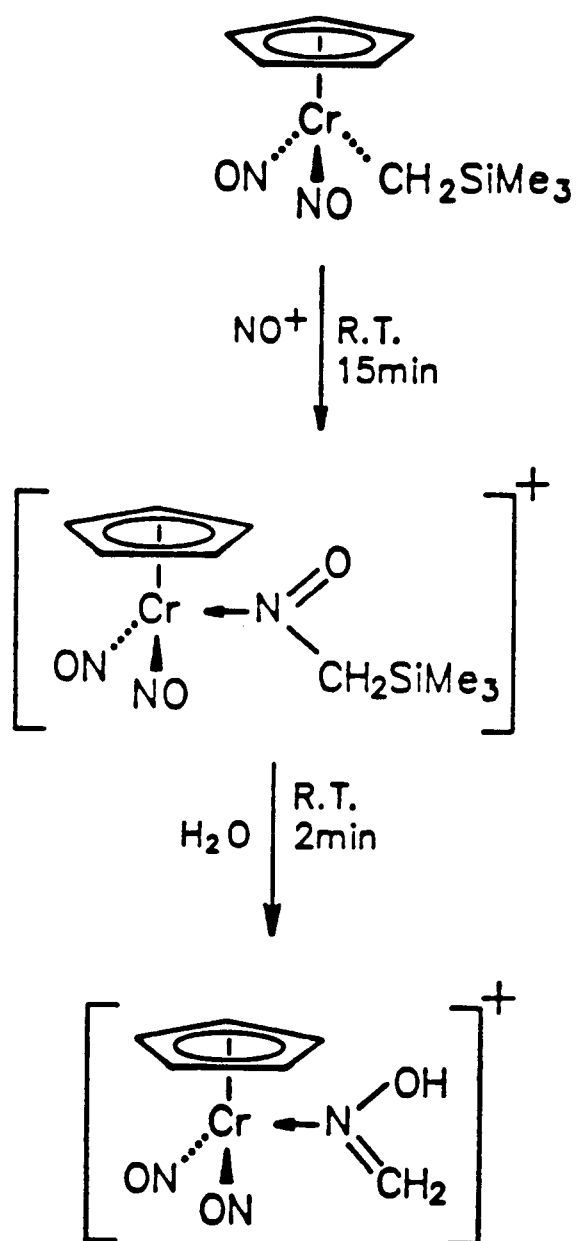


In this instance, the final green salt, $[\text{CpCr}(\text{NO})_2\{\text{N}(\text{OD})\text{CD}_2\}]\text{PF}_6$, is isolable in 61% yield. The occurrence of this conversion thus verifies that the hydroxyl H atom of the formaldoxime ligand in reaction 3.5 does indeed originate from the methyl group in the organometallic reactant and not from some other source such as the solvent. The presence of the perdeuterated formaldoxime ligand in the final complex is clearly evident in its IR [Nujol mull; ν_{OD} 2581 cm^{-1} ; $\nu_{\text{OH}}/\nu_{\text{OD}}$ calcd: 1.37; found: 1.35] and ^2H NMR [CH_3NO_2 ; three singlets of equal intensity at δ 8.89, 7.61 and 7.25] spectra. However, this ligand undergoes facile deuterium-hydrogen exchange at the OD position in the presence of even trace amounts of H_2O , i.e.



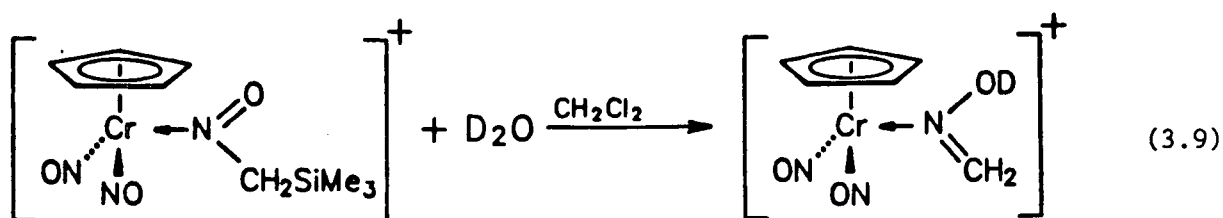
Thus, as reaction 3.7 progresses, there appears and grows a ν_{OH} band at 3480 cm^{-1} in the Nujol mull IR spectrum, and the ^2H NMR signal (CH_3NO_2) at δ 8.89 diminishes.

When $\text{R} = \text{CH}_2\text{SiMe}_3$ in the general transformation 3.4, the NO^+ inserted product can be precipitated as its PF_6^- salt by the addition of hexanes to the final reaction mixture. Isolated in this manner, the complex is a slightly impure, dark green tar which exhibits IR and ^1H NMR spectra (see Experimental Section for details) that are completely consistent with its cation possessing the molecular structure shown in the middle of eqn 3.8 below. Also as indicated in eqn 3.8, this cation is readily hydrolyzed to the ubiquitous formaldoxime-containing complex. Interestingly, if D_2O rather than H_2O is employed to effect the second step of reaction 3.8, the final product displays deuterium

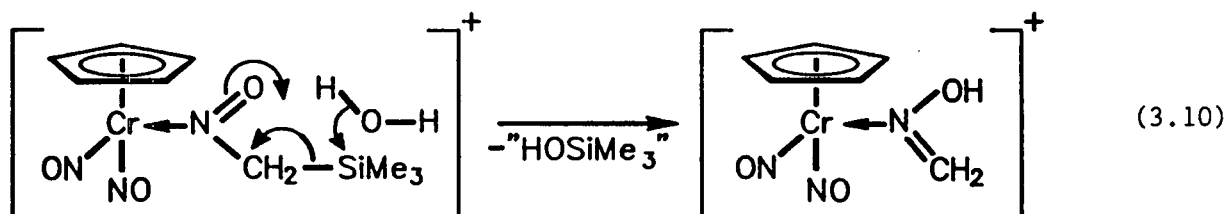


(3.8)

incorporation solely at the hydroxyl position, i.e.



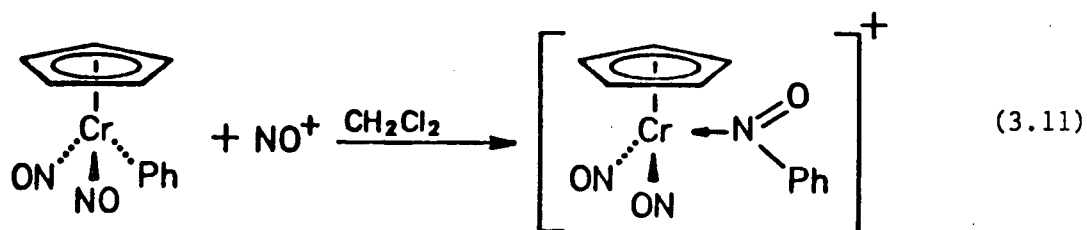
This latter observation is indicative of the hydrolysis reaction proceeding so as to afford the formaldoxime complex directly, e.g.



Had the cleavage of the C-Si link by D_2O proceeded so as to generate initially the CH_2DNO -containing cation which would then isomerize to the final product (eqn 3.5), a distribution of the deuterium label amongst the hydroxyl and methylene sites of the formaldoxime ligand would have been observed. For comparison, it may be noted that the analogous carbon-silicon bond in the neutral $\text{CpCr}(\text{NO})_2\text{CH}_2\text{SiMe}_3$ reactant is much less prone to cleavage. Thus, the complex is inert to H_2O and MeOH , and I_2 cleanly breaks the Cr-C bond instead

to produce $\text{CpCr(NO)}_2\text{I}$.

Finally, the NO^+ insertion reaction (eqn 3.4) can also be extended to encompass chromium-aryl linkages as well. For instance,

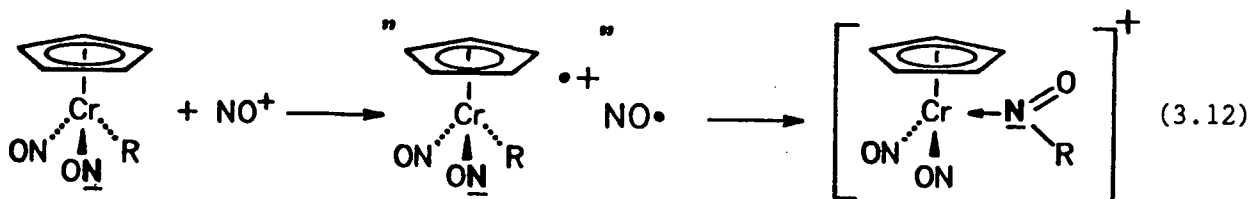


and the $[\text{CpCr(NO)}_2\{\text{N(O)Ph}\}]\text{PF}_6$ product is isolable in 76% yield as a red, microcrystalline solid. This nitrosobenzene complex is very soluble under ambient conditions in noncoordinating solvents such as CH_2Cl_2 and CH_3NO_2 , but can be crystallized from them at -20°C . The physical and spectroscopic properties of the complex are fully in accord with its cation having the molecular structure depicted in eqn 3.11. In particular, the fact that the ν_{NO} exhibited by the PhNO ligand is 17 cm^{-1} lower than in the free state is indicative of it being coordinated in a monodentate fashion through N.^{18,19}

Possible Mechanisms for the Nitrosonium Insertion Reactions. Although there are many mechanistic pathways that can be envisaged for the unprecedented reactions 3.4, the most likely ones involve (a) oxidatively induced, intramolecular insertion of bound NO into the Cr-C σ bonds, (b) direct attack of NO^+ at the metal center followed by migration into the Cr-C σ bonds, or (c) charge-controlled, intermolecular attacks by NO^+ at the Cr-R groups. Each pathway is next considered in some detail.

(a) **Oxidatively Induced Migratory Insertion of Bound NO.** Ample evidence exists in the chemical literature that during its reactions with organo-

metallic substrates the nitrosonium cation may, on occasion, simply function as a one-electron oxidant.²⁰ Hence, it is conceivable that the insertion reactions 3.4 may well proceed in the manner summarized in eqn 3.12. As indicated, the NO^+



cation could oxidize the $\text{CpCr}(\text{NO})_2\text{R}$ reagent to its 17-electron radical cation while being itself reduced to $\text{NO} \cdot$. The organometallic cation thus formed could then insert a bound NO into its Cr-R bond, presumably via intramolecular nucleophilic attack of R onto the nitrogen atom of a nitrosyl ligand (underlined in eqn 3.12).²¹ Finally, the resulting 15-electron $[\text{CpCr}(\text{NO})\{\text{N}(\text{O})\text{R}\}]^{\bullet+}$ species would be trapped by the still present $\text{NO} \cdot$ radical to afford the final dinitrosyl cation shown in eqn 3.12. Note that if this mechanism is indeed operative, then it would be a nitrosyl ligand originally in the chromium's coordination sphere (as opposed to the external NO^+) that would finally constitute a part of the bound RNO group.

Any discussion concerning the viability of this mechanism must first involve a consideration of the relative ease of oxidation of the various $\text{CpCr}(\text{NO})_2\text{R}$ complexes. Consequently, I have investigated the oxidation behavior of these compounds in CH_2Cl_2 by employing cyclic voltammetry at a platinum-bead electrode with $[\text{n-Bu}_4\text{N}]\text{PF}_6$ as the support electrolyte. A typical cyclic voltammogram, that of $\text{CpCr}(\text{NO})_2\text{Me}$, is shown in Figure 3.2, and data for the oxidations of all three compounds are collected in Table 3.1.²² The pertinent

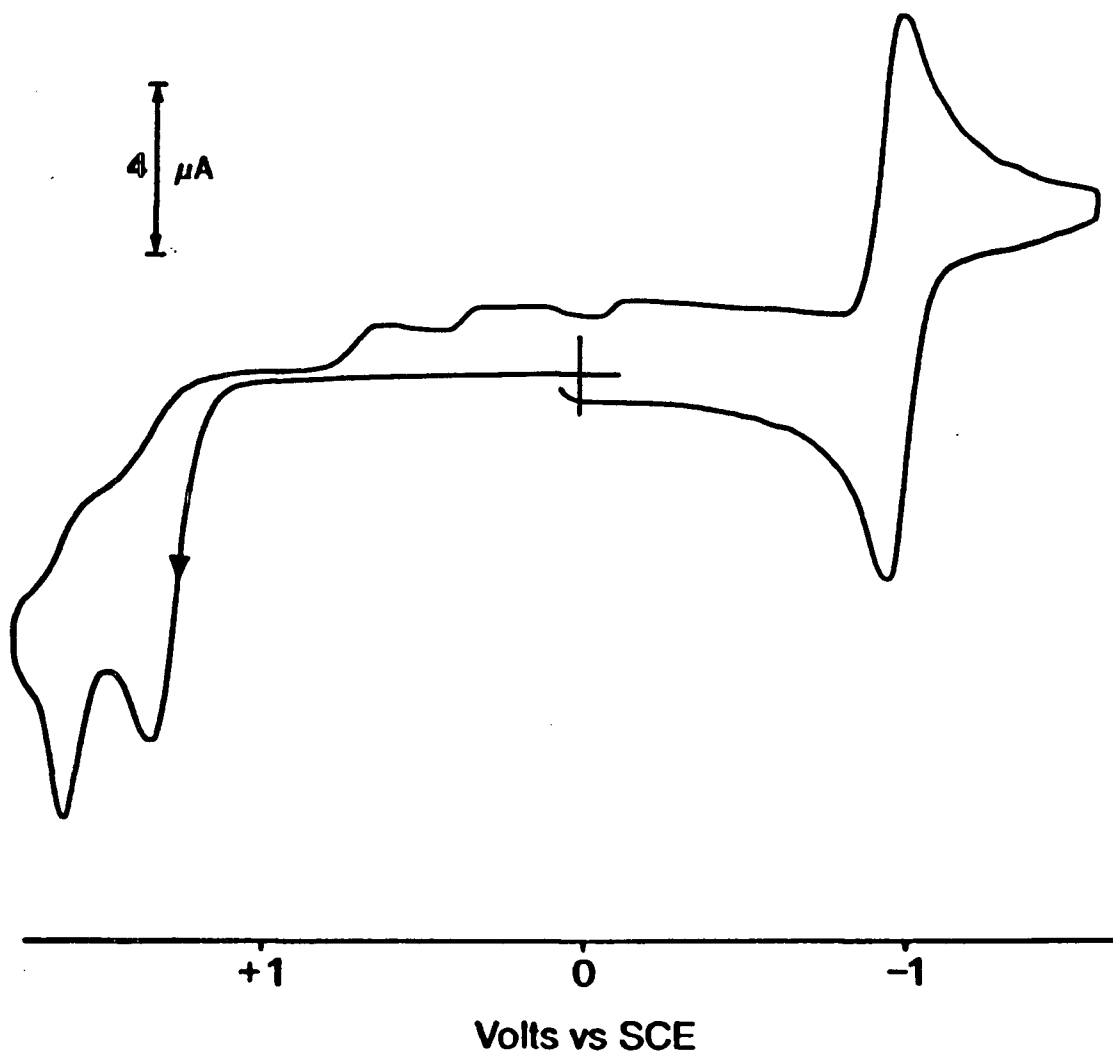


Figure 3.2. Ambient temperature cyclic voltammogram of 5×10^{-4} M $\text{CpCr}(\text{NO})_2\text{Me}$ in CH_2Cl_2 containing 0.1 M $[\text{n-Bu}_4\text{N}]\text{PF}_6$ measured at a platinum-bead electrode at a scan rate of 0.30 V s^{-1} .

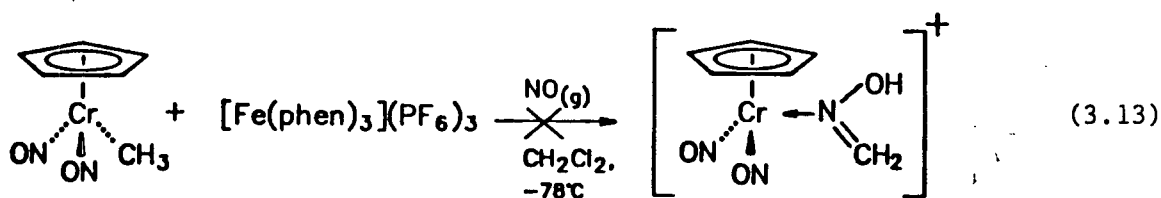
Table 3.1. Cyclic Voltammetry Data for the Oxidations of Some $\text{CpCr}(\text{NO})_2\text{R}$ Complexes.

compd ^a	$E_{p,a}^b$	Scan rate (V s^{-1})
$\text{CpCr}(\text{NO})_2\text{Me}$	+1.33, +1.55	0.30
$\text{CpCr}(\text{NO})_2\text{CH}_2\text{SiMe}_3$	+1.42	0.39
$\text{CpCr}(\text{NO})_2\text{Ph}$	+1.32	0.19

^a In $\text{CH}_2\text{Cl}_2/0.1 \text{ M } [\text{n-Bu}_4\text{N}]\text{PF}_6$.

^b V vs. SCE, for which the $\text{Cp}_2\text{Fe}/\text{Cp}_2\text{Fe}^+$ couple occurs at +0.46 V ($i_{p,a}/i_{p,c} = 1$), $\Delta E = 70 \text{ mV}$).

feature that is immediately evident is that the $\text{CpCr(NO)}_2\text{R}$ complexes all undergo irreversible oxidations at fairly high potentials > 1.3 V vs SCE. (For comparison, isoelectronic $\text{CpFe(CO)}_2\text{Me}$ undergoes a similar irreversible oxidation at $+1.10$ V under identical experimental conditions.) Since the reduction potential of NO^+ in CH_2Cl_2 has been estimated as being in the range -0.22 to -0.11 V,²³ it is unlikely that NO^+ would be able to oxidize the $\text{CpCr(NO)}_2\text{R}$ species cleanly and completely. To do just that, I chose instead the more potent one-electron oxidant $[\text{Fe(phen)}_3]^{3+}$ whose standard reduction potential is 1.13 V at 25°C .^{24,25} Indeed, at room temperature in CH_2Cl_2 , $\text{CpCr(NO)}_2\text{Me}$ (ν_{NO} 1777 (s), 1669 (vs) cm^{-1}) is completely converted by 1 equiv of $[\text{Fe(phen)}_3]^{3+}$ into a CpCr(NO)_2^+ -containing product (ν_{NO} 1846 (s), 1745 (vs) cm^{-1}). However, when this oxidation product is treated with NO gas, none of the formaldoxime complex is produced. This state of affairs persists even if the sequential transformations are effected at -78°C , i.e.

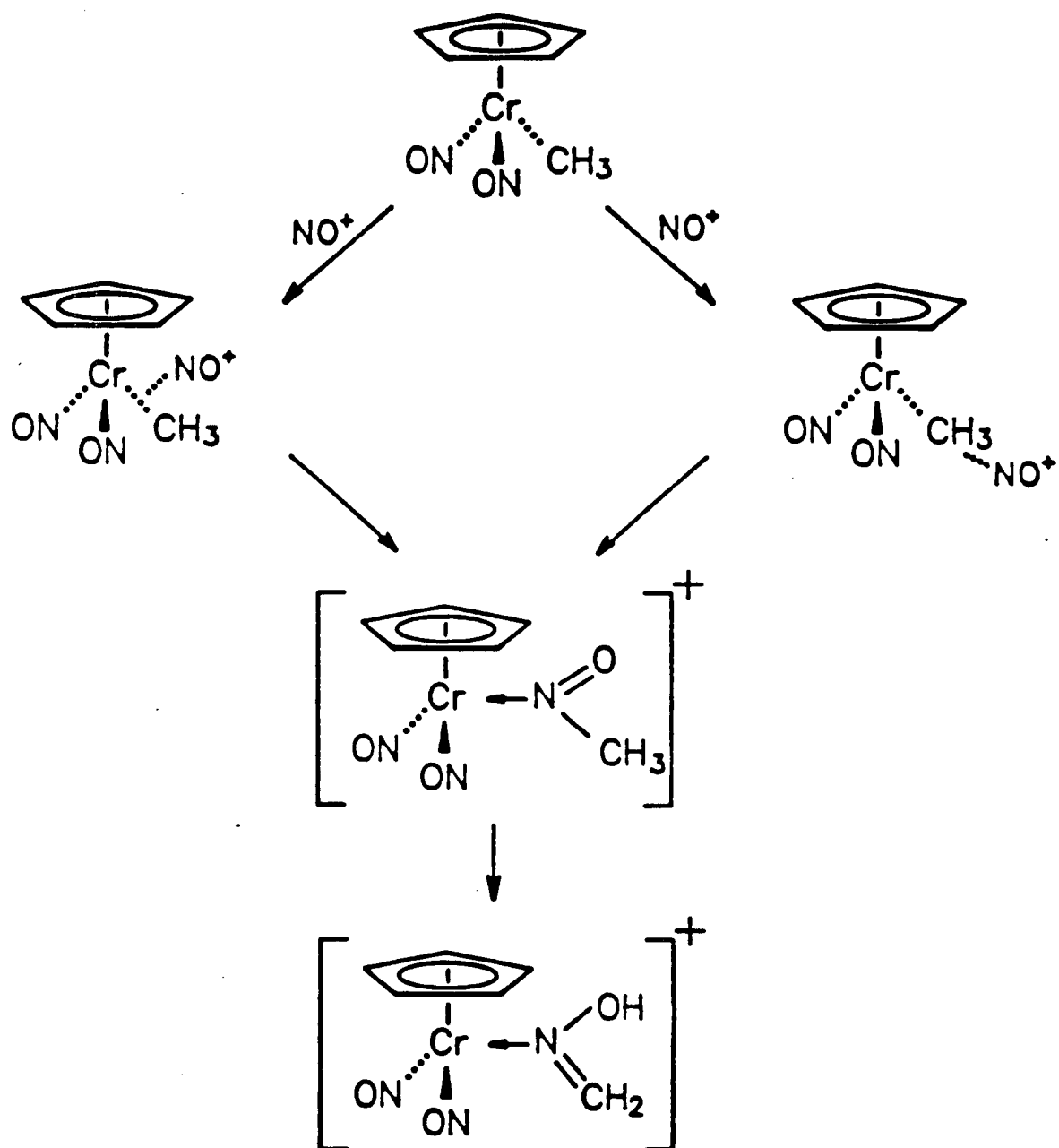


Furthermore, there is no spectroscopic evidence for the formation of the NO-inserted products when $\text{CpCr(NO)}_2\text{CH}_2\text{SiMe}_3$ and $\text{CpCr(NO)}_2\text{Ph}$ are treated in the manner depicted in eqn 3.13. While the exact natures of the organometallic products formed in these latter conversions remain to be ascertained, the

evidence presently at hand thus argues against reactions 3.4 proceeding via the mechanistic steps outlined in eqn 3.12.

(b) Attack of NO^+ at the Metal Center. Another possible mechanistic pathway for the insertion reactions 3.4 involves the direct attack of the NO^+ electrophile at the chromium center in $\text{CpCr}(\text{NO})_2\text{R}$ to initially generate the 20-electron, four-legged "piano-stool" $[\text{CpCr}(\text{NO})_3\text{R}]^+$ intermediate complex (which may attain an 18-electron configuration by adopting either $\eta^3\text{-Cp}$ or bent NO geometries). Subsequent insertion of one of the NO ligands into the Cr-R link may then occur to afford the final $[\text{CpCr}(\text{NO})_2\{\text{N}(\text{O})\text{R}\}]^+$ complex. In this mechanistic pathway, it can be envisaged that either one of the following two possibilities could arise, namely (i) any one of the three NO ligands in $[\text{CpCr}(\text{NO})_3\text{R}]^+$ could insert into the Cr-R bond to yield the insertion product, or (ii) only the incoming NO^+ inserts, a process that necessitates the "preferential activation" of the now-bonded NO^+ electrophile. Clearly, the crucial experiment to perform to unambiguously determine the mode of reaction is the one that involves the use of the ^{15}N -labelled nitrosonium salt, $^{15}\text{NOPF}_6$, in the reactions 3.4. Regrettably, this salt is not readily available, nor are any of its convenient precursors such as $^{15}\text{NOCl}$. It has not been possible, therefore, to demonstrate whether it is the "external" NO^+ or the bound NO that eventually ends up in the Cr-R group.

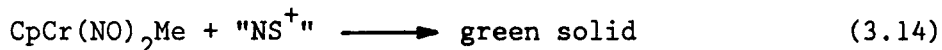
(c) Direct Electrophilic Attack at the Chromium-Carbon Bonds. The third plausible mechanistic pathway for the formation of the NO^+ -inserted products of reactions 3.4 involves charge-controlled, intermolecular attacks by NO^+ at the chromium-carbon σ bonds of the $\text{CpCr}(\text{NO})_2\text{R}$ reactants. Such a pathway is illustrated for $\text{CpCr}(\text{NO})_2\text{Me}$ in Scheme 3.1 in which the attack by NO^+ is



Scheme 3.1

portrayed as being a classical S_E2 process.²⁶ The isomerization of the CH_3NO ligand to bound $CH_2=NOH$ shown in the last step of Scheme 3.1 has already been demonstrated to occur for the perdeuteromethyl analogue (eqn 3.6) and is probably facilitated by the acidic species present in the reaction mixture.²⁷ Note that if this mechanism is indeed operative, then it is the external NO^+ (as opposed to a nitrosyl ligand in the organometallic reactant) that finally is a constituent part of the formaldoxime ligand. In other words, treatment of the various $CpCr(NO)_2R$ complexes with electrophiles NE^+ which are formally valence isoelectronic with NO^+ should result in the insertion of NE^+ (and not NO^+) into the Cr-C σ bonds if mechanisms analogous to that portrayed in Scheme 3.1 hold.

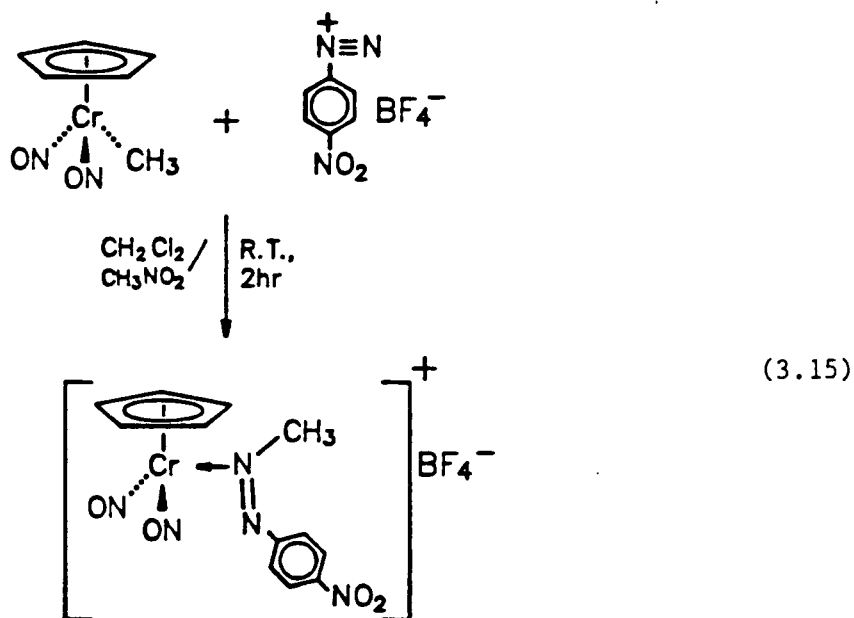
Unfortunately, the reaction of $CpCr(NO)_2Me$ and " NS^+ " (generated in situ) affords a green solid of unknown composition. An IR spectrum of this solid as



a Nujol mull (see Appendix) displays absorptions attributable to ν_{NO} at 1829 and 1723 cm^{-1} , and also to (possibly) ν_{NH} at 3331 cm^{-1} . Unfortunately, this green solid is thermally unstable, decomposing to a brown species slowly in the solid state and rapidly in solutions. This proclivity of the impure complex to decompose has prevented the determination of consistent elemental analyses or acquisition of NMR spectra for it. Its true identity, therefore, remains unknown.

Fortunately, when an aryldiazonium cation (also valence isoelectronic with the nitrosonium cation) is used in place of NS^+ in reaction 3.14, a tractable and thermally stable product is obtained. Thus, treatment of a green

CH_2Cl_2 solution of $\text{CpCr}(\text{NO})_2\text{Me}$ at room temperature with a light orange CH_3NO_2 solution of $[\text{p-O}_2\text{NC}_6\text{H}_4\text{N}_2]^+\text{BF}_4^-$ results in the mixture becoming red-brown in color as the following conversion occurs:



The final product salt is isolable as a green-brown crystalline solid whose spectroscopic properties are consistent with it possessing the molecular structure shown in eqn 3.15. For instance, a Nujol mull IR spectrum of this moderately air-stable solid displays bands at 1605, 1590 and 1560 cm^{-1} that are assignable to the newly-formed diazene ligand. Furthermore, a ^1H NMR spectrum of the complex in CD_3NO_2 (Figure 3.3) exhibits an AX pattern in the δ 8.5-7.2 region due to the protons of a para-substituted phenyl ring, and singlets at δ 6.12 and 4.26 due to the cyclopentadienyl and methyl protons, respectively. To confirm the mode of linkage of the paranitrophenylmethyldiazene ligand to the $\text{CpCr}(\text{NO})_2$ fragment, the salt was subjected to a single-crystal X-ray crystallo-

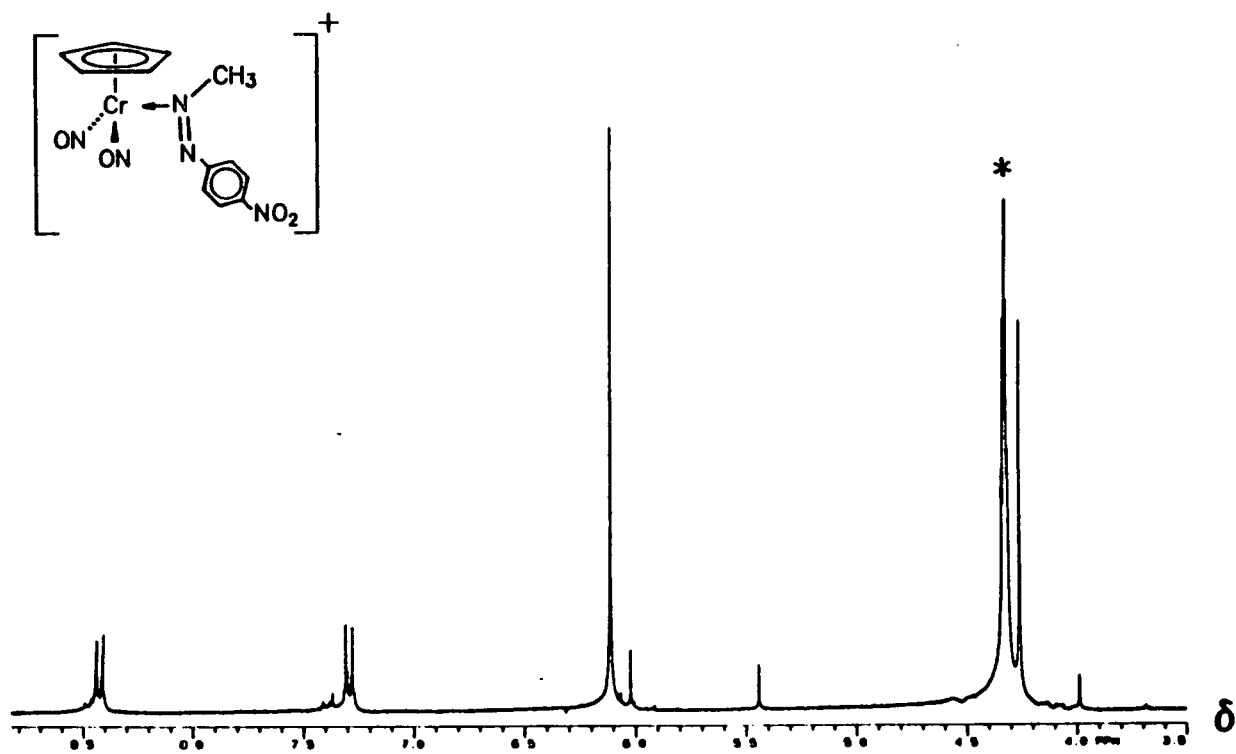


Figure 3.3. The 300 MHz ^1H NMR spectrum of $[\text{CpCr}(\text{NO})_2\{\text{N}(\text{NC}_6\text{H}_4\text{NO}_2)\text{Me}\}]\text{BF}_4$ in CD_3NO_2 (*).

graphic analysis.¹⁵ Two views of the solid-state molecular structure of the organometallic cation are shown in Figure 3.4, and selected intramolecular dimensions of the cation are presented in Table 3.2. As for the formaldoxime-containing cation (*vide supra*), the $\text{CpCr}(\text{NO})_2$ fragment in the $[\text{CpCr}(\text{NO})_2\{\text{N}(\text{NC}_6\text{H}_4\text{NO}_2)\text{Me}\}]^+$ cation is normal, and the internal dimensions of the diazene ligand are fully in accord with it functioning as a Lewis base towards the chromium center.²⁸ Interestingly, the diazene ligand adopts a cis-configuration, probably for steric reasons, and there is no evidence for the existence of the trans-diazene-containing isomer either in the solid state or in solutions. Certainly, the atomic connectivity of the diazene-containing cation in the solid state is consistent with it being formed by the electrophilic attack of external $[\text{p-O}_2\text{NC}_6\text{H}_4\text{NN}]^+$ at the Cr-Me bond $\text{CpCr}(\text{NO})_2\text{Me}$.

The successful incorporation of the aryldiazonium cation into the Cr-Me links thus suggests that the formal NO^+ insertion into this and related $\text{CpCr}(\text{NO})_2\text{R}$ compounds (eqn 3.4) also probably proceeds by direct electrophilic attack as depicted in Scheme 3.1 for $\text{R} = \text{Me}$.

A Stoichiometric Cycle for the Formation of New Carbon-Nitrogen Bonds.

As pointed out in the preceding sections, the newly-formed nitrosoalkane and diazene ligands in the cationic products of transformations 3.4 and 3.15 may be simply viewed as Lewis bases coordinated to the cationic metal center. Consequently, they should, in principle, be displaceable from the chromium's coordination sphere by other, more strongly coordinating two-electron donors. For practical reasons, I have found that the chloride anion is the Lewis base of choice for effecting these displacement reactions. For example, treatment of a red dichloromethane solution of $[\text{CpCr}(\text{NO})_2\{\text{N}(\text{O})\text{Ph}\}]^+$ at 20°C with one equiva-

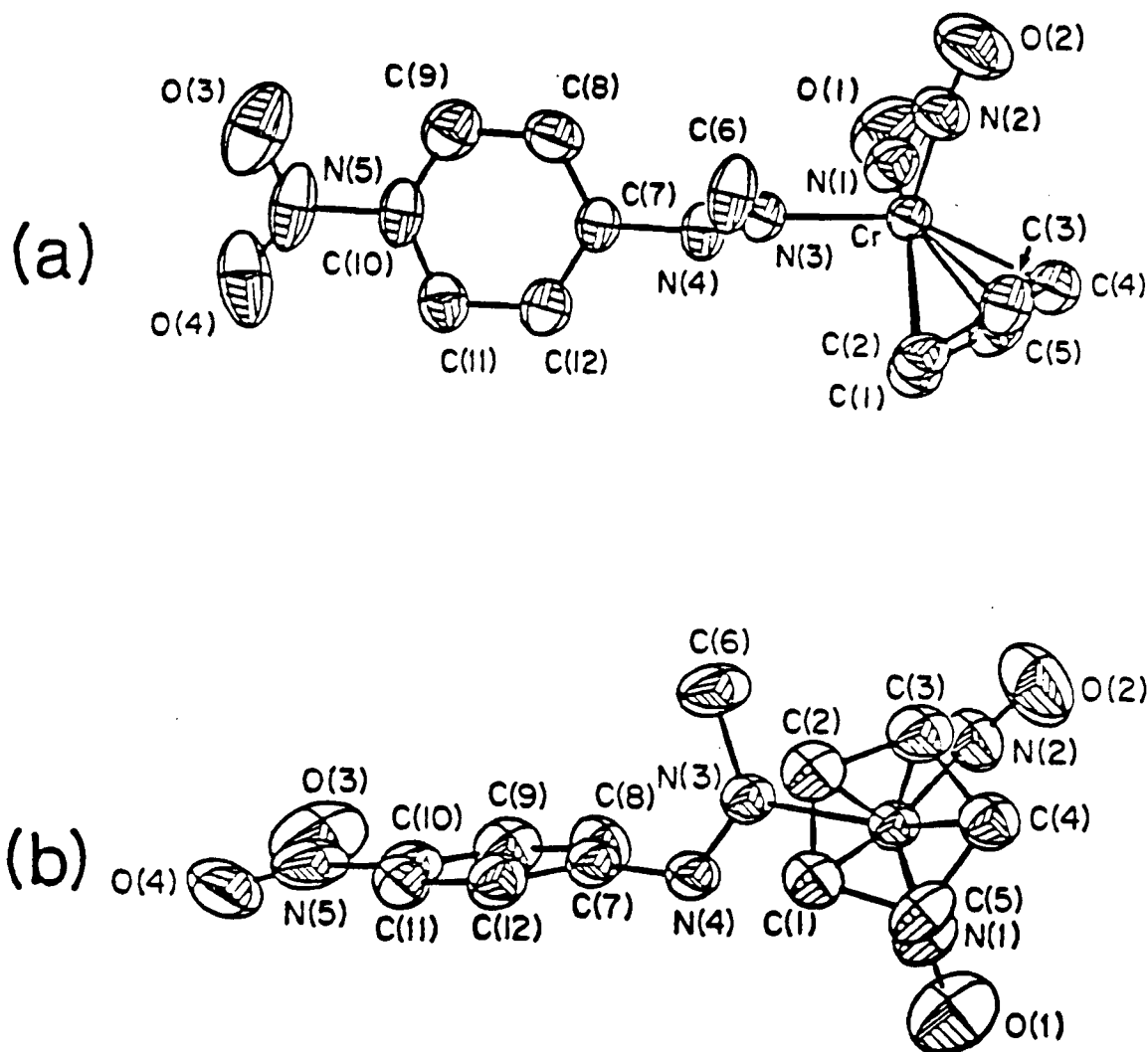
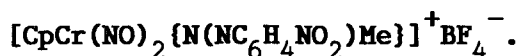


Figure 3.4. Views of the molecular structure of the $[\text{CpCr}(\text{NO})_2\{\text{N}(\text{NC}_6\text{H}_4\text{NO}_2)\text{Me}\}]^+$ cation (a) approximately parallel to the Cp ligand and (b) approximately perpendicular to the Cp ligand. Only non-hydrogen atoms are shown.

Table 3.2. Selected Bond Lengths (Å) and Angles (deg) for



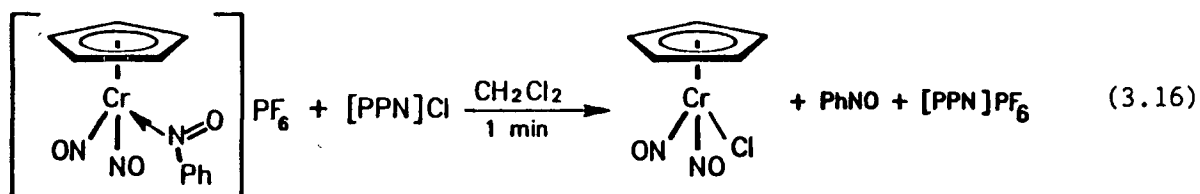
Cr - N(1)	1.709(5)	Cr - N(2)	1.699(5)
Cr - N(3)	2.057(4)	Cr - C(1)	2.191(5)
Cr - C(2)	2.201(5)	Cr - C(3)	2.212(5)
Cr - C(4)	2.181(5)	Cr - C(5)	2.189(5)
N(1) - O(1)	1.152(7)	N(2) - O(2)	1.167(7)
N(3) - N(4)	1.225(6)	N(3) - C(6)	1.478(7)
N(4) - C(7)	1.450(6)	C(7) - C(12)	1.375(8)
C(7) - C(8)	1.374(8)	C(12) - C(11)	1.397(8)
C(11) - C(10)	1.368(9)	C(8) - C(9)	1.371(8)
C(9) - C(10)	1.368(10)	C(10) - N(5)	1.490(7)
N(5) - O(3)	1.218(11)	N(5) - O(4)	1.213(11)
C(1) - C(2)	1.383(9)	C(2) - C(3)	1.389(9)
C(3) - C(4)	1.413(10)	C(4) - C(5)	1.409(9)
C(5) - C(1)	1.396(9)		
N(1) - Cr - N(2)	95.6(3)°	N(1) - Cr - N(3)	95.3°(2)
N(2) - Cr - N(3)	97.8(2)	Cr - N(1) - O(1)	173.2(5)
Cr - N(2) - O(2)	172.4(5)	Cr - N(3) - C(6)	120.4(3)
Cr - N(3) - N(4)	118.1(3)	N(4) - N(3) - C(6)	121.5(4)
N(3) - N(4) - C(7)	121.3(4)	N(4) - C(7) - C(12)	117.8(5)
N(4) - C(7) - C(8)	119.7(5)	C(12) - C(7) - C(8)	121.9(5)
C(7) - C(12) - C(11)	118.9(5)	C(12) - C(11) - C(10)	117.7(5)
C(11) - C(10) - C(9)	123.7(5)	C(10) - C(9) - C(8)	118.3(6)

continued...

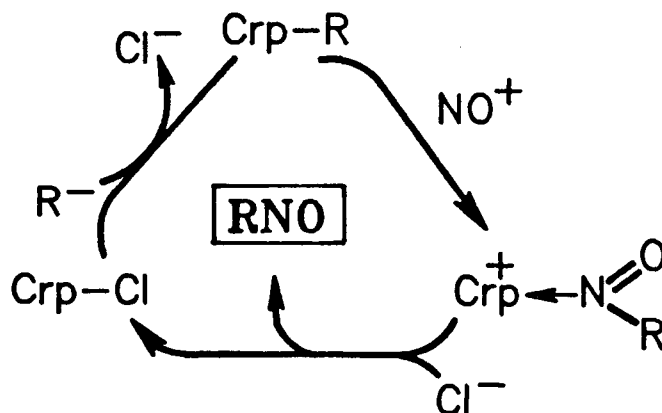
Table 3.2. (continued)

C(7) - C(8) - C(9)	119.6(5)	C(11) - C(10) - N(5)	117.9(6)
C(9) - C(10) - N(5)	118.4(6)	C(10) - N(5) - O(3)	117.7(7)
C(10) - N(5) - O(4)	118.3(7)	O(3) - N(5) - O(4)	124.0(6)
C(1) - C(2) - C(3)	109.2(5)	C(2) - C(3) - C(4)	107.3(5)
C(3) - C(4) - C(5)	107.6(5)	C(4) - C(5) - C(1)	107.6(5)
C(5) - C(1) - C(2)	108.3(5)		

lent of bis(triphenylphosphine)iminium chloride ([PPN]Cl) results in the reaction mixture rapidly becoming green. Monitoring the progress of this transformation by IR spectroscopy reveals the clean conversion of the organometallic reactant to $\text{CpCr}(\text{NO})_2\text{Cl}$ (ν_{NO} at 1817 and 1711 cm^{-1}) and the formation of free nitrosobenzene (diagnostic bands at 1506 and 1439 cm^{-1}). The balanced chemical equation for this process is thus



the nitrosobenzene being isolable from the final reaction mixture by sublimation after removal of the CH_2Cl_2 solvent in vacuo. The success of reaction 3.16 thus permits the construction of a cycle of stoichiometric reactions for the formation of new carbon-nitrogen bonds mediated by the $\text{CpCr}(\text{NO})_2$ group. Such a cycle is shown below for the particular case of NO^+ insertion, Crp representing the $\text{CpCr}(\text{NO})_2$ group:



Thus, when $R = \text{Ph}$, reaction 3.16 is shown at the bottom of the cycle. The $\text{CpCr}(\text{NO})_2\text{Cl}$ by-product of this reaction may be reconverted to the original $\text{CpCr}(\text{NO})_2\text{Ph}$ reactant simply by treatment with Ph_3Al ,⁷ and the insertion of NO^+ may then be effected again. In principle, cycles similar to that shown above should also hold for $R = \text{Me}$ or CH_2SiMe_3 and for $[\text{p-O}_2\text{NC}_6\text{H}_4\text{N}_2]^+$ as the electrophile in place of NO^+ . Preliminary investigations indicate that this is indeed true and that it usually is not necessary to isolate the intermediate insertion products. Thus, sequential treatment of $\text{CpCr}(\text{NO})_2\text{Ph}$ with $[\text{p-O}_2\text{NC}_6\text{H}_4\text{N}_2]\text{BF}_4$ and then $[\text{PPN}]\text{Cl}$ affords good yields of the unsymmetrical diazene, $\text{p-O}_2\text{NC}_6\text{H}_4\text{N}=\text{NPh}$, and $\text{CpCr}(\text{NO})_2\text{Cl}$.

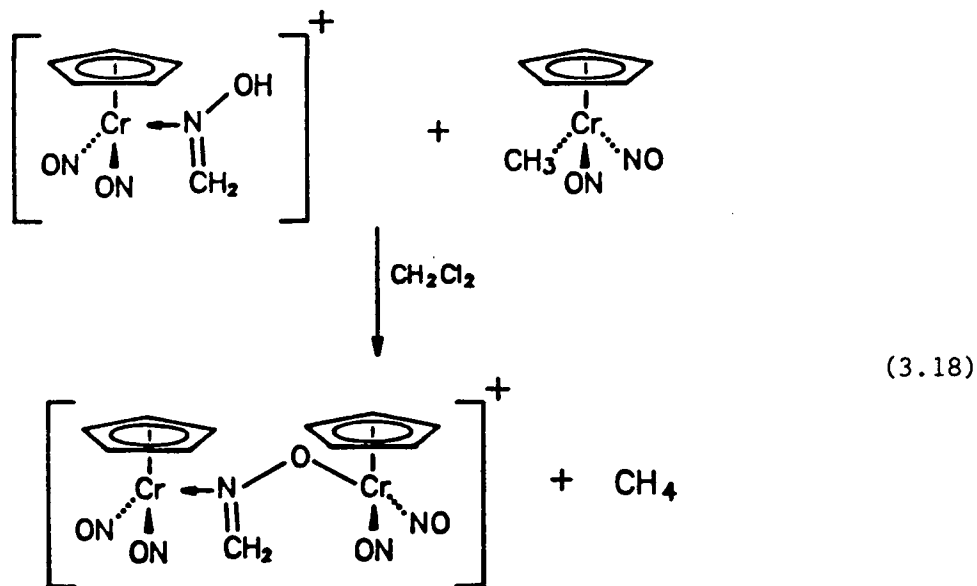
The net organic transformations mediated by the $\text{CpCr}(\text{NO})_2\text{R}$ groups in cycles such as that shown above are thus



where NE^+ is the external nitrogen-containing electrophile and R^- is the organic group initially σ -bonded to chromium. The final N(E)R product is formed selectively, the new C-N linkage being generated exclusively at the carbon atom originally attached to the metal center.²⁹

Deprotonation of the Formaldoxime Ligand in $[\text{CpCr}(\text{NO})_2\{\text{N}(\text{OH})\text{CH}_2\}]\text{PF}_6$.

Interestingly, the $[\text{CpCr}(\text{NO})_2\{\text{N}(\text{OH})\text{CH}_2\}]\text{PF}_6$ compound reacts with $\text{CpCr}(\text{NO})_2\text{Me}$ to generate an unprecedented type of an oximato-bridged bimetallic complex. The specific transformation being considered is presented in eqn 3.18:



This bimetallic complex is air-stable and is most soluble in good solvating solvents such as nitromethane.

Single-crystal X-ray crystallographic analysis¹⁵ of the dichromium cation (as its BPh_4^- salt) revealed a new type of an oximato-bridged molecular structure (Figure 3.5). The intramolecular dimensions of the bimetallic cation (Table 3.3) indicate two structurally normal $\text{CpCr}(\text{NO})_2$ groups¹⁶ held together

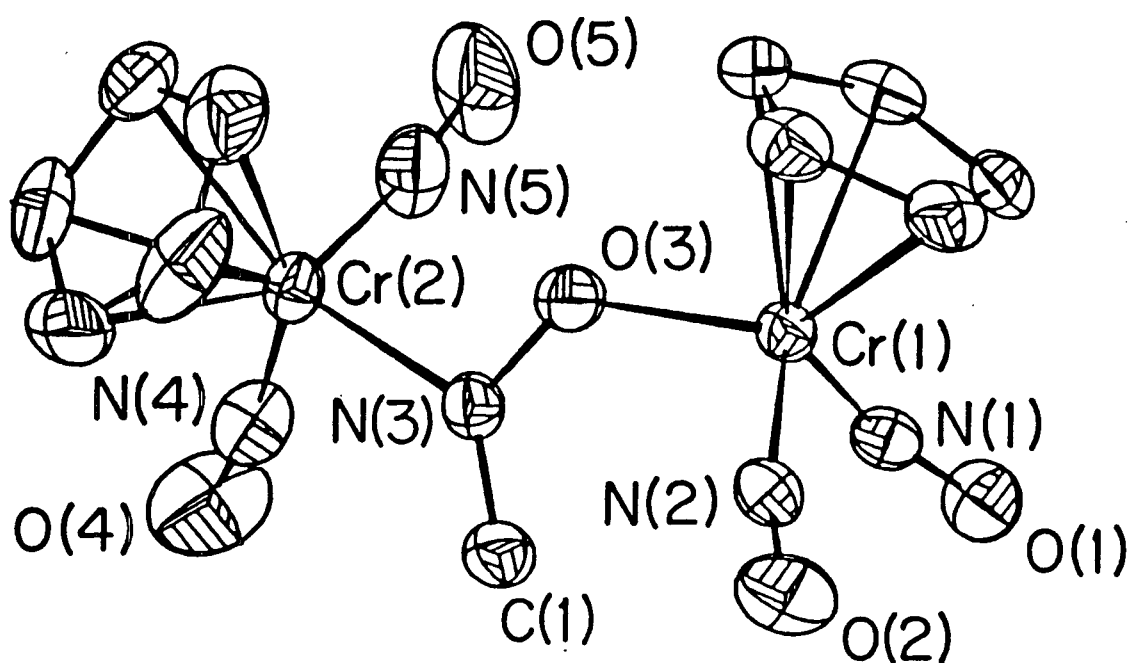


Figure 3.5. Solid-state molecular structure of the $[\{\text{CpCr}(\text{NO})_2\}_2\{\mu,\eta^2\text{-N}(\text{CH}_2)\text{O}\}]^+$ cation as it exists in its BPh_4^- salt. Hydrogen atoms have been omitted for clarity.

Table 3.3. Selected Bond Lengths (Å) and Angles (deg) for the

$[\{\text{CpCr}(\text{NO})_2\}_2\{\mu,\eta^2\text{-N}(\text{CH}_2)_2\text{O}\}]^+$ cation as it exists in its BPh_4^- salt.

Cr(1) - N(1) = 1.725(4)	N(1) - O(1) = 1.169(5)
Cr(1) - N(2) = 1.718(4)	N(2) - O(2) = 1.174(5)
Cr(1) - O(3) = 1.956(3)	N(3) - O(3) = 1.348(5)
Cr(2) - N(3) = 2.206(4)	N(3) - C(1) = 1.282(4)
Cr(2) - N(4) = 1.714(4)	N(4) - O(4) = 1.160(5)
Cr(2) - N(5) = 1.706(5)	N(5) - O(5) = 1.170(6)
N(1) - Cr(1) - N(2) = 94.5(2)	Cr(1) - N(1) - O(1) = 165.7(4)
N(1) - Cr(2) - O(3) = 103.6(2)	Cr(1) - O(3) - N(3) = 128.5(5)
N(3) - Cr(2) - N(4) = 99.9(2)	Cr(2) - N(3) - O(3) = 109.3(3)
N(4) - Cr(2) - N(5) = 94.2(3)	Cr(2) - N(4) - O(4) = 171.7(4)

only by single bonds to the N and O atoms of the formaldoximato ligand, respectively. All other structurally characterized bimetallic complexes having an oximato ligand spanning the two metal centers possess a metal-metal bond.^{30,31} The spectroscopic properties of the $[(\text{CpCr}(\text{NO})_2)_2\{\mu, \eta^2\text{-N}(\text{CH}_2)\text{O}\}]^+$ cation (as its more soluble PF_6^- salt) are readily interpretable in terms of its solid-state molecular structure, a fact which indicates that the basic dichromium structural units persist in solutions. For example, the ^1H NMR spectrum of the compound in CD_2Cl_2 is shown in Figure 3.6 and contains signals due to the methylene and cyclopentadienyl protons (see Experimental Section for details).

Particularly interesting is the ^{13}C NMR spectrum of the compound in CD_3NO_2 (Figure 3.7) which exhibits two Cp carbon signals at δ 105.94 and 105.06. Each appears as a doublet of quintets because of short-range ^{13}C - ^1H coupling of 182 Hz and long-range coupling of 6.5 Hz to the four other protons of the Cp ring. Furthermore, the signal due to the methylene carbon of the bridging formaldoximato group appears as a doublet of doublets at δ 153.33 ($^1J_{^{13}\text{C}-^1\text{H}} = 185, 173$ Hz), the coupling constants being fully consistent with this carbon retaining its sp^2 hybridization.^{32,33}

The sequence of reactions leading to the production of the oximato-bridged bimetallic complex may thus be represented as

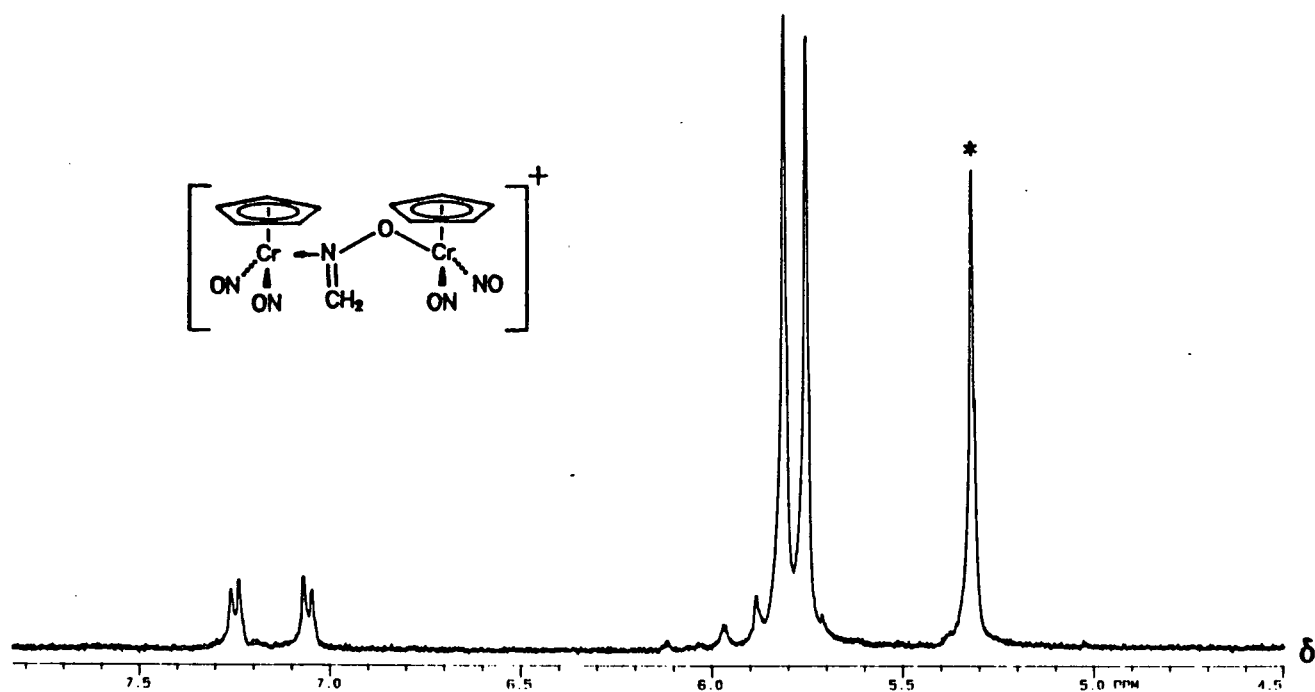


Figure 3.6. The 300 MHz ^1H NMR spectrum of $[\{\text{CpCr}(\text{NO})_2\}_2\{\mu, \eta^2\text{-N}(\text{CH}_2)\text{O}\}]\text{PF}_6$ in CD_2Cl_2 .

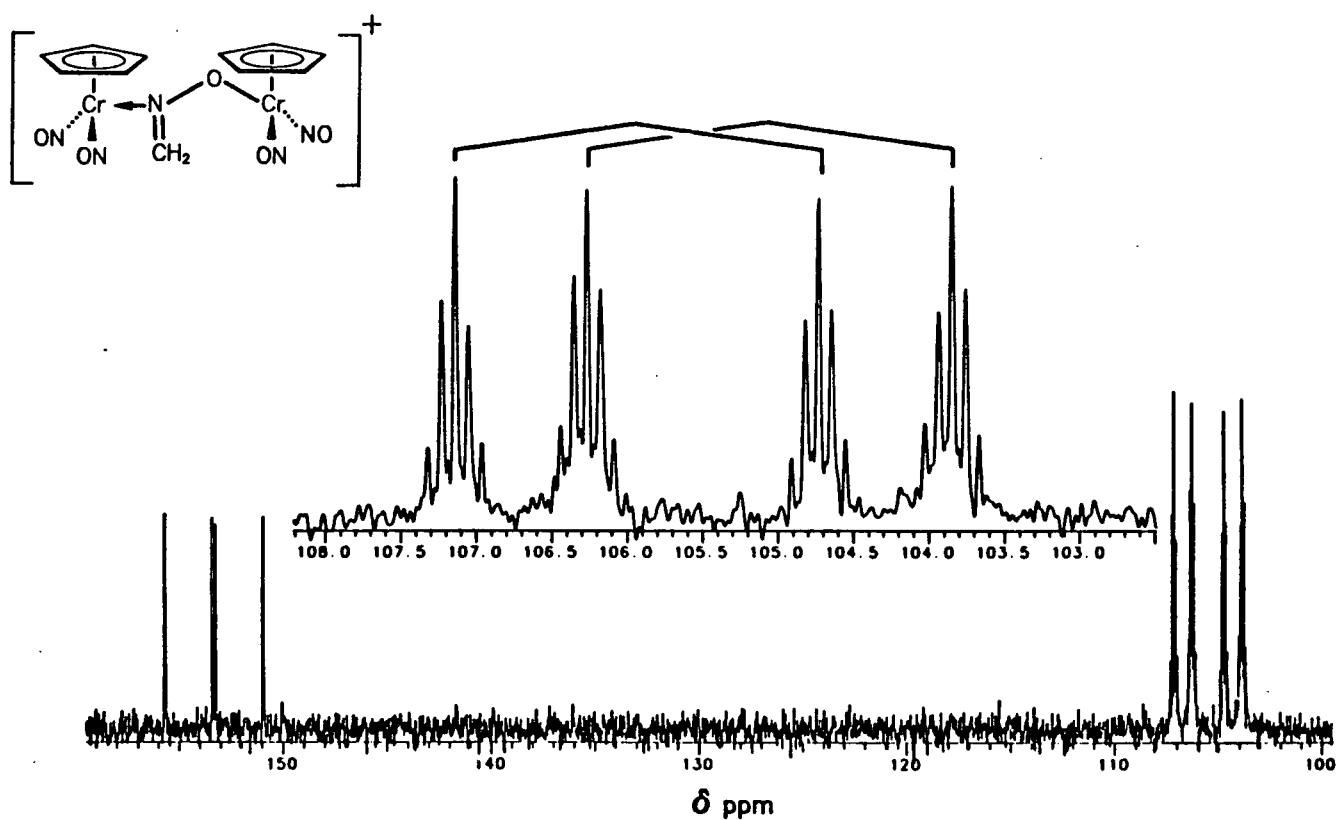
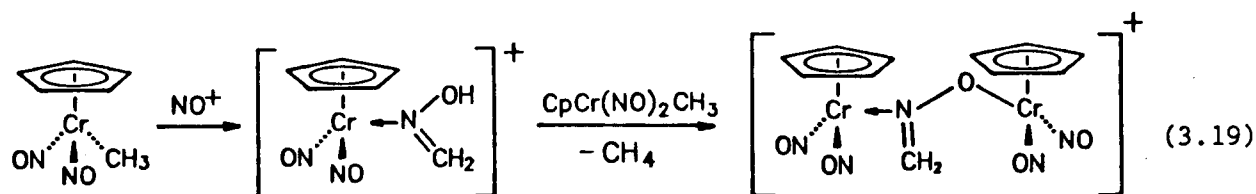
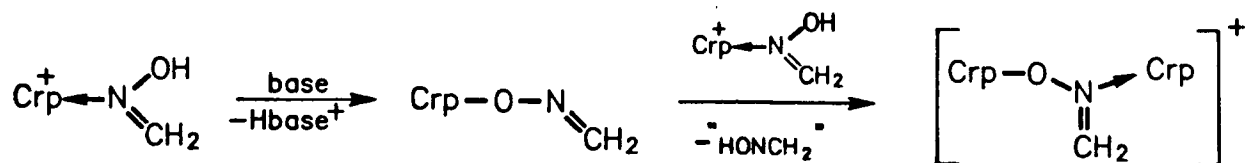


Figure 3.7. The 75 HMz ^{13}C NMR spectrum of $[\{\text{CpCr}(\text{NO})_2\}_2\{\mu, \eta^2\text{-N}(\text{CH}_2)\text{O}\}]\text{PF}_6$ in CD_3NO_2 . The inset contains an expansion of the signals due to the Cp carbons at δ 105.94 and 105.06 ppm.



Certainly, the occurrence of reaction 3.18 explains why low yields of the formaldoxime complex are obtained³ (during its synthesis from CpCr(NO)₂Me and NOPF₆, vide supra) if (a) an excess of CpCr(NO)₂Me is used or (b) the insoluble NOPF₆ is not finely ground (in effect causing (a) locally).

Also, the occurrence of reaction 3.18 is of fundamental significance since free oximes such as diacetyl monoxime (pK_a = 9.3)³⁴ or even carboxylic acids such as p-fluorobenzoic acid (pK_a = 4.14)³⁵ do not react with CpCr(NO)₂Me under identical experimental conditions. The role of the electrophilic [CpCr(NO)₂]⁺ cation in activating formaldoxime by coordination is thus to increase substantially its Brønsted acidity above that which it possesses in its free state. Once activated, the bound formaldoxime can then undergo deprotonation by CpCr(NO)₂Me to afford the observed products.³⁶ Surprisingly, the reaction of [CpCr(NO)₂{N(OH)CH₂}]PF₆ with Proton Sponge also results in the production of the oximato-bridged bimetallic complex (in 55% yield based on Cr). This transformation occurs presumably via the initial formation of CpCr(NO)₂-ON=CH₂ (IR ν_{NO} 1800 and 1690 cm⁻¹) which then readily displaces the formaldoxime ligand in unreacted [CpCr(NO)₂{N(OH)CH₂}]⁺ as shown in Scheme 3.2.



Scheme 3.2

Regrettably, attempts to isolate the intermediate $\text{CpCr}(\text{NO})_2\text{-ON=CH}_2$ compound have not been fruitful.

Summary

The NE^+ electrophiles ($\text{E} = \text{O}$ or $\text{p-O}_2\text{NC}_6\text{H}_4\text{N}$) undergo unprecedented insertions into the Cr-C σ bonds of various $\text{CpCr}(\text{NO})_2\text{R}$ compounds to afford $[\text{CpCr}(\text{NO})_2\{\text{N(E)R}\}]^+$ cationic complexes. When $\text{R} = \text{Me}$ and $\text{E} = \text{O}$, the initially formed product isomerizes intramolecularly to $[\text{CpCr}(\text{NO})_2\{\text{N(OH)CH}_2\}]^+$, which then reacts further with $\text{CpCr}(\text{NO})_2\text{Me}$ to give the oximato-bridged complex, $[\{\text{CpCr}(\text{NO})_2\}_2\{\mu, \eta^2\text{-N(CH}_2\text{)O}\}]^+$. At present, it appears that the $\text{CpCr}(\text{NO})_2\text{R}$ compounds undergo the requisite insertion of NE^+ into the Cr-R bonds because these bonds are prone to non-oxidative attack by electrophiles and the compounds themselves are relatively difficult to oxidize. Nevertheless, the newly-formed N(E)R ligands may be displaced from the chromium's coordination sphere by the more strongly coordinating Cl^- anion. The resulting $\text{CpCr}(\text{NO})_2\text{Cl}$ can be reconverted to $\text{CpCr}(\text{NO})_2\text{R}$ by treatment with the appropriate Grignard or

organoaluminum reagent, thereby completing a cycle by regenerating the initial organometallic reactant. The entire sequence of stoichiometric reactions forming the cycle thus constitutes a selective method for the formation of new carbon-nitrogen bonds, the net organic conversions mediated by the $\text{CpCr}(\text{NO})_2$ group being $\text{NE}^+ + \text{R}^- \rightarrow \text{N(E)R}$. In principle, therefore it should be possible to broaden the scope of this synthetic methodology by extending this chemistry to encompass a wide range of $\text{CpCr}(\text{NO})_2$ -containing organometallic complexes and other electrophiles.

References and Notes

- (1) Collman, J. P.; Hegedus, L. S.; Norton, J. R.; Finke, R. G. *Principles and Applications of Organotransition Metal Chemistry*; University Science Books: Mill Valley, CA, 1987.
- (2) Alexander, J. J. In *The Chemistry of the Metal-Carbon Bond*; Hartley, F. R.; Patai, S., Eds.; Wiley: Toronto, 1985; Vol. 2, Chapter 5.
- (3) Legzdins, P.; Wassink, B.; Einstein, F. W. B.; Willis, A. C. *J. Am. Chem. Soc.* **1986**, *108*, 317.
- (4) Goldhaber, A.; Vollhardt, K. P. C.; Walborsky, E. C.; Wolfgruber, M. *J. Am. Chem. Soc.* **1986**, *108*, 516.
- (5) Migratory insertions of neutral nitric oxide into transition-metal-carbon bonds also result in the formation of new C-N linkages.⁶
- (6) Seidler, M. D.; Bergman, R. G. *J. Am. Chem. Soc.* **1984**, *106*, 6110 and references therein.
- (7) Hoyano, J. K.; Legzdins, P.; Malito, J. T. *J. Chem. Soc., Dalton Trans.* **1975**, 1022.
- (8) Hoyano, J. K.; Legzdins, P.; Malito, J. T. *Inorg. Synth.* **1978**, *18*, 126.
- (9) Whitmore, F. C.; Sommer, L. H. *J. Am. Chem. Soc.* **1946**, *68*, 481.
- (10) Herberhold, M.; Haumaier, L. *Organomet. Synth.* **1986**, *3*, 281.
- (11) Balz, G.; Schiemann, G. *Chem. Ber.* **1927**, *60*, 1186.
- (12) Using a DBI-30W (5 μ) column at 5° C and a Kratos MS-80 mass spectrometer.

- (13) For comparison, free MeNO exhibits a ν_{NO} of 1564 cm^{-1} ; see Feuer, H. *The Chemistry of the Nitroso and Nitro Groups*; Wiley-Interscience: Toronto, 1969; Vol. 1, p. 140.
- (14) Drago, R. S. *Pure Appl. Chem.* **1980**, *52*, 2261.
- (15) The X-ray structural analysis was performed by Drs. F. W. B. Einstein and R. H. Jones of Simon Fraser University.
- (16) Greenhough, T. J.; Kolthammer, B. W. S.; Legzdins, P.; Trotter, J. *Acta Crystallogr., Sect. B* **1980**, *B36*, 795.
- (17) Levine, I. N. *J. Chem. Phys.* **1963**, *38*, 2326.
- (18) Boyd, A. S. F.; Browne, G.; Gowenlock, B. G.; McKenna, P. J. *Organomet. Chem.* **1988**, *345*, 217 and references therein.
- (19) For leading references to other RNO complexes of transition metals, see (a) Stella, S.; Floriani, C.; Chiesi-Villa, A.; Guastini, C. *J. Chem. Soc., Dalton Trans.* **1988**, 545. (b) Pizzotti, M.; Porta, F.; Cenini, S.; Demartin, F.; Masciocchi, N. *J. Organomet. Chem.* **1987**, *330*, 265 and references therein.
- (20) Caulton, K. G. *Coord. Chem. Rev.* **1975**, *14*, 317.
- (21) Related oxidatively promoted alkyl to acyl migratory insertions involving CpFe(CO)(L)Me complexes which are isoelectronic with $\text{CpCr(NO)}_2\text{Me}$ have been documented: see Magnuson, R. H.; Meirowitz, R.; Zulu, S.; Giering, W. P. *J. Am. Chem. Soc.* **1982**, *104*, 5790 and references therein.
- (22) All three complexes undergo reversible 1-electron reductions in CH_2Cl_2 . For $\text{CpCr(NO)}_2\text{CH}_2\text{SiMe}_3$ this redox couple occurs at $E^{\circ'} = -1.03 \text{ V}$, and for $\text{CpCr(NO)}_2\text{Ph}$ this occurs at $E^{\circ'} = -1.07 \text{ V}$. The reduction behaviour of the $\text{CpCr(NO)}_2\text{Me}$ compound has been analyzed in some detail previously,

- see: Legzdins, P.; Wassink, B. *Organometallics* **1988**, *7*, 482.
- (23) Connelly, N. G.; Demidowicz, Z.; Kelly, R. L. *J. Chem. Soc., Dalton Trans.* **1975**, 2335.
- (24) Rieger, P. H. *Electrochemistry*; Prentice-Hall: Englewood Cliffs, NJ, 1987; p. 455.
- (25) The $\text{Fe}(\text{phen})_3^{3+}/\text{Fe}(\text{phen})_3^{2+}$ redox couple is also reported to be at +1.83 V in CH_3CN , see: Schmid, R.; Kirchner, K.; Dickert, F. L. *Inorg. Chem.* **1988**, *27*, 1530.
- (26) Rogers, W. N.; Page, J. A.; Baird, M. C. *Inorg. Chem.* **1981**, *20*, 3521 and references therein.
- (27) Boyer, J. H. In *The Chemistry of the Nitro and Nitroso Groups*; Feuer, H., Ed.; Wiley-Interscience: Toronto, 1969; Part 1.
- (28) Einstein, F. W. B.; Sutton, D.; Tyers, K. G. *Inorg. Chem.* **1987**, *26*, 111 and references therein.
- (29) For comparison, PhMgCl reacts with NOCl to produce diphenylamine (Ph_2NH) and not the expected PhNO .^{29a} Also, the reaction of PhCH_2MgCl (or $t\text{-BuMgCl}$) with $[\text{p-R-C}_6\text{H}_4\text{N}_2]\text{BF}_4$ ($\text{R} = \text{H, Me, OMe, NO}_2, \text{COMe}$) results in the elimination of N_2 and the production of coupled products such as $\text{pRC}_6\text{H}_4\text{CH}_2\text{Ph}$ and $\text{p-RC}_6\text{H}_4\text{-C}_6\text{H}_4\text{R}$,^{29b} see: (a) Marsh, P. G. *Diss. Abstr. Int. B.* **1975**, *35(8)*, 3838. (b) Singh, P. R.; Khanna, R. K.; Jayaraman, B. *Tetrahedron Lett.* **1982**, *23*, 5475.

- (30) (a) Khare, G. P.; Doedens, R. J. *Inorg. Chem.* **1976**, *15*, 86.
(b) Aime, S.; Gervasio, G.; Milone, L.; Rossetti, R.; Stanghellini, P. L. *J. Chem. Soc., Chem. Commun.* **1976**, 370.
- (31) For an example of a monometallic complex containing a bidentate oximate ligand, see: Khare, G. P.; Doedens, R. J. *Inorg. Chem.* **1977**, *16*, 907.
- (32) (a) Levy, G. C.; Lichter, R. L.; Nelson, G. L. *Carbon-13 Nuclear Magnetic Resonance Spectroscopy* 2nd ed.; John Wiley and Sons: New York, 1980. (b) Mann, B. E.; Taylor, B. F. ¹³C NMR Data for Organometallic Compounds; Academic: London, England, 1981. (c) Becker, E. B. *High Resolution NMR: Theory and Chemical Applications*, 2nd ed.; Academic: New York, 1980.
- (33) The related Cp^{*}Ru(PMe₃)₂-ON=CH(Me) compound has been assigned its structure on the basis of the magnitude of this ¹³C-H coupling constant.⁶
- (34) Krueger, P. J. In *The Chemistry of the Hydrazo, Azo and Azoxy Groups*, Part 1; Patai, S., Ed; Wiley-Interscience: New York, 1975, p. 167.
- (35) Dean, J. A. *Handbook of Organic Chemistry*; McGraw-Hill: New York, 1987, Section 8.
- (36) Cp₂Zr(Cl)Me has also been employed recently to deprotonate other organic groups bound to organotransition-metal centers.³⁷
- (37) Tso, C. T.; Cutler, A. R. *J. Am. Chem. Soc.* **1986**, *108*, 6069.

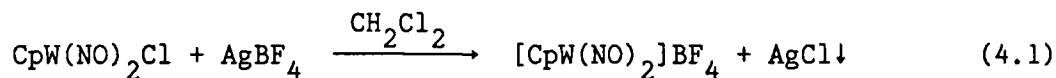
CHAPTER 4

Some Characteristic Chemistry of the Electrophilic $[\text{Cp}'\text{M}(\text{NO})_2]\text{BF}_4$

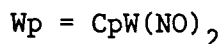
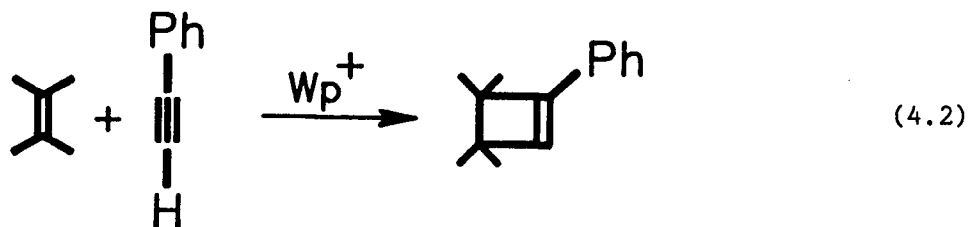
Complexes ($\text{Cp}' = \text{Cp}$ or Cp^* ; $\text{M} = \text{Cr}, \text{Mo}$ or W)

Introduction

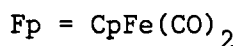
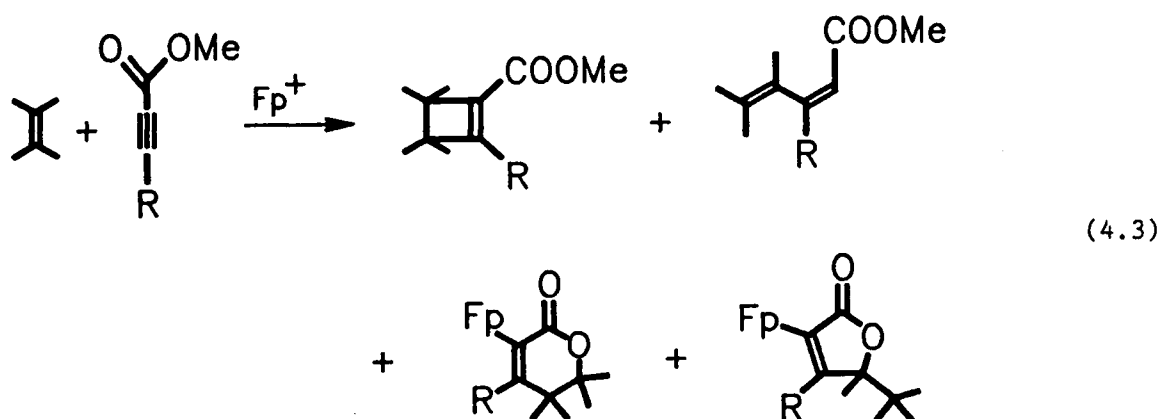
The $[\text{CpW}(\text{NO})_2]^+$ cation is a versatile organometallic electrophile.¹ It is generated by the reaction of the chloro precursor with AgBF_4 as shown in equation 4.1



and is best formulated as a coordinatively unsaturated 16-electron compound, although it may incorporate a solvent molecule into the tungsten's coordination sphere.¹ Not surprisingly, it readily forms 1:1 adducts with various 2-electron donor ligands such as phosphines and phosphites.^{1,2} Curiously, the only isolable olefin adduct of this cationic compound is $[\text{CpW}(\text{NO})_2(\eta^2\text{-C}_8\text{H}_{14})]\text{BF}_4$ (C_8H_{14} = cyclooctene).^{1,3} Other unsaturated hydrocarbons simply do not react with $[\text{CpW}(\text{NO})_2]^+$, or undergo dimerization or isomerization probably via the electrophile-induced formation of carbocations. Furthermore, 2,3-dimethyl-2-butene and phenylacetylene undergo a rapid $[2 + 2]$ cycloaddition reaction in the presence of $[\text{CpW}(\text{NO})_2]^+$ to form the cyclobutene shown in equation 4.2.⁴



Several years ago, Rosenblum and coworkers reported that some olefins and acetylenic esters condense in the presence of the $[\text{CpFe}(\text{CO})_2]^+$ cation (commonly referred to as the Fp^+ cation) to yield cyclobutenes, 1,3-dienes and some $\text{Fp}(\eta^1\text{-lactone})$ products, as shown in the general equation 4.3.^{5,6}



As mentioned in Chapter 3 of this thesis, the Fp^+ cation is valence isoelectronic with $[\text{Cp}'\text{M}(\text{NO})_2]^+$ ($\text{Cp}' = \text{Cp}$ or Cp^* ; $\text{M} = \text{Cr}, \text{Mo}$ or W). Prompted by Rosenblum's report, I decided to attempt transformations analogous to reactions 4.3 by employing the isoelectronic $[\text{Cp}'\text{M}(\text{NO})_2]^+$ complexes. In this Chapter, I present the results of this study, and also describe the chemistry of some of the $[\text{Cp}'\text{M}(\text{NO})_2]^+$ cationic complexes that further delineates their electrophilic character.

Experimental Section

All reactions and subsequent manipulations were performed under anaerobic and anhydrous conditions unless specified otherwise. General experimental procedures employed in this study were the same as those described in the preceding two chapters. Methyl propiolate (99%), 2,3-dimethyl-2-butene (98%), AgBF_4 and NaBPh_4 (Gold label) were purchased from Aldrich and were used without further purification. Isobutylene (C.P. grade) was purchased from Matheson Gas Company. The $\text{CpM}(\text{NO})_2\text{Cl}$ compounds ($\text{M} = \text{Cr}, \text{Mo}$ or W)⁷ and $\text{Cp}^*\text{W}(\text{NO})_2\text{Cl}$ ¹ were prepared by published procedures. The $\text{Cp}^*\text{M}(\text{NO})_2\text{Cl}$ compounds for Cr and Mo were synthesized in a manner similar to that employed for the W analogue, and their purity was checked by elemental analyses. Preparatory gas chromatography was performed on a Varian Model 90-P gas chromatograph, and GC-MS samples were run on a Varian Vista 6000 gas chromatograph interfaced with a Nermag R10-10 quadrupole mass spectrometer with the assistance of Ms. C.M. Moxham.

Preparation of $[\text{Cp}'\text{M}(\text{NO})_2]\text{BF}_4$ ($\text{Cp}' = \text{Cp}$ or Cp^* ; $\text{M} = \text{Cr}, \text{Mo}$ or W). These complexes were prepared by treating CH_2Cl_2 solutions of their $\text{Cp}'\text{M}(\text{NO})_2\text{Cl}$ precursors with AgBF_4 in the manner described previously for $\text{M} = \text{W}$.¹ The reactions were monitored by IR spectroscopy and took 15 to 45 min to go to completion. (The IR data for these complexes are listed in Table 4.1.) In each case, the conversion was clean (by IR) and assumed to be quantitative. The AgCl precipitate was removed by filtration through a medium-porosity frit, and the filtrates were then allowed to react with the desired organic substrates.

Reaction of $[\text{CpW}(\text{NO})_2]\text{BF}_4$ with Isobutylene. To a cold, green dichloromethane solution (-10°C , 40 mL) of $[\text{CpW}(\text{NO})_2]\text{BF}_4$ (4 mmol) was added an

excess of isobutylene (25 mL, ~60 fold excess, previously condensed and maintained at -78°C). The reaction mixture was stirred for 2.5 h while being maintained at $\sim -10^{\circ}\text{C}$. After this period, the reaction mixture was filtered through alumina (3 x 4 cm, Woelm neutral, activity 1) supported on a medium-porosity frit. The clear, colorless filtrate was concentrated under reduced pressure to ~20 mL, and a gas chromatographic analysis of this mixture showed it to contain four products. Analyses by GC-MS and ^1H NMR spectroscopy of the fractions separated by preparatory GC revealed these products to be:

(i) 2,4,4,6,6-pentamethyl-2-heptene (28% of product mixture⁸): ^1H NMR (CDCl_3) δ 5.16 (m, 1H, $=\text{CH}$), 1.68 (m, 6H, 2 x CH_3), 1.43 (s, 2H, CH_2), 1.13 (s, 6H, 2 x CH_3), 0.93 (s, 9H, 3 x CH_3). Low resolution mass spectrum (probe temperature 80°C) m/z 168 (P^+).

(ii) 2,4,4,6,6-pentamethyl-1-heptene (27% of product mixture): ^1H NMR (CDCl_3) δ 4.86 (m, 1H, $=\text{CH}_\text{A}\text{H}_\text{B}$), 4.65 (m, 1H, $=\text{CH}_\text{A}\text{H}_\text{B}$), 2.00 (s, 2H, CH_2), 1.78 (s, 3H, CH_3), 1.30 (s, 2H, CH_2), 1.00 (s, 15H, 5 x CH_3). Low resolution mass spectrum (probe temperature 80°C) m/z 168 (P^+).

(iii) 2,4,4,6,6,8,8-heptamethyl-2-nonene (26% of product mixture): ^1H NMR (CDCl_3) δ 5.16 (m, 1H, $=\text{CH}$), 1.70 (m, 6H, 2 x CH_3), 1.55 (s, 2H, CH_2), 1.32 (s, 2H, CH_2), 1.15 (s, 6H, 2 x CH_3), 1.03 (s, 6H, 2 x CH_3), 0.97 (s, 9H, 3 x CH_3). Low resolution mass spectrum (probe temperature 80°C) m/z 224 (P^+).

(iv) 2,4,4,6,6,8,8-heptamethyl-1-nonene (19% of product mixture): ^1H NMR (CDCl_3) δ 4.87 (m, 1H, $=\text{CH}_\text{A}\text{H}_\text{B}$), 4.66 (m, 1H, $=\text{CH}_\text{A}\text{H}_\text{B}$), 2.00 (s, 2H, CH_2), 1.78 (s, 3H, CH_3), 1.37 (s, 2H, CH_2), 1.33 (s, 2H, CH_2), 1.10 (s, 6H, 2 x CH_3), 1.03 (s, 6H, 2 x CH_3), 1.00 (s, 9H, 3 x CH_3). Low resolution mass spectrum (probe temperature 80°C) m/z 224 (P^+).

Reactions of $[\text{CpM}(\text{NO})_2]\text{BF}_4$ with NaBPh_4 ($\text{M} = \text{Cr}$ or Mo). These reactions proceeded similarly for both Cr and Mo, and that for Cr is outlined below.

To a stirred, green CH_2Cl_2 solution (40 mL) of $[\text{CpCr}(\text{NO})_2]\text{BF}_4$ (2.0 mmol) was added solid NaBPh_4 (0.68 g, 2.0 mmol). An IR spectrum of the reaction mixture after 2 min showed a decrease in intensity of the ν_{NO} 's at 1844 and 1740 cm^{-1} due to the starting dinitrosyl reagent, and the appearance of new, strong ν_{NO} 's at 1819 and 1712 cm^{-1} attributable to $[\text{CpCr}(\text{NO})_2]\text{BPh}_4$. These latter bands decreased in intensity with time, and after a period of ~ 1 h, the only ν_{NO} 's evident in the IR spectrum of the reaction mixture were at 1790 and 1685 cm^{-1} . The reaction mixture was then filtered through alumina (2 x 5 cm, Woelm neutral, activity 1). The alumina was washed with CH_2Cl_2 (20 mL) and the combined filtrates taken to dryness in vacuo to obtain 0.19 g (74% yield) of $\text{CpCr}(\text{NO})_2\text{Ph}$,⁹ which was identified by its characteristic spectroscopic properties: IR (hexanes) ν_{NO} 1794 (s) and 1694 (s) cm^{-1} . ^1H NMR (C_6D_6) δ 7.30 (m, 5H, C_6H_5), 4.73 (s, 5H, C_5H_5). Low resolution mass spectrum (probe temperature 120°C) m/z 254 (P^+).

The known $\text{CpMo}(\text{NO})_2\text{Ph}$ ⁹ compound was similarly obtained as a green oil (75% yield) presumably via the initial formation of $[\text{CpMo}(\text{NO})_2]\text{BPh}_4$ in CH_2Cl_2 (IR ν_{NO} 1769 and 1670 cm^{-1}).

Reactions of $[\text{Cp}'\text{M}(\text{NO})_2]\text{BF}_4$ with 2,3-Dimethyl-2-butene and Methyl Propiolate. These reactions were performed using a four- to five-fold excess of the organic reagents.

(a) $\text{M} = \text{Cr}$. To a stirred, green dichloromethane solution (40 mL) of $[\text{CpCr}(\text{NO})_2]\text{BF}_4$ (3.2 mmol) was added a dichloromethane solution (about 10 mL

total volume) of methyl propiolate (1.0 mL, 13 mmol) and 2,3-dimethyl-2-butene (1.0 mL, 17 mmol). The reaction mixture was then refluxed for 1 h. After this period, the reaction mixture was cooled to room temperature, and Et₂O (200 mL) was added to precipitate an olive-green solid. The supernatant solution was decanted, and the remaining solid was washed with Et₂O (40 mL) and then dried in vacuo for 1 h to afford the lactone salt,

$[\text{CpCr}(\text{NO})_2-\text{C}=\text{C}(\text{H})\text{C}(\text{Me})_2\text{C}(\text{Me})_2\text{OC}(\text{OMe})]\text{BF}_4$ (compound 1), as an analytically pure olive-green solid in 73% yield based on CpCr(NO)₂Cl.

The pentamethylcyclopentadienyl analogue, 2, was similarly generated from [Cp^{*}Cr(NO)₂]⁺BF₄⁻, but this reaction required refluxing the reaction mixture for 2 h.

The numbering scheme for these lactone complexes is presented in Table 4.2, and their analytical, IR, ¹H NMR and ¹³C NMR data are collected in Tables 4.3 - 4.5.

(b) **M = Mo.** These reactions were performed in a manner similar to that described for the chromium analogues, but the reaction mixtures were simply stirred at room temperature for 45 min, and the products were isolated as outlined above.

(c) **M = W.** Unlike the conversions involving Cr and Mo, the W reaction mixtures had to be filtered after 45 min of stirring at room temperature, and the filtrates then treated with Et₂O to obtain the lactone salts in pure form. The cyclopentadienyl case is presented as a representative example.

To a stirred, green dichloromethane solution of [CpW(NO)₂]⁺BF₄⁻ (3.36 mmol

in 70 mL) was added a CH_2Cl_2 solution (~10 mL total volume) of methyl propiolate (1.0 mL, 13 mmol) and 2,3-dimethyl-2-butene (1.0 mL, 17 mmol). The reaction mixture immediately became very dark green, and after 2 min, a bright green solid precipitated. After 45 min, this precipitate was collected by filtration, washed with CH_2Cl_2 (5 mL) and dried in vacuo to obtain 0.48 g (30% yield) of bright green $[\text{CpW}(\text{NO})_2\text{-O=C(OMe)C}\equiv\text{CH}]\text{BF}_4$. This solid was formulated as such based on its characteristic IR spectrum: IR (Nujol mull) ν_{NO} 1757 (s) and 1661 (s) cm^{-1} ; also $\nu_{\text{C}\equiv\text{C}}$ 2122 (m) cm^{-1} ; ν_{CO} 1603 (m) cm^{-1} . Unfortunately, this compound decomposed (turned brown) in < 15 min at room temperature under an atmosphere of N_2 , and immediately upon exposure to air.

Nevertheless, when the filtrate obtained from the above procedure was treated with Et_2O (120 mL), the desired lactone salt precipitated and was isolated in the usual manner (vide supra) in 25% yield.

Reaction of $[\text{CpW}(\text{NO})_2\text{-O=C(OMe)C}\equiv\text{CH}]\text{BF}_4$ with $\text{P}(\text{OPh})_3$. To a stirred slurry of $[\text{CpW}(\text{NO})_2\text{-O=C(OMe)C}\equiv\text{CH}]\text{BF}_4$ (0.24 g, 0.5 mmol) in dichloromethane (30 mL) was added excess $\text{P}(\text{OPh})_3$ (1.0 mL, 3.8 mmol). The reaction mixture became homogeneous in < 2 min, and then Et_2O (80 mL) was added to precipitate a bright green solid. This solid was collected by filtration, washed with Et_2O (10 mL) and then dried in vacuo for 1 h to obtain 0.26 g (77% yield) of $[\text{CpW}(\text{NO})_2\{\text{P}(\text{OPh})_3\}]\text{BF}_4$, which was identified by its characteristic spectroscopic properties:^{1,2} IR (CH_2Cl_2) ν_{NO} 1788 (s) and 1711 (s) cm^{-1} . ¹H NMR (acetone- d_6) δ 7.70–7.40 (m, 15H, 3 x C_6H_5), 6.43 (d, 5H, C_5H_5 , $J_{\text{PH}} = 1$ Hz).

Preparation of the Neutral Lactone Complexes 7-12. The preparations of these six compounds were similar; the procedure employed for the cyclopentadienylchromium complex is outlined below.

To a stirred, green solution of $[\text{CpCr}(\text{NO})_2-\text{C}=\text{C}(\text{H})\text{C}(\text{Me})_2\text{C}(\text{Me})_2\text{OC}(=\text{OMe})]\text{BF}_4$ (0.910 g, 2.11 mmol) in acetone (50 mL) was added solid NaI (0.33 g, 2.2 mmol). The reaction mixture was stirred for 45 min and then taken to dryness in vacuo to obtain a dark green solid. This solid was then redissolved in Et_2O (70 mL) and filtered through alumina (2 x 3 cm, Woelm neutral, activity 1). The alumina was then washed with THF (30 mL), and the combined filtrates were taken to dryness to yield $\text{CpCr}(\text{NO})_2-\text{C}=\text{C}(\text{H})\text{C}(\text{Me})_2\text{C}(\text{Me})_2\text{OC}(=\text{O})$, compound **7**, as an analytically pure olive-green solid in 74% yield based on Cr.

The physical, analytical, mass spectral, IR and ^1H NMR data for these complexes are presented in Tables 4.6 and 4.7. The ^{13}C NMR data for the cyclopentadienyl compounds are also listed in Table 4.5.

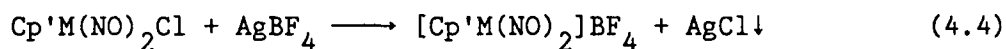
Decomposition of the Tungsten Lactone Complexes in Air. When a green dichloromethane solution (30 mL) of $\text{CpW}(\text{NO})_2-\text{C}=\text{C}(\text{H})\text{C}(\text{Me})_2\text{C}(\text{Me})_2\text{OC}(=\text{O})$ (0.41 g, 0.89 mmol) was exposed to air, it became orange after ~1 h and then pale yellow after ~2 h. Drying the pale yellow solution with anhydrous Na_2SO_4 , filtering off the used drying agent, and removal of the solvent from the filtrate under reduced pressure, led to the isolation of 0.28 g (73% yield) of pale yellow $\text{CpW}(\text{O})_2-\text{C}=\text{C}(\text{H})\text{C}(\text{Me})_2\text{C}(\text{Me})_2\text{OC}(=\text{O})$: IR (Nujol mull) $\nu_{\text{W=O}}$ 953 (m) and 910 (m) cm^{-1} ; also 1686 (s) and 1578 (w). ^1H NMR (acetone- d_6) δ 7.08 (s, 1H, =CH), 6.66 (s, 5H, C_5H_5), 1.38 (s, 6H, 2 x CH_3), 1.23 (s, 6H, 2 x CH_3). Low resolution mass spectrum (probe temperature 200°C) m/z 434 (P^+).

The pentamethylcyclopentadienyl analogue,

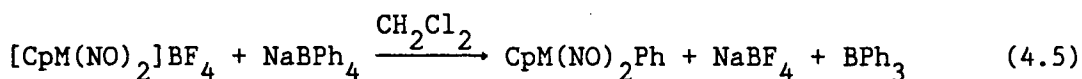
$\text{Cp}^* \text{W}(\text{O})_2 - \overline{\text{C}=\text{C}(\text{H})\text{C}(\text{Me})_2\text{C}(\text{Me})_2\text{OC}(=\text{O})}$, was prepared in a manner similar to that outlined above in 78% yield: IR (Nujol mull) $\nu_{\text{W=O}}$ 945 (m) and 899 (m) cm^{-1} . ^1H NMR (acetone- d_6) δ 6.87 (s, 1H, $=\text{CH}$), 2.18 (s, 15H, $\text{C}_5(\text{CH}_3)_5$), 1.37 (s, 6H, 2 x CH_3), 1.18 (s, 6H, 2 x CH_3). Low resolution mass spectrum (probe temperature 200°C) $\underline{m/z}$ 504 (P^+).

Results and Discussion

Generation of $[\text{Cp}'\text{M}(\text{NO})_2]\text{BF}_4$ ($\text{Cp}' = \text{Cp}$ or Cp^* ; $\text{M} = \text{Cr}, \text{Mo}$ or W). All the $[\text{Cp}'\text{M}(\text{NO})_2]^+$ cations are generated by chloride abstraction from their $\text{Cp}'\text{M}(\text{NO})_2\text{Cl}$ precursors by reaction with AgBF_4 , i.e.



These reactions 4.4 (called 4.1 for $\text{Cp}' = \text{Cp}$ and $\text{M} = \text{W}$, vide supra) are conveniently monitored by IR spectroscopy and take 15 - 45 min to go to completion. As may be noted from Table 4.1, the ν_{NO} 's shift to higher wavenumbers (by $\sim 30 \text{ cm}^{-1}$) as a result of the replacement of the coordinating Cl^- ligand by the weakly coordinating BF_4^- anion.^{1,10} [The IR data for the PF_6^- analogues (obtained by employing AgPF_6 instead of AgBF_4 in reactions 4.4) are also listed in the Table, and in general the physical properties of the BF_4^- salts are indistinguishable from those of their PF_6^- analogues.] These complexes are best formulated as 16-electron, coordinatively unsaturated $[\text{Cp}'\text{M}(\text{NO})_2]^+$ cations which may be stabilized by solvation.^{1,2,11} Nevertheless, the chemistry of these cations is dominated by their electrophilic character. For example, all the $[\text{CpM}(\text{NO})_2]^+$ cations are sufficiently electrophilic to abstract a Ph^- group from the BPh_4^- anion to form the known $\text{CpM}(\text{NO})_2\text{Ph}$ compounds, i.e.



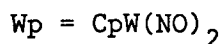
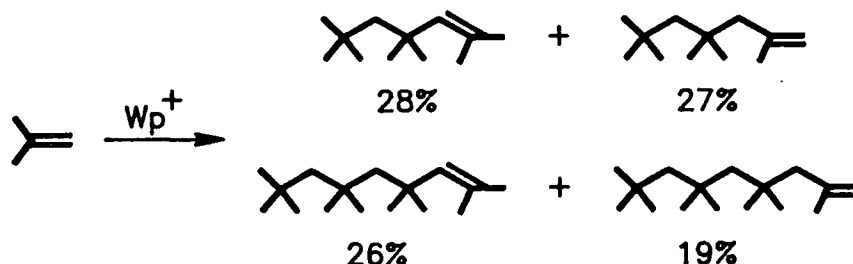
($\text{M} = \text{Cr}, \text{Mo}$ or W^1)

Table 4.1. IR Data for Various $\text{Cp}'\text{M}(\text{NO})_2\text{X}$ Complexes in CH_2Cl_2 .

Compound	$\nu_{\text{NO}}(\text{s}), \text{cm}^{-1}$		
	X = Cl	X = BF_4	X = PF_6
$\text{CpCr}(\text{NO})_2\text{X}$	1817 1711	1844 1740	1840 1736
$\text{Cp}^*\text{Cr}(\text{NO})_2\text{X}$	1782 1680	1809 1709	1806 1709
$\text{CpMo}(\text{NO})_2\text{X}$	1760 1669	1790 1698	1784 1695
$\text{Cp}^*\text{Mo}(\text{NO})_2\text{X}$	1726 1642	1757 1671	1750 1667
$\text{CpW}(\text{NO})_2\text{X}$	1733 1650	1765 1682	1748 1663
$\text{Cp}^*\text{W}(\text{NO})_2\text{X}$	1705 1624	1734 1654	1723 1644

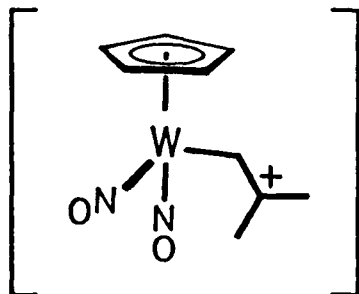
presumably via the initial formation of $[\text{CpM}(\text{NO})_2]\text{BPh}_4$ (see Experimental Section). Certainly, the clean production of the $\text{CpM}(\text{NO})_2\text{Ph}$ compounds provides a more convenient (and higher yield) route to these phenyl derivatives than obtaining them by treatment of their chloro precursors with Ph_3Al .⁹

The electrophilic nature of the $[\text{Cp}'\text{M}(\text{NO})_2]^+$ cations is further exemplified by the reaction of the cyclopentadienyltungsten compound with isobutylene (Scheme 4.1).



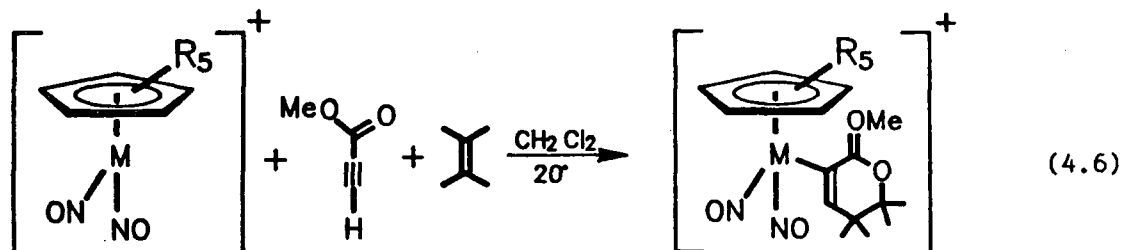
Scheme 4.1

The fact that oligomerization of the isobutylene occurs in this reaction is indicative of the ability of the electrophilic $[\text{CpW}(\text{NO})_2]^+$ cation to generate incipient carbocations. It is thus proposed that adduct formation between $[\text{CpW}(\text{NO})_2]^+$ and isobutylene occurs to yield a carbocation as shown below.



Such an organometallic carbocation could then be attacked by another molecule of the olefin,¹²⁻¹⁴ a process that may account for the linear oligomerization observed.¹⁵⁻¹⁷ Regrettably, it has not been possible to obtain a suitable crystal of any $[\text{Cp}'\text{M}(\text{NO})_2(\eta^2\text{-olefin})]^+$ compound for X-ray crystallographic studies in order to ascertain the nature of the bonding in these complexes.

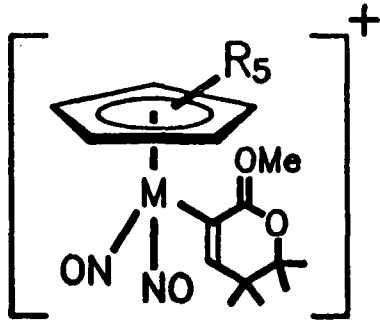
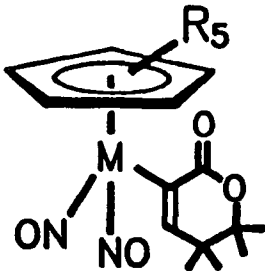
Reactions of $[\text{Cp}'\text{Mo}(\text{NO})_2]\text{BF}_4$ with 2,3-Dimethyl-2-butene and Methyl Propiolate. When exposed to dichloromethane solutions of $[\text{Cp}'\text{M}(\text{NO})_2]\text{BF}_4$, 2,3-dimethyl-2-butene and methyl propiolate condense to yield the methylated lactone salts 1 - 6 (equation 4.6).



1 - 6

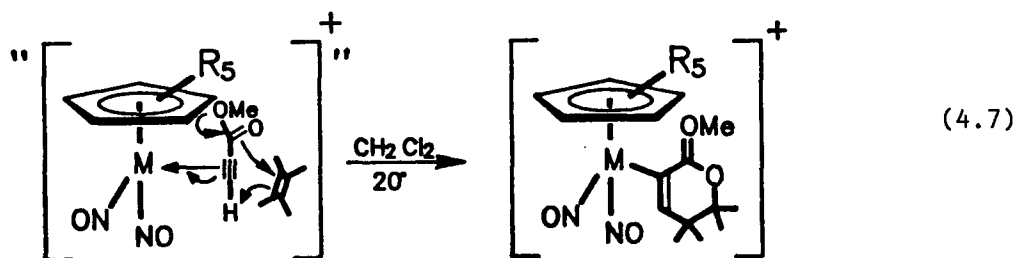
(M = Cr, Mo or W; R = H or Me)

Table 4.2. Numbering Scheme for the Cationic and Neutral Lactone Complexes.

			
Compound	Number	Compound	Number
$[\text{CpCr}(\text{NO})_2-\text{C}=\text{C}(\text{H})\text{C}(\text{Me})_2\text{C}(\text{Me})_2\text{OC}(\text{OMe})]\text{BF}_4$	1	$\text{CpCr}(\text{NO})_2-\text{C}=\text{C}(\text{H})\text{C}(\text{Me})_2\text{C}(\text{Me})_2\text{OC}(=\text{O})$	7
$[\text{Cp}^*\text{Cr}(\text{NO})_2-\text{C}=\text{C}(\text{H})\text{C}(\text{Me})_2\text{C}(\text{Me})_2\text{OC}(\text{OMe})]\text{BF}_4$	2	$\text{Cp}^*\text{Cr}(\text{NO})_2-\text{C}=\text{C}(\text{H})\text{C}(\text{Me})_2\text{C}(\text{Me})_2\text{OC}(=\text{O})$	8
$[\text{CpMo}(\text{NO})_2-\text{C}=\text{C}(\text{H})\text{C}(\text{Me})_2\text{C}(\text{Me})_2\text{OC}(\text{OMe})]\text{BF}_4$	3	$\text{CpMo}(\text{NO})_2-\text{C}=\text{C}(\text{H})\text{C}(\text{Me})_2\text{C}(\text{Me})_2\text{OC}(=\text{O})$	9
$[\text{Cp}^*\text{Mo}(\text{NO})_2-\text{C}=\text{C}(\text{H})\text{C}(\text{Me})_2\text{C}(\text{Me})_2\text{OC}(\text{OMe})]\text{BF}_4$	4	$\text{Cp}^*\text{Mo}(\text{NO})_2-\text{C}=\text{C}(\text{H})\text{C}(\text{Me})_2\text{C}(\text{Me})_2\text{OC}(=\text{O})$	10
$[\text{CpW}(\text{NO})_2-\text{C}=\text{C}(\text{H})\text{C}(\text{Me})_2\text{C}(\text{Me})_2\text{OC}(\text{OMe})]\text{BF}_4$	5	$\text{CpW}(\text{NO})_2-\text{C}=\text{C}(\text{H})\text{C}(\text{Me})_2\text{C}(\text{Me})_2\text{OC}(=\text{O})$	11
$[\text{Cp}^*\text{W}(\text{NO})_2-\text{C}=\text{C}(\text{H})\text{C}(\text{Me})_2\text{C}(\text{Me})_2\text{OC}(\text{OMe})]\text{BF}_4$	6	$\text{Cp}^*\text{W}(\text{NO})_2-\text{C}=\text{C}(\text{H})\text{C}(\text{Me})_2\text{C}(\text{Me})_2\text{OC}(=\text{O})$	12

These salts are isolated as analytically pure solids, and are air-stable as solids. In solution, they may be handled in air for at least 4 h without any noticeable decomposition. Their spectroscopic properties are fully consistent with their formulations. For example, the ^1H NMR spectrum of the cyclopentadienylmolybdenum compound, 3, is shown in Figure 4.1. [The physical, analytical and spectral data for complexes 1 - 6 are collected in Tables 4.3 - 4.5.] As illustrated by this example, the assignments of the signals in the ^1H NMR spectra for all the complexes are quite straightforward, and are as indicated. However, an apparently inconsistent feature of this spectrum is the low intensity of the resonance due to the Cp protons. Indeed, a measurement of the T_1 relaxation time for these protons¹⁸ indicates it to be very long, 21 s.¹⁹ Thus, in recording the ^1H NMR spectra for these and other compounds synthesized in this work, pulse delays of >50 s must be used in order to obtain meaningful integrations of the signals.

It is proposed that reactions 4.6 occur via coordination of the acetylenic ester to the metal center (through the acetylene link) followed by nucleophilic attack at the bound acetylenic ester by the incoming olefin, as shown below in equation 4.7.



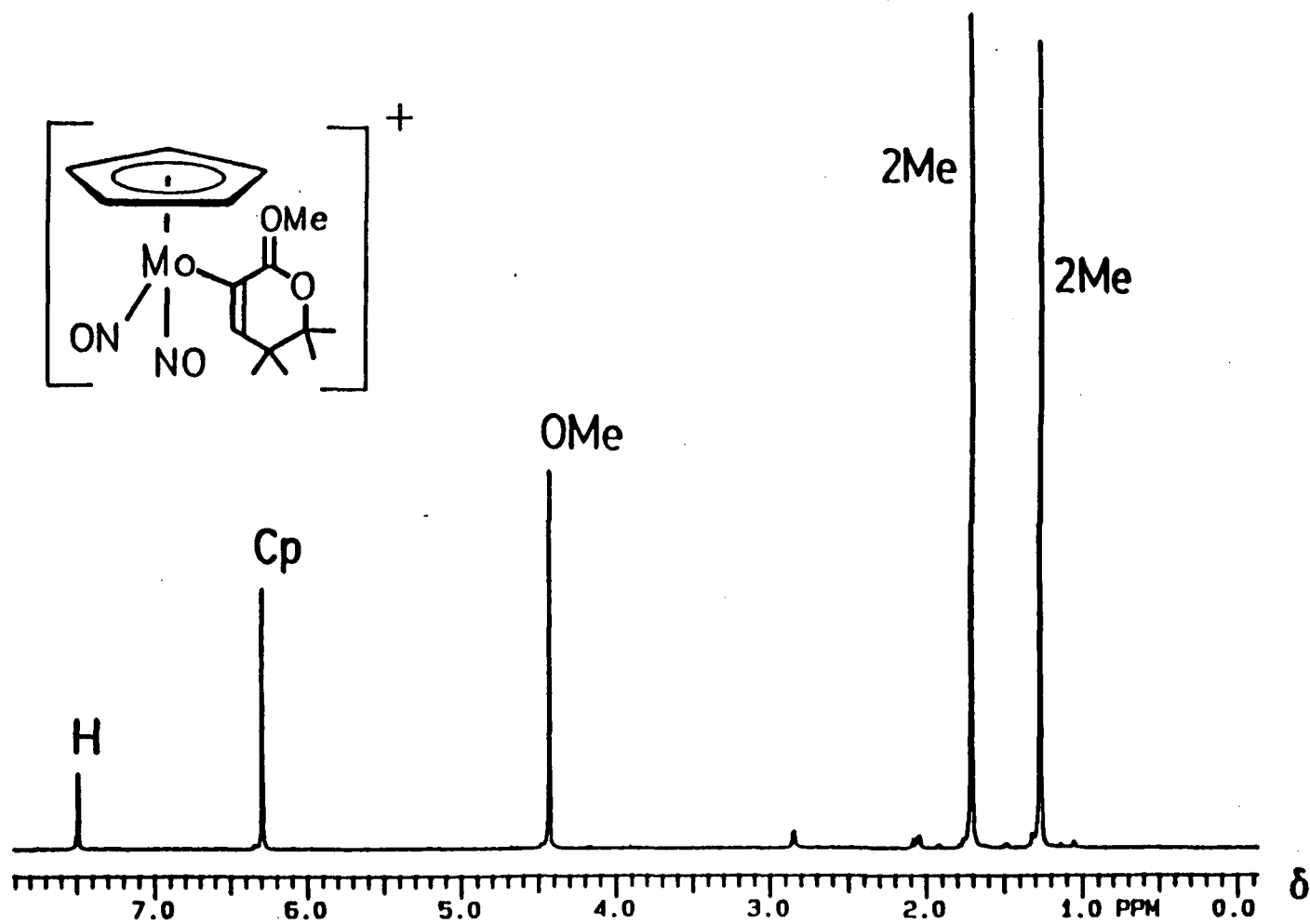


Figure 4.1. The 300 MHz ^1H NMR spectrum of complex 3 in $\text{acetone-}d_6$.

Table 4.3. Physical Data for the Cationic Lactone Complexes 1 - 6.

Compound	Color	Yield %	Analytical Data			IR (Nujol) ^a (cm ⁻¹)
			C (calcd)	H (calcd)	N (calcd)	
$[\text{CpCr}(\text{NO})_2-\text{C}=\text{C}(\text{H})\text{C}(\text{Me})_2\text{C}(\text{Me})_2\text{OC}(\text{OMe})]\text{BF}_4$ 1	olive green	73	41.90 (41.67)	4.93 (4.86)	6.48 (6.48)	1800(s), 1721(s), 1665(s), 1564(w), 1518(m)
$[\text{Cp}^*\text{Cr}(\text{NO})_2-\text{C}=\text{C}(\text{H})\text{C}(\text{Me})_2\text{C}(\text{Me})_2\text{OC}(\text{OMe})]\text{BF}_4$ 2	olive green	68	47.68 (47.81)	6.09 (6.18)	5.57 (5.58)	1763(s), 1682(s), 1659(s), 1561(w), 1512(m)
$[\text{CpMo}(\text{NO})_2-\text{C}=\text{C}(\text{H})\text{C}(\text{Me})_2\text{C}(\text{Me})_2\text{OC}(\text{OMe})]\text{BF}_4$ 3	bright green	66	38.00 (37.82)	4.35 (4.41)	5.91 (5.88)	1752(s), 1680(s), 1630(s), 1564(m), 1518(m)
$[\text{Cp}^*\text{Mo}(\text{NO})_2-\text{C}=\text{C}(\text{H})\text{C}(\text{Me})_2\text{C}(\text{Me})_2\text{OC}(\text{OMe})]\text{BF}_4$ 4	pale brown	82	44.03 (43.96)	5.63 (5.68)	4.96 (5.13)	1709(s), 1624(s), 1561(m), 1520(m)
$[\text{CpW}(\text{NO})_2-\text{C}=\text{C}(\text{H})\text{C}(\text{Me})_2\text{C}(\text{Me})_2\text{OC}(\text{OMe})]\text{BF}_4$ 5	bright green	25	31.69 (31.91)	3.78 (3.72)	4.90 (4.96)	1732(s), 1669(s), 1618(s), 1564(m), 1522(m)
$[\text{Cp}^*\text{W}(\text{NO})_2-\text{C}=\text{C}(\text{H})\text{C}(\text{Me})_2\text{C}(\text{Me})_2\text{OC}(\text{OMe})]\text{BF}_4$ 6	pale green	63	37.84 (37.85)	4.93 (4.89)	4.29 (4.42)	1692(s), 1613(s), 1560(m), 1522(m)

^a In the 1900 - 1500 cm⁻¹ region.

Table 4.4. ^1H NMR Chemical Shifts of the Cationic Lactone Complexes 1 - 6.

Compound	Chemical Shifts $[(\text{CD}_3)_2\text{C}=\text{O}, \delta \text{ in ppm}]$				
	Cp	H	$\text{C}(\text{CH}_3)_2$	$\text{C}(\text{CH}_3)_2\text{-O}$	OCH_3
$[\text{CpCr}(\text{NO})_2\text{-}\overline{\text{C}=\text{C}(\text{H})\text{C}(\text{Me})_2\text{C}(\text{Me})_2\text{OC}(\text{OMe})}] \text{BF}_4$ 1	5.87 (s)	7.33 (s)	1.24 (s)	1.68 (s)	4.41 (s)
$[\text{Cp}^* \text{Cr}(\text{NO})_2\text{-}\overline{\text{C}=\text{C}(\text{H})\text{C}(\text{Me})_2\text{C}(\text{Me})_2\text{OC}(\text{OMe})}] \text{BF}_4$ 2	1.87 (s) ^a	7.19 (s)	1.29 (s)	1.72 (s)	4.48 (s)
$[\text{CpMo}(\text{NO})_2\text{-}\overline{\text{C}=\text{C}(\text{H})\text{C}(\text{Me})_2\text{C}(\text{Me})_2\text{OC}(\text{OMe})}] \text{BF}_4$ 3	6.30 (s)	7.50 (s)	1.28 (s)	1.72 (s)	4.44 (s)
$[\text{Cp}^* \text{Mo}(\text{NO})_2\text{-}\overline{\text{C}=\text{C}(\text{H})\text{C}(\text{Me})_2\text{C}(\text{Me})_2\text{OC}(\text{OMe})}] \text{BF}_4$ 4	2.01 (s) ^a	7.42 (s)	1.32 (s)	1.74 (s)	4.50 (s)
$[\text{CpW}(\text{NO})_2\text{-}\overline{\text{C}=\text{C}(\text{H})\text{C}(\text{Me})_2\text{C}(\text{Me})_2\text{OC}(\text{OMe})}] \text{BF}_4$ 5	6.41 (s)	7.59 (s)	1.28 (s)	1.72 (s)	4.44 (s)
$[\text{Cp}^* \text{W}(\text{NO})_2\text{-}\overline{\text{C}=\text{C}(\text{H})\text{C}(\text{Me})_2\text{C}(\text{Me})_2\text{OC}(\text{OMe})}] \text{BF}_4$ 6	2.10 (s) ^a	7.49 (s)	1.33 (s)	1.75 (s)	4.52 (s)

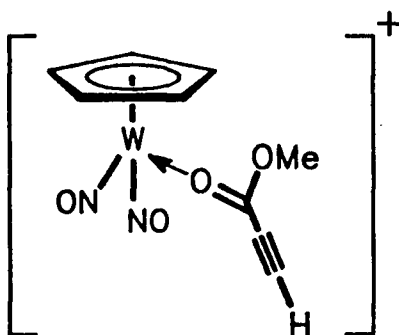
^a this is $\eta^5\text{-C}_5\text{Me}_5$

Table 4.5. ^{13}C NMR Chemical Shifts of Some Lactone Complexes.

Compound	Chemical Shifts [$(\text{CD}_3)_2\text{CO}$, δ in ppm] ^a								
	Cp	M-C=	=CH	CMe ₂	C(Me) ₂	C(Me) ₂ O	C(Me) ₂ O	C=O	O-Me
$[\text{CpCr}(\text{NO})_2-\text{C}=\text{C}(\text{H})\text{C}(\text{Me})_2\text{C}(\text{Me})_2\text{OC}(\text{OMe})]\text{BF}_4$ 1	102.01	137.70	178.76	42.66	22.46	23.05	99.91	n.o.	60.72
$\text{CpCr}(\text{NO})_2-\text{C}=\text{C}(\text{H})\text{C}(\text{Me})_2\text{C}(\text{Me})_2\text{OC}(=\text{O})$ 7	101.23	n.o.	161.18	41.20	23.99	24.09	83.75	n.o.	n.a.
$[\text{CpMo}(\text{NO})_2-\text{C}=\text{C}(\text{H})\text{C}(\text{Me})_2\text{C}(\text{Me})_2\text{OC}(\text{OMe})]\text{BF}_4$ 3	104.18	134.76	182.59	43.22	22.66	23.23	101.74	n.o.	61.31
$\text{CpMo}(\text{NO})_2-\text{C}=\text{C}(\text{H})\text{C}(\text{Me})_2\text{C}(\text{Me})_2\text{OC}(=\text{O})$ 9	103.74	144.94	166.29	41.56	24.07	24.07	85.48	170.44	n.a.
$[\text{CpW}(\text{NO})_2-\text{C}=\text{C}(\text{H})\text{C}(\text{Me})_2\text{C}(\text{Me})_2\text{OC}(\text{OMe})]\text{BF}_4$ 5	102.78	130.01	182.13	42.89	22.66	22.95	100.80	n.o.	61.32
$\text{CpW}(\text{NO})_2-\text{C}=\text{C}(\text{H})\text{C}(\text{Me})_2\text{C}(\text{Me})_2\text{OC}(=\text{O})$ 11	102.24	n.o.	166.05	41.00	23.74	23.89	84.17	n.o.	n.a.

^a all peaks appear as singlets n.o. not observed n.a. not applicable

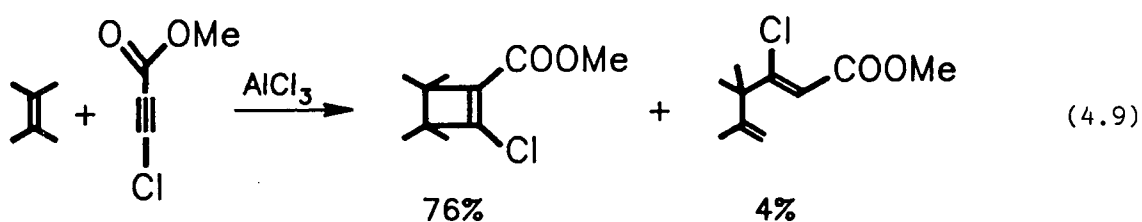
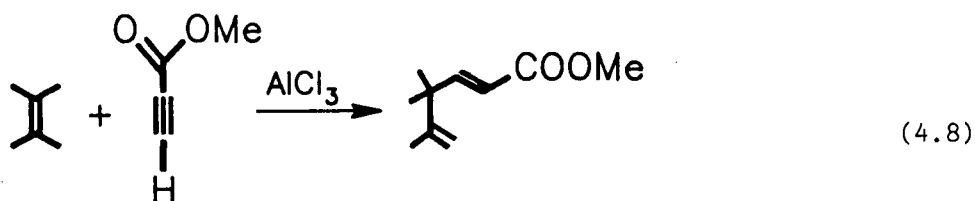
Indeed, in the case where $M = W$ and $R = H$, the overall reaction 4.6 is hampered by the precipitation of the O-bound methyl propiolate adduct,



This compound is fairly insoluble in dichloromethane, and it decomposes in the solvents in which it dissolves. Consequently, no consistent ^1H NMR data have been obtained for this complex. However, an IR spectrum of it (as a Nujol mull) contains bands attributable to a coordinated methyl propiolate ligand. Thus, although the $\text{C}\equiv\text{C}$ stretching frequency does not change significantly upon the coordination of the acetylenic ester ($\nu_{\text{C}\equiv\text{C}}$ 2122 cm^{-1} bound vs 2128 cm^{-1} free), the $\text{C}=\text{O}$ stretching frequency does by 118 cm^{-1} ($\nu_{\text{C}=\text{O}}$ 1603 cm^{-1} bound vs 1721 cm^{-1} free) consistent with this ligand binding through the carbonyl oxygen.²¹ Nevertheless, the methyl propiolate is readily displaced by $\text{P}(\text{OPh})_3$ to give the known $[\text{CpW}(\text{NO})_2\{\text{P}(\text{OPh})_3\}]\text{BF}_4$ compound in high yield. Therefore it appears that in addition to the observed reaction leading to lactone salt formation, there is a competing reaction pathway which involves the formation

of the insoluble $[\text{CpW}(\text{NO})_2 \leftarrow \text{O}=\text{C}(\text{OMe})\text{C}\equiv\text{CH}]\text{BF}_4$ complex. The precipitation of this latter product effectively reduces the availability of the $[\text{CpW}(\text{NO})_2]^+$ cation for reaction 4.7, and accounts for the low yield (25%) of the lactone salt obtained in this instance.

In a sense, the attachment of the $[\text{CpW}(\text{NO})_2]^+$ cation to the carbonyl oxygen of the acetylenic ester is reminiscent of the AlCl_3 catalyzed condensation reactions 4.8 and 4.9 in which the Lewis acid (in this case,

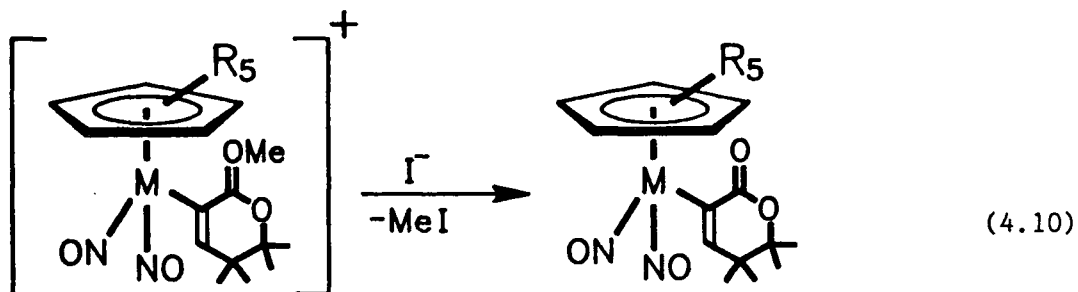


AlCl_3) is believed to coordinate to the carbonyl oxygen of the acetylenic esters in the transition states of these transformations.²² However, no $[2 + 2]$ cycloaddition or ene products are observed in any of the $[\text{Cp}'\text{M}(\text{NO}_2)]^+$

reactions with 2,3-dimethyl-2-butene and methyl propiolate (compare with equation 4.2), and thus it is probable that in the $[\text{Cp}'\text{M}(\text{NO})_2]^+$ reactions, entirely different transition states (such as in equation 4.7) are involved during the production of the organometallic lactone salts.

Thus, it can be concluded from the results of this study that the reactions of $[\text{Cp}'\text{M}(\text{NO})_2]^+$ (equation 4.6) resemble those of the valence isoelectronic $[\text{CpFe}(\text{CO})_2]^+$ compound (equation 4.3) rather than those of other Lewis acids such as AlCl_3 (equation 4.8). Also, the reactions of all the $[\text{Cp}'\text{M}(\text{NO})_2]^+$ complexes with 2,3-dimethyl-2-butene and methyl propiolate lead to the selective formation of 6-membered-ring lactones in high yields. No 5-membered-ring lactones are observed in any of the reactions involving the dinitrosyl complexes.

Preparation of the Neutral $\text{Cp}'\text{M}(\text{NO})_2$ - $\overline{\text{C}=\text{C}(\text{H})\text{C}(\text{Me})_2\text{C}(\text{Me})_2\text{OC}(=\text{O})}$ Lactone Complexes (7 - 12). The organometallic complexes 7 - 12 are obtainable by exposure of acetone solutions of their precursor methylated lactone salts (1 - 6) to equimolar amounts of NaI as shown in equation 4.10.



(4.10)

(M = Cr, Mo or W; R = H or Me)

1 - 6

7 - 12

Compounds 7 - 12 are green to brown solids, and their physical, analytical, mass spectral and IR data are collected in Table 4.6. The ^1H NMR data for these complexes are presented in Table 4.7, and the ^1H NMR spectrum of the cyclopentadienyl compound 9 is shown in Figure 4.2. This spectrum qualitatively resembles that exhibited by its precursor lactone salt (Figure 4.1), and the measured T_1 value for the Cp proton resonance is also very large (38 s). Furthermore, the notable absence of the resonance around 4 ppm is consistent with the successful accomplishment of the O-dealkylation²³ reaction outlined in equation 4.10. The low resolution mass spectra for these complexes all show the parent ions as the highest m/z peaks.

The connectivity of the atoms in these monomeric complexes has been confirmed by a single-crystal X-ray crystallographic analysis of the cyclopentadienylmolybdenum compound (9).²⁴ The molecular structure of this compound in the solid state is depicted in Figure 4.3, and selected bond lengths and angles are listed in Tables 4.8 and 4.9 respectively. Although there are no other structurally characterized neutral compounds containing the $\text{CpMo}(\text{NO})_2$ fragment, the intramolecular dimensions of this unit appear normal in comparison to the intramolecular dimensions of the related $\text{CpM}(\text{NO})_2\text{Cl}$ compounds ($\text{M} = \text{Cr}$ or W)²⁵ already discussed in Chapter 3 of this thesis. Thus the $\text{N}(1)\text{-Mo-N}(2)$ bond angle of $92.3(1)^\circ$ is close to that found for the $\text{CpM}(\text{NO})_2\text{Cl}$ compounds (93.9° for Cr , and 92° for W).²⁵ Also, the $\text{O}(1)\text{-N}(1)\text{-Mo}$ and $\text{O}(2)\text{-N}(2)\text{-Mo}$ bond angles of $174.4(2)^\circ$ and $174.3(2)^\circ$ indicate that the nitrosyl ligands are essentially linear. Interestingly, the $\text{C}(15)\text{-O}(4)$ bond is short [$1.354(3)\text{\AA}$] in comparison to the $\text{C}(14)\text{-O}(4)$ bond [$1.477(3)\text{\AA}$] and may be



indicative of some participation of the -C=O- resonance form in the complex,

Table 4.6. Physical and Mass Spectral Data for the Neutral Lactone Complexes.

Compound	Color	Yield %	Analytical Data			Mass Spectrum m/z	IR (Nujol)	
			C (calcd)	H (calcd)	N (calcd)		$\nu_{\text{NO}}, \text{cm}^{-1}$	$\nu_{\text{C=O}}, \text{cm}^{-1}$
$\text{CpCr}(\text{NO})_2-\overline{\text{C}=\text{C}(\text{H})\text{C}(\text{Me})_2\text{C}(\text{Me})_2\text{OC}(=\text{O})}$ 7	olive green	74	50.67 (50.91)	5.60 (5.45)	8.39 (8.48)	330 (P^+)	1786 1661	1678
$\text{Cp}^*\text{Cr}(\text{NO})_2-\overline{\text{C}=\text{C}(\text{H})\text{C}(\text{Me})_2\text{C}(\text{Me})_2\text{OC}(=\text{O})}$ 8	olive green	72	57.02 (57.00)	7.11 (7.00)	7.00 (7.00)	400 (P^+)	1757 1649	1684
$\text{CpMo}(\text{NO})_2-\overline{\text{C}=\text{C}(\text{H})\text{C}(\text{Me})_2\text{C}(\text{Me})_2\text{OC}(=\text{O})}$ 9	bright green	51	44.49 (44.92)	4.87 (4.81)	7.13 (7.49)	376 (P^+)	1737 1630	1656
$\text{Cp}^*\text{Mo}(\text{NO})_2-\overline{\text{C}=\text{C}(\text{H})\text{C}(\text{Me})_2\text{C}(\text{Me})_2\text{OC}(=\text{O})}$ 10	green brown	57	51.60 (51.35)	6.35 (6.31)	6.19 (6.13)	446 (P^+)	1709 1610	1680
$\text{CpW}(\text{NO})_2-\overline{\text{C}=\text{C}(\text{H})\text{C}(\text{Me})_2\text{C}(\text{Me})_2\text{OC}(=\text{O})}$ 11	bright green	71	36.60 (36.36)	4.02 (3.90)	6.02 (6.06)	462 (P^+)	1717 1617	1672
$\text{Cp}^*\text{W}(\text{NO})_2-\overline{\text{C}=\text{C}(\text{H})\text{C}(\text{Me})_2\text{C}(\text{Me})_2\text{OC}(=\text{O})}$ 12	bright green	63	42.95 (42.86)	5.35 (5.26)	5.19 (5.26)	532 (P^+)	1692 1599	1680

Table 4.7. ^1H NMR Chemical Shifts of the Neutral Lactone Complexes.

Compound	Chemical Shifts $[(\text{CD}_3)_2\text{C}=\text{O}, \delta \text{ in ppm}]$			
	Cp	H	$\text{C}(\text{CH}_3)_2$	$\text{C}(\text{CH}_3)_2\text{-O}$
$\text{CpCr}(\text{NO})_2\text{-}\overline{\text{C}=\text{C}(\text{H})\text{C}(\text{Me})_2\text{C}(\text{Me})_2\text{OC}(=\text{O})}$ 7	5.66 (s)	6.42 (s)	1.06 (s)	1.32 (s)
$\text{Cp}^*\text{Cr}(\text{NO})_2\text{-}\overline{\text{C}=\text{C}(\text{H})\text{C}(\text{Me})_2\text{C}(\text{Me})_2\text{OC}(=\text{O})}$ 8	1.81 (s) ^a	6.20 (s)	1.08 (s)	1.32 (s)
$\text{CpMo}(\text{NO})_2\text{-}\overline{\text{C}=\text{C}(\text{H})\text{C}(\text{Me})_2\text{C}(\text{Me})_2\text{OC}(=\text{O})}$ 9	6.16 (s)	6.63 (s)	1.12 (s)	1.38 (s)
$\text{Cp}^*\text{Mo}(\text{NO})_2\text{-}\overline{\text{C}=\text{C}(\text{H})\text{C}(\text{Me})_2\text{C}(\text{Me})_2\text{OC}(=\text{O})}$ 10	1.94 (s) ^a	6.43 (s)	1.10 (s)	1.33 (s)
$\text{CpW}(\text{NO})_2\text{-}\overline{\text{C}=\text{C}(\text{H})\text{C}(\text{Me})_2\text{C}(\text{Me})_2\text{OC}(=\text{O})}$ 11	6.23 (s)	6.77 (s)	1.07 (s)	1.33 (s)
$\text{Cp}^*\text{W}(\text{NO})_2\text{-}\overline{\text{C}=\text{C}(\text{H})\text{C}(\text{Me})_2\text{C}(\text{Me})_2\text{OC}(=\text{O})}$ 12	2.02 (s) ^a	6.54 (s)	1.11 (s)	1.33 (s)

^a this is $\eta^5\text{-C}_5\text{Me}_5$

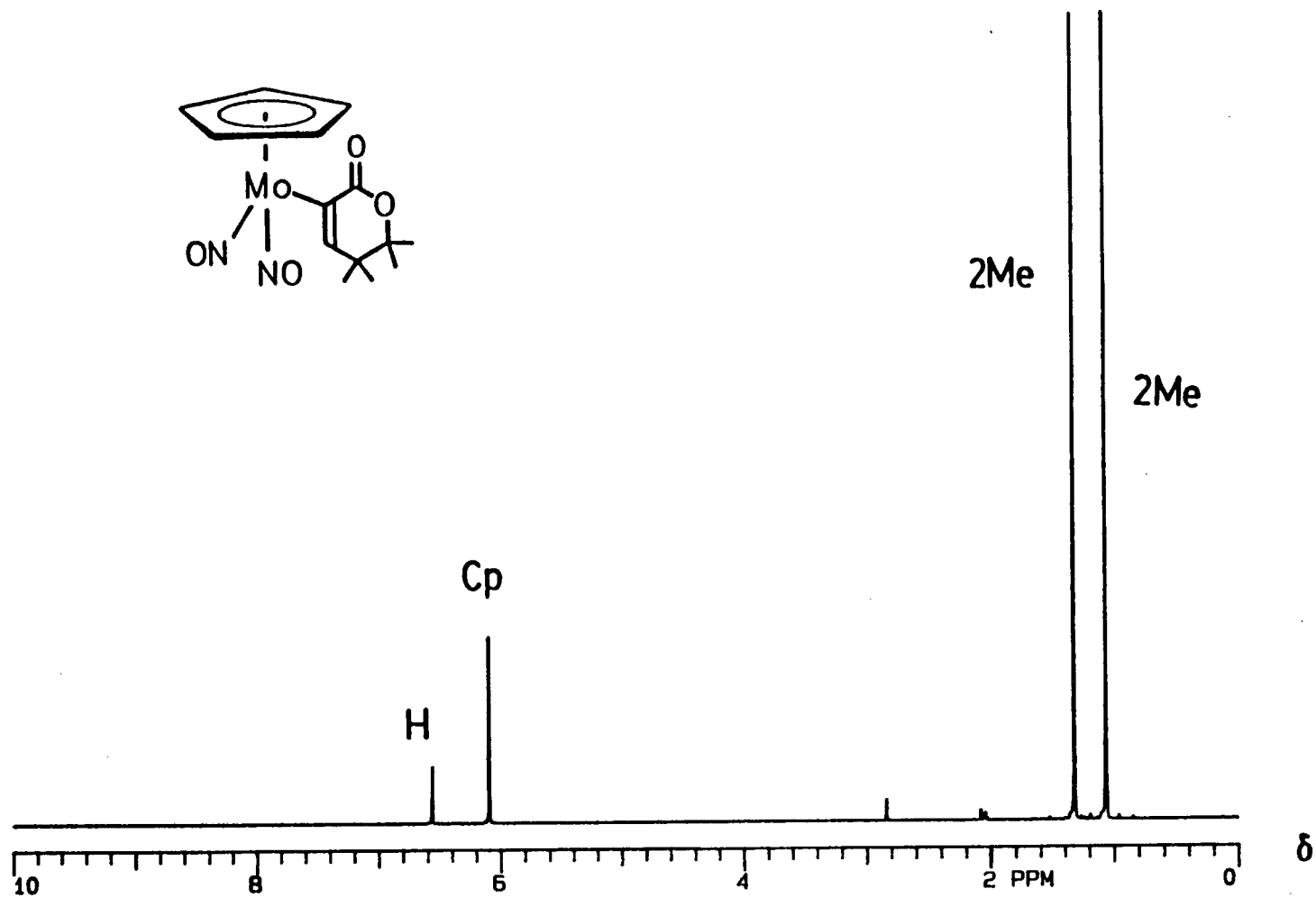


Figure 4.2. The 300 MHz ^1H NMR spectrum of complex **9** in $\text{acetone-}d_6$.

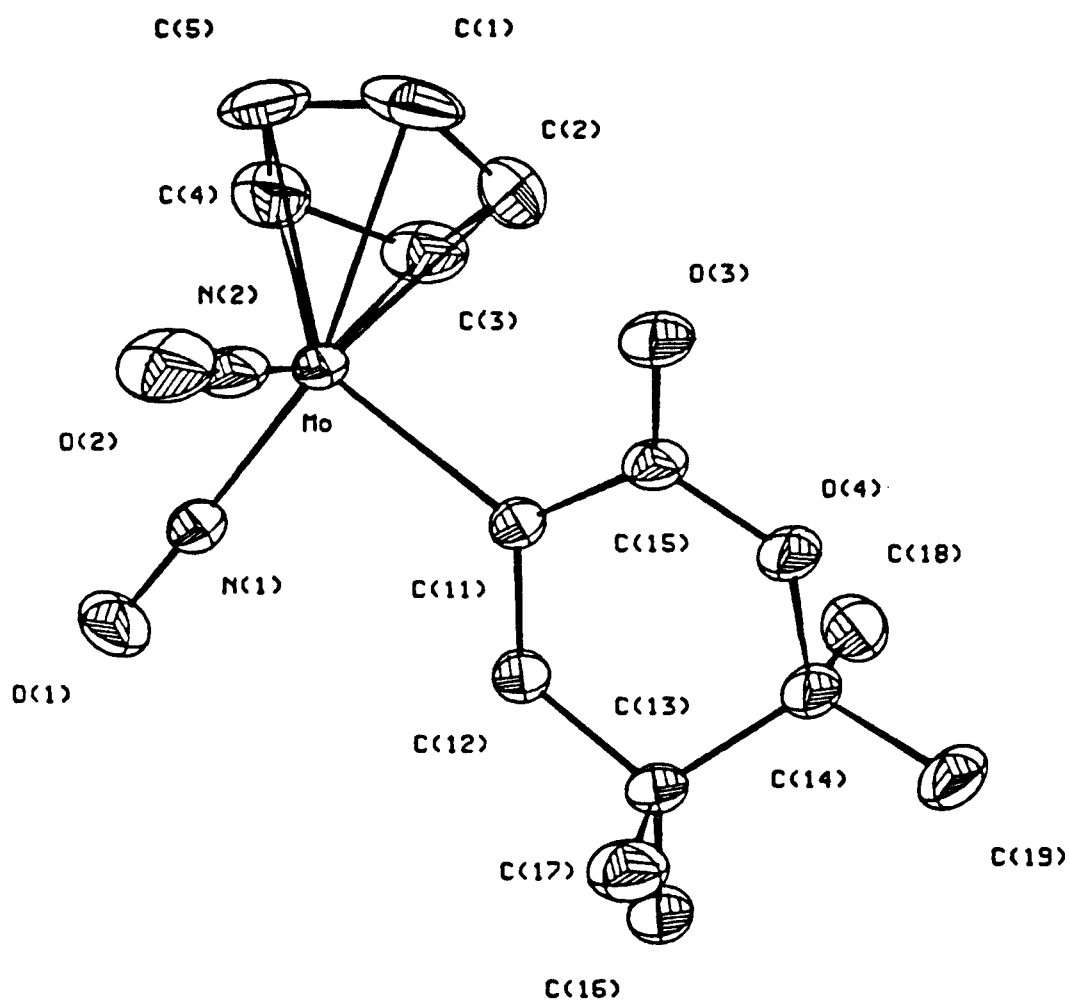


Figure 4.3. Solid-state molecular structure of the $\text{CpMo}(\text{NO})_2(\eta^1\text{-lactone})$ complex 9.

Table 4.8. Selected Bond Lengths (Å) for the $\text{CpMo(NO)}_2(\eta^1\text{-lactone})$ Compound 9.

Bond	Length ^a
Mo - N(1)	1.813(2)
Mo - N(2)	1.823(2)
Mo - C(1)	2.360(3)
Mo - C(11)	2.170(2)
N(1) - O(1)	1.181(3)
N(2) - O(2)	1.180(3)
O(3) - C(15)	1.212(3)
O(4) - C(15)	1.354(3)
C(11) - C(12)	1.331(3)
C(11) - C(15)	1.478(3)
C(12) - C(13)	1.506(3)
C(12) - H(12)	0.93(3)
O(4) - C(14)	1.477(3)

^a E.s.d.'s are in parentheses.

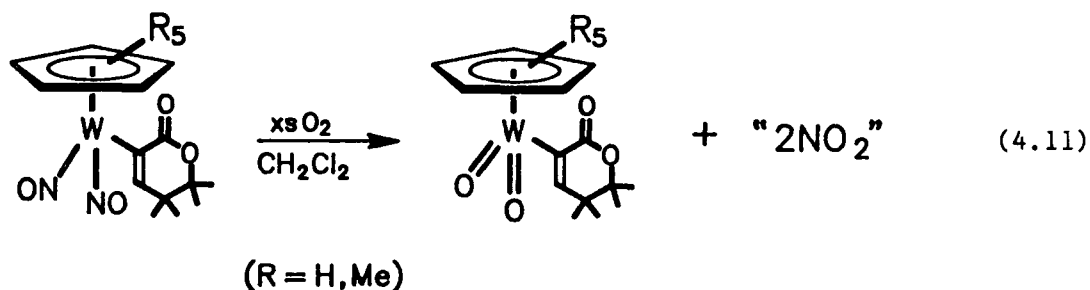
Table 4.9. Selected Bond Angles (deg) for the $\text{CpMo}(\text{NO})_2(\eta^1\text{-lactone})$ Compound 9.^a

N(2) - Mo - N(1)	92.3(1)
C(11) - Mo - N(1)	92.8(1)
O(1) - N(1) - Mo	174.4(2)
O(2) - N(2) - Mo	174.3(2)
C(12) - C(11) - Mo	123.8(2)
C(13) - C(12) - C(11)	125.7(2)
C(14) - C(13) - C(12)	107.3(2)
C(15) - O(4) - C(14)	120.5(2)
O(4) - C(15) - O(3)	116.5(2)
C(11) - C(15) - O(3)	124.2(2)
C(11) - C(15) - O(4)	119.3(2)
H(12) - C(12) - C(11)	121 (2)

^a E.s.d.'s are in parentheses.

which would then impose some partial double-bond character onto the C(15)-O(4) bond.²⁶ Furthermore, the C(11)-C(15) bond distance of 1.478(3) Å is shorter than that expected for an unconjugated C-C bond of this type (1.497 Å)²⁷ and is close to the value expected for the (conjugated) α,β -unsaturated ketone form (1.47 Å),²⁸ a feature thus suggesting some delocalization of electron density over the whole C(12)-O(4) fragment.

Decomposition of the $\text{Cp}'\text{W}(\text{NO})_2\text{-C}=\text{C}(\text{H})\text{C}(\text{Me})_2\text{C}(\text{Me})_2\text{OC}(=\text{O})$ Complexes in Air. The initially green dichloromethane solutions of the neutral tungsten lactone complexes (11 and 12) turn orange and then yellow over the course of hours (2 h for the Cp complex, and 6 h for the Cp^* complex) when exposed to air, cleanly producing the corresponding dioxo compounds in high yields (70-80%).

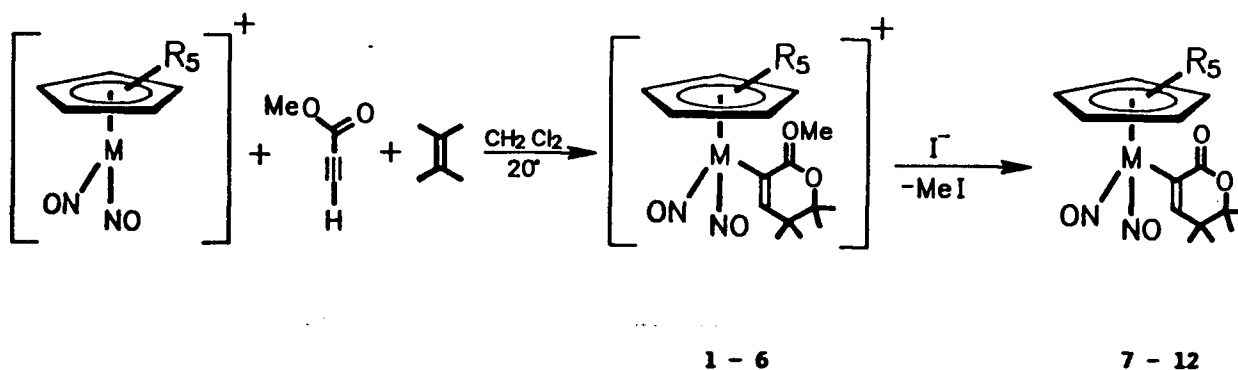


These dioxo derivatives have been characterized fully by spectroscopic methods.²⁹ Thus, their IR spectra are devoid of nitrosyl absorptions and now contain bands assignable to $\nu_{\text{W}=\text{O}}$ (see Experimental Section). Also, the ^1H NMR spectra for these dioxo products are very similar to those of their dinitrosyl precursors, indicating that the $\{\text{Cp}'\text{W}(\eta^1\text{-lactone})\}$ group remains intact during

reaction 4.11. Furthermore, the low resolution mass spectra of these complexes display the expected parent ion peaks as their highest m/z peaks. The success of the reactions 4.11 therefore implies that a possible extension of this chemistry to the chromium analogues may indeed be the preferred route to the unknown $\text{Cp}'\text{Cr}(\text{O})_2\text{R}$ type compounds. Regrettably, initial attempts to effect this extension have not been fruitful.

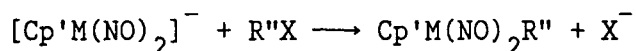
Summary

This work has shown that the $[\text{Cp}'\text{M}(\text{NO})_2]^+$ organometallic cations ($\text{Cp}' = \text{Cp}$ or Cp^* ; $\text{M} = \text{Cr}, \text{Mo}$ or W) are potent electrophiles. For instance, 2,3-dimethyl-2-butene and methyl propiolate condense in their presence to form the cationic lactone salts 1 - 6.



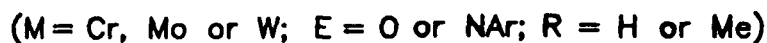
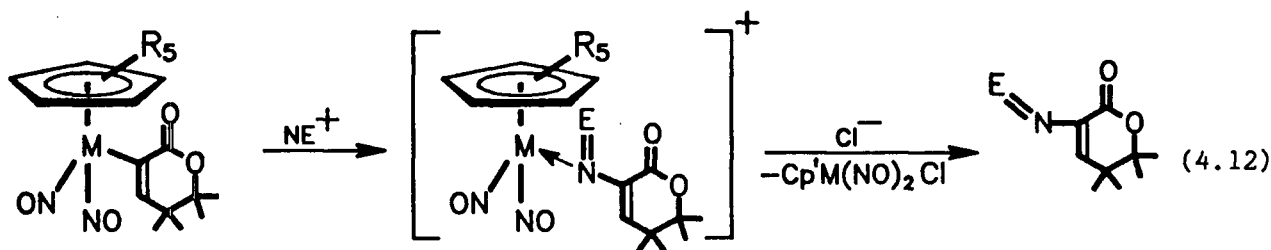
These salts are converted to their neutral lactone compounds (7 - 12) upon

treatment with NaI in acetone. Furthermore, the tungsten complexes **11** and **12** decompose to their dioxo derivatives, $\text{Cp}'\text{W}(\text{O})_2(\eta^1\text{-lactone})$, by exposure of their dichloromethane solutions to air. Most interestingly, the new $\text{Cp}'\text{M}(\text{NO})_2(\eta^1\text{-lactone})$ complexes (**7** - **12**) now join a rare class of $\text{Cp}'\text{M}(\text{NO})_2\text{R}''$ compounds (R'' = heteroatomic organic ligand) which cannot be synthesized in the more common manner used for the carbonyl analogues. This



pathway is unavailable to the dinitrosyl complexes since the $[\text{Cp}'\text{M}(\text{NO})_2]^-$ anions are presently unknown.

Following the chemistry outlined in Chapter 3 of this thesis, the question arises as to whether the transformations outlined in equation 4.12 may be cleanly carried out.



If they can, this would then lead to the formation of new types of α -substituted lactones, the formation of which (to the best of my knowledge) does not appear to have any precedent. Preliminary experiments in this regard

do suggest that these transformations are indeed feasible, although the proper reaction conditions to isolate the products in pure form have yet to be determined. It is possible that the NE^+ electrophiles may not attack the metal-carbon bonds of the organometallic complexes alone, but may also be involved in electrophilic attack at the carbonyl oxygen of the lactone ligands (to obtain the $[\text{C=ONE}]^+$ analogues of the cationic lactone salts 1 - 6). Nevertheless, the reactions outlined in equation 4.12 above constitute a promising area of research and, hopefully, will have an impact in the development of synthetic methods for the production of new organic compounds.

References and Notes

1. Legzdins, P.; Martin, D. T. *Organometallics* **1983**, *2*, 1785.
2. Stewart, R. P., Jr.; Moore, G. T. *Inorg. Chem.* **1975**, *14*, 2699.
3. The molybdenum analogue of this compound has been briefly described, see: Hames, B. W.; Legzdins, P. *Organometallics* **1982**, *1*, 118.
4. Martin, D. T. Ph.D. Dissertation, the University of British Columbia, 1984.
5. (a) Rosenblum, M.; Scheck, D. *Organometallics* **1982**, *1*, 397.
(b) Samuels, S.-B.; Berryhill, S. R.; Rosenblum, M. *J. Organomet. Chem.* **1979**, *166*, C9.
6. The course of this reaction is strongly dependent on the structure of the olefin reactant. For example, 1,2-disubstituted olefins yield cyclobutenes and 1,3-dienes in addition to the lactone products, whereas 1,1-disubstituted or trisubstituted olefins yield only the lactone products.^{5a}
7. Legzdins, P.; Malito, J. T. *Inorg. Chem.* **1975**, *14*, 1875.
8. The yields were determined by GC.
9. Hoyano, J. K.; Legzdins, P.; Malito, J. T. *J. Chem. Soc., Dalton Trans.* **1975**, 1022.
10. (a) Beck, W.; Sünkel, K. *Chem. Rev.* in press. (b) Regina, F. J.; Wojcicki, A. *Inorg. Chem.* **1980**, *19*, 3803.
11. Thus, coordinating solvents such as acetonitrile coordinate to the metal center to give the isolable $[\text{Cp}'\text{M}(\text{NO})_2(\text{solvent})]^+$ compounds.

- Richter-Addo, G. B.; Legzdins, P. *Chem. Rev.* in press.
12. It has been calculated that indeed, it is such linkages that render bound olefins susceptible to nucleophilic attack.¹³ However, X-ray crystallographic analyses of some $[\text{CpFe}(\text{CO})_2(\text{olefin})]^+$ complexes reveal that it is the complexes having the symmetrically bound olefin that are reactive. Those having the unsymmetrically bound olefin are unreactive towards nucleophiles.¹⁴
 13. Eisenstein, O.; Hoffmann, R. *J. Am. Chem. Soc.* **1980**, *102*, 6148.
 14. Chang, T. C. T.; Foxman, B. M.; Rosenblum, M.; Stockman, C. *J. Am. Chem. Soc.* **1981**, *103*, 7361.
 15. These oligomers were identified by their characteristic ^1H NMR spectra.¹⁶
 16. Francis, S. A.; Archer, E. D. *Anal. Chem.* **1963**, *35*, 1363.
 17. Procedures for the isolation and identification of complex hydrocarbon mixtures have been outlined. (a) Stehling, F. C.; Bartz, K. W. *Anal. Chem.* **1966**, *38*, 1467. (b) Archer, E. D.; Shively, J. H.; Francis, S. A. *Anal. Chem.* **1963**, *35*, 1369 and references therein.
 18. The T_1 measurements were performed with the assistance of Dr. S. O. Chan of the Departmental NMR laboratory.
 19. Long relaxation times (of ~ 15 s) are frequently observed for the cyclopentadienyl proton resonances for some $\text{CpM}(\text{NO})$ -containing compounds ($\text{M} = \text{Mo}$ or W).²⁰ A pulse delay of 0 s was used to obtain the spectra shown in Figures 4.1 and 4.2
 20. (a) Hunter, A. D.; Legzdins, P. *Organometallics* **1986**, *5*, 1001. (b) Legzdins, P.; Martin, J. T.; Oxley, J. C. *Organometallics*

- 1985, 4, 1263. (c) Martin, J. T. Ph.D. Dissertation, The University of British Columbia, 1987.
21. For a general discussion of the bonding of aldehyde and ketone ligands in organometallic chemistry, see: Huang, Y.-H.; Gladysz, J. A. *J. Chem. Ed.* **1988**, 65, 298.
22. (a) Snider, B. B. *Acc. Chem. Res.* **1980**, 13, 426. (b) Snider, B. B.; Roush, D. M.; Rodini, D. J.; Gonzalez, D.; Spindell, D. *J. Org. Chem.* **1980**, 45, 2773. (c) Snider, B. B.; Rodini, D. J.; Conn, R. S. E.; Sealfon, S. *J. Am. Chem. Soc.* **1979**, 101, 5283. (d) Snider, B. B.; Roush, D. M. *J. Am. Chem. Soc.* **1979**, 101, 1906.
23. For other examples of O-dealkylation in organometallic chemistry, see (a) Davison, A.; Reger, D. L. *J. Am. Chem. Soc.* **1972**, 94, 9237. (b) Bodner, G. S.; Smith, D. E.; Hatton, W. G.; Heah, P. C.; Georgiou, S.; Rheingold, A. L.; Geib, S. J.; Hutchinson, J. P.; Gladysz, J. A. *J. Am. Chem. Soc.* **1987**, 109, 7688.
24. The structural analysis was performed by Drs. R. H. Jones and F. W. B. Einstein of Simon Fraser University.
25. Greenhough, T. J.; Kolthammer, B. W. S.; Legzdins, P.; Trotter, J. *Acta Crystallogr., Sect. B: Struct. Crystallogr. Cryst. Chem.* **1980**, B36, 795.
26. Similar situations have been well documented for various structurally characterized carboxylic esters. Schweizer, W. B.; Dunitz, J. D. *Helv. Chim. Acta.* **1982**, 65, 1547.
27. Handbook of Chemistry and Physics; Weast, R. C.; Astle, M. J., Eds.; CRC: Florida, 1980; 60th Ed., F216.

28. Allen, F. H. *Acta Crystallogr., Sect. B: Struct. Crystallogr. Cryst. Chem.* **1981**, B37, 890.
29. The $\text{CpW(NO)}_2\text{Fc}$ compound (Fc = ferrocenyl) is reported to undergo a similar conversion to $\text{CpW(O)}_2\text{Fc}$. Herberhold, M.; Kniesel, H.; Haumaier, L.; Gieren, A.; Ruiz-Pérez, C. *Z. Naturforsch., B: Anorg. Chem, Org. Chem.* **1986**, 41b, 1431.

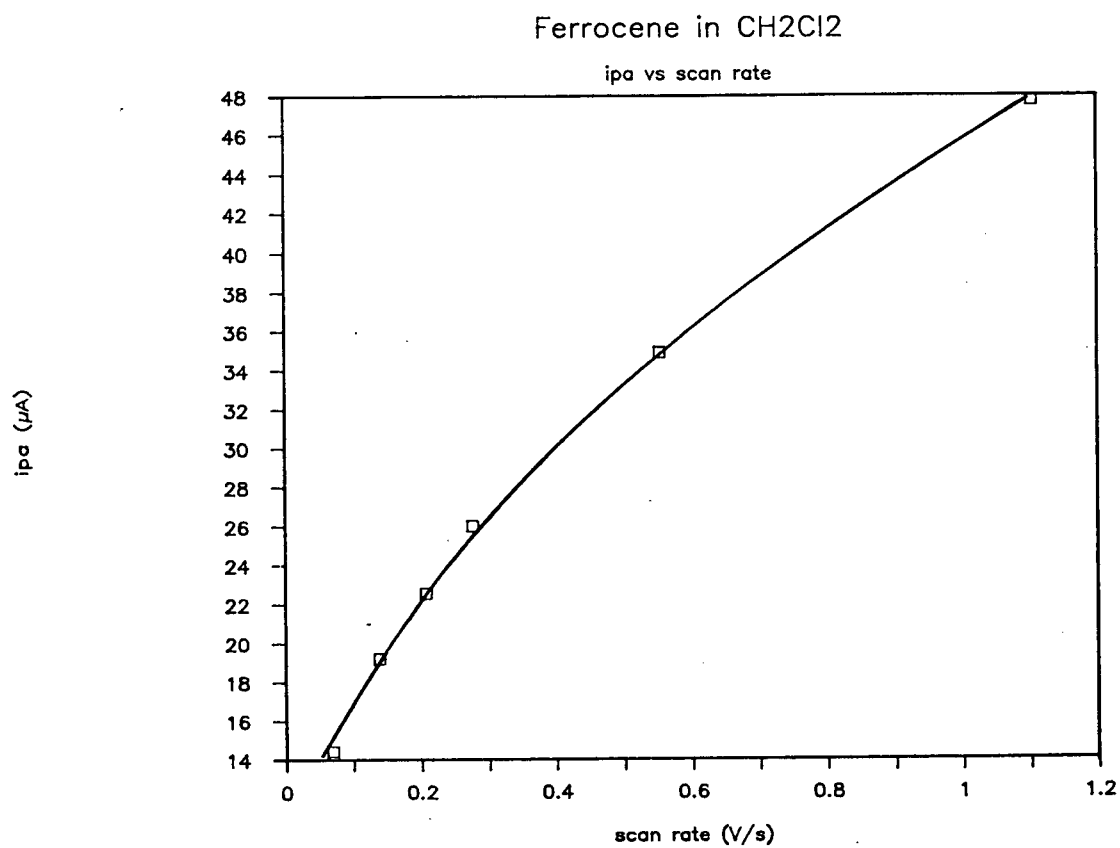
Epilogue

The work presented in this thesis shows that a knowledge of the redox behavior of a class of compounds may help to explain some of the chemistry observed for these complexes. As a result of cyclic voltammetry (and ESR) studies on a series of organometallic nitrosyl-dihalo complexes, new routes to previously unknown $\text{Cp}'\text{Mo}(\text{NO})\text{R}_2$ complexes (R = alkyl or aryl) have been found. Clearly, the extensions of such studies (described in Chapter 2) to other organometallic-halide systems for which no alkyl (or aryl) derivatives are known, are warranted. It is not assumed, however, that trends similar to those observed for the nitrosyl-dihalo complexes studied will be seen in such extensions.

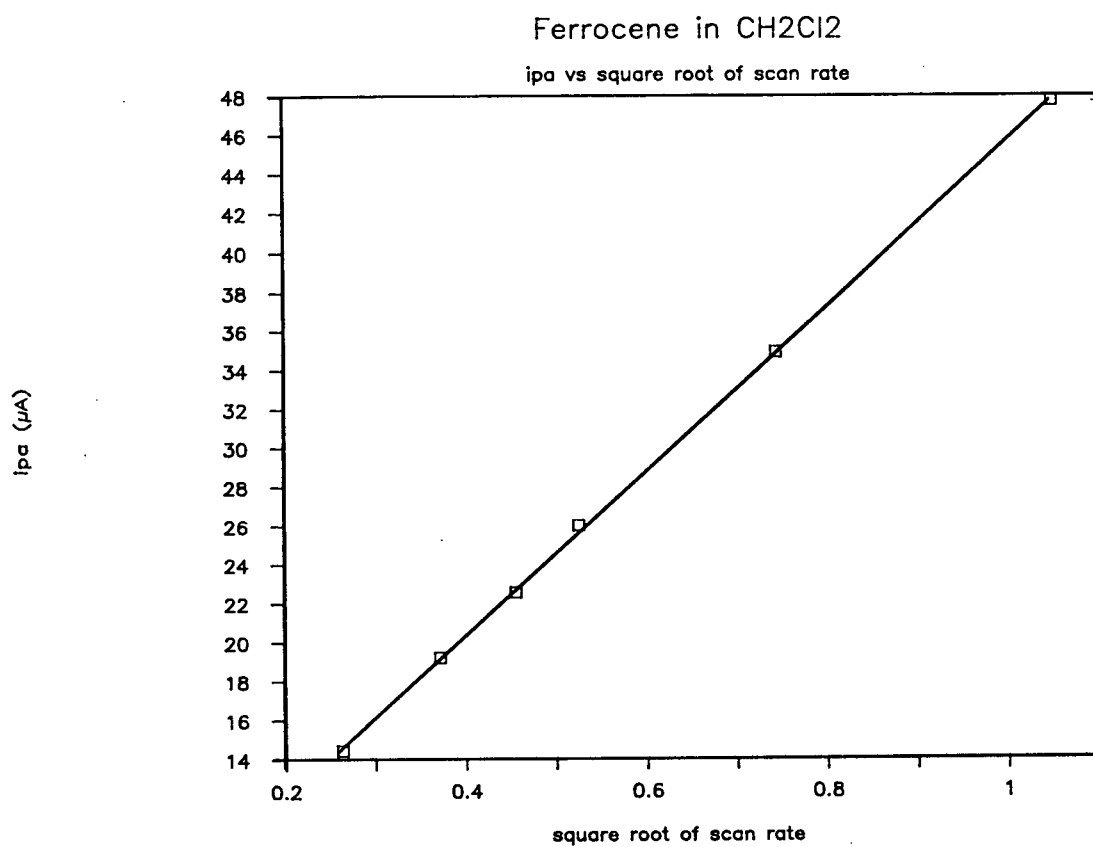
The use of organometallic nitrosyl complexes in organic synthesis has only received little attention, although the potential applications are enormous. Detailed studies of the reactions of nitrogen-containing electrophiles with various $\text{CpCr}(\text{NO})_2\text{R}$ compounds have ultimately led to the creation of a stoichiometric cycle for the formation of carbon-nitrogen bonds. Furthermore, the application of the Group 6 organometallic nitrosyl compounds for the formation of carbon-carbon and carbon-oxygen bonds has been developed in the last chapter of this thesis. It is my hope that this work will draw more attention to the potential applications of organometallic nitrosyl complexes as catalysts and specific reagents for organic transformations.

APPENDIX

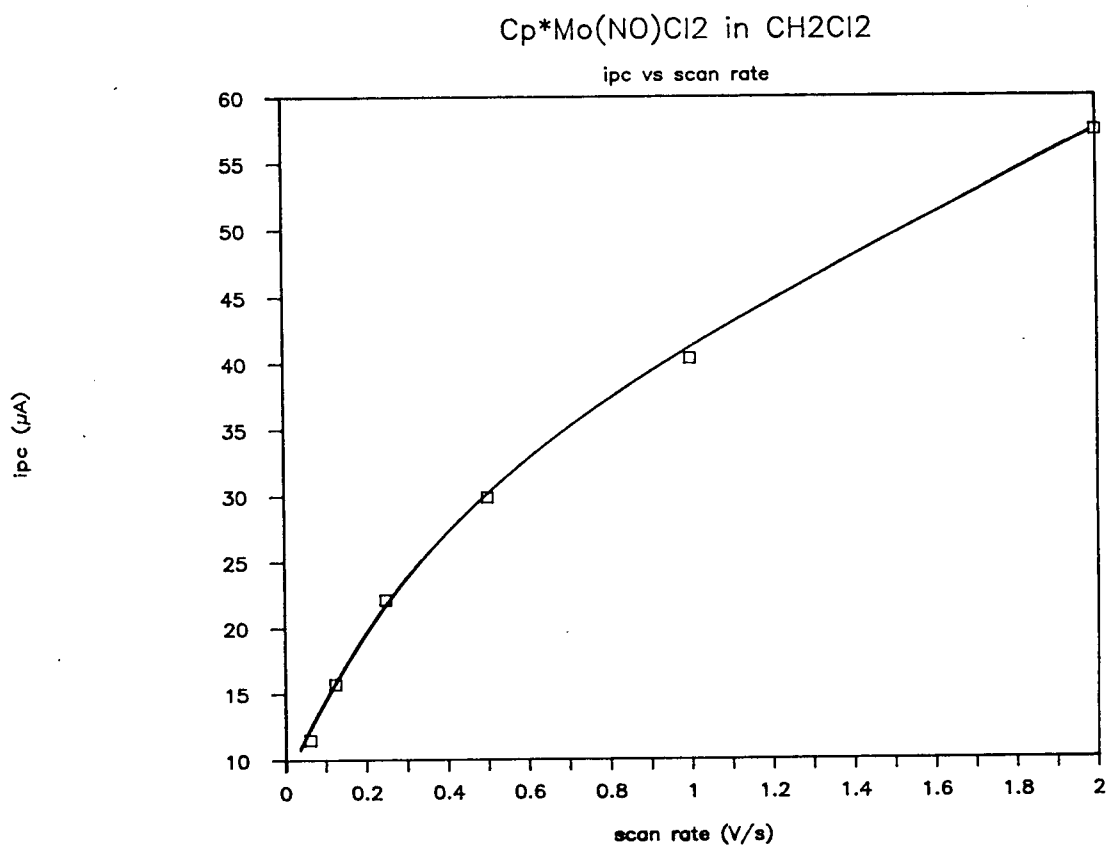
Plot of $i_{p,a}$ vs scan rate for the electrochemical oxidation of Cp_2Fe in CH_2Cl_2 .



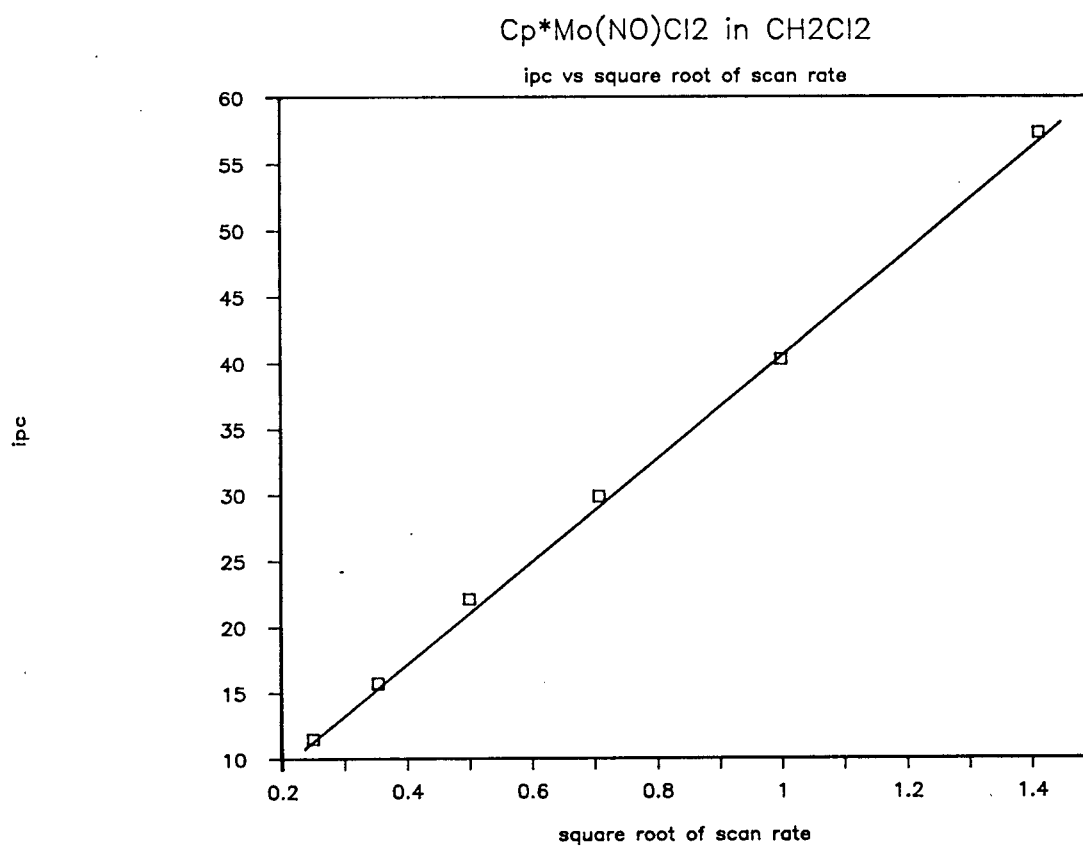
Plot of $i_{p,a}$ vs square root of scan rate for the electrochemical oxidation of Cp_2Fe in CH_2Cl_2 .



Plot of $i_{p,c}$ vs scan rate for the electrochemical reduction of $\text{Cp}^*\text{Mo}(\text{NO})\text{Cl}_2$ in CH_2Cl_2 .



Plot of $i_{p,c}$ vs square root of scan rate for the electrochemical reduction of $\text{Cp}^*\text{Mo}(\text{NO})\text{Cl}_2$ in CH_2Cl_2 .



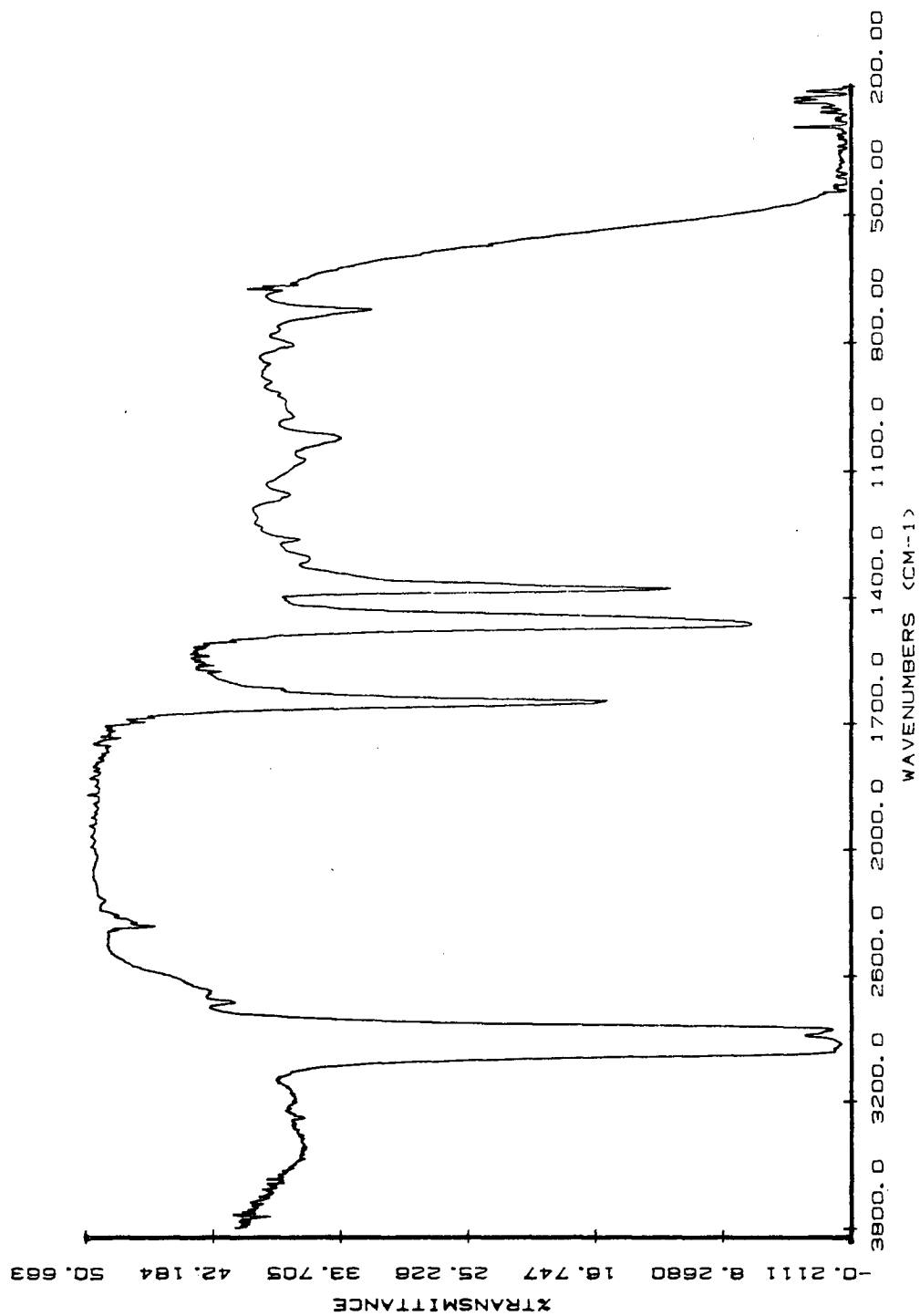
Oxidation Peak Potentials and Associated Redox Data of Some Cp'(M(NO)X₂ and
Related Complexes.

Compound ^a	Scan Rate (<u>v</u> , Vs ⁻¹)	<u>E</u> ¹ _{p,a}	<u>E</u> ² _{p,a}	<u>E</u> ³ _{p,a}	<u>E</u> ¹ _{p,c}	<u>E</u> ² _{p,c}	<u>E</u> ³ _{p,c}	Comments
CpMo(NO)Cl ₂	0.21	1.67	1.91					Broad
Cp [*] Mo(NO)Cl ₂	0.43	1.47	1.68					Broad
CpMo(NO)Br ₂	0.41	1.93			0.41			<u>E</u> ¹ _{p,c} broad and weak
Cp [*] Mo(NO)Br ₂	0.41	1.49	1.74		1.19	0.36		<u>E</u> _{p,c} 's broad and weak
CpMo(NO)I ₂ _b	0.17	1.05			0.46	-0.04		<u>E</u> ² _{p,c} is <u>E</u> _{1/2} (see text)
CpMo(NO)I ₂ _b	0.44	0.33	0.96	1.79	1.69	0.58	0.19	<u>E</u> ³ _{p,c} associated with broad and weak
Cp [*] Mo(NO)I ₂	0.36	1.64			0.58	0.33		<u>E</u> ² _{p,a}
CpW(NO)I ₂	0.40	1.54						
Cp [*] W(NO)I ₂	0.40	1.35	1.75		1.46	0.61		<u>E</u> _{p,c} 's broad
CpMo(NO)I ₂ PMePh ₂	0.20	0.98	1.47	1.70	1.41	0.53		<u>E</u> ² _{p,a} weak and broad
CpW(NO)(CH ₂ SiMe ₃) ₂	0.15	1.15						
Cp [*] W(NO)(CH ₂ SiMe ₃) ₂	0.20	0.97			-0.10	-0.45		<u>E</u> ¹ _{p,c} broad <u>E</u> ² _{p,c} broad

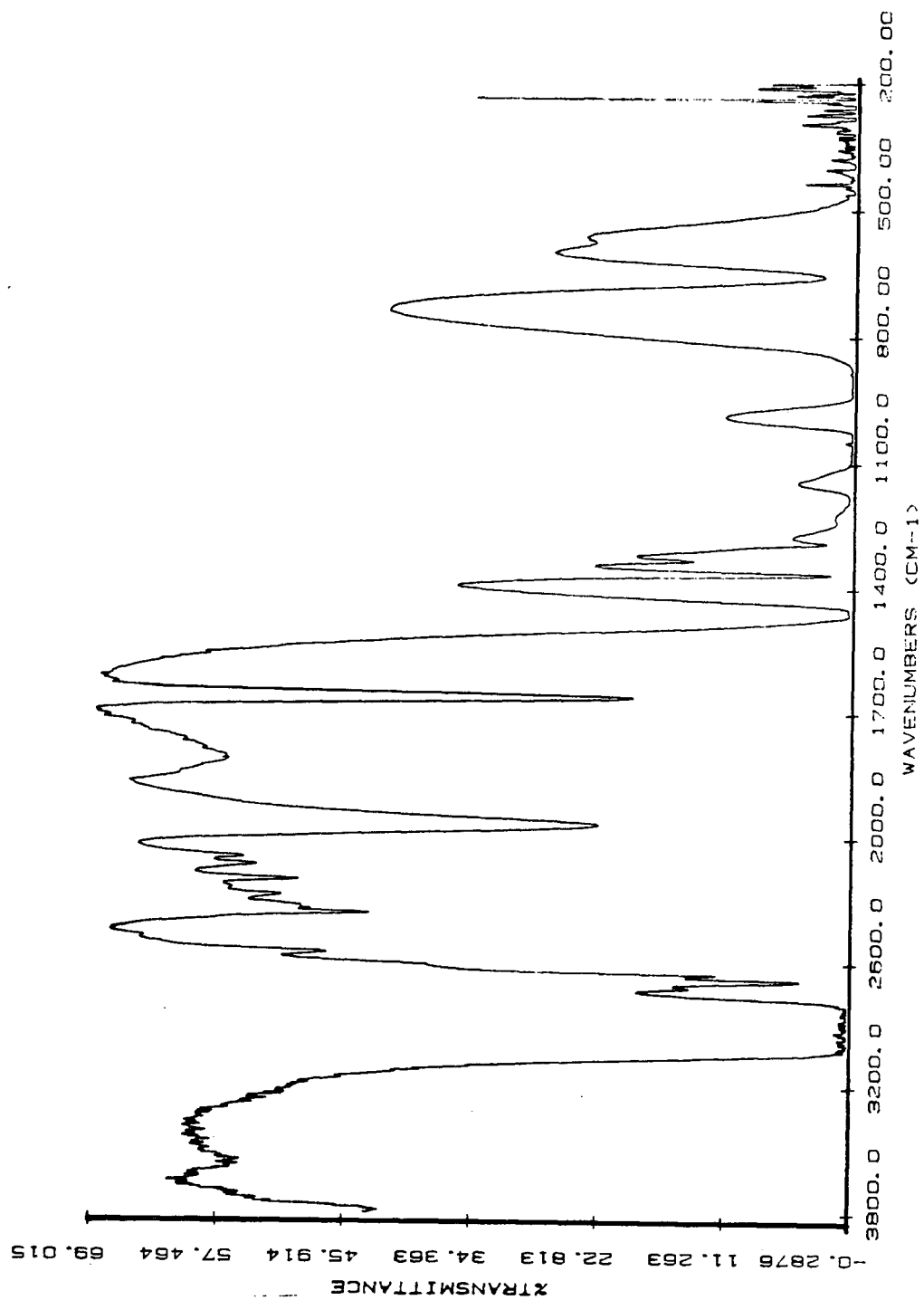
^a in CH₂Cl₂ (0.1 M [n-Bu₄N]PF₆)

^b in CH₃CN (0.1 M [n-Bu₄N]PF₆)

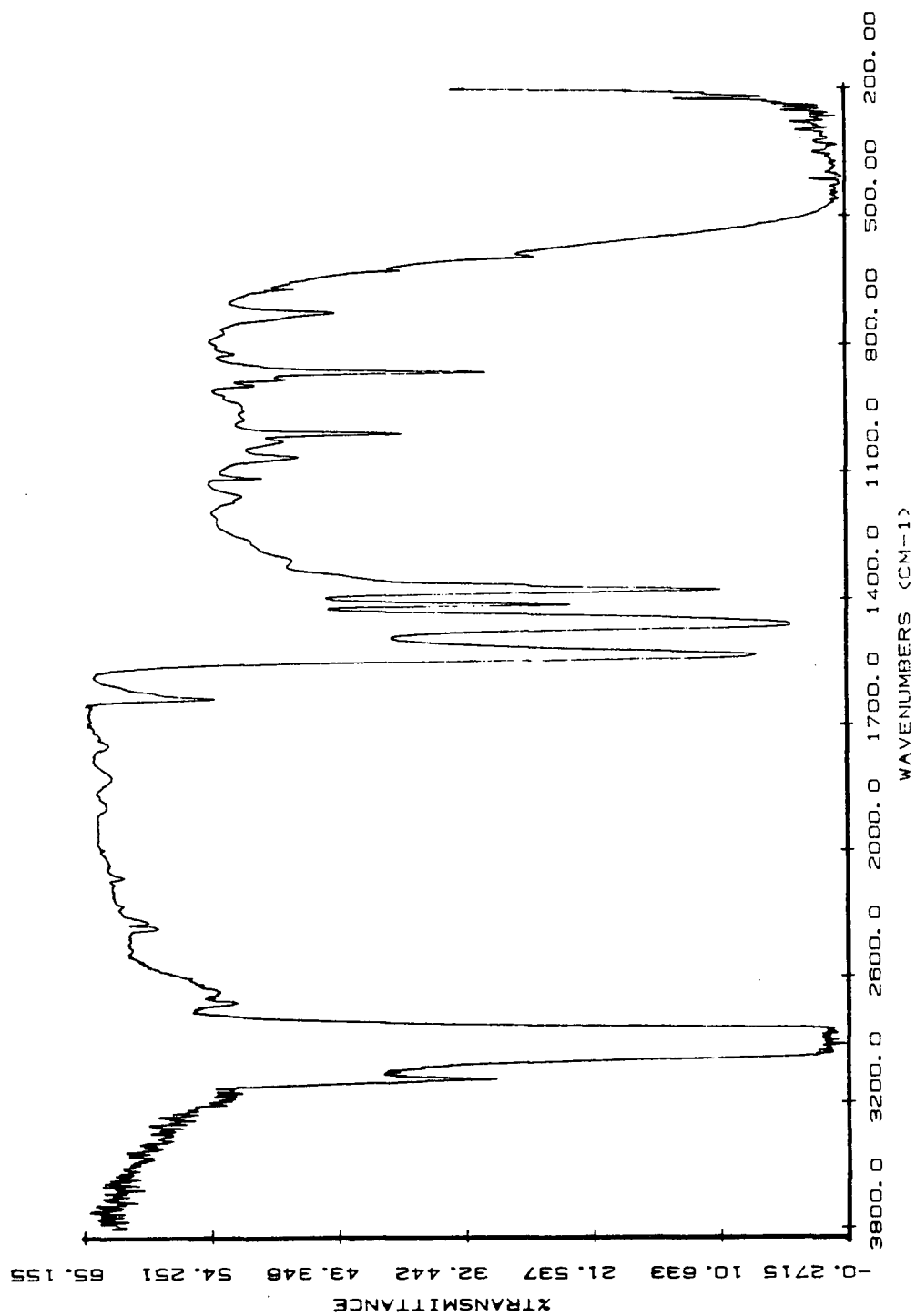
IR spectrum of $\text{Cp}^*\text{Mo}(\text{NO})\text{Cl}_2$ as a Nujol mull.



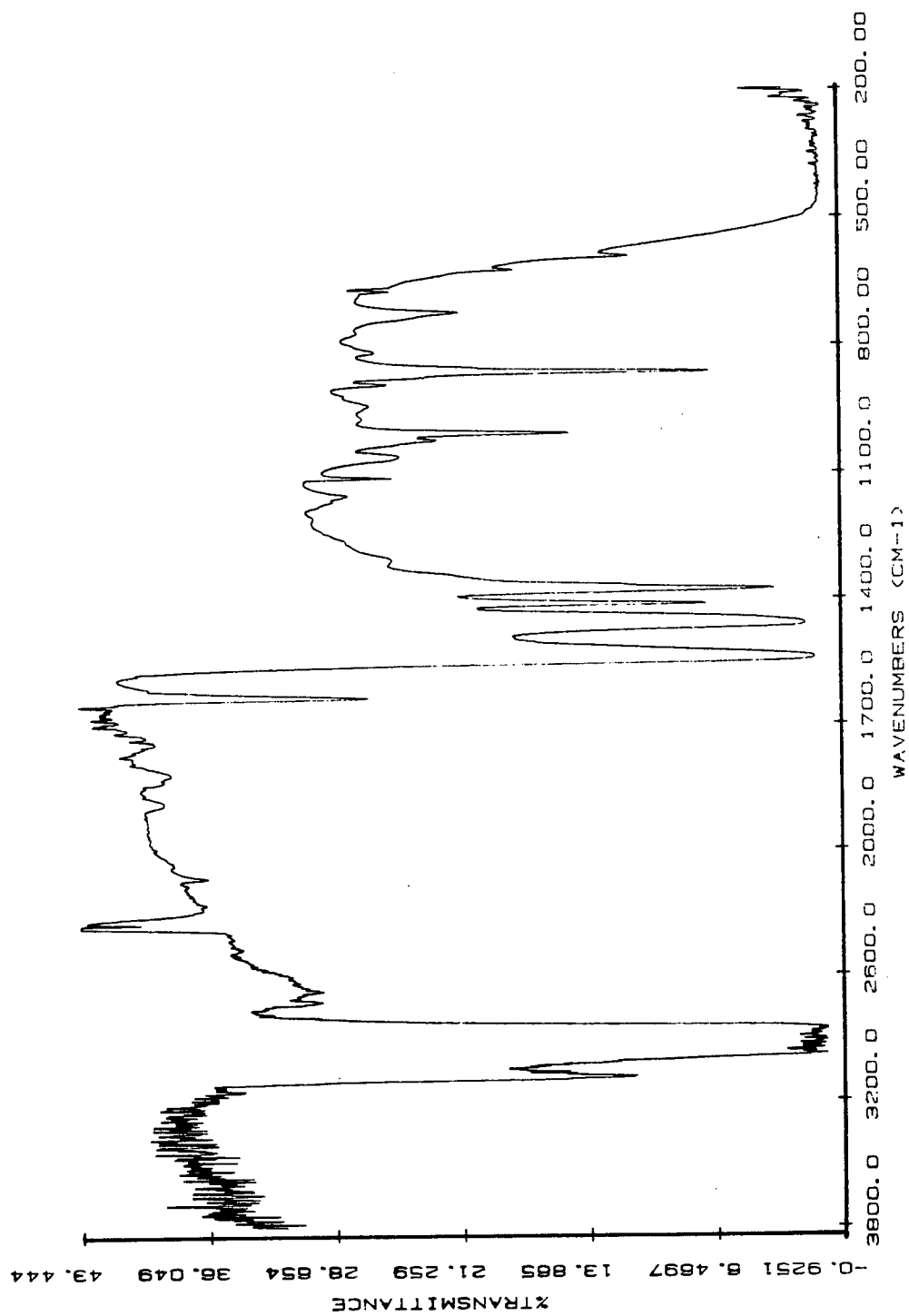
IR spectrum of $\text{Cp}^*\text{Mo}(\text{NO})\text{Br}_2$ in THF.



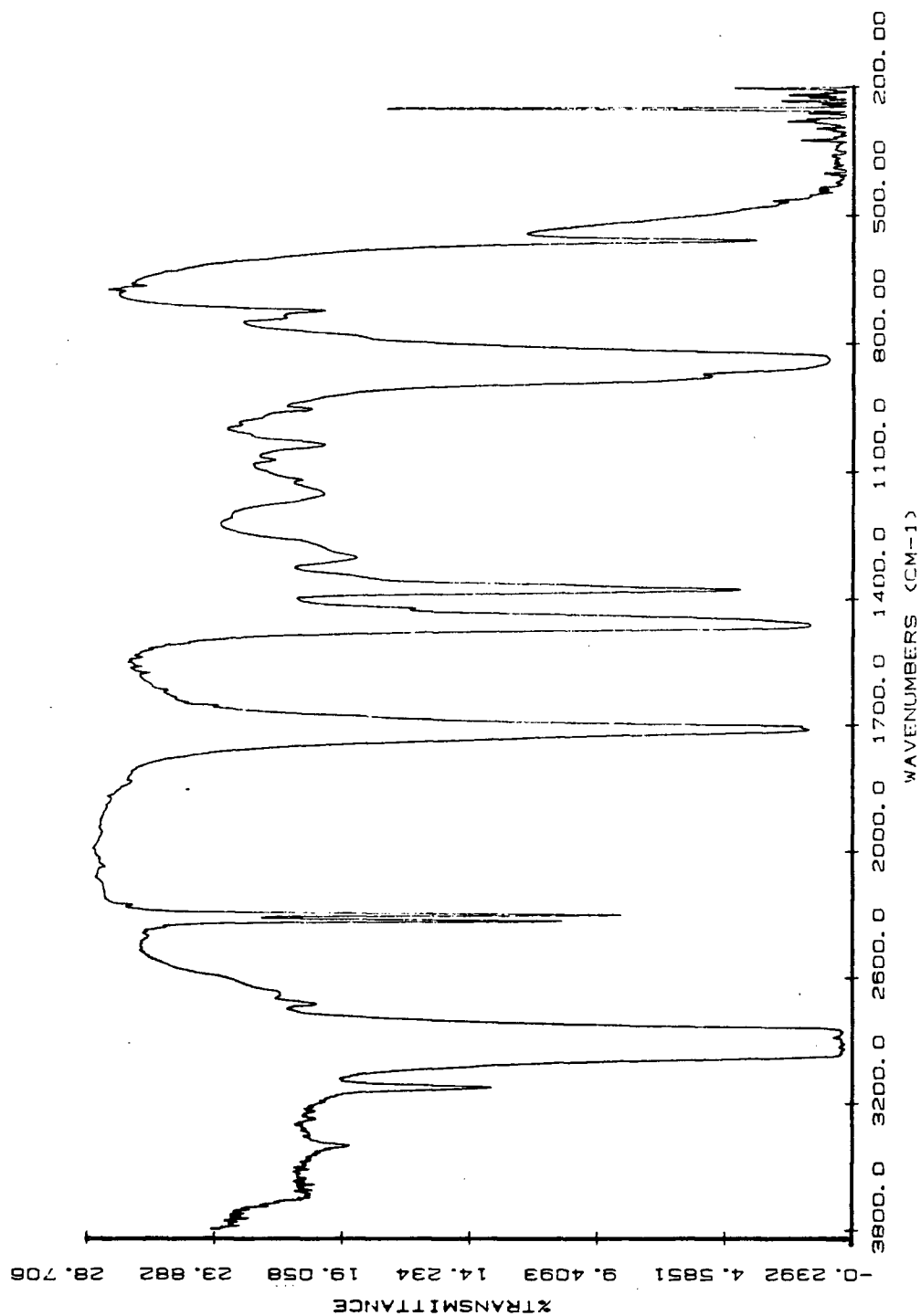
IR spectrum of $[\text{Cp}_2\text{Co}][\text{Cp}^*\text{Mo}(\text{NO})\text{Br}_2]$ as a Nujol mull.



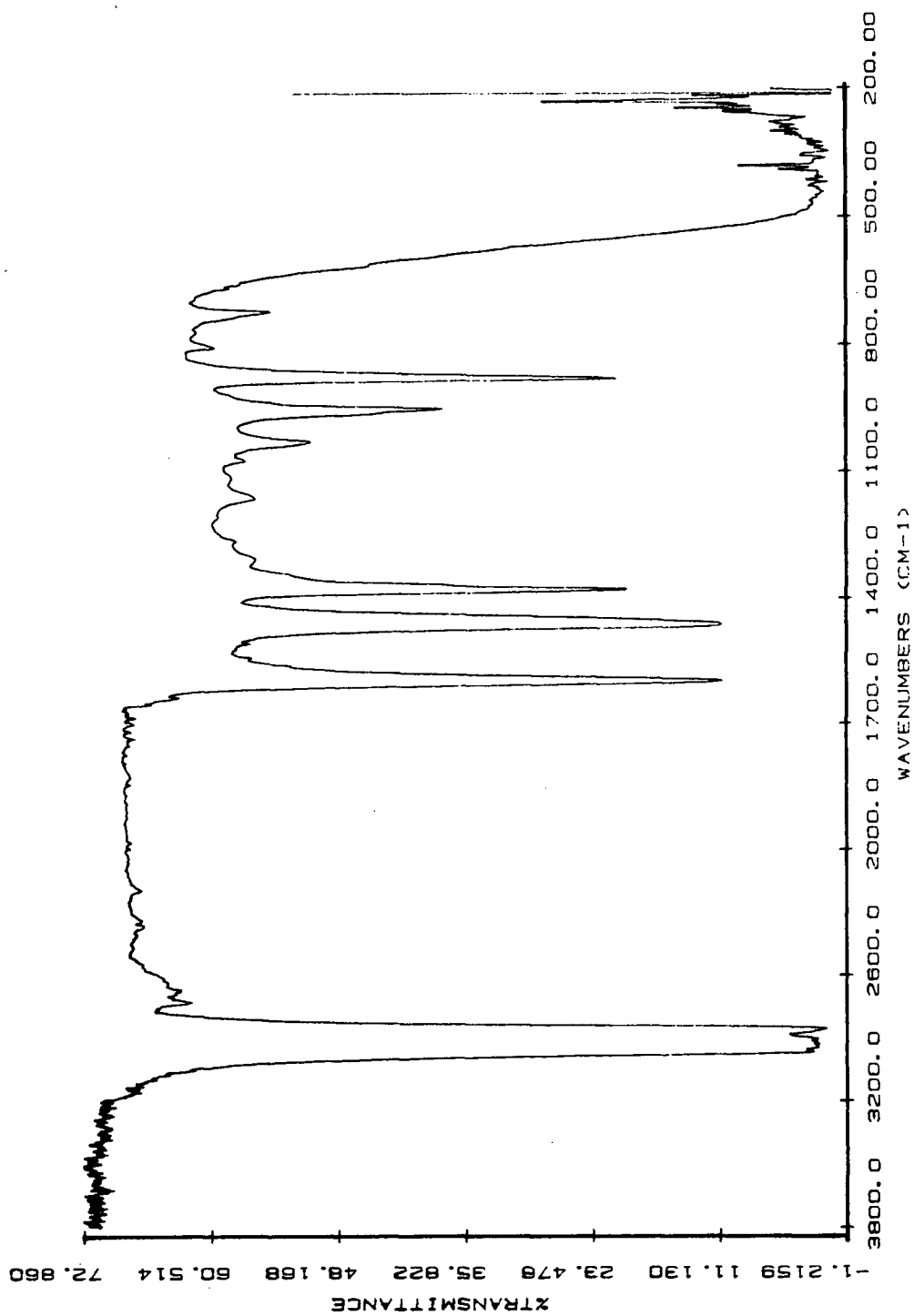
IR spectrum of $[\text{Cp}_2\text{Co}][\text{Cp}^*\text{Mo}(\text{NO})\text{I}_2]$ as a Nujol mull.



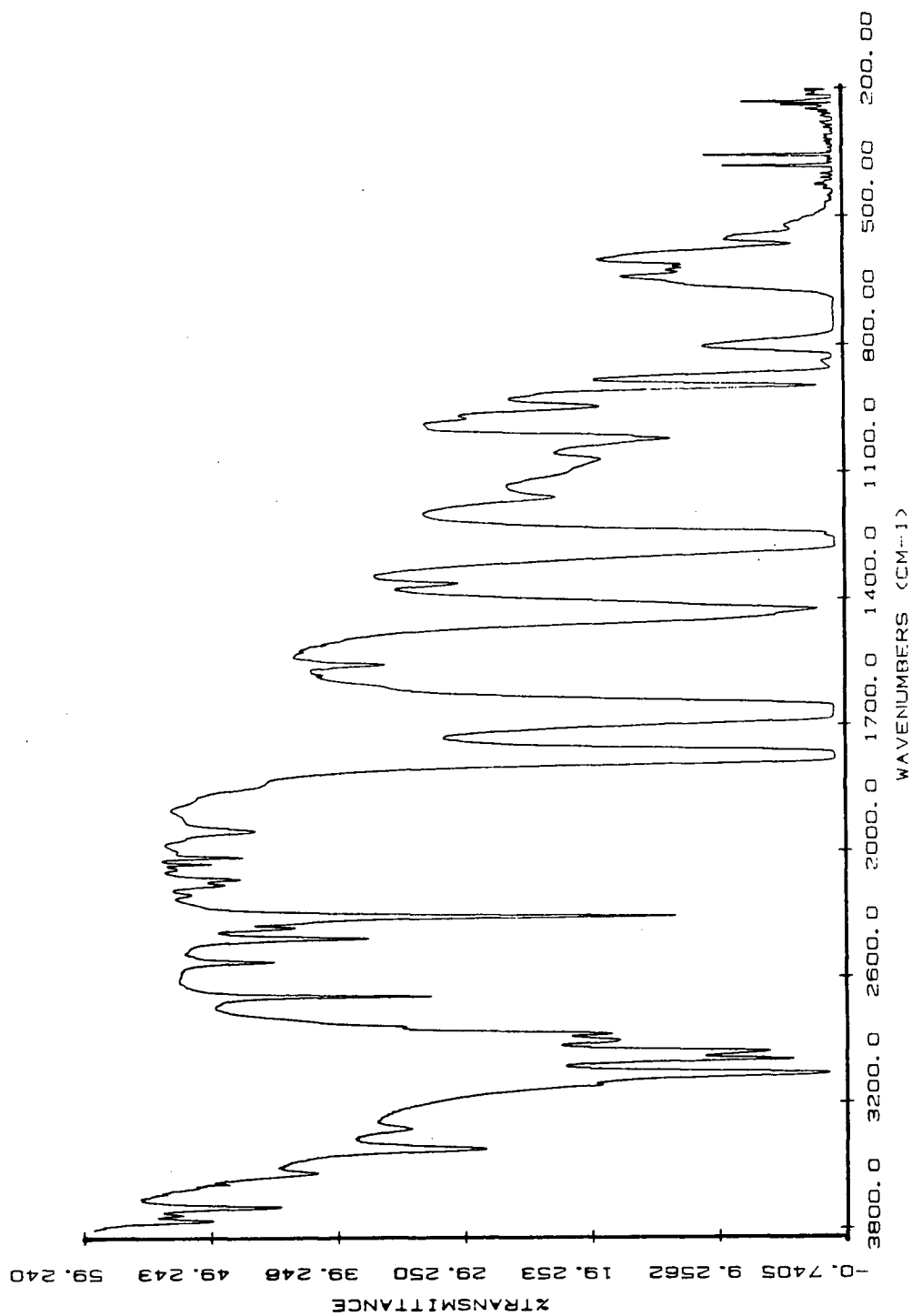
IR spectrum of $[\text{CpMo}(\text{NO})(\text{CH}_3\text{CN})_3](\text{I})(\text{PF}_6)$ as a Nujol mull.

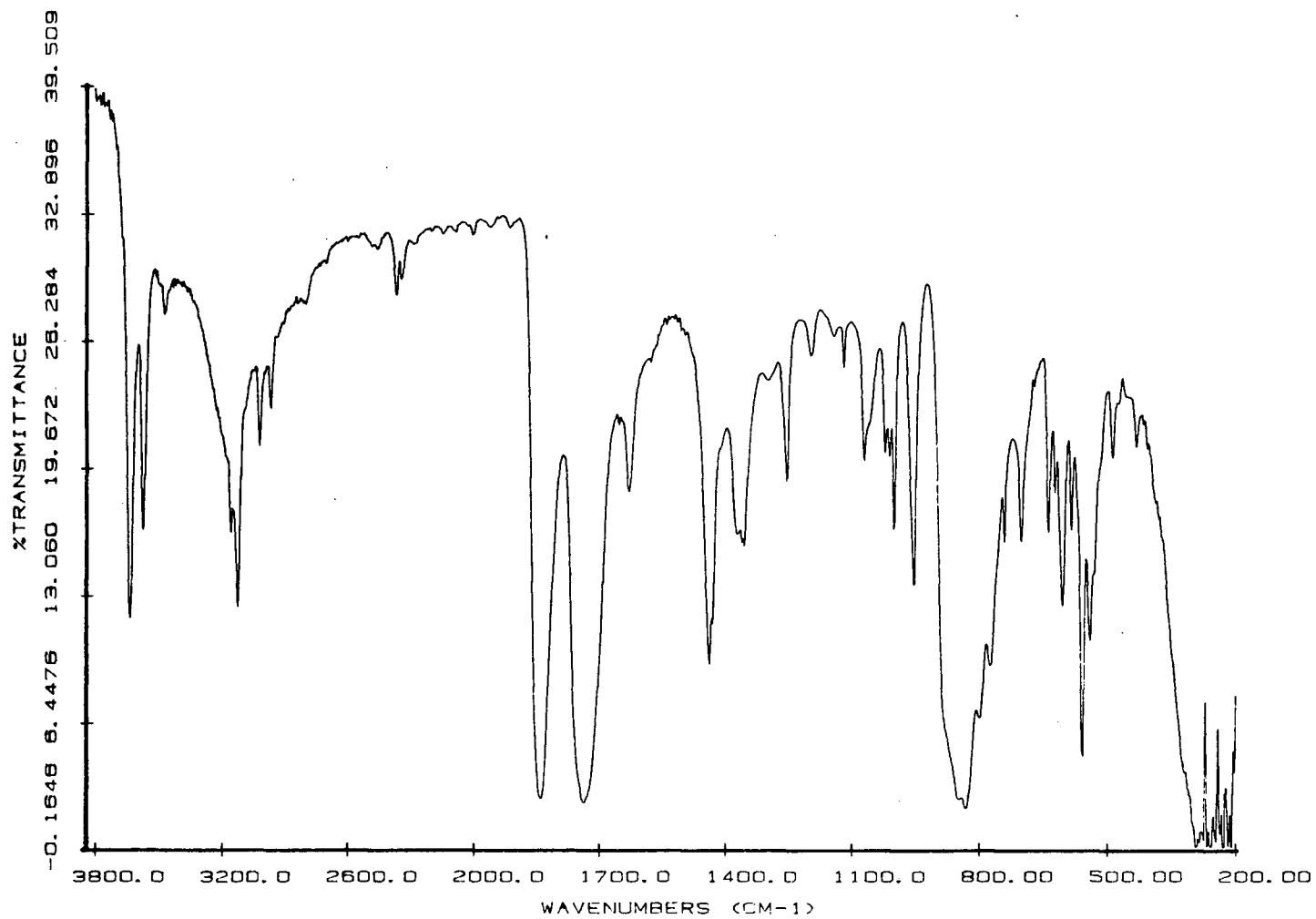


IR spectrum of $[\text{Cp}^*\text{W}(\text{NO})\text{I}]_2$ as a Nujol mull.

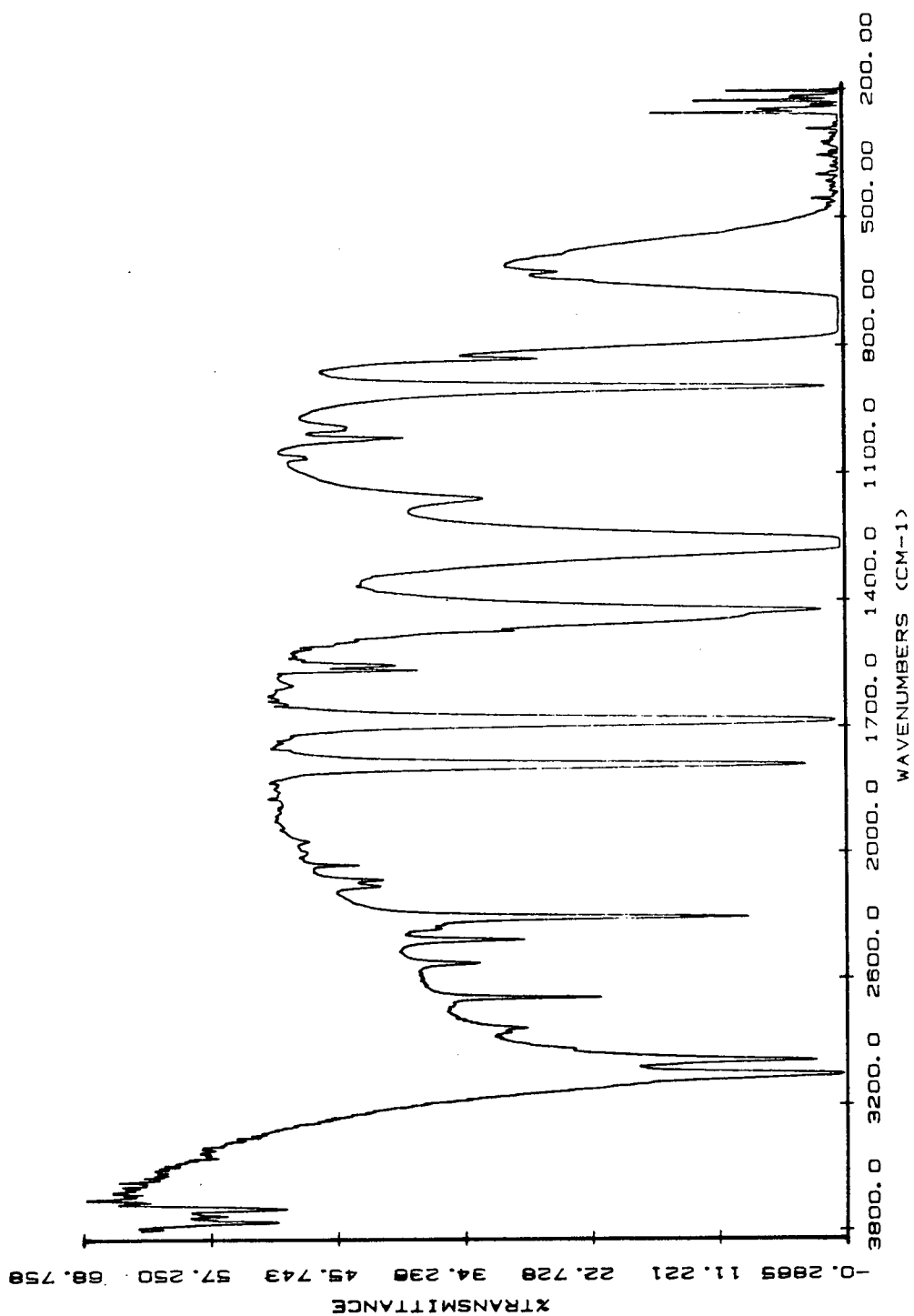


IR spectrum of $\text{CpCr}(\text{NO})_2\text{CH}_2\text{SiMe}_3$ in CH_2Cl_2 .

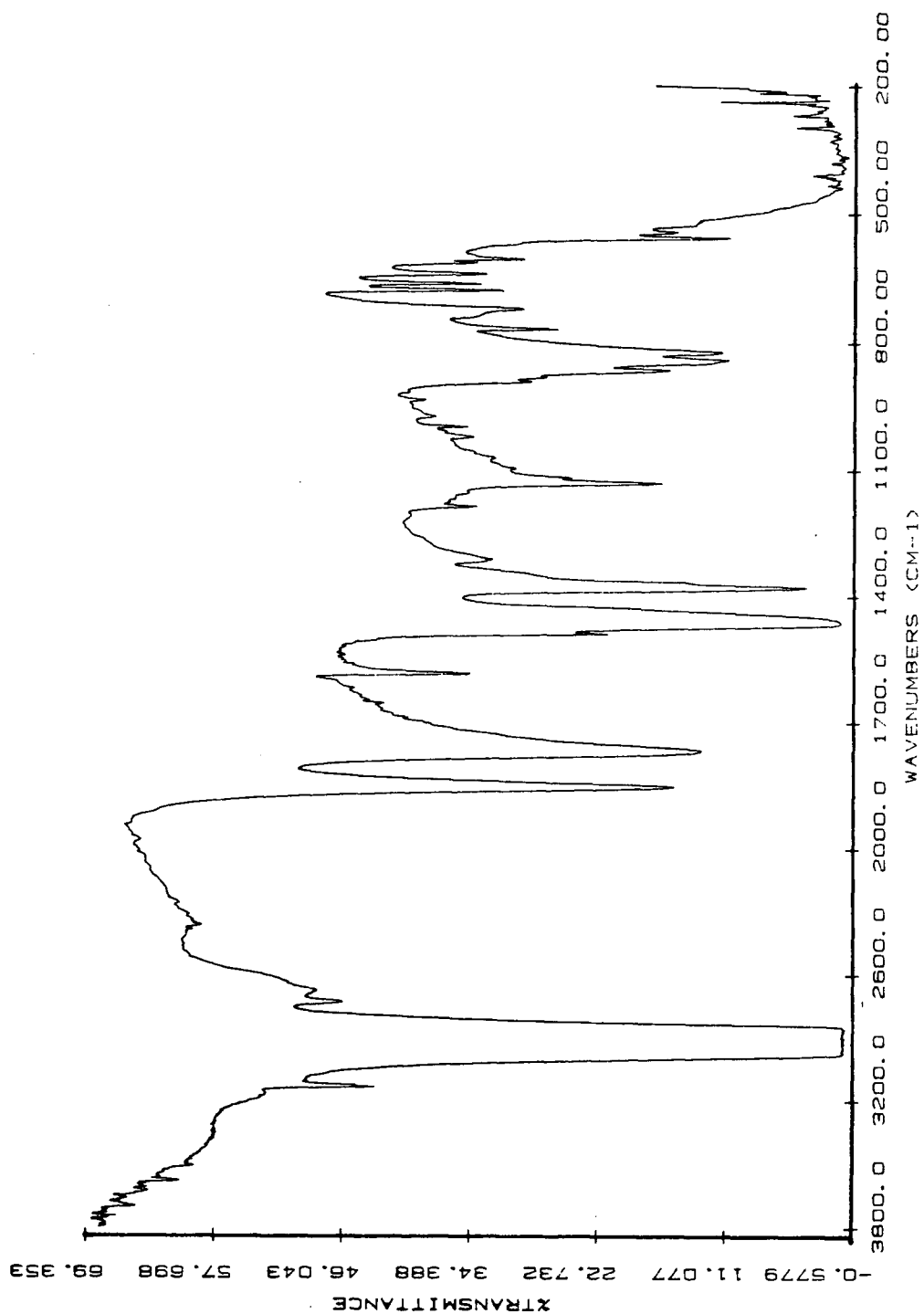




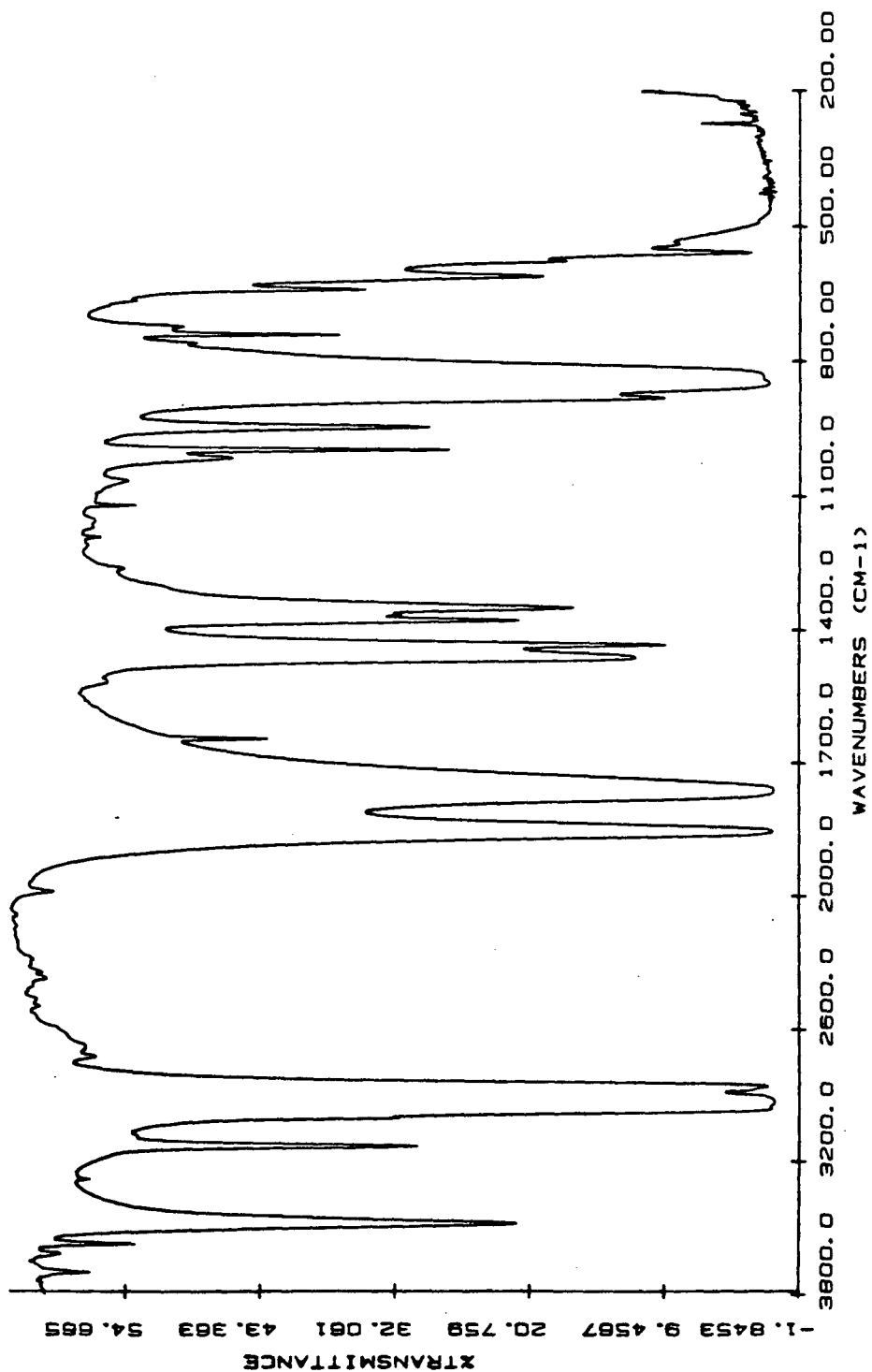
IR spectrum of $\text{CpCr}(\text{NO})_2\text{Ph}$ in CH_2Cl_2 .



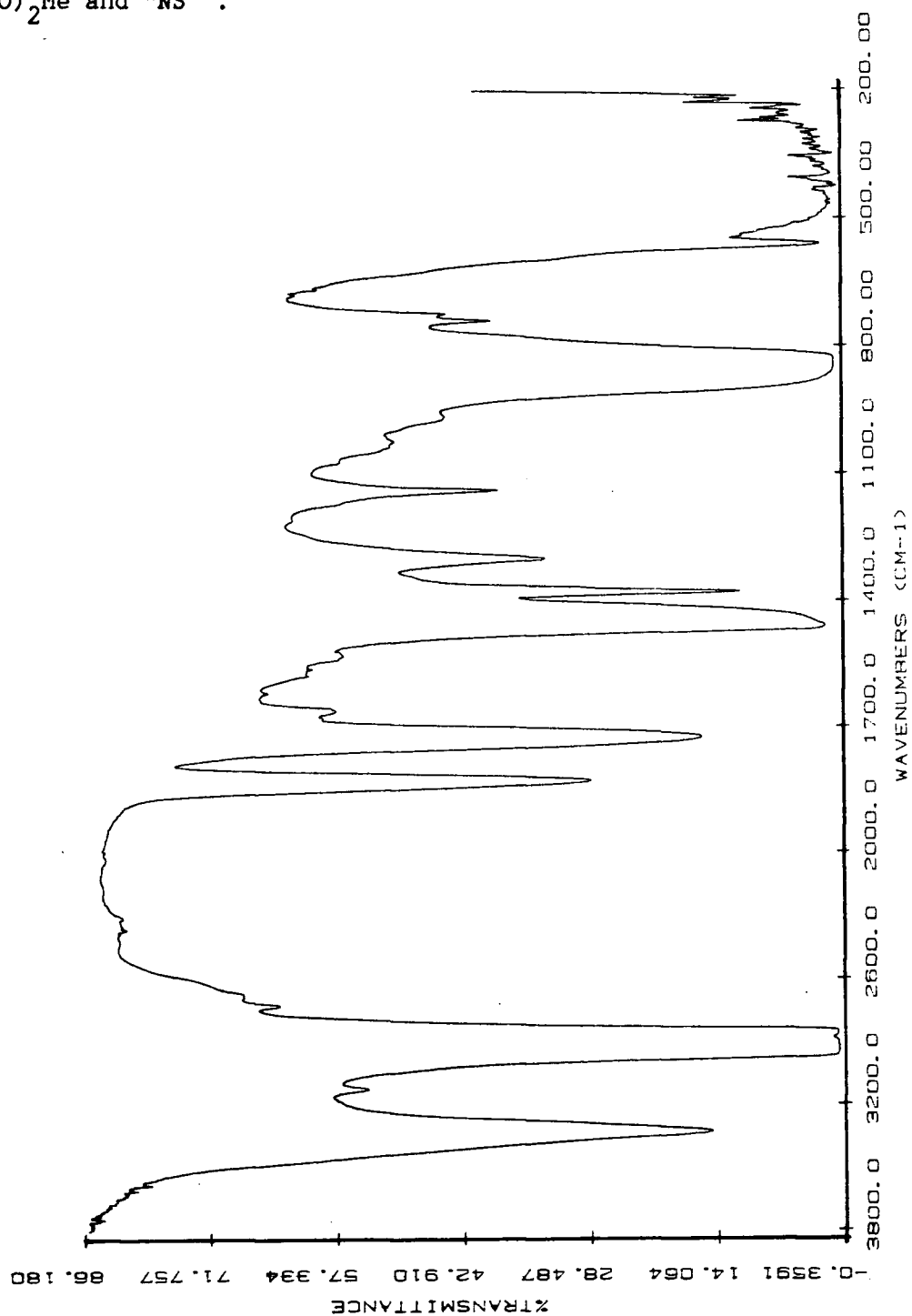
IR spectrum of $[\text{CpCr}(\text{NO})_2\{\text{N}(\text{O})\text{Ph}\}]\text{PF}_6$ as a Nujol mull.



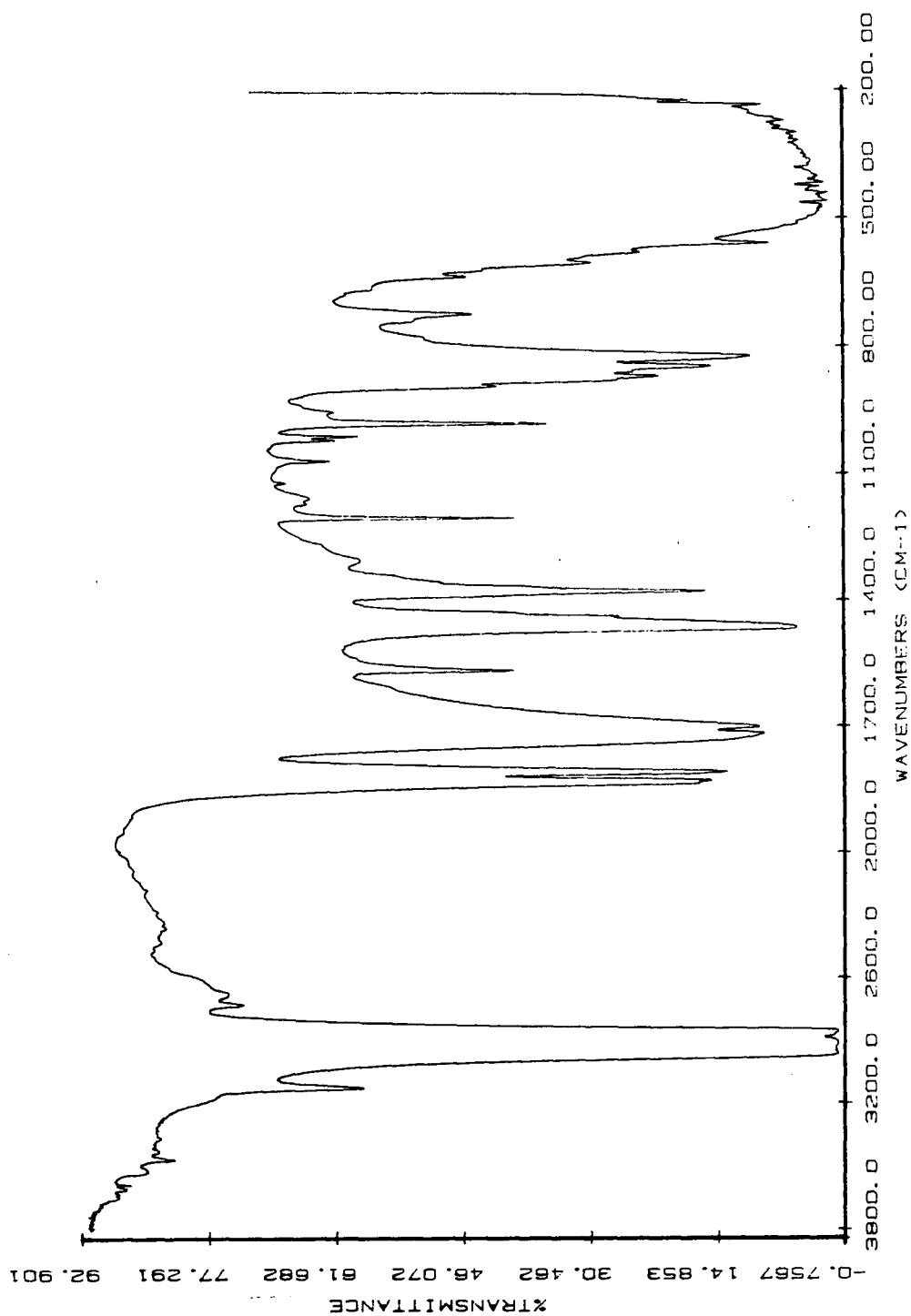
IR spectrum of $[\text{CpCr}(\text{NO})_2\{\text{N}(\text{OH})\text{CH}_2\}]\text{PF}_6$ as a Nujol mull.



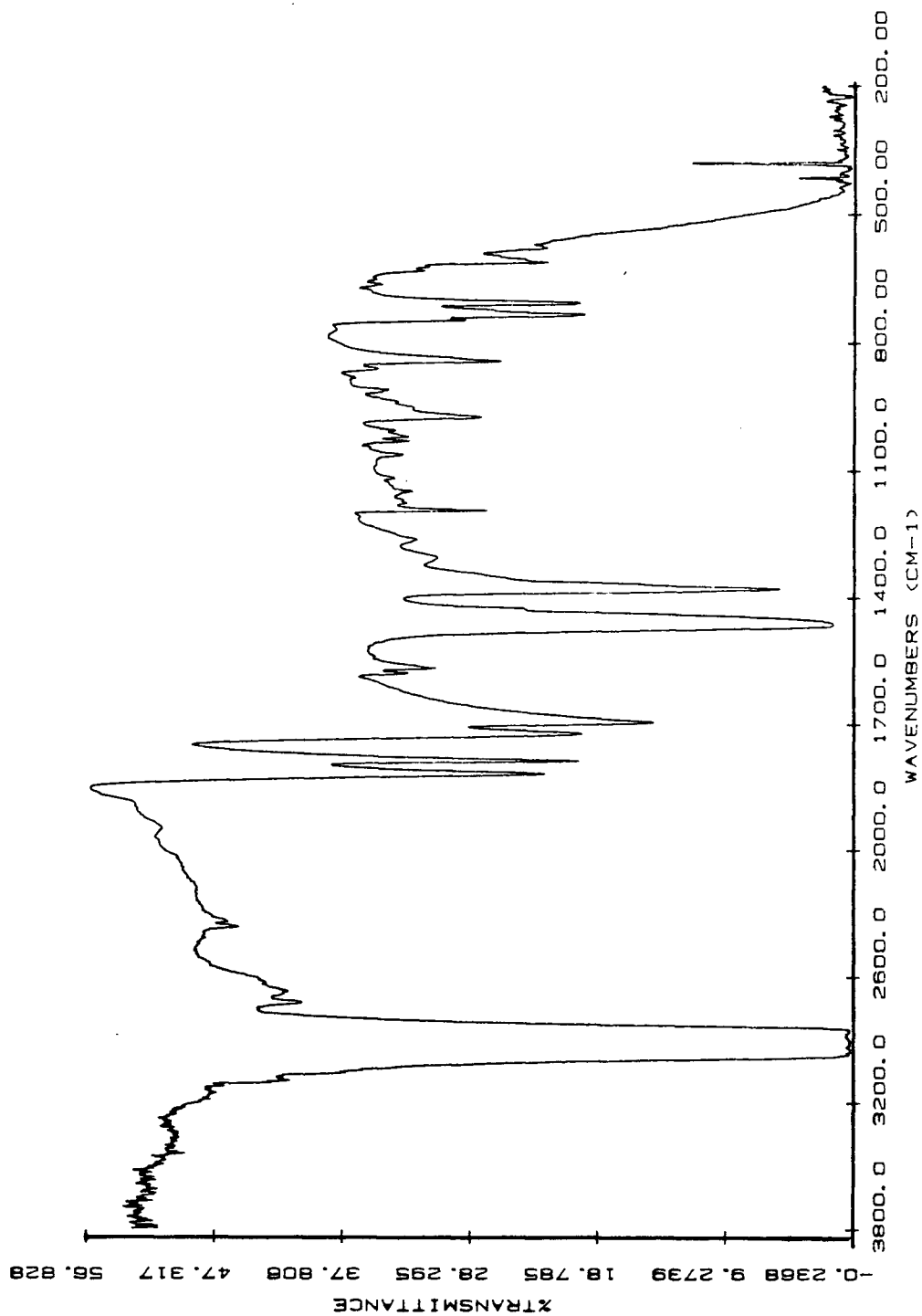
IR spectrum of the green solid (as a Nujol mull) from the reaction of $\text{CpCr}(\text{NO})_2\text{Me}$ and " NS^+ ".



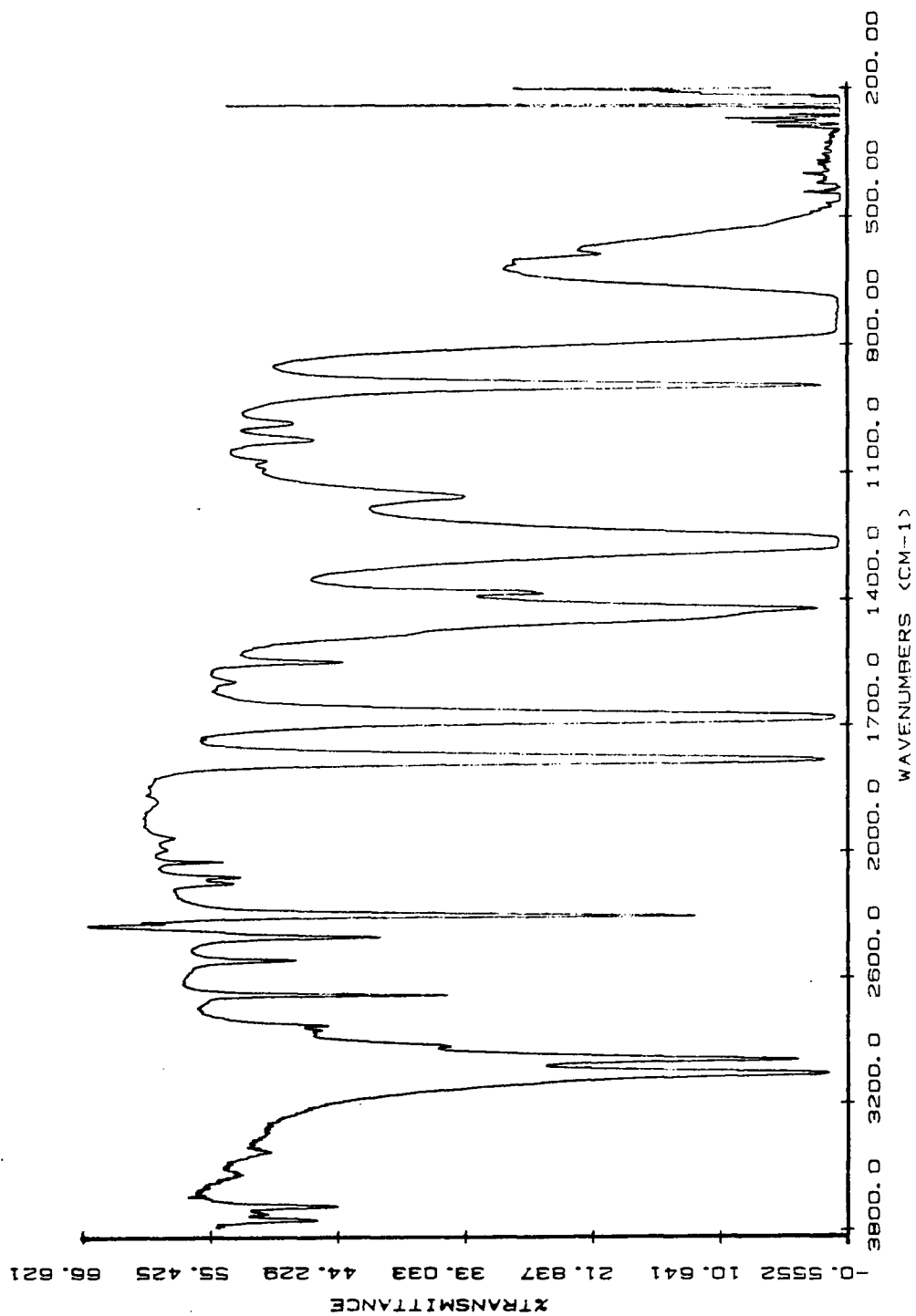
IR spectrum of $[(\text{CpCr}(\text{NO})_2)_2(\mu, \eta^2\text{-N}(\text{CH}_2)\text{O})]\text{PF}_6$ as a Nujol mull.



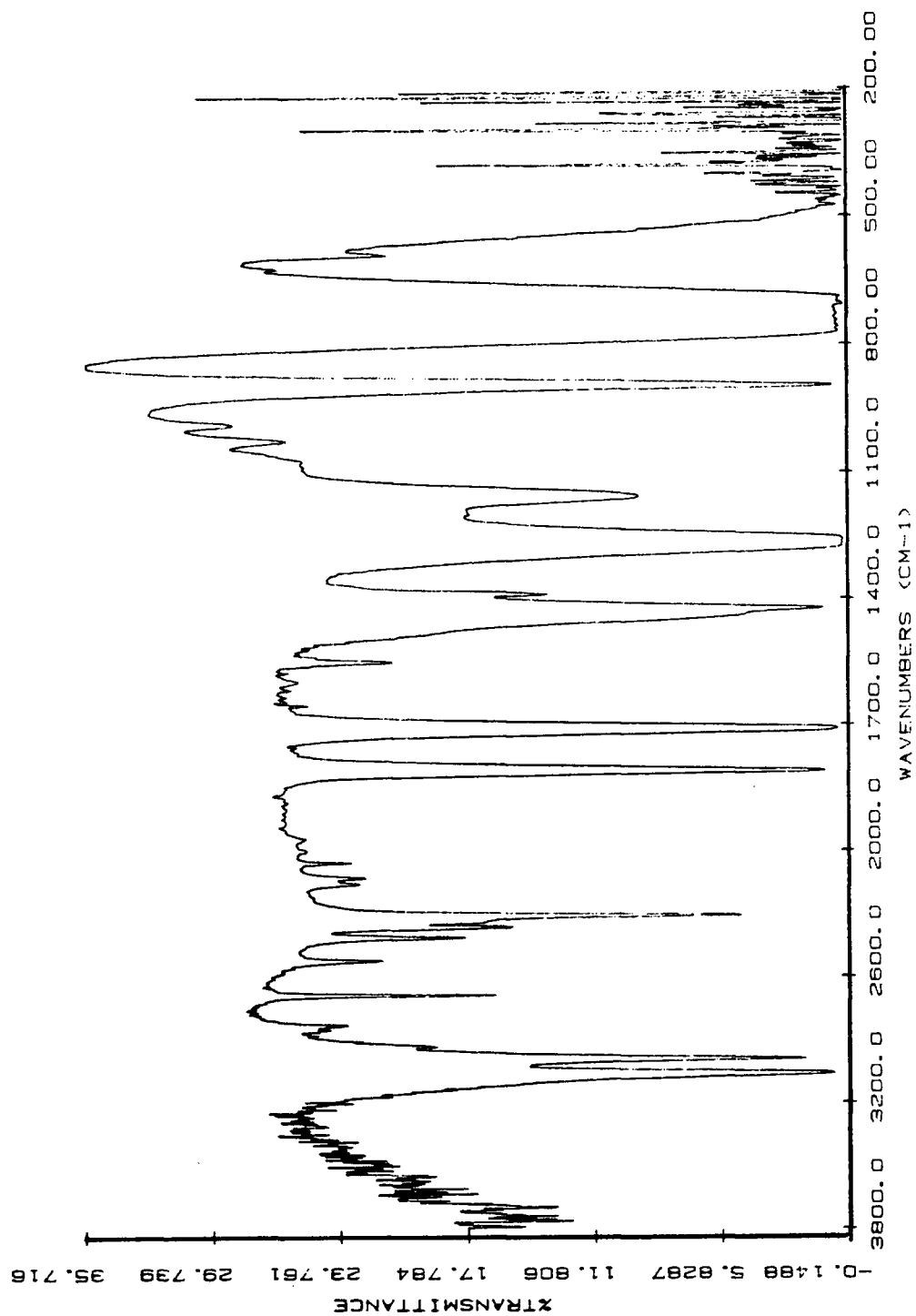
IR spectrum of $[(\text{CpCr}(\text{NO})_2)_2\{\mu, \eta^2\text{-N}(\text{CH}_2\text{O})\}]\text{BPh}_4$ as a Nujol mull.



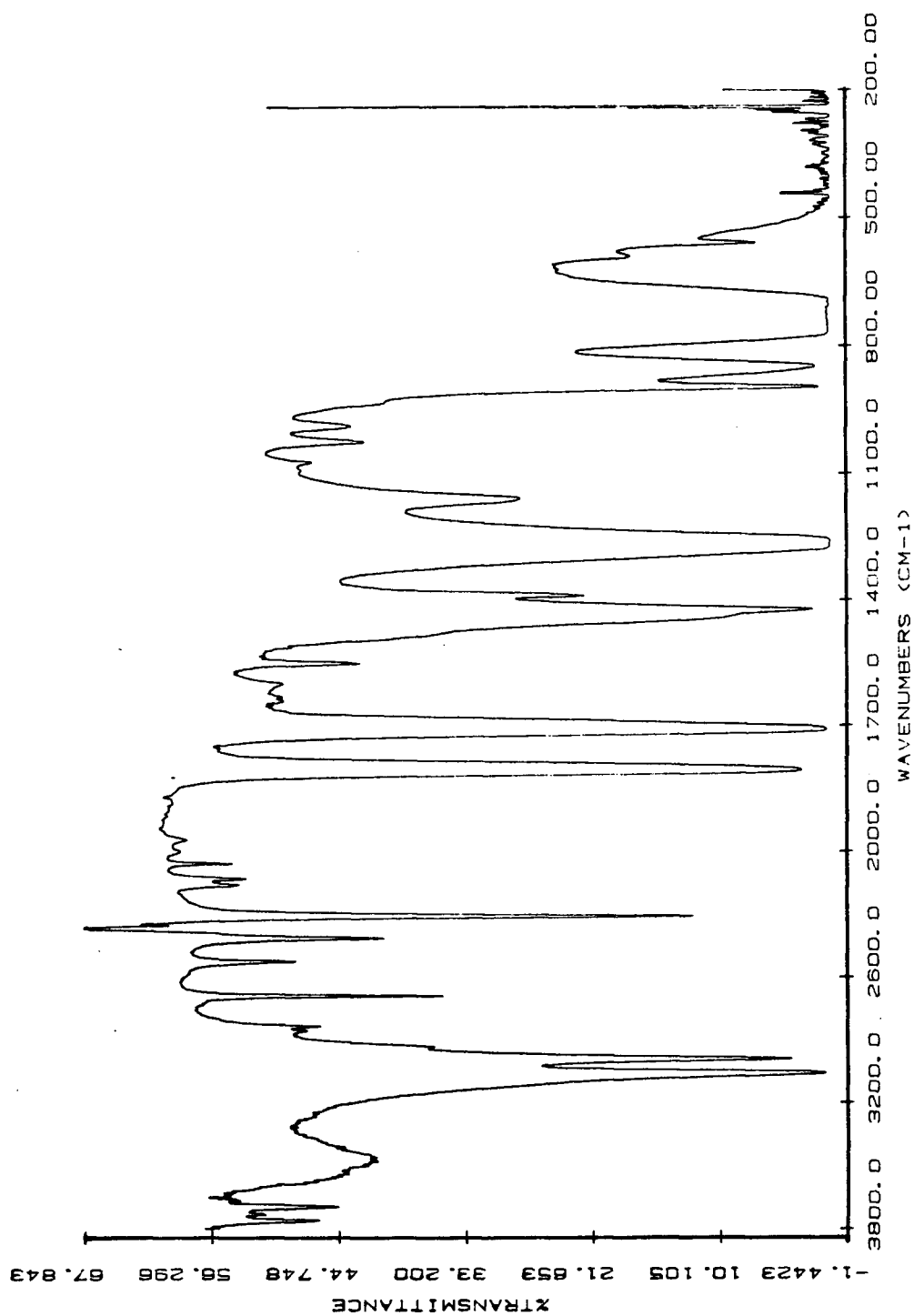
IR spectrum of $\text{Cp}^*\text{Cr}(\text{NO})_2\text{Cl}$ in CH_2Cl_2 .



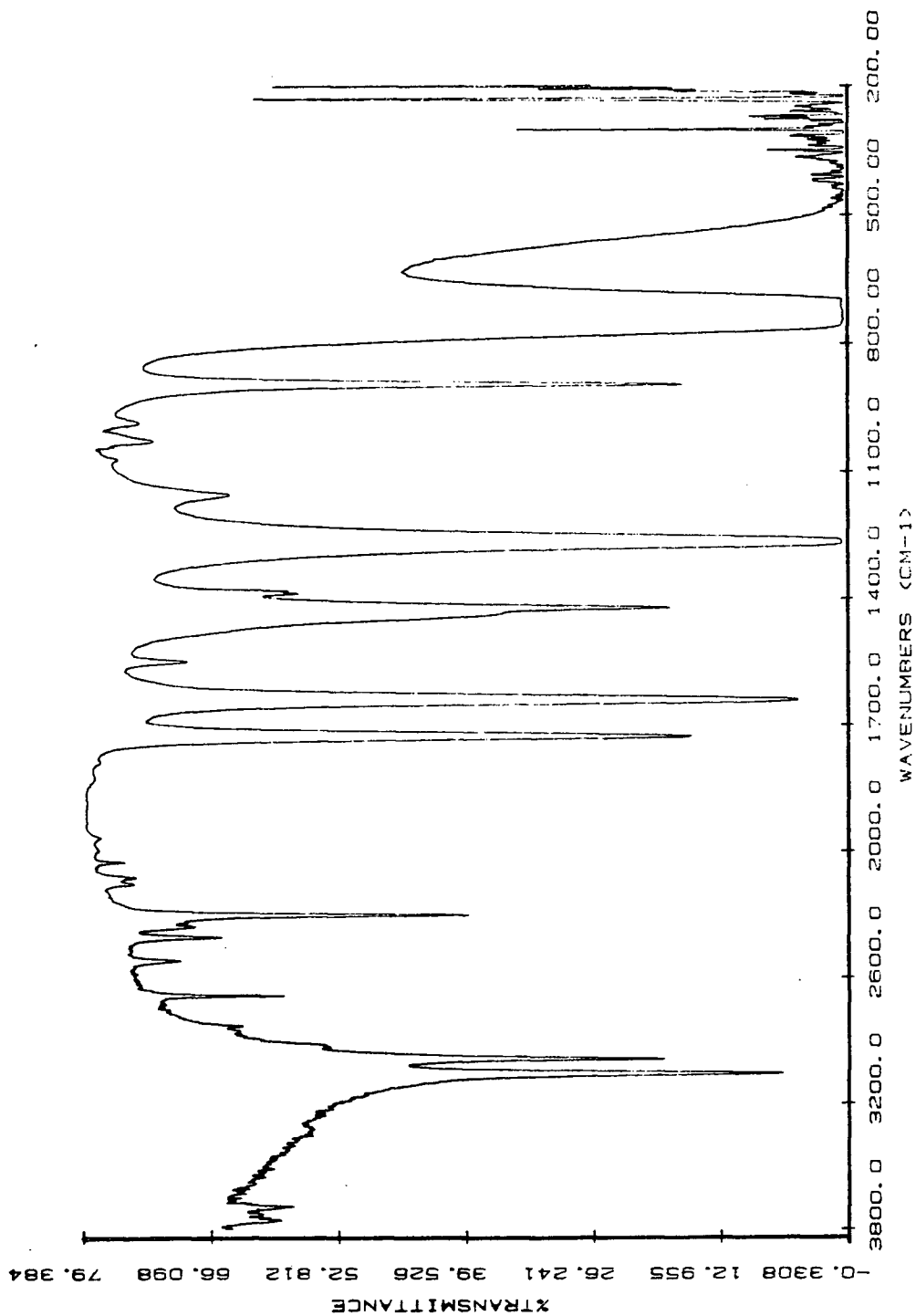
IR spectrum of $[\text{Cp}^* \text{Cr}(\text{NO})_2]\text{BF}_4$ in CH_2Cl_2 .



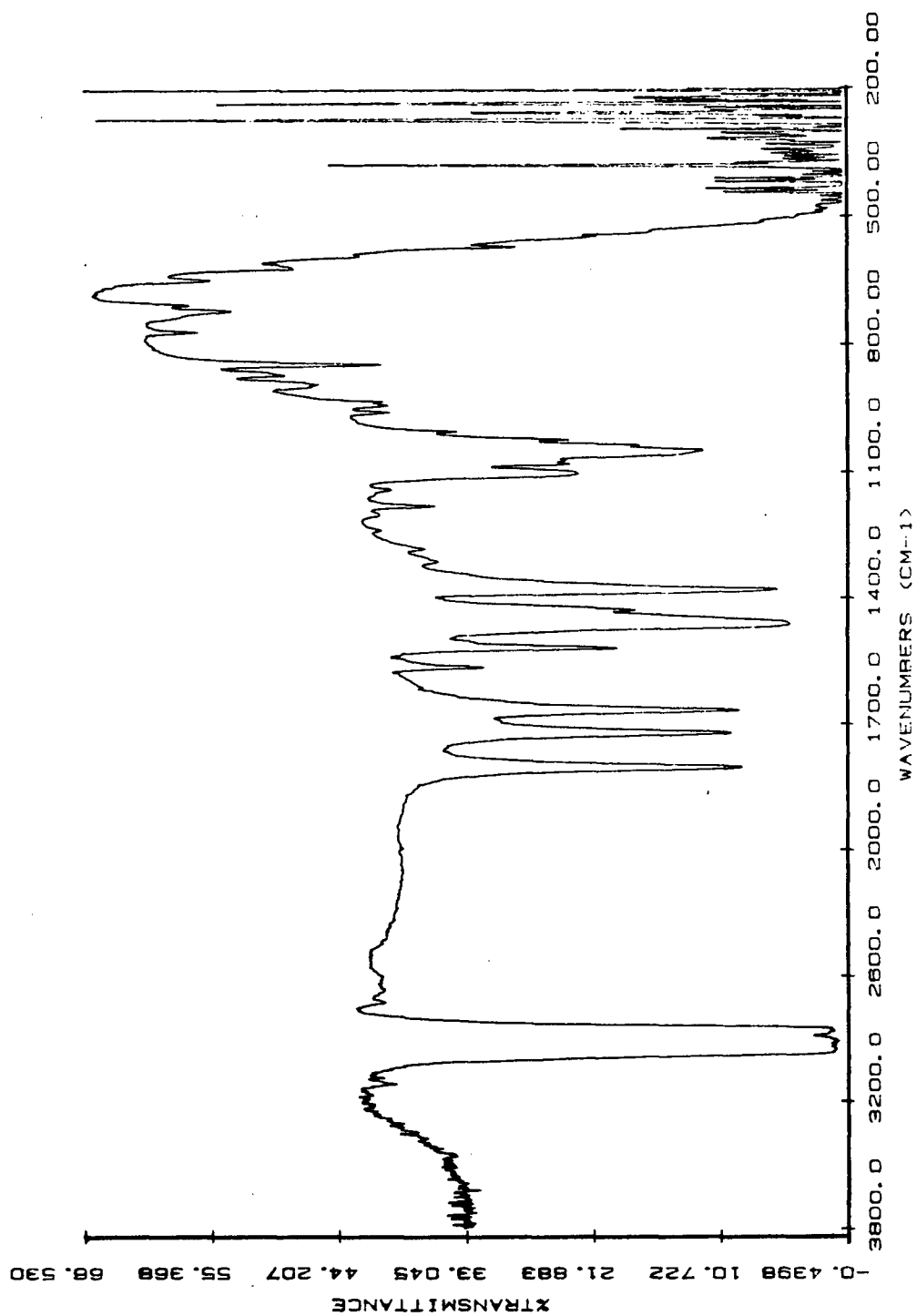
IR spectrum of $[\text{Cp}^* \text{Cr}(\text{NO})_2]\text{PF}_6$ in CH_2Cl_2 .



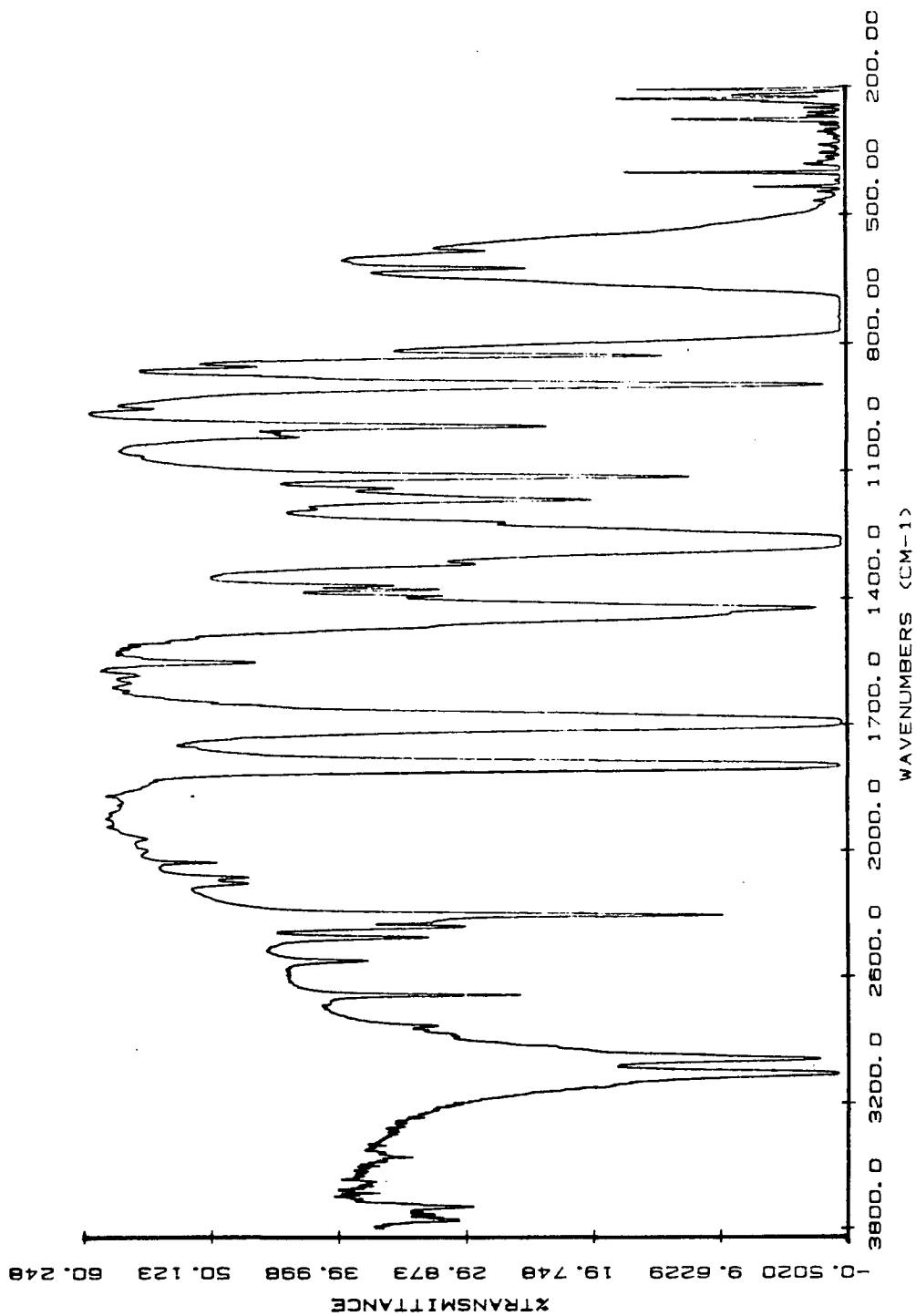
IR spectrum of $\text{Cp}^* \text{Mo}(\text{NO})_2 \text{Cl}$ in CH_2Cl_2 .



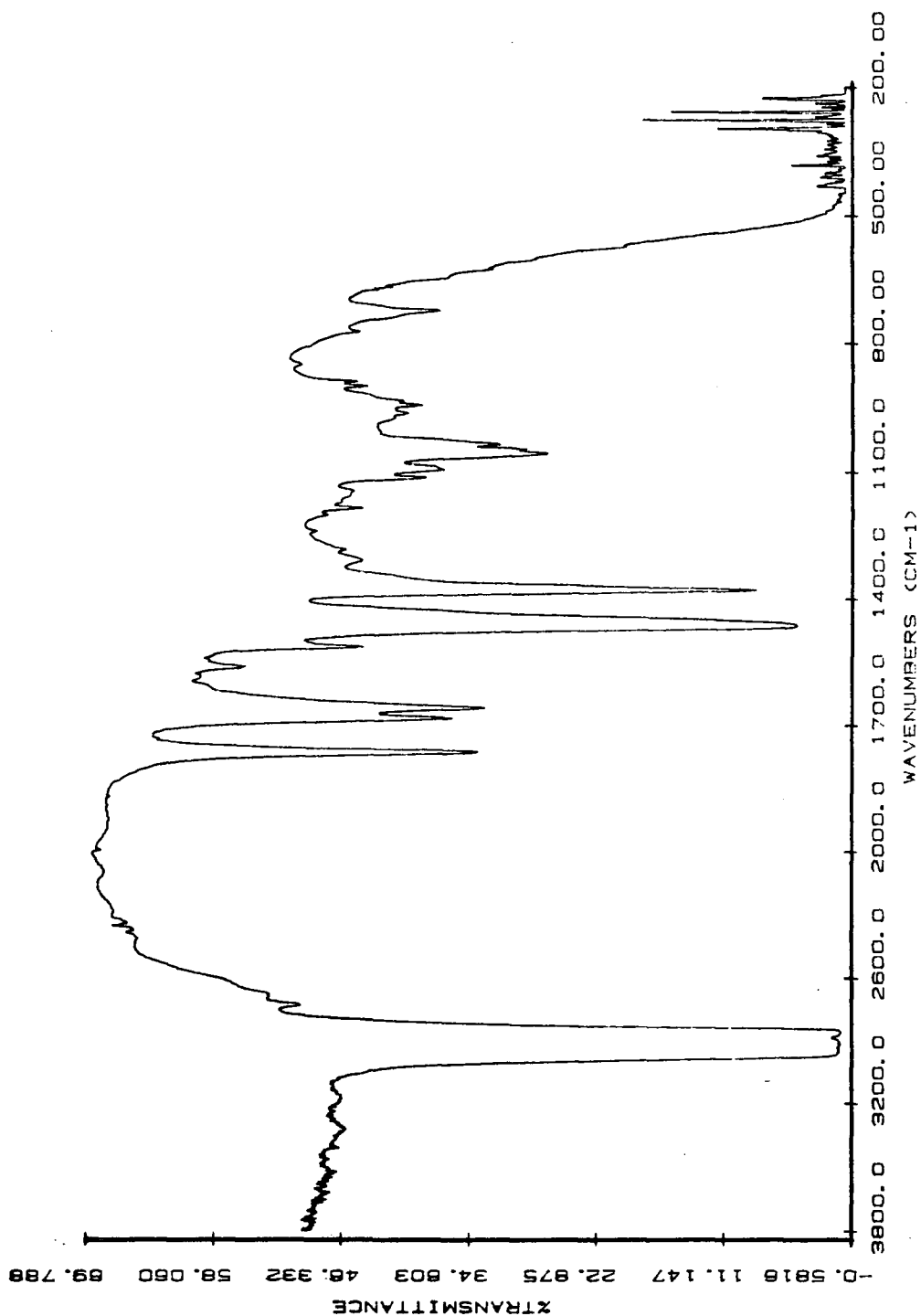
IR spectrum of $[\text{CpCr}(\text{NO})_2-\overline{\text{C}=\text{C}(\text{H})\text{C}(\text{Me})_2\text{C}(\text{Me})_2\text{OC}(\text{OMe})}]\text{BF}_4$ as a Nujol mull.



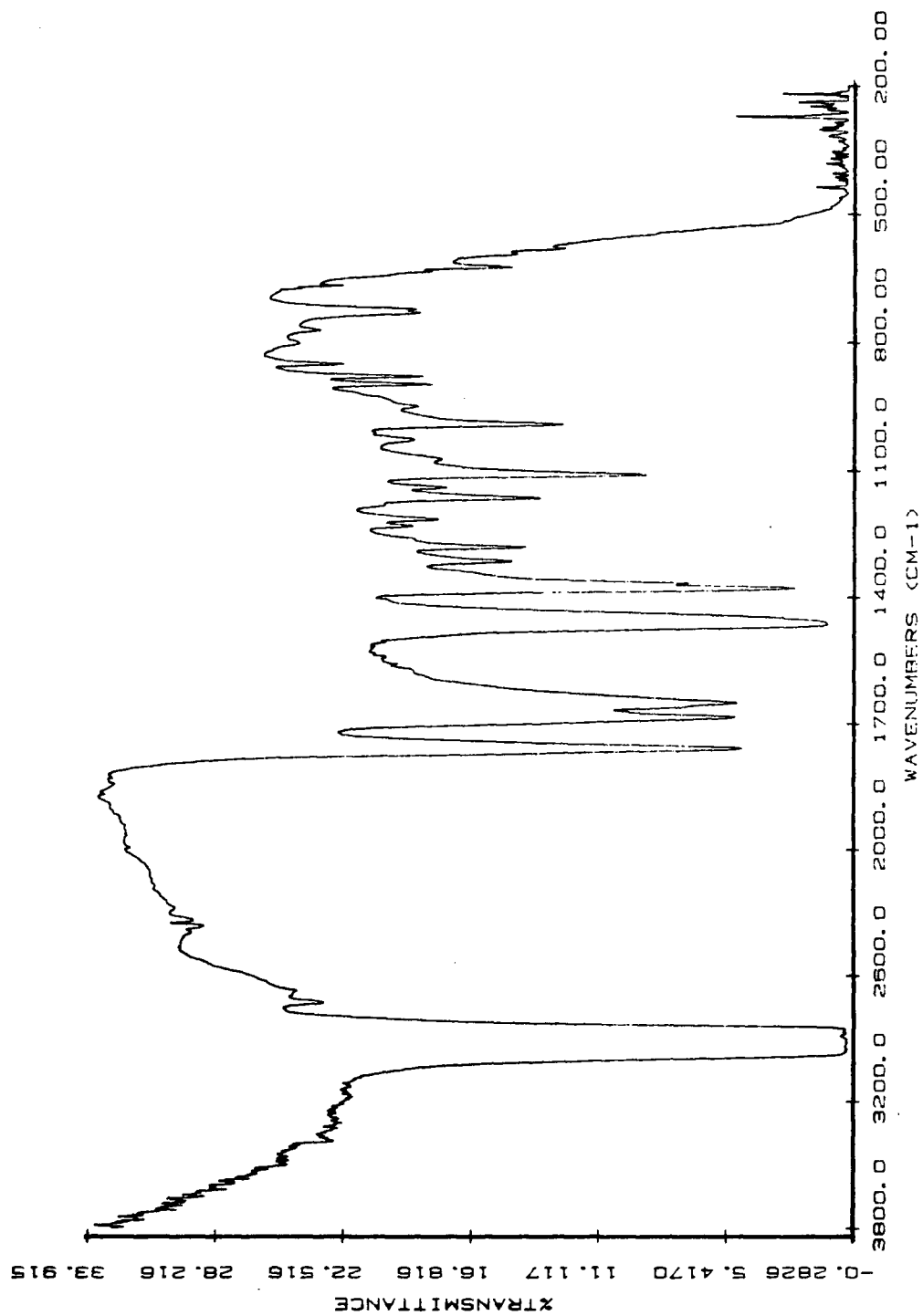
IR spectrum of $\text{CpCr(NO)}_2\text{-}\overline{\text{C}=\text{C(H)C(Me)}_2\text{C(Me)}_2\text{OC(=O)}}$ in CH_2Cl_2 .



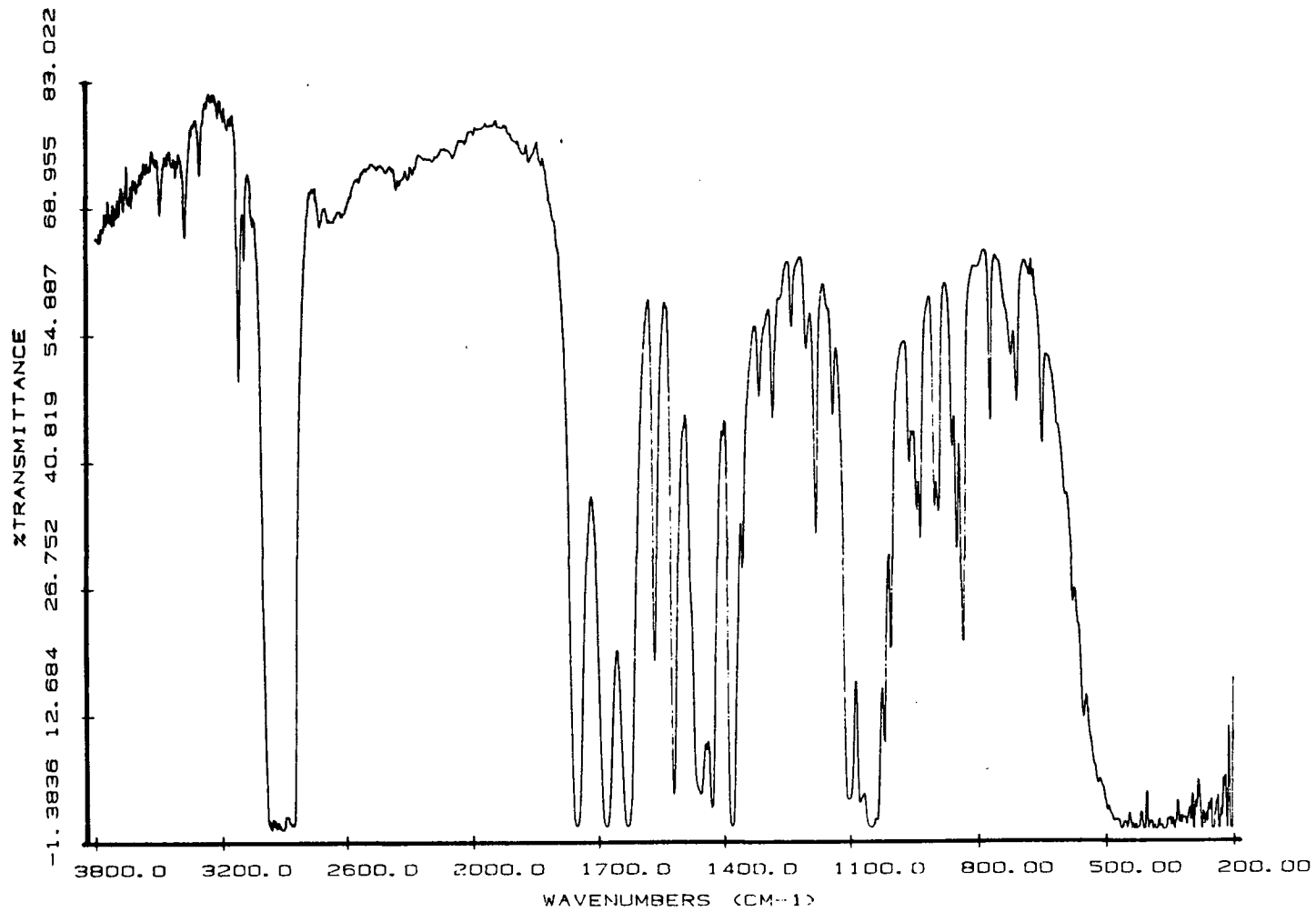
IR spectrum of $[\text{Cp}^* \text{Cr}(\text{NO})_2 - \overline{\text{C}=\text{C}(\text{H})\text{C}(\text{Me})_2\text{C}(\text{Me})_2\text{OC}(\text{OMe})}] \text{BF}_4$ as a Nujol mull.



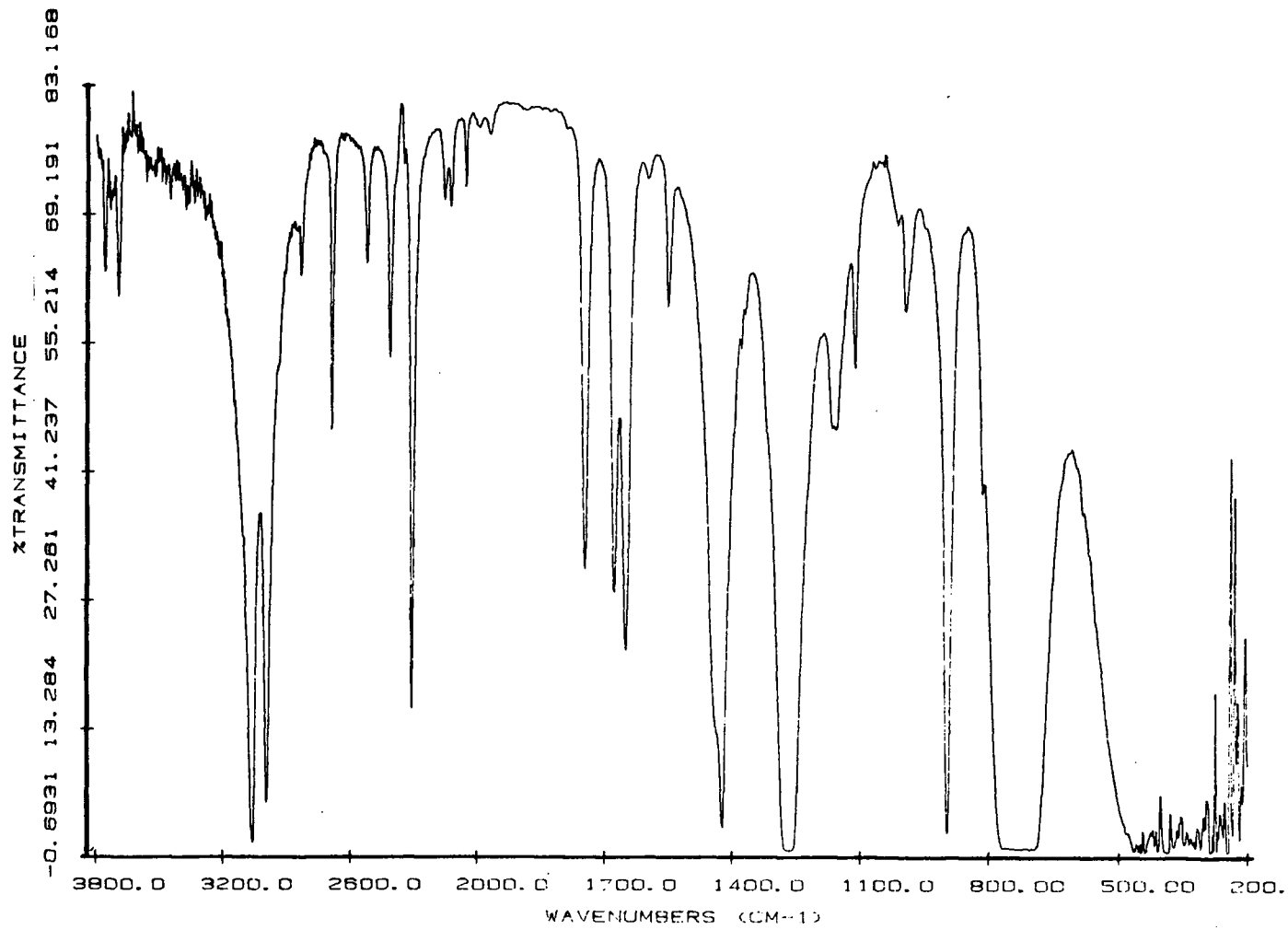
IR spectrum of $\text{Cp}^* \text{Cr}(\text{NO})_2 - \text{C}=\text{C}(\text{H})\text{C}(\text{Me})_2\text{C}(\text{Me})_2\text{OC}(=\text{O})$ as a Nujol mull.



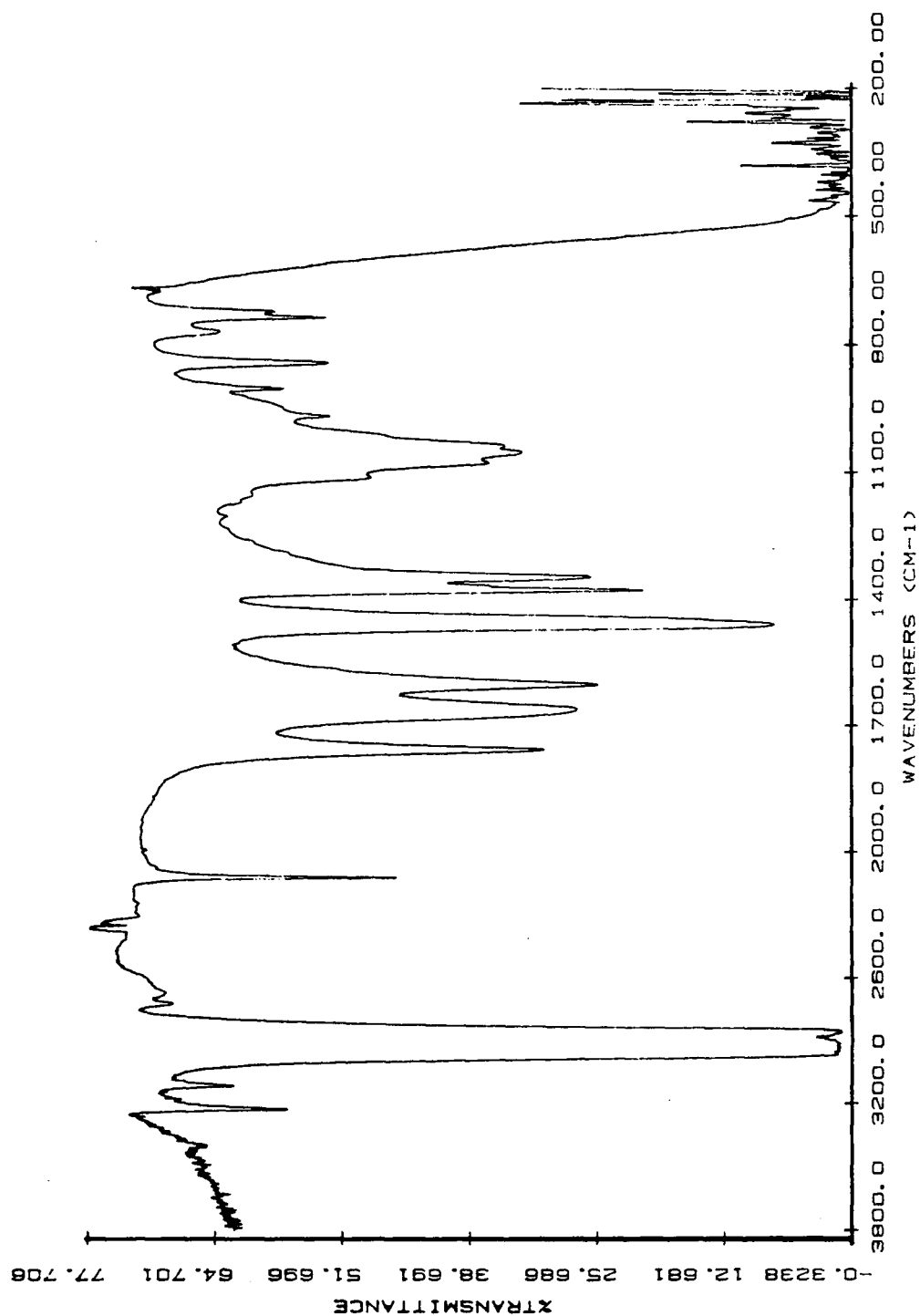
IR spectrum of $[\text{CpMo}(\text{NO})_2-\text{C}(\text{H})\text{C}(\text{Me})_2\text{C}(\text{Me})_2\text{OC}(\text{OMe})] \text{BF}_4$ as a Nujol mull.



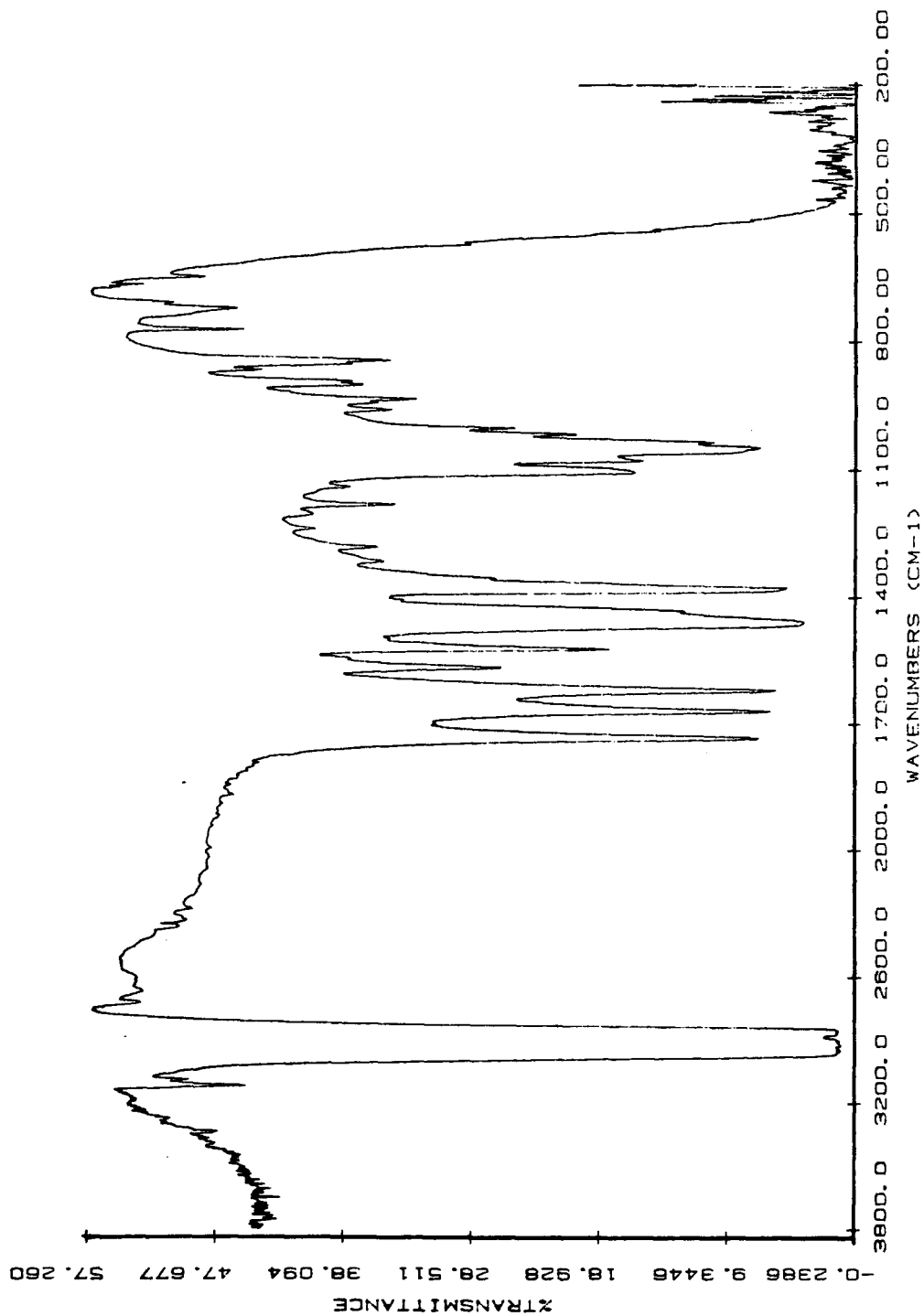
IR spectrum of $\text{CpMo(NO)}_2\text{-}\overline{\text{C=C(H)C(Me)}_2\text{C(Me)}_2\text{OC(=O)}}$ in CH_2Cl_2 .



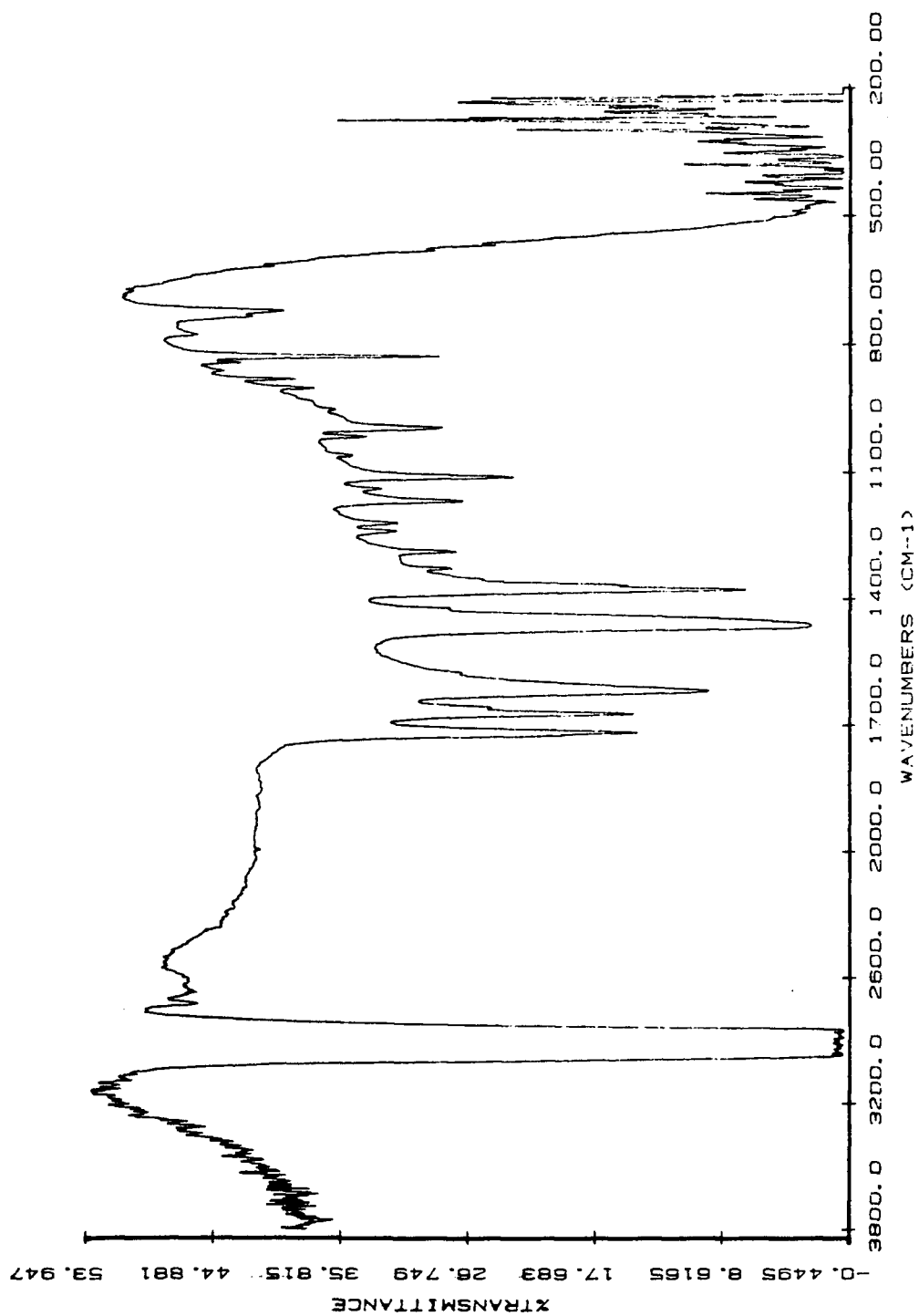
IR spectrum of $[\text{CpW}(\text{NO})_2\text{-O}=\text{C}(\text{OMe})\text{C}\equiv\text{CH}]\text{BF}_4$ as a Nujol mull.



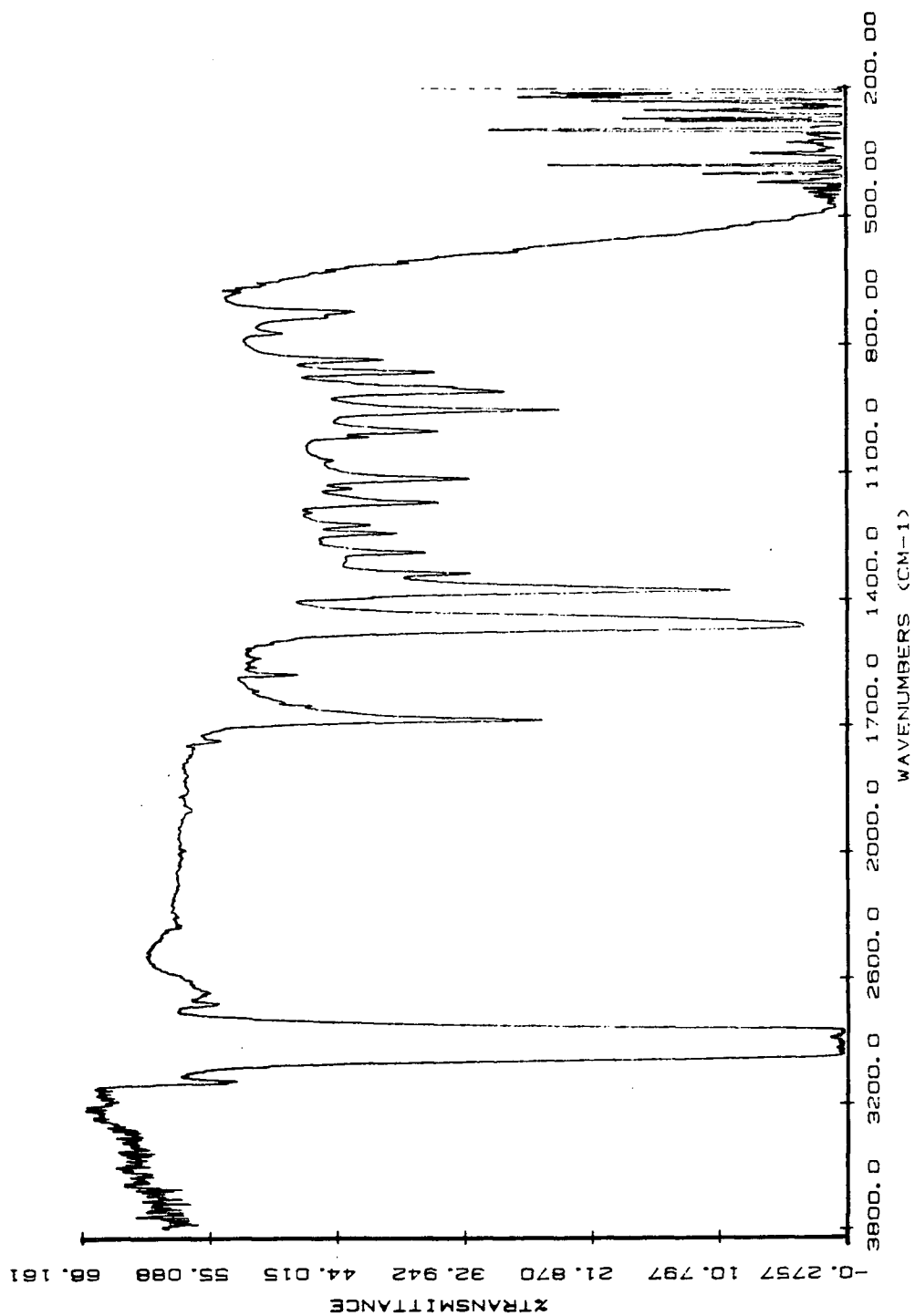
IR spectrum of $[\text{CpW}(\text{NO})_2-\text{C}=\text{C}(\text{H})\text{C}(\text{Me})_2\text{C}(\text{Me})_2\text{OC}(\text{OMe})]\text{BF}_4$ as a Nujol mull.



IR spectrum of $\text{CpW(NO)}_2\text{-}\overline{\text{C}=\text{C}(\text{H})\text{C}(\text{Me})_2\text{C}(\text{Me})_2\text{OC(=O)}}$ as a Nujol mull.



IR spectrum of $\text{CpW(O)}_2\text{-}\overline{\text{C}=\text{C}(\text{H})\text{C}(\text{Me})_2\text{C}(\text{Me})_2\text{OC(=O)}}$ as a Nujol mull.



IR spectrum of $\text{Cp}^* \text{W}(\text{NO})_2 - \overbrace{\text{C}=\text{C}(\text{H})\text{C}(\text{Me})_2\text{C}(\text{Me})_2\text{OC}(=\text{O})}^{\text{---}}$ in CH_2Cl_2 .

